6.0 CONTAINMENT REQUIREMENTS

6.0.1 Introduction

Because of the amount of material presented in Chapter 6.0 and its complexity, the U.S. Department of Energy (DOE) has provided an introductory summary of Chapter 6.0. Detailed discussions of the topics covered in this summary are found in the remainder of the chapter, which is organized as follows:

- Section 6.1 – the overall system performance assessment methodology used to evaluate compliance with the containment requirements.
- Section 6.2 – a comprehensive list of features, events, and processes (FEPs) that might affect disposal system performance, the screening methodology applied to that list, and the results of the screening process.
- Section 6.3 – development of the scenarios that are considered in the system-level consequence analysis.
- Section 6.4 – the conceptual and computational models used to perform the system-level consequence analysis (performance assessment), the overall flow of information in the performance assessment, the scenario probabilities, and the construction of a performance measure for comparison with the standard.
- Section 6.5 – the results of the performance assessment.

Additional information supporting this chapter is provided in appendices. See Table 1-6 in Chapter 1.0 for a list of these appendices.

6.0.2 Overview of Chapter 6.0

The DOE has determined that the Waste Isolation Pilot Plant (WIPP) is in compliance with the Containment Requirements of Title 40 Code of Federal Regulations (CFR) § 191.13. These requirements are stringent and state that the DOE must demonstrate a reasonable expectation that the probabilities of cumulative radionuclide releases from the disposal system during the 10,000 years following closure will fall below specified limits. The performance assessment analyses supporting this determination must be quantitative and must consider uncertainties caused by all significant processes and events that may affect the disposal system, including inadvertent human intrusion into the repository during the future. A quantitative performance assessment is conducted using a series of linked computer models in which uncertainties are addressed by a Monte Carlo procedure for the sampling of selected input parameters.

As required by regulation, results of the performance assessment are displayed as complementary cumulative distribution functions (CCDFs) that display the probability that cumulative radionuclide releases from the disposal system will exceed the values calculated

for each scenario considered in the analysis. These CCDFs are calculated using reasonable and, in some cases conservative, conceptual models that are based on the scientific understanding of the behavior of the disposal system. Parameters used in these models are derived from experimental data, field observations, and relevant technical literature. The overall mean CCDF lies entirely below and to the left of the specified limits, and the WIPP is therefore in compliance with the containment requirements of 40 CFR Part 191. Sensitivity analysis of results shows the location of the mean CCDF is dominated by releases of radionuclides that could occur directly at the ground surface during the inadvertent penetration of the repository by a future drilling operation. Releases of radionuclides to the accessible environment resulting from transport in groundwater through the shaft seal systems and the subsurface geology are negligible, with or without human intrusion, and make no contribution to the location of the mean CCDF. No releases whatsoever are predicted to occur at the ground surface in the absence of human intrusion. The natural and engineered barrier systems of the WIPP provide robust and effective containment of transuranic (TRU) waste even if the repository is penetrated by multiple borehole intrusions.

6.0.2.1 Conceptual Basis for the Performance Assessment

The foundations of the performance assessment lie in a thorough understanding of the disposal system and the possible future interactions among the repository, the waste, and the surrounding geology. This application is organized such that site characterization, facility design, and waste characterization are described separately in Chapters 2.0, 3.0, and 4.0. The DOE's confidence in the results of the performance assessment is based in part on the strength of the research done during site characterization, the robustness of the facility design, and the knowledge of the inventory. Quality assurance activities, described in Chapter 5.0, demonstrate that the information gathered during these activities is qualified to support the compliance decision.

Chapters 2.0, 3.0, and 4.0 provide the basic descriptions of the main components of the disposal system. The interactions of the repository and waste with the geologic system, and the response of the disposal system to possible future inadvertent human intrusion are described in Section 6.4.

6.0.2.2 Undisturbed Performance

An evaluation of undisturbed performance, which is defined by regulation (see 40 CFR § 191.15 and § 191.2) to exclude human intrusion and unlikely disruptive natural events, is required by regulation (see 40 CFR § 191.12). Evaluation of past and present natural geologic processes in the region indicate that none has the potential to breach the repository within 10,000 years. Behavior of the disposal system is dominated by the coupled processes of deformation of the rock surrounding the excavation, fluid flow, and waste degradation. Each of these processes can be described independently, but the extent to which each process occurs will be affected by the others.

Deformation of the rock immediately around the repository begins as soon as excavation creates a disturbance in the stress field. Stress relief results in some degree of brittle fracturing and the formation of a disturbed rock zone (DRZ) surrounding excavations in all deep mines. For the WIPP, the DRZ is characterized by an increase in permeability and a decrease in pore pressure, and may ultimately extend a few meters from the excavated region. Salt will also deform due to deviatoric stress by creep processes and move inward to fill voids. This process of salt creep will continue until deviatoric stress is dissipated and the system is once again at stress equilibrium.

The ability of salt to creep, thereby healing fractures and filling porosity, is one of the fundamental advantages of using it as a medium for geologic disposal of radioactive waste and is one of the reasons it was recommended for use by the National Academy of Sciences. For the WIPP, salt creep provides the basis for the design of the compacted crushed salt components of the shaft seal system that will compact to yield properties approaching those of the intact salt within 200 years. The salt creep will also cause the DRZ surrounding the shaft to heal rapidly around the concrete components of the seal system. In the absence of elevated pressure in the repository, salt creep would also eventually result in substantial compaction of the waste and the healing of the DRZ around the disposal region. Understanding the coupling of salt creep with fluid flow and waste degradation processes suggests that fluid pressure within the waste disposal region will be sufficient to maintain significant porosity within the disposal region throughout the performance period.

Characterization of the Salado Formation indicates that fluid flow does not occur on time scales of interest in the absence of an artificially imposed hydraulic gradient. This lack of fluid flow is the second fundamental reason for the choice of salt as a medium for geologic disposal of radioactive waste. Lack of fluid flow is a result of the extremely low permeability of the evaporite rocks that make up the Salado. Excavation of the repository has disturbed the natural hydraulic gradient and rock properties and has resulted in fluid flow. Small quantities of interstitial brine present in the Salado move toward regions of low hydraulic potential and brine seeps are observed in the underground. The slow flow of brine from halite into more permeable anhydrite marker beds and then through the DRZ into the repository is expected to continue as long as the hydraulic potential within the repository is below the hydraulic potential in the far field. The repository environment will also involve gas, and fluid flow there must be modeled as a two-phase process. Initially, the gas phase will consist primarily of air trapped at the time of closure, although other gases will form as a result of waste degradation. The gas phase pressure will rise due to creep closure, gas generation, and brine inflow, creating the potential for flow outward from the excavated region.

Consideration of waste degradation processes indicates that the role of the gas phase in fluid flow and the pressure history of the repository will be far more important than would be expected if the initial air were the only gas present. Degradation of waste can generate significant additional gas by two processes:

(1) the generation of hydrogen gas by anoxic corrosion of iron, iron alloys, and aluminum, and

(2) the generation of carbon dioxide and methane by anaerobic microbial degradation of waste containing cellulose, rubber, or plastic.

The coupling of these gas generation reactions to the processes of fluid flow and salt creep is complex. Gas generation will increase fluid pressure in the repository, thereby decreasing the hydraulic gradient and deviatoric stress between the far field and the excavated region and inhibiting the processes of brine inflow and salt creep. Anoxic corrosion will also consume brine as it breaks down water to oxidize iron and release hydrogen gas. Thus, corrosion has the potential to be a self-limiting process, in that as it consumes all water in contact with iron, it will cease. Microbial reactions are also considered to be dependent on the presence of water to occur, although their net effect is uncertain. It is assumed that microbial reactions will result in neither the consumption nor creation of water.

The total volume of gas that may be generated by corrosion and microbial degradation may be sufficient to result in repository pressures that approach lithostatic. Sustained pressures above lithostatic are not physically reasonable within the disposal system, and fracturing of the more brittle anhydrite layers is expected to occur if sufficient gas is present. The conceptual model implemented in the performance assessment causes permeability and porosity of the anhydrite marker beds to increase rapidly as pore pressure approaches and exceeds lithostatic. This conceptual model for pressure-dependent fracturing approximates the hydraulic effect of pressure-induced fracturing and allows gas and brine to move more freely within the marker beds at higher pressures.

Overall, the behavior of the undisturbed disposal system will result in extremely effective isolation of the radioactive waste. Concrete, clay, and asphalt components of the shaft seal system will provide an immediate and effective barrier to fluid flow through the shafts, isolating the repository until salt creep has consolidated the compacted crushed salt components that will permanently seal the shafts. Around the shafts, the DRZ in halite layers will heal rapidly because the presence of the solid material within the shafts will provide rigid resistance to creep. The DRZ around the shaft, therefore, will not provide a continuous pathway for fluid flow. The DRZ is not expected to heal completely around the disposal region or the operations and experimental regions, and pathways for fluid flow may exist indefinitely to the overlying and underlying anhydrite layers (Marker Beds [MB] 138 and 139 and anhydrites a and b). Some quantity of brine is expected to be present in the repository under most conditions and this brine may contain actinides (which dominate the radionuclide inventory and are therefore the elements of primary regulatory interest) mobilized as both dissolved and colloidal species. Gas generation by corrosion and microbial degradation is expected to occur and will result in elevated pressures within the repository. These pressures will not significantly exceed lithostatic, because fracturing within the more brittle anhydrite layers will occur and provide a pathway for gas to leave the repository. Fracturing is expected to enhance gas and brine migration from the repository, but gas transport will not contribute to the release of actinides from the disposal system. Brine flowing out of the waste disposal region through anhydrite layers may transport actinides as dissolved and colloidal species, but the quantity of actinides that may reach the accessible environment boundary during undisturbed performance through the interbeds is insignificant and has no effect on the

compliance determination. No migration of radionuclides whatsoever is expected to occur vertically through the Salado or through the shaft seal system.

6.0.2.3 Disturbed Performance

Performance assessment is required by regulation to consider scenarios that include intrusions into the repository by inadvertent and intermittent drilling for resources. The probability of these intrusions is based on a future drilling rate of 46.8 boreholes per square kilometer per 10,000 years. This rate is based on consideration of the past record of drilling events in the Delaware Basin consistent with regulatory criteria. Active institutional controls are assumed to be completely effective in preventing intrusion during the first 100 years after closure and passive institutional controls are assumed to be effective in reducing the drilling rate by two orders of magnitude for the 600 years that follow the 100 years of active control. Future drilling practices are assumed to be the same as current practice, also consistent with regulatory criteria. These practices include the type and rate of drilling, emplacement of casing in boreholes, and the procedures implemented when boreholes are plugged and abandoned.

Results of the performance assessment indicate that human intrusion provides the only mechanism for significant releases of radionuclides from the disposal system. These releases may occur by five mechanisms:

(1) cuttings, which include material intersected by the rotary drilling bit,

(2) cavings, which include material eroded from the borehole wall during drilling,

(3) spallings, which include solid material carried into the borehole during rapid depressurization of the waste-disposal region,

(4) direct brine releases, which include contaminated brine that may flow to the surface during drilling, and

(5) long-term brine releases, which include the contaminated brine that may flow through a borehole after it is abandoned.

The first four of these mechanisms operate immediately following the intrusion event and are collectively referred to as direct releases. The accessible environment boundary for these releases is the ground surface. The fifth mechanism, actinide transport by long-term groundwater flow, begins when concrete plugs are assumed to degrade in an abandoned borehole and may continue throughout the regulatory period. The accessible environment boundary for these releases may be the land surface or the lateral subsurface limit of the controlled area.

Repository conditions prior to intrusion will be the same as those described for undisturbed performance and all processes active in undisturbed performance will continue to occur

following intrusion. Because intrusion provides a pathway for radionuclides to reach the ground surface and to enter the geological units above the Salado, additional processes will occur that are less important in undisturbed performance. These processes include the mobilization of radionuclides as dissolved and colloidal species in repository brine and groundwater flow and actinide transport in the overlying units. Flow and transport in the Culebra Member of the Rustler Formation are of particular interest because this is the unit to which modeling indicates most flow from a borehole will occur.

6.0.2.3.1 Cuttings and Cavings

In a rotary drilling operation, the volume of material brought to the surface as cuttings is the cylinder defined by the thickness of the unit being drilled and the diameter of the drill bit. The quantity of radionuclides released as cuttings is therefore a function only of the activity of the intersected waste and the diameter of the intruding drill bit. Like all parameters that describe future drilling activities, the diameter of a drill bit that may intersect waste is speculative. The DOE uses a constant value of 12.25 inches (0.311 meters), consistent with bits used at the WIPP depth in the Delaware Basin today. The activity of the intersected waste may vary depending on the type of waste intersected, and the DOE considers random penetrations into remote-handled (RH)-TRU waste and each of the 569 different waste types identified for contact-handled (CH)-TRU waste.

The volume of particulate material eroded from the borehole wall and brought to the surface as cavings may be affected by the drill bit diameter, the effective shear resistance of the intruded material, the speed of the drill bit, the viscosity of the drilling fluid and the rate at which it is circulated in the borehole, and other properties related to the drilling process. The most important of these parameters, after drill bit diameter, is the effective shear resistance of the intruded material. In the absence of data describing the reasonable and realistic future properties of degraded waste and backfill, the DOE has used conservative parameter values based on the properties of fine-grained sediment. Other properties are assigned fixed values consistent with current practice. The quantity of radionuclides released as cavings depends on the volume of eroded material and its activity, which is treated in the same manner as the activity of the cuttings.

6.0.2.3.2 Spallings

Unlike releases from cuttings and cavings, which will occur with every borehole intrusion, spalling releases will occur only if pressure in the waste-disposal region exceeds the hydrostatic pressure in the borehole. At lower pressures, below about 8 megapascals, fluid in the waste-disposal region will not flow toward the borehole. At higher pressures, gas flow toward the borehole may be sufficiently rapid to entrain particulate waste. If spalling occurs, the volume of spalled material is affected by the physical properties of the waste, specifically its tensile strength and particle diameter. As is the case for the effective shear resistance for the waste, WIPP-specific experimental data are not available to support parameter values for the tensile strength and average particle diameter of degraded waste and backfill. The DOE

has based the parameter values used in the performance assessment on reasonable and conservative assumptions.

The quantity of radionuclides released as spalled material depends on the volume of spalled waste and its activity. Because spalling may occur at a greater distance from the borehole than cuttings and cavings, spalled waste is assumed to have the volume-averaged activity of CH-TRU waste rather than the sampled activities of individual waste streams. RH-TRU waste is isolated from the spallings process and does not contribute to the volume or activity of spalled material.

6.0.2.3.3 Direct Brine Flow

Radionuclides may be released to the accessible environment if repository brine enters the borehole during drilling and flows to the ground surface. The quantity of radionuclides released by direct brine flow depends on the volume of brine reaching the ground surface and the concentration of radionuclides contained in the brine. As is the case for spallings, direct releases of brine will not occur if repository pressure is below the hydrostatic pressure in the borehole. At higher repository pressures, if mobile brine is present in the repository, it will flow toward the borehole. If the volume of brine flowing from the repository into the borehole is small, it will not affect the drilling operation and flow may continue until the driller reaches the base of the evaporite section and installs casing in the borehole. This length of time is estimated to be 72 hours, consistent with current practice. Larger brine flows or large gas flows could cause the driller to lose control of the borehole and fluid flow, in this case, could continue until repository pressure drops or the hole is contained. The maximum length of time that such flow would be allowed to continue before the borehole would be controlled by the driller is 11 days, consistent with current drilling practice in the Delaware Basin.

6.0.2.3.4 Mobilization of Actinides in Repository Brine

Actinides may be mobilized in repository brine in two principal ways:

(1) as dissolved species, and

(2) as colloidal species.

The solubilities of actinides differ among the different oxidation states in which they may exist, with the more reduced forms (for example, Pu-III or Pu-IV rather than Pu-V or Pu-VI) being less soluble. Conditions within the repository will be reducing because of the large quantity of iron in the waste and containers and, in some cases, only the lower solubility oxidation states will be present. Solubilities also vary with pH. The DOE will therefore emplace magnesium oxide (MgO) in the waste disposal region with the waste to ensure conditions that favor minimum actinide solubility. Solubilities in the performance assessment are based on reducing conditions, MgO backfill, and the chemistry of brines that can be present in the waste disposal region.

The waste contains organic ligands that, under some circumstances, can enhance actinide concentrations in brine by forming soluble complexes containing actinide ions. However, these organic ligands also bond strongly to other metals, such as magnesium, that will be present in far larger quantities in repository brine. Because of this competition effect, organic ligands will not have a significant effect on overall actinide concentrations in brine.

Colloidal transport of actinides has been examined and four types have been determined to represent the possible behavior at the WIPP. These include microbes, humic substances, actinide intrinsic colloids, and mineral fragments. Concentrations of actinides mobilized as these colloidal forms are included in the estimates of total actinide concentrations used in the performance assessment.

6.0.2.3.5 Long-Term Brine Flow up an Intrusion Borehole

Long-term releases to the ground surface or into groundwater in the Rustler or overlying units may occur after the borehole has been plugged and abandoned. In keeping with regulatory criteria, borehole plugs are assumed to have the properties consistent with current practice in the basin. Thus, boreholes are assumed to have concrete plugs emplaced at various locations. Initially, concrete plugs will be effective in limiting fluid flow in the borehole. However, under most circumstances, these plugs cannot be expected to remain fully effective indefinitely. For the purposes of performance assessment, discontinuous borehole plugs above the repository are assumed to degrade 200 years after emplacement. From then on, the borehole is assumed to be filled with a silty-sand like material containing degraded concrete, corrosion products resulting from degradation of casing, and material that sloughs into the hole from the walls. Of six possible plugged borehole configurations in the Delaware Basin, three are considered either likely or found to adequately represent other possible configurations; one configuration (a two-plug configuration) is explicitly modeled.

If sufficient brine is available in the repository, and if pressure in the repository is higher than that in the overlying units, brine may flow up the borehole following degradation of the plugs. In principle, this brine could flow into any permeable unit or to the ground surface if repository pressure were high enough. For modeling purposes, brine is allowed to flow only into the higher permeability units and to the surface. Lower permeability anhydrite and mudstone layers in the Rustler are treated as if they were impermeable, to simplify the analysis while maximizing the amount of flow occurring into units where it has a potential to contribute to releases from the disposal system. Model results indicate that essentially all flow occurs into the Culebra, which has been recognized since the early stages of site characterization as the most transmissive unit above the repository and the most likely pathway for subsurface transport.

6.0.2.3.6 Groundwater Flow in the Culebra

Site characterization activities in the units above the Salado have focused on the Culebra. These activities have shown that the direction of groundwater flow in the Culebra varies somewhat regionally, but in the area that lies over the site, flow is southward. Regional

variation in groundwater flow direction in the Culebra is influenced by the regional variation in transmissivity observed and also by the shape of and distribution of rock types in the groundwater basin in which the WIPP is located. Site characterization activities have demonstrated that there is no evidence of karst groundwater systems in the controlled area, although groundwater flow in the Culebra is affected by the presence of fractures, fracture fillings, and vuggy pore features. A zone of relatively high transmissivity in the Culebra in the southeast portion of the controlled area has been identified as the most important flow path away from the waste disposal panels, based on analysis of regional groundwater pumping tests. Other laboratory and field activities have focused on the behavior of dissolved and colloidal actinides in the Culebra. These characterization and modeling activities conducted in the units above the Salado confirm that the Culebra is the most transmissive unit above the Salado. The Culebra is the unit into which actinides are likely to be introduced from long-term flow up an abandoned borehole.

Basin-scale regional modeling of three-dimensional groundwater flow in the units above the Salado demonstrates that it is appropriate, for the purposes of estimating radionuclide transport, to conceptualize the Culebra as a two-dimensional confined aquifer. As modeled in the performance assessment, the steady-state flow field within the Culebra is affected only by the initial head distribution and the spatial variability of the transmissivity of the unit. Field data for both transmissivity and head are available from many locations in the Culebra. Uncertainty in the flow field is incorporated in the analysis through the use of 100 different geostatistically-based transmissivity fields, each of which is consistent with available head and transmissivity data.

Groundwater flow in the Culebra is modeled as a steady-state process, but two mechanisms are considered in the performance assessment that could affect flow in the future. Potash mining in the McNutt Potash Zone (hereafter referred to as the McNutt) of the Salado, which occurs now in the Delaware Basin outside the controlled area and which may continue to occur in the future, has the potential to affect flow in the Culebra if subsidence over mined areas causes fracturing or other changes in rock properties. Climatic changes during the next 10,000 years may also affect groundwater flow by altering recharge to the Culebra.

Consistent with regulatory criteria, mining outside the controlled area is assumed to occur in the near future, and mining within the controlled area is assumed to occur with a probability of 1 in 100 per century (adjusted for the effectiveness of institutional controls during the first 700 years following closure). Consistent with regulatory guidance, the effects of mine subsidence are incorporated in the performance assessment by increasing the transmissivity of the Culebra over the areas identified as mineable by a factor sampled from a uniform distribution between 1 and 1000. Transmissivity fields used in the performance assessment are therefore adjusted and steady-state flow fields calculated accordingly, once for the case in which mining is assumed to occur only outside the controlled area and once for the case in which mining is assumed to occur both inside and outside the controlled area. Mining outside the controlled area is considered in both undisturbed and disturbed performance.

The extent to which climate will change during the next 10,000 years and the extent to which such change will affect groundwater flow in the Culebra are uncertain. Regional three-dimensional modeling of groundwater flow in the units above the Salado indicates that flow velocities in the Culebra may be increased by a factor of between 1 and 2.25 for reasonably possible future climates. This uncertainty is incorporated in the performance assessment by scaling the calculated steady-state specific discharge within the Culebra by a sampled parameter within this range.

6.0.2.3.7 Actinide Transport in the Culebra

Field tests have shown that the Culebra is best characterized as a double porosity medium for the purposes of estimating contaminant transport in groundwater. Groundwater flow and advective transport of dissolved species or colloidal particles occurs primarily in a small fraction of the total porosity of the rock and thus corresponds to the porosity of open and interconnected fractures and vugs. Diffusion and slower flow occur in the remainder of the porosity, which is associated with the low-permeability dolomite matrix. Transported species, including actinides if present, will diffuse into this porosity.

Diffusion out of the advective porosity into the dolomite matrix will retard actinide transport by two mechanisms. Physical retardation occurs simply because actinides that diffuse into the matrix are no longer transported with the flowing groundwater. Transport is interrupted until they diffuse back into the advective porosity. In situ tracer tests have been conducted to demonstrate this phenomenon. Chemical retardation also occurs within the matrix as actinides are sorbed onto dolomite grains. The relationship between sorbed and liquid concentrations is assumed to be linear, and the distribution coefficients (K_ds) that characterize the extent to which actinides will sorb on dolomite are based on experimental data.

Modeling indicates that physical and chemical retardation, as supported by field tests and laboratory experiments, will be extremely effective in reducing the transport of dissolved actinides in the Culebra. Experimental work has demonstrated that transport of colloidal actinides is not a significant mechanism in the Culebra. As a result, actinide transport through the Culebra to the subsurface boundary of the controlled area is not a significant pathway for releases from the WIPP. As discussed in Section 6.5.3, the location of the mean CCDF that demonstrates compliance with the containment requirements of 40 CFR § 191.13 is determined entirely by direct releases at the ground surface during drilling (cuttings, cavings, and spallings).

6.0.2.3.8 Intrusion Scenarios

Human intrusion scenarios evaluated in the performance assessment include both single intrusion events and combinations of multiple boreholes. Two different types of boreholes are considered:

(1) those that penetrate a pressurized brine reservoir in the underlying Castile Formation, and

(2) those that do not.

The presence of a brine reservoir under the repository is speculative, but cannot be ruled out by available information. A pressurized brine reservoir was encountered at the WIPP-12 borehole within the controlled area to the northwest of the disposal region and other pressurized brine reservoirs have been encountered elsewhere in the Delaware Basin that are associated with regions of deformation in the Castile. Based on a geostatistical analysis of the distribution of brine encounters in the region, the DOE has estimated that there is a 0.08 probability that any random borehole that penetrates waste in the WIPP will also penetrate an underlying brine reservoir. Properties are assigned to the hypothetical reservoir (for example, its pressure and volume) that are consistent with the available information from tests at WIPP-12 and other boreholes. These properties are also made consistent with the hypothetical reservoir's location under the waste disposal region.

The primary consequence of penetrating a pressurized reservoir will be to provide an additional source of brine beyond that which flows into the repository from the Salado. Direct releases at the ground surface resulting from the first intrusion into the repository will be unaffected by the presence of additional Castile brine even if it flows to the surface, because brine moving straight up a borehole will not mix significantly with waste. The presence of Castile brine has the potential to increase radionuclide releases significantly in two ways, however. First, the volume of contaminated brine that could flow to the surface may be greater for a second or subsequent intrusion into a repository that has already been connected to a Castile reservoir. Second, the volume of contaminated brine that may flow up an abandoned borehole after plugs have degraded may be greater for combinations of two or more boreholes that intrude the same panel if one of the boreholes penetrates a pressurized reservoir. Both processes are modeled in the performance assessment.

6.0.2.4 Compliance Demonstration Method

The DOE's approach to demonstrating compliance is the performance assessment methodology described in Section 6.1. The performance assessment process is based on a comprehensive consideration of the features, events, and processes that are relevant to disposal system performance. Those features, events, and processes that are shown by screening analyses to have the potential to affect performance are included in quantitative calculations using a system of linked computer models to describe the interaction of the repository with the natural system, both with and without human intrusion. Uncertainty is incorporated in the analysis through a Monte Carlo approach in which multiple simulations (or realizations) are completed using sampled values for 57 imprecisely known or naturally variable input parameters. Distribution functions are constructed that characterize the state of knowledge for these parameters, and each realization of the modeling system uses a different set of sampled input values. A sample size of 100 results in 100 different values of each parameter. Therefore, there are 100 different sets (vectors) of input parameter values. Quality assurance activities, described in Chapter 5.0, demonstrate that the parameters, software, and analysis used in the performance assessment were the result of a rigorous process conducted under controlled conditions.

Probabilities of scenarios composed of specific combinations of features, events, and processes are estimated based on regulatory criteria (applying to the probability of future human action) and the understanding of the natural and engineered systems. Cumulative radionuclide releases from the disposal system are calculated for each scenario considered and probabilities of the scenarios are summed for each realization of the modeling system to construct distributions of CCDFs. Sampling of the input parameters was performed in three separate replicates resulting in three independent distributions of CCDFs and allowing the construction of three independent mean CCDFs, each based on 100 individual CCDFs.

6.0.2.5 Results of the Performance Assessment

Section 6.5 addresses the Containment Requirements of 40 CFR Part 191 and the associated criteria of 40 CFR § 194.34. Section 6.5 presents distributions of CCDFs for each replication of the analysis, mean CCDFs, and an overall mean CCDF, together with the 95 percent confidence interval estimated from the distribution of the three independent means.

Families of CCDFs and mean CCDFs for each of the three replicates are also shown in Section 6.5. All 300 individual CCDFs lie below and to the left of the limits specified in 40 CFR § 191.13(a). The overall mean CCDF determined from the three replicates lies entirely below and to the left of the limits specified in 40 CFR § 191.13(a). Thus, the WIPP is in compliance with the containment requirements of 40 CFR Part 191. Comparison of the results of the three replicates indicates that the sample size of 100 in each replicate is sufficient to generate a stable distribution of outcomes. Within the region of regulatory interest (that is, at probabilities greater than $10^{-3}/10^{4}$ yr), the mean CCDFs from each replicate are essentially indistinguishable from the overall mean.

As discussed in Section 6.5, examination of the normalized releases resulting from cuttings and cavings, spallings, and direct brine release provides insight into the relative importance of each release mode in terms of its contribution to the location of the mean CCDF and the compliance determination. Releases from cuttings and cavings dominate the mean CCDF. Spallings make a small contribution. Direct brine releases are less important and have very little effect on the location of the mean. Subsurface releases resulting from groundwater transport are less than 10^{-6} EPA units and make no contribution to the location of the mean CCDF.

Uncertainties characterized in the natural system and the interaction of waste with the disposal system environment have little effect on the location of the mean CCDF, providing additional confidence in the compliance determination. The natural and engineered barrier systems of the WIPP provide robust and effective containment of TRU waste even if the repository is penetrated by multiple borehole intrusions.

6.1 Performance Assessment Methodology

The U.S. Environmental Protection Agency (EPA), in 40 CFR Part 191, specifies the generally applicable environmental standards for the protection of public health and the

environment for the disposal of TRU and high-level radioactive wastes. In this chapter, the DOE addresses compliance with the Containment Requirements of 40 CFR § 191.13 and the associated portions of 40 CFR Part 194.

The complete text of the 40 CFR § 191.13 Containment Requirements follows:

> (a) Disposal systems for spent nuclear fuel or high-level or transuranic radioactive wastes shall be designed to provide a reasonable expectation, based on performance assessments, that the cumulative releases of radionuclides to the accessible environment for 10,000 years after disposal from all significant processes and events that may affect the disposal system shall:
>
> (1) Have a likelihood of less than one chance in 10 of exceeding the quantities calculated according to Table 1 (Appendix A); and
>
> (2) Have a likelihood of less than one chance in 1,000 of exceeding ten times the quantities calculated according to Table 1 (Appendix A).
>
> (b) Performance assessments need not provide complete assurance that the requirements of § 191.13(a) will be met. Because of the long time period involved and the nature of the events and processes of interest, there will inevitably be substantial uncertainties in projecting disposal system performance. Proof of the future performance of a disposal system is not to be had in the ordinary sense of the word in situations that deal with much shorter time frames. Instead, what is required is a reasonable expectation, on the basis of the record before the implementing agency, that compliance with § 191.13(a) will be achieved.

The term accessible environment is defined as "(1) The atmosphere; (2) land surfaces; (3) surface waters; (4) oceans; and (5) all of the lithosphere that is beyond the controlled area" (40 CFR § 191.12). Further, controlled area means "(1) A surface location, to be identified by passive institutional controls, that encompasses no more than 100 square kilometers and extends horizontally no more than five kilometers in any direction from the outer boundary of the original location of the radioactive wastes in a disposal system; and (2) the subsurface underlying such a surface location" (40 CFR § 191.12). The controlled area established by the Land Withdrawal Act is shown in Figure 3-1 (see Chapter 3.0). The release limits listed in Appendix A of 40 CFR Part 191 are reproduced as Table 6-1.

For a release to the accessible environment that involves a mix of radionuclides, the limits in Table 6-1 are used to determine a normalized release (nR) of radionuclides for comparison with the release limits

(1)

where

Q_i = cumulative release in curies (*Ci*) of radionuclide *i* into the accessible environment during the 10,000-year period following closure of the repository.
L_i = release limit in curies for radionuclide *i* given in Table 6-1.
C = amount of curies of TRU waste emplaced in the repository. (As described in Section 4.1, TRU wastes contain alpha-emitting transuranic radionuclides with half-lives greater than 20 years.)

Table 6-1. Release Limits for the Containment Requirements (EPA 1985, Appendix A, Table 1)

Radionuclide	Release Limit L_i per 1,000 MTHM[a] or Other Unit of Waste (curies)
Americium-241 or -243	100
Carbon-14	100
Cesium-135 or -137	1,000
Iodine-129	100
Neptunium-237	100
Plutonium-238, -239, -240, or -242	100
Radium-226	100
Strontium-90	1,000
Technetium-99	10,000
Thorium-230 or -232	10
Tin-126	1,000
Uranium-233, -234, -235, -236, or -238	100
Any other alpha-emitting radionuclide with a half-life greater than 20 years	100
Any other radionuclide with a half-life greater than 20 years that does not emit alpha particles	1,000

[a] Metric tons of heavy metal exposed to a burnup between 25,000 megawatt-days per metric ton of heavy metal (MWd/MTHM) and 40,000 MWd/MTHM.

As indicated in Note 1(e) to Table 1 in Appendix A of 40 CFR Part 191, the "other unit of waste" for TRU waste shall be "an amount of transuranic wastes containing 1 million curies of alpha-emitting transuranic radionuclides with half-lives greater than 20 years."

Performance assessments are the basis for addressing the containment requirements. 40 CFR § 191.12 defines performance as follows:

> "Performance assessment" means an analysis that: (1) identifies the processes and events that might affect the disposal system; (2) examines the effects of these processes and events on the performance of the disposal system; and (3) estimates the cumulative releases of radionuclides, considering the associated uncertainties, caused by all significant processes and events.

The DOE's methodology for performance assessment uses information about the disposal system and the waste to evaluate performance in a regulatory context over the 10,000-year regulatory time period.

The general theory for conducting a performance assessment is presented in this section together with details specific to the performance assessment conducted for the WIPP. Figure 6-1 illustrates the general, high-level steps used by the DOE for this final performance assessment of the WIPP. In this figure, the sections of this chapter are indicated in which these steps are discussed in detail, and it shows several important features of the WIPP performance assessment. It indicates the points at which regulatory standards and guidance (40 CFR Part 191 and related documents) are most influential, and it shows that there can be an iterative process between site characterization and performance assessment that facilitates improvement in both characterization data and performance assessment. Through this process, the DOE has used early site characterization information and design specifications to develop preliminary performance assessments, from which sensitivity analyses were used to guide further characterization of important features of the site data collection on specific topics and to further develop the repository design.

Section 6.1 presents the basis for the methodology shown in Figure 6-1. Section 6.1.1 presents the conceptualization of risk, Section 6.1.2 discusses the characterization of uncertainty in risk, Section 6.1.3 discusses regulatory criteria for the quantification of risk, Section 6.1.4 discusses calculation of risk, and Section 6.1.5 discusses techniques for probabilistic analysis.

6.1.1 Conceptualization of Risk

Performance assessment of the WIPP is fundamentally concerned with the evaluation of risk, for which comparative measures are defined by regulatory standards. For comparison with these standards, the DOE uses a conceptualization for risk similar to that developed for risk assessments of nuclear power plants. This description provides a structure on which both the representation and calculation of risk can be based.

Kaplan and Garrick (1981, 11 – 12) have presented the representation of risk as a set of ordered triples. The DOE uses this representation and defines risk to be a set R of the form

$$R = [(S_i, pS_i, \mathbf{cS}_i), i = 1, ..., nS] , \quad (2)$$

where

S_i = a set of similar occurrences
pS_i = probability that an occurrence in set S_i will take place
$\mathbf{cS}_i$ = a vector of consequences associated with S_i
nS = number of sets selected for consideration

and the sets S_i have no occurrences in common (that is, the S_i are disjoint sets). This representation formally decomposes risk into what can happen (the S_i), how likely things are to happen (the pS_i), and the consequences of what can happen (the $\mathbf{cS}_i$). In the WIPP performance assessment, the S_i are scenarios, the pS_i are scenario probabilities, and the vector $\mathbf{cS}_i$ contains consequences associated with scenario S_i. Development of scenarios for the WIPP is discussed in Sections 6.1.2, 6.2, and 6.3. Scenario probabilities and consequence determination are discussed in Section 6.4.

As discussed in the following sections of this chapter, risk in the set R can be displayed using CCDFs, as required by the EPA. As stated in 40 CFR § 194.34(a),

> The results of performance assessments shall be assembled into "complementary, cumulative distribution functions" (CCDFs) that represent the probability of exceeding various levels of cumulative release caused by all significant processes and events.

In the context of Equation 2, CCDFs provide information about the consequences $\mathbf{cS}_i$ and the probabilities pS_i associated with the scenarios S_i. The probability that **cS** exceeds a specific consequence value x is determined by the CCDF F defined by

(3)

where the particular consequence result **cS** under consideration is ordered so that $\mathbf{cS}_i \leq \mathbf{cS}_{i+1}$ for i=1, …, nS-1, and i is the smallest integer such that $\mathbf{cS}_i > x$. The function F represents the probabilities that consequence values plotted on the abscissa will be exceeded. A diagrammatic example of an estimation of F is shown in Figure 6-2. The steps in the CCDF shown in Figure 6-2 result from the evaluation of F with a discrete number of possible occurrences (that is, futures) represented in the sets S_i. Unless the underlying processes are inherently disjoint, the use of more sets S_i will tend to reduce the size of these steps and, in the limit, will result in a smooth curve. To avoid a broken appearance, the DOE plots estimated CCDFs with vertical lines added at the discontinuities.

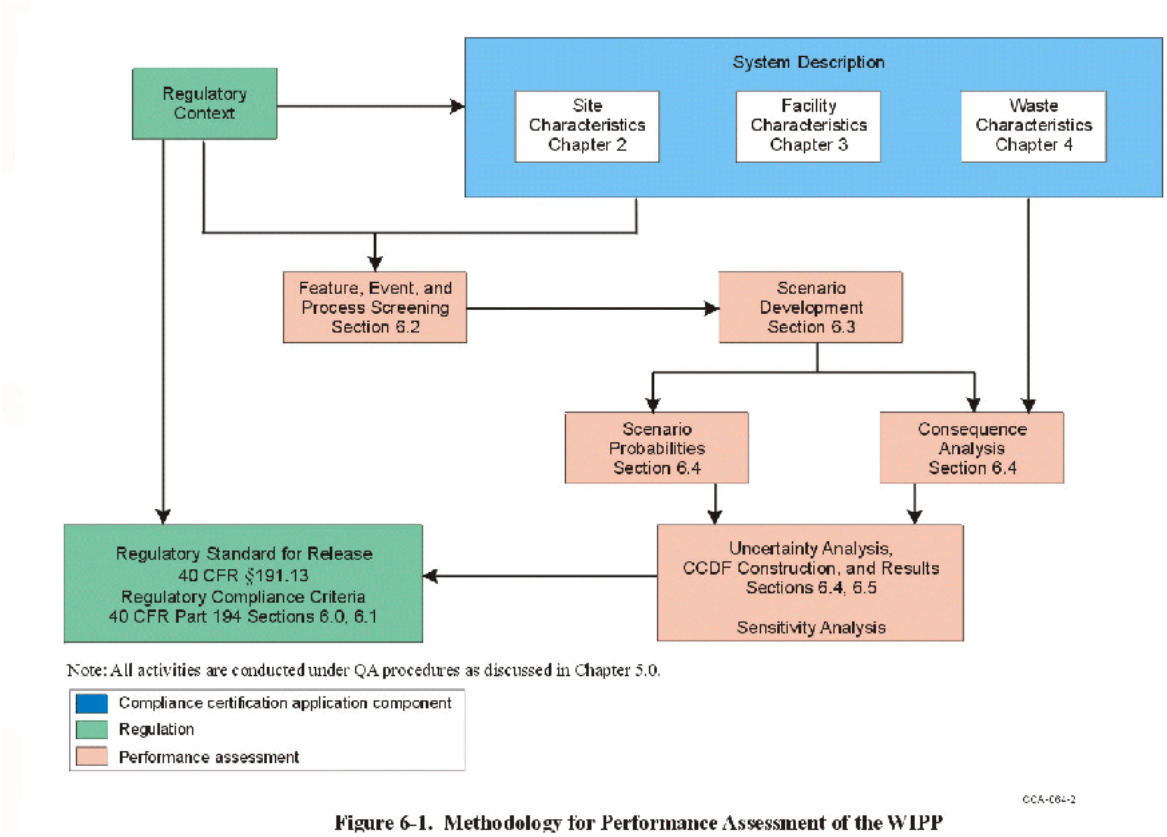

Figure 6-1. Methodology for Performance Assessment of the WIPP

1 **THIS PAGE INTENTIONALLY LEFT BLANK**

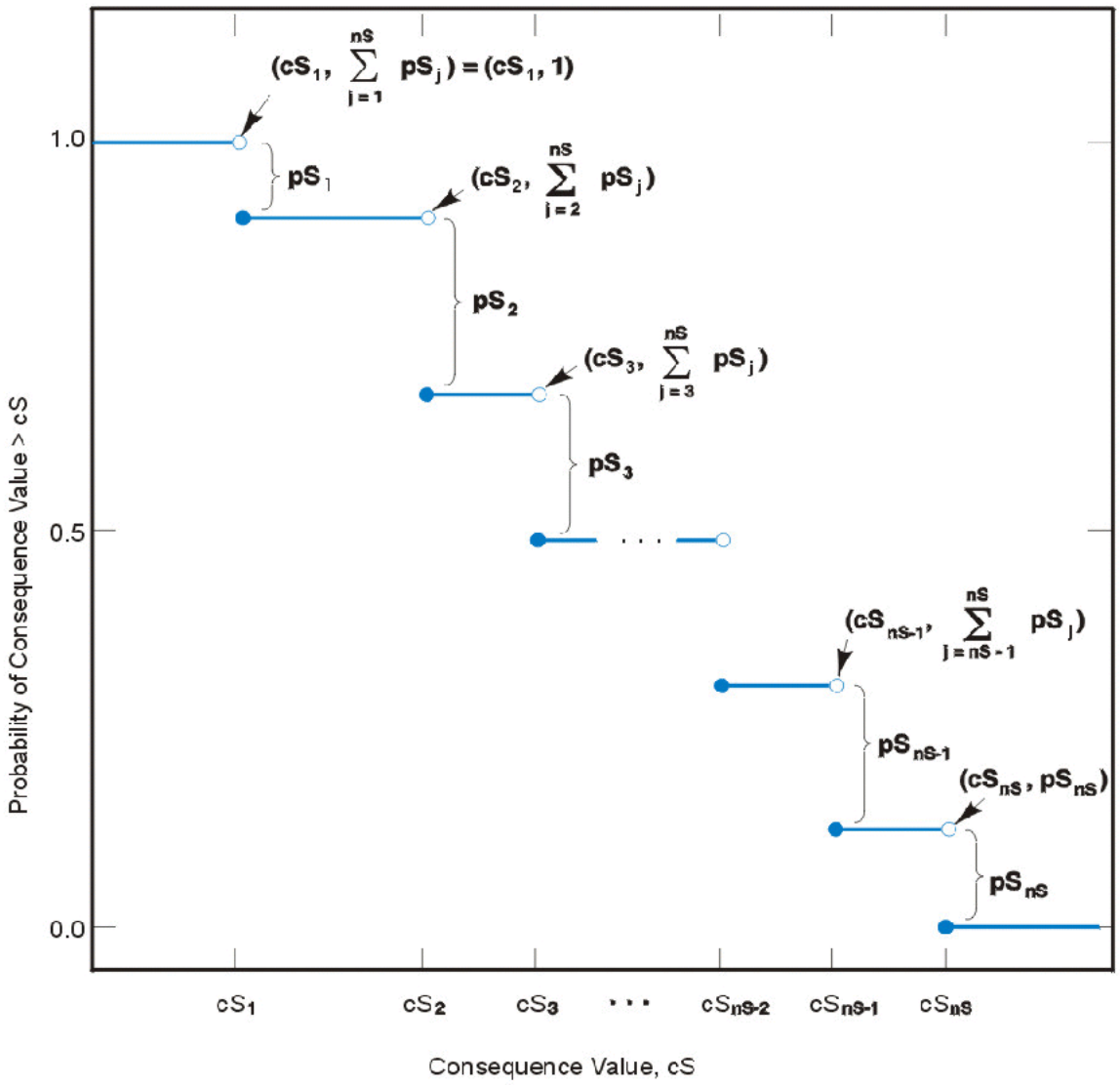

Note: The open and solid circles at the discontinuities indicate the points included on (solid circles) and excluded from (open circles) the CCDF.

CCA 006 2

Figure 6-2. Estimated CCDF For Consequence Results

1

1 **THIS PAGE INTENTIONALLY LEFT BLANK**

6.1.2 Characterization of Uncertainty in Risk

The DOE defines uncertainty in the analysis as either stochastic uncertainty or subjective uncertainty. Stochastic uncertainty derives from lack of knowledge about the future. Subjective uncertainty derives from lack of knowledge about quantities, properties, or attributes that are believed to have single or certain values. Stochastic uncertainty can be further subdivided into completeness, aggregation, and stochastic variation. Completeness refers to the extent that a performance assessment includes all possible occurrences for the system under consideration. In terms of the risk representation in Equation 2, completeness deals with whether all significant occurrences are included in the union of the sets S_i. The DOE addresses completeness in its development of scenarios, discussed here and in Sections 6.2 and 6.3. Aggregation refers to the division of the possible occurrences into the sets S_i. Resolution is lost if the S_i are defined too coarsely (for example, if nS is too small). Computational efficiency is affected if nS is too large. Aggregation gives rise to the steps in a single CCDF, as shown in Figure 6-2. The DOE addresses aggregation uncertainty in Sections 6.1.4 and 6.4.13. Stochastic variation is represented by the probabilities pS_i, which are functions of the many factors that affect the occurrence of the individual sets S_i. The DOE addresses stochastic variation in Sections 6.1.4 and 6.4.12.

Stochastic uncertainty can be characterized in performance assessment by evaluating the probability of future events (for example, by assuming that the occurrence of certain future events will be random in space and time), and by consideration of imprecisely known system properties directly associated with the future events. These imprecisely known system properties can be expressed as variables represented by the vector

$$\mathbf{x_{st}} = [x_{st,1}, x_{st,2}, \ldots, x_{st,nV(st)}] , \tag{4a}$$

where each $x_{st,j}$ [$j = 1, 2, \ldots, nV(st)$] is an imprecisely known property required in the analysis, nV is the total number of such properties associated with stochastic uncertainty, and the subscript st denotes stochastic uncertainty.

Subjective uncertainty results from incomplete data or measurement uncertainty. These uncertainties are addressed in Section 6.4. Subjective quantities, properties, or attributes may be associated with stochastic uncertainties (events that might occur in the future).

Subjective uncertainty can be characterized in performance assessment by consideration of system properties that are imprecisely known. These imprecisely known system properties can be expressed as variables represented by vectors

$$\mathbf{x_{su}} = [x_{su,1}, x_{su,2}, \ldots, x_{su,nV(su)}] , \tag{4b}$$

where each $x_{su,j}$ [$j = 1, 2, \ldots, nV(su)$] is an imprecisely known property required in the analysis, nV is the total number of such properties associated with subjective uncertainty, and the subscript su denotes subjective uncertainty.

If the analysis has been developed such that each x_j is a quantity for which the overall analysis requires a single value, the representation for risk in Equation 2 can be restated as a function of $\mathbf{x}_{st}$ and $\mathbf{x}_{su}$:

$$R(\mathbf{x}_{su}) = [S_i(\mathbf{x}_{su}), pS_i(\mathbf{x}_{su}), \mathbf{cS}_i(\mathbf{x}_{st,i}, \mathbf{x}_{su}), i = 1, ..., nS(\mathbf{x}_{st}, \mathbf{x}_{su})] , \quad (5)$$

where $x_{st,i}$ is included in S_i. Probability distributions are then assigned to the individual variables $x_{su,j}$ and $x_{st,j}$ as defined in Equation 4. These probability distributions are of the form

$$D_{st,1}, D_{st,2}, \ldots, D_{st,nV(st)} , \quad (6a)$$
$$D_{su,1}, D_{su,2}, \ldots, D_{su,nV(su)} , \quad (6b)$$

where the D_j's are the distributions developed for the variables x_j, $j = 1, 2, ...nV$, and the subscripts *st* and *su* denote distributions associated with $\mathbf{x}_{st}$ or $\mathbf{x}_{su}$. The definition of these distributions may also be accompanied by the specification of correlations and various restrictions that further define the possible relations among the x_j. These distributions (along with specified correlations or restrictions) probabilistically specify what the appropriate input to use in the performance assessment calculations might be, given that the analysis is structured so that only one value can be used for each variable, x_j, under consideration for a particular calculation.

Monte Carlo techniques can be used to determine the uncertainty in $R(\mathbf{x}_{su})$ associated with both $\mathbf{x}_{st}$ and $\mathbf{x}_{su}$. The theory of this technique is similar for characterization of both stochastic and subjective uncertainty. This technique as applied to determining the risk $R(\mathbf{x}_{su})$ associated with $\mathbf{x}_{su}$ is developed in the following paragraphs.

Once the distributions in Equation 6b have been developed, a sample

$$\mathbf{x}_k = (x_{k1}, x_{k2}, \ldots, x_{k,nV}), k = 1, \ldots, nK \quad (7)$$

is generated according to the specified distributions and restrictions where *nK* is the size of the sample. Performance assessment calculations are then performed for each sample element $\mathbf{x}_k$, which yields a sequence of risk results of the form

$$R(\mathbf{x}_k) = \{[S_i(\mathbf{x}_k), pS_i(\mathbf{x}_k), \mathbf{cS}_i(\mathbf{x}_k)], i = 1, \ldots, nS(\mathbf{x}_k)\} . \quad (8)$$

Each set $R(\mathbf{x}_k)$ is the result of one complete set of calculations performed with a set of inputs (that is, $\mathbf{x}_k$) obtained from the distributions assigned in Equation 6b. Further, associated with each risk result $R(\mathbf{x}_k)$ in Equation 8 is a weight[1] that can be used in making probabilistic statements about the distribution of $R(\mathbf{x})$.

[1] In random or Latin hypercube sampling (LHS), this weight is the reciprocal of the sample size (that is, $1/nK$) and can be used in estimating means, cumulative distribution functions, and other statistical properties. This weight is often referred to as the probability for each observation (that is, sample $\mathbf{x}_k$). However, this usage is not technically correct. If continuous distributions are involved, the actual probability of each observation is zero.

A single CCDF can be produced for each set $R(\mathbf{x}_k)$ of results shown in Equation 8, yielding a family of CCDFs of the form shown in Figure 6-3. The distribution of CCDFs in Figure 6-3 can be summarized with the mean and percentile curves shown in Figure 6-4. These curves result from connecting the mean and percentile values corresponding to individual consequence values on the abscissa of Figure 6-3. The percentile curves provide a probabilistic representation of the estimated exceedance probability given a fixed consequence value. For example, the probability is 0.8 that the exceedance probability for a particular normalized release is located between the 10 and 90 percentile curves.

To summarize, consideration of a family of CCDFs allows a distinction between stochastic uncertainty that controls the shape of a single CCDF and subjective uncertainty that results in a distribution of CCDFs. The stepwise shape of a single CCDF reflects aggregation of future events into similar groups. A family of CCDFs arises from imperfect knowledge of quantifiable properties, or, in other words, subjective uncertainty. The distribution arising from subjective uncertainty involves an infinite number of CCDFs; a family of CCDFs is a sample of finite size.

6.1.3 Regulatory Criteria for the Quantification of Risk

The representation for risk in Equation 2 provides a conceptual basis for the calculation of the CCDF for normalized releases specified in 40 CFR § 194.34(a). Further, this representation provides a structure that can be used for both the incorporation of uncertainties and the representation of the effects of uncertainties, as stated in 40 CFR § 194.34.

In 40 CFR § 194.34(b), the EPA states that "probability distributions for uncertain disposal system parameter values used in performance assessments shall be developed and documented in any compliance application." The treatment of uncertain parameter values in the performance assessment is discussed in Sections 6.1.4, 6.1.5, and 6.4. Further discussion of distributions assigned to uncertain parameter values is provided in Appendix PAR (Section PAR.2).

In 40 CFR § 194.34(c), the EPA states that documentation shall be provided of the computational techniques used to generate random samples. The sampling techniques used are discussed in Section 6.1.5.2. Sampled values are reproduced in tabular form in Appendix IRES (Section IRES.1).

In 40 CFR § 194.34(d), the EPA states that "the number of CCDFs generated shall be large enough such that, at cumulative releases of 1 and 10, the maximum CCDF generated exceeds the 99th percentile of the population of CCDFs with at least a 0.95 probability." The CCDFs resulting from this performance assessment are provided in Section 6.5, together with a demonstration that the total number of CCDFs is sufficiently large.

In 40 CFR § 194.34(e), the EPA states that "any compliance application shall display the full range of CCDFs generated." The full range of CCDFs generated is displayed in Section 6.5.

In 40 CFR § 194.34(f), the EPA states that "any compliance application shall provide information which demonstrates that there is at least a 95 percent level of confidence that the mean of the population of CCDFs meets the containment requirements . . . ." Section 6.5 contains a display of the mean CCDF and evidence demonstrating level of confidence.

6.1.4 Calculation of Risk

The methodology presented in Sections 6.1.1 and 6.1.2 is based on the work of Kaplan and Garrick (1981) and is one way to estimate the effects of uncertain but characterizable futures. In Kaplan and Garrick's procedure, the possible futures are defined as literal entities (S_i), and each is associated with a probability of occurrence (pS_i) and a consequence of occurrence ($\mathbf{cS}_i$). Preliminary performance assessments of the WIPP have used this procedure (for example, see Sandia National Laboratories 1991; 1992-1993, Vol. 1, Section 4), but definition of the futures S_i as discrete entities resulted in a great number of possible futures to be defined. The method of analysis used in preliminary performance assessments was called importance sampling.

For this performance assessment, an alternative method for calculating futures has been used that is based on developing futures by direct probabilistic sampling of the possible events leading to uncertain futures rather than a priori definition of possible futures. This modification from the calculational techniques of previous preliminary performance assessments is consistent with the fundamental concepts of Kaplan and Garrick and does not alter the results of the analysis. Both techniques will lead to the same CCDF. Adoption of this new procedure was prompted by two practical considerations. First, it is difficult to define futures as literal entities as required by importance sampling and to develop probabilities for each one. Second, generation of the futures by probabilistic methods allows for greater resolution in a CCDF, for equal effort, than the importance sampling procedure used in preliminary performance assessments.

The concept of a scenario is important in this performance assessment. There is a universe of possible futures, which is the set of all possible occurrences within the 10,000-year regulatory time frame. For analysis, this universe is divided into subsets of occurrences—scenarios—that are defined practically to include similar future occurrences. It should be noted that scenarios would not necessarily have to be defined as subsets of similar future occurrences, but by defining a scenario as a subset of similar futures, the DOE gains a practical advantage

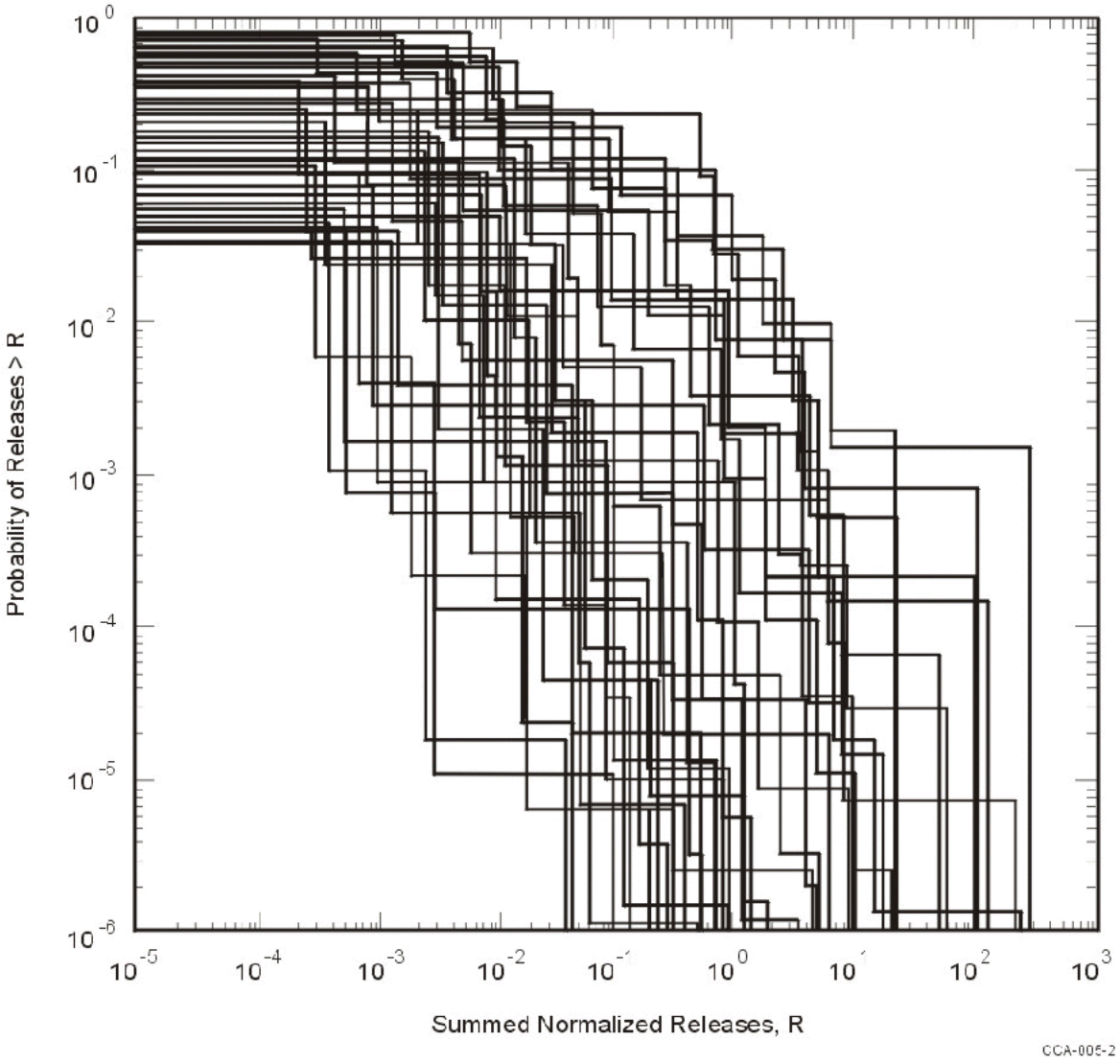

Figure 6-3. Example Distribution of a Family of CCDFs Obtained by Sampling Imprecisely Known Variables

1

1 **THIS PAGE INTENTIONALLY LEFT BLANK**

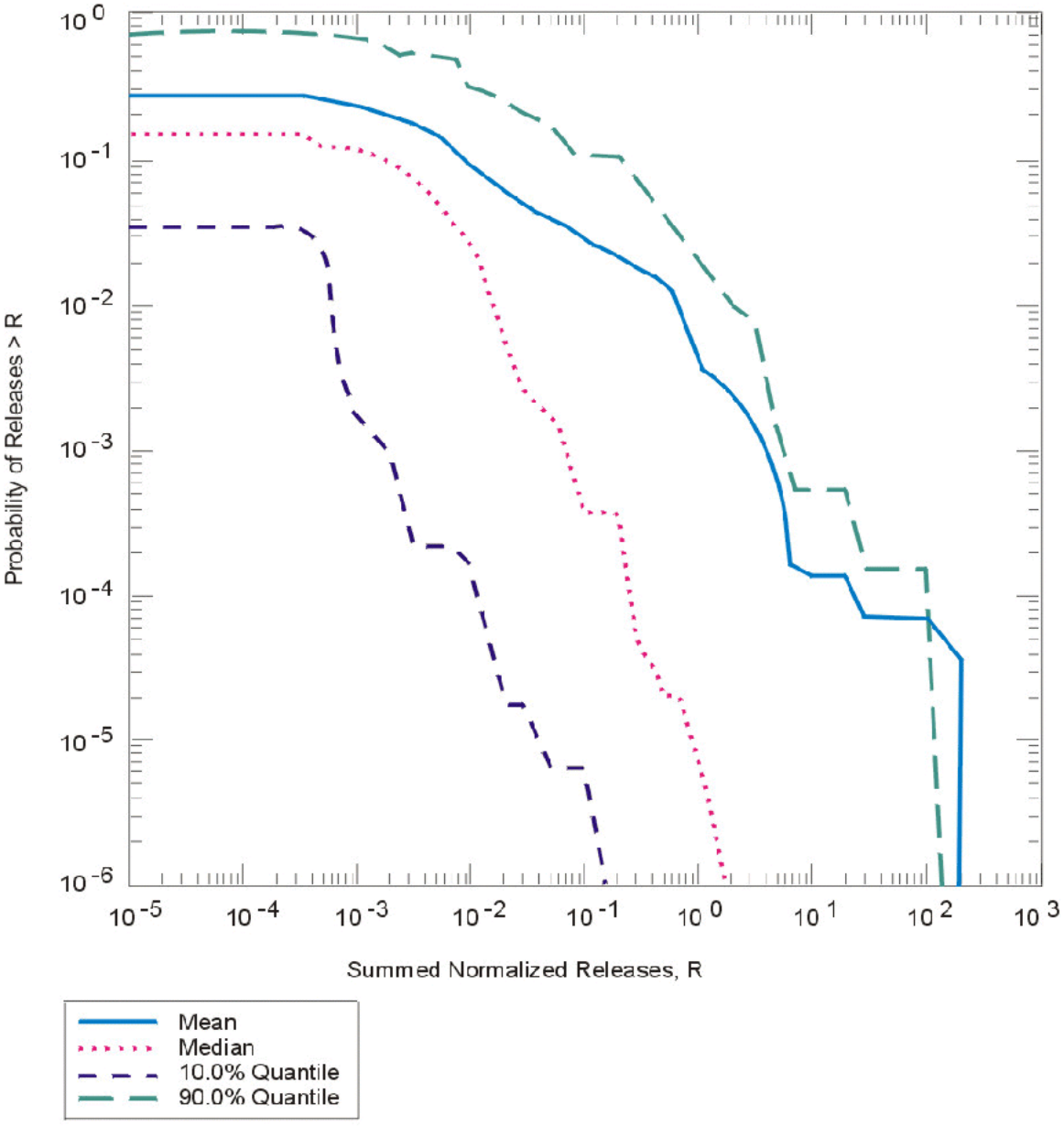

Note: The curves in this figure were obtained by calculating the mean and the indicated percentiles for each consequence value on the abscissa in Figure 6-3. The 90th-percentile curve crosses the mean curve because of highly skewed distributions for exceedance probability. This skew also results in the mean curve being above the median curve.

Figure 6-4. Example Summary Curves Derived from an Estimated Distribution of CCDFs

1 **THIS PAGE INTENTIONALLY LEFT BLANK**

because the consequences of futures falling within one scenario can be calculated with the same model configuration. Because the term scenario is defined simply as a subset of futures with similar occurrences, any size subset of similar futures can be called a scenario. In general, applying the term scenario for larger subsets of futures is useful in discussions of concepts; whereas, applying the term scenario for smaller subsets of futures is useful when constructing a CCDF.

The calculation of the probabilities and consequences of future occurrences begins with the determination of the sets S_i, which are the scenarios to be analyzed. Scenarios are determined through a formal process similar to that proposed by Cranwell et al. (1990, 5 – 10), and the process used in preliminary performance assessments for the WIPP. This process has four steps:

(1) FEPs (features, events, and processes) potentially relevant to the WIPP are identified and classified.

(2) Certain FEPs are eliminated according to well-defined screening criteria as not important or not relevant to the performance of the WIPP.

(3) Scenarios are formed from the remaining FEPs, in the context of regulatory performance criteria.

(4) Scenarios are specified for consequence analysis.

Through steps (1) and (2) of the scenario development process, the DOE identifies "all significant processes and events that may affect the disposal system" as required by 40 CFR § 191.13(a) and as further addressed in 40 CFR § 194.32. These steps are described in Section 6.2. The grouping of retained FEPs to form scenarios, and the specification of scenarios for consequence analysis, is presented in Section 6.3.

As discussed in Section 6.2, the DOE has developed a comprehensive initial list of FEPs for this performance assessment. This comprehensive initial list assures that the identification of significant processes and events is complete, that potential interactions between FEPs are not overlooked, and that responses to possible questions are available and well documented.

Once scenarios have been defined, a calculational methodology for evaluating their consequences must be developed. The calculational methodology must address stochastic uncertainty related to aggregation and stochastic variation, and subjective uncertainty because of, for example, measurement difficulties or incomplete data. The DOE uses a system of linked computer models to calculate scenario consequences cS_i. As discussed in Section 6.4, these computer models are based on conceptual models that describe the processes relevant to disposal system performance for the defined scenarios. These conceptual models are in turn based on site-specific experimental and observational data and the general scientific understanding of natural and engineered systems.

For practical purposes, the DOE separates the calculation of risk because of stochastic uncertainty, represented in an individual CCDF, from risk because of subjective uncertainty, which is represented by the family of CCDFs. This can be represented mathematically as a double integral of a function with the function representing the probability of exceedance associated with any particular consequence. The inner integral evaluates stochastic uncertainty, or the probability of exceedance associated with any particular consequence; the outer integral evaluates subjective uncertainty and leads to a distribution of exceedance probabilities for any given consequence value. Because of the complexity of this double integral for the WIPP, an analytical method for its solution is not available. Instead, the DOE approximates the solution of this double integral with a linked system of computer codes. In this computational framework, the performance assessment analysis can be thought of as a double sum, presented here in a stylized form for clarity,

(9)

Here, $F(x)$ is a procedure for estimating the normalized release to the accessible environment associated with each scenario that could occur at the WIPP site. The inner sum denoted with the subscript *st* is a probabilistic characterization of the uncertainty associated with parameters used to characterize stochastic uncertainty (the $\mathbf{x}_{st}$ and D_{st} in equations 4a and 6a, respectively). It is the evaluation of $F(x)$ through the inner sum that develops an individual CCDF, as shown in Figure 6-2. The outer sum denoted with the subscript *su* is a probabilistic characterization of the uncertainty associated with parameters used to characterize subjective uncertainty (the $\mathbf{x}_{su}$ and D_{su} in Equations 4b and 6b, respectively). It is the combined evaluation in the outer sum of the inner sum with $F(x)$ that develops the family of CCDFs, as shown in Figure 6-3.

A separate probabilistic analysis is required to evaluate each sum. Associated with each analysis are parameter distributions representing uncertainty (the D_{st} and D_{su} of Equations 6a and 6b). For example, associated with the inner sum may be uncertainty in the number and time of intrusion boreholes. The outer sum includes a probabilistic characterization of site properties, such as the permeability of specific rock types.

For the methodology adopted by the DOE for the evaluation of stochastic uncertainty in the inner sum, consequence calculations are required for model configurations with a set of fixed values for subjective parameters $\mathbf{x}_{su}$ taken from their distributions D_{su}, as well as for defined sequences and times of events associated with scenarios. These calculations are referred to in Section 6.4.11 and later sections as deterministic calculations (or deterministic futures). For the evaluation of stochastic uncertainty and construction of a CCDF, the consequences of futures generated probabilistically by random sampling (probabilistic futures) are evaluated in the context of these deterministic futures. This process is discussed in detail in Sections 6.4.12 and 6.4.13.

In certain cases, it may not be obvious whether a particular uncertainty should be classified as subjective or stochastic. For example, whether currently observed geologic properties persist

through time could be thought of as either subjective or stochastic uncertainty. For the WIPP, the DOE treats uncertainty associated with significant future human actions as stochastic (for example, drilling for natural resources), and uncertainty in disposal system properties that are subject to ongoing physical processes as subjective (for example, climate change or gas generation). In particular, the DOE's formal separation of the evaluation of stochastic uncertainty from subjective uncertainty into different probabilistic analyses allows clear understanding as to how any particular uncertainty is incorporated.

Once the scenarios have been determined and their consequences calculated using the appropriate conceptual and computational models, scenario probabilities must be determined for a CCDF to be constructed. This process is described in Section 6.4.12. CCDF construction is also described in Section 6.4.13.

6.1.5 Techniques for Probabilistic Analysis

Once scenarios have been defined, conceptual models defined, and the computational modeling system developed, the DOE uses probabilistic techniques to evaluate the double sum presented above. Monte Carlo analysis is the general name for the technique used for probabilistic analysis of the WIPP. Monte Carlo analyses can involve five steps: (1) selection of the variables to be examined and the ranges and distributions for their possible values, (2) generation of the samples to be analyzed, (3) propagation of the samples through the analysis, (4) uncertainty analysis, and (5) sensitivity analysis. These steps are described briefly in the following sections.

Within the general framework of Monte Carlo analysis, performance assessment uses two methods for generating the samples propagated through the model system. One method is used for the assessment of stochastic uncertainty, and another method is used for the characterization of subjective uncertainty. Each of these methods utilizes the five steps summarized in the preceding paragraph but differs in methodology in Steps 2 through 5.

6.1.5.1 Selection of Variables and Their Ranges and Distributions

Monte Carlo analyses use a probabilistic procedure for the selection of model input. Therefore, the first step in a Monte Carlo analysis is the selection of uncertain variables and the assignment of ranges and distributions that characterize them. These variables are typically input parameters to computer models, and the impact of the assigned ranges and distributions can be great; for a given set of conceptual and mathematical models, performance assessment results are largely controlled by the choice of input. Results of uncertainty and sensitivity analyses, in particular, strongly reflect the characterization of uncertainty in the input data.

Information about the ranges and distributions of possible values can be drawn from a variety of sources, including field data, laboratory data, and literature. In instances where sufficient data are not available, the documented solicitation of experts may be used. A review process leads from the available data to the construction of the distribution functions used in the

performance assessment to characterize uncertainty in input parameters. In part, this review process addresses the scaling of data collected at experimental scales of observation to the development of the parameter ranges applied to scales of interest in the disposal system. Because of the nature of the available data and the type of analysis, this review process unavoidably involves some judgment of the investigators and analysts involved. For this performance assessment, a discussion of parameter ranges developed by this process is provided in Appendix PAR (Sections PAR.1, PAR.2, and PAR.3). The QA procedures associated with this review process are identified in Section 5.1.4 and Appendix PAR (Section PAR.1).

The outcome of the review process is a cumulative distribution function (CDF) *D(x)* of the form shown in Figure 6-5 for each independent variable of interest. For a particular variable x_j, the function D is defined such that

$$prob(x < x_j \leq x+\Delta x) = D(x+\Delta x) - D(x) \; . \qquad (10)$$

That is, $D(x+\Delta x) - D(x)$ is equal to the probability that the appropriate value to use for x_j in the particular analysis under consideration falls between x and $x+\Delta x$.

6.1.5.2 Generation of the Sample

Various techniques are available for generating samples from the assigned distribution functions for the variables, including random sampling, stratified sampling, and Latin hypercube sampling (LHS). The DOE's performance assessment for WIPP uses random sampling and LHS.

Random sampling of the occurrence of possible future events is used to generate the possible futures (probabilistic futures) that comprise a CCDF. This sampling is used to select values of uncertain parameters associated with future human activities, or in other words, it is used to incorporate stochastic uncertainty into the WIPP performance assessment. This sampling is used for parameters evaluated in the inner sum of the double sum and included in the parameter set $\mathbf{x}_{st}$ with associated distributions D_{st}, as shown in Equations 4a and 6a, respectively. Generation of the futures comprising a CCDF by random sampling, rather than importance or stratified sampling as used in previous preliminary performance assessments, largely eliminates errors from aggregation.

LHS, in which the full range of each variable is subdivided into intervals of equal probability and samples are drawn from each interval, is used to select values of uncertain parameters associated with the physical system being simulated. In other words, LHS incorporates subjective uncertainty into the WIPP performance assessment. This sampling is used for

1

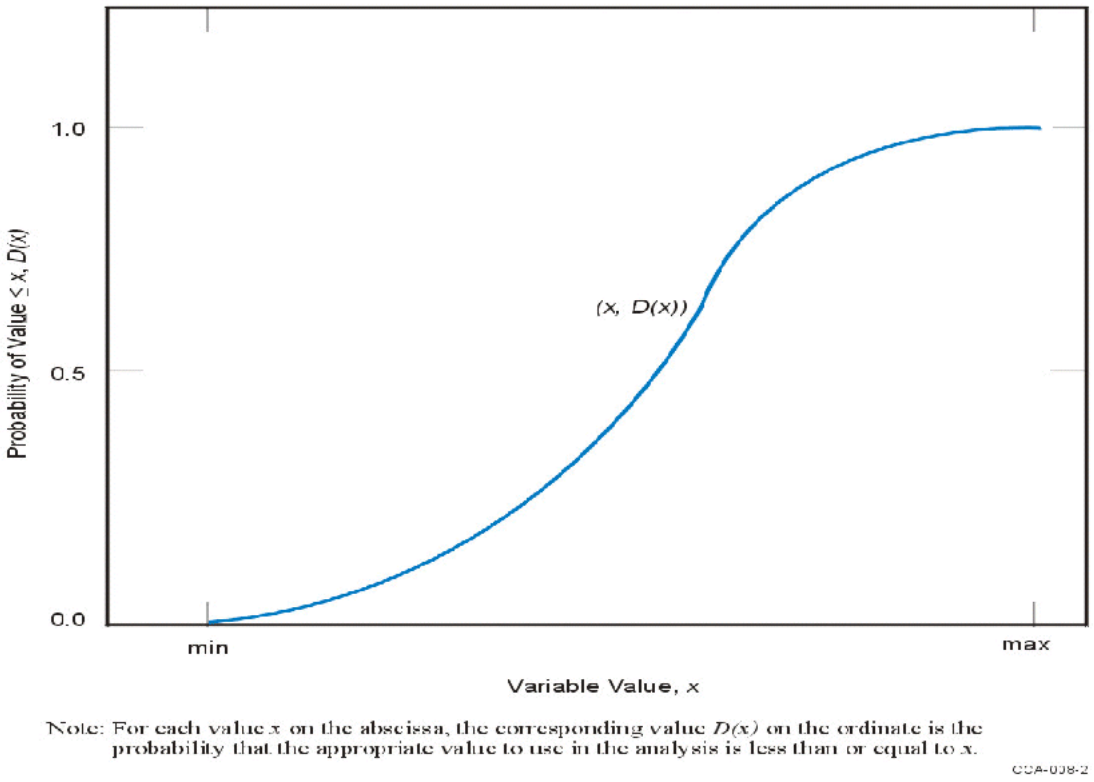

Note: For each value x on the abscissa, the corresponding value $D(x)$ on the ordinate is the probability that the appropriate value to use in the analysis is less than or equal to x.

CCA-038-2

Figure 6-5. Distribution Function for an Imprecisely Known Variable

1 **THIS PAGE INTENTIONALLY LEFT BLANK**

parameters that are evaluated in the outer sum of the double sum and are included in the parameter set $\mathbf{x}_{su}$ with associated distributions D_{su}, as shown in Equations 4b and 6b, respectively. The restricted pairing technique of Iman and Conover (1982, 314 – 319) is used to prevent spurious correlations within the sample.

6.1.5.3 Propagation of the Sample through the Analysis

The next step is the propagation of the sample through the analysis. Each element of the sample is supplied to the model system as input, and the corresponding model system predictions are saved for use in later uncertainty and sensitivity studies. The Software Configuration Management System (SCMS) has been developed to facilitate the complex calculations performed by the model system and to store the input and output files from each program.

6.1.5.4 Uncertainty Analysis

Uncertainty analyses evaluate uncertainty in performance estimates that results from uncertainty about imprecisely known input parameters. Once a sample has been generated and propagated through the modeling system, uncertainty in the outcome can be interpreted directly from the display of the results. For the WIPP performance assessment, stochastic uncertainty is represented by the shape of the individual CCDFs displayed in Section 6.5. Subjective uncertainty is represented by the family of CCDFs displayed in Section 6.5.

6.1.5.5 Sensitivity Analysis

Sensitivity analyses determine the contribution of individual input variables to the uncertainty in model predictions. This is the final step in a probabilistic study. Sensitivity analyses can identify those parameters for which reductions in uncertainty (that is, narrowing of the range of values from which the sample used in the Monte Carlo analysis is drawn) have the greatest potential to increase confidence in the estimate of the disposal system's performance. However, because results of these analyses are inherently conditional on the models, data distributions, and techniques used to generate them, the analyses cannot provide insight to the correctness of the conceptual models and data distributions used. Qualitative judgment about the modeling system must be used with sensitivity analyses to set priorities for performance assessment data acquisition and model development. Sensitivity analyses conducted as part of the WIPP performance assessment are described in Appendix SA.

6.2 Identification and Screening of Features, Events, and Processes

The EPA has provided criteria concerning the scope of performance assessments in 40 CFR § 194.32. In particular, criteria relating to the identification of potential processes and events that may affect the performance of the disposal system are provided in 40 CFR § 194.32(e), which states that

> Any compliance application(s) shall include information which:

> (1) Identifies all potential processes, events or sequences and combinations of processes and events that may occur during the regulatory time frame and may affect the disposal system;
>
> (2) Identifies the processes, events or sequences and combinations of processes and events included in performance assessments; and
>
> (3) Documents why any processes, events or sequences and combinations of processes and events identified pursuant to paragraph (e)(1) of this section were not included in performance assessment results provided in any compliance application.

This section and Appendix SCR fulfill these criteria by documenting DOE's identification, screening, and screening results of all potential processes and events consistent with the criteria specified in 40 CFR § 194.32(e).

As discussed in Section 6.1.4, the first two steps in scenario development involve the identification and screening of FEPs (features, events, and processes) potentially relevant to the performance of the disposal system. This section contains a discussion of the development of a comprehensive initial set of FEPs, the methodology and criteria used for screening, and a summary of the FEPs retained for scenario development. Detailed discussion of the basis for eliminating or retaining particular FEPs is provided in Appendix SCR. The formation of scenarios from retained FEPs is discussed in Section 6.3, and the specification of scenarios for consequence analysis is addressed in Section 6.4.12.

6.2.1 Identification of FEPs

The first step of the scenario development procedure is identification and classification of FEPs potentially relevant to the performance of the disposal system. Catalogs of FEPs have been developed in several national radioactive waste disposal programs as well as internationally. In constructing a comprehensive list of FEPs for the WIPP, the DOE drew on the work of these other radioactive waste disposal programs.

As a starting point, the DOE assembled a list of potentially relevant FEPs from the compilation developed by Stenhouse et al. (1993) for the Swedish Nuclear Power Inspectorate *Statens Kärnkraftinspektion* (SKI). The SKI list was based on a series of FEP lists developed for other disposal programs and is considered to be the best documented and most comprehensive starting point for the WIPP. For the SKI study, an initial raw FEP list was compiled based on nine different FEP identification studies (Table 6-2).

The compilers of the SKI list eliminated a number of FEPs as irrelevant to the particular disposal concept under consideration in Sweden; these FEPs were reinstated for the WIPP effort, and several FEPs on the SKI list were subdivided to facilitate screening for the WIPP. Finally, to ensure comprehensiveness, other FEPs specific to the WIPP were added based on review of key project documents and broad examination of the preliminary WIPP list by both project participants and stakeholders. The initial unedited list is contained in Attachment 1 of

Table 6-2. FEP Identification Studies Used in the SKI Study

Study	Country	Number of FEPS Identified
Atomic Energy of Canada Limited (AECL) study of disposal of spent fuel in crystalline rock (Goodwin et al. 1994)	Canada	275
SKI & Swedish Nuclear Fuel and Waste Management Company (SKB) study of disposal of spent fuel in crystalline rock (Andersson 1989)	Sweden	157
National Cooperative for the Storage of Radioactive Waste (NAGRA) Project Gewähr study (NAGRA 1985)	Switzerland	44
UK Department of the Environment Dry Run 3 study of deep disposal of low- and intermediate-level waste (L/ILW) (Thorne 1992)	United Kingdom	305
UK Department of Environment assessment of L/ILW disposal in volcanic rock at Sellafield (Miller and Chapman 1992)	United Kingdom	79
UK Nuclear Industry Radioactive Waste Executive (NIREX) study of the deep disposal of L/ILW (Hodgkinson and Sumerling 1989)	United Kingdom	131
SNL study of deep disposal of spent fuel (Cranwell et al. 1990)	United States	29
NEA Working Group on Systematic Approaches to Scenario Development (OECD 1992)	International	122
International Atomic Energy Agency (IAEA) Safety Series (IAEA 1981)	International	56

Appendix SCR. The initial unedited FEP list was restructured and revised to derive the comprehensive WIPP FEP list used in this application. The number of FEPs has been reduced to approximately 240 for this application to avoid the ambiguities caused by the use of a generic list. Restructuring the list for this application did not remove any substantive issues from the discussion. As discussed in more detail in Attachment 1 to Appendix SCR, the following steps have been used to derive the WIPP FEP list used in this application from the initial unedited list.

- References to subsystems have been eliminated because the SKI subsystem classification is not appropriate for the WIPP disposal concept. For example, in contrast to the Swedish disposal concept, canister integrity does not have a role in postoperational performance of the WIPP, and the terms near-field, far-field, and biosphere are not unequivocally defined for the WIPP site.

- Duplicate FEPs have been eliminated. Duplicate FEPs arose in the SKI list because individual FEPs could act in different subsystems. FEPs have a single entry in this application list whether they are applicable to several parts of the disposal system or to a single part only. For example, the FEP *Gas Effects: Disruption* appears in the seals,

backfill, waste, canister, and near-field subsystems in the initial FEP list. These FEPs are represented by the single FEP *Disruption Due to Gas Effects* for this application.

- FEPs that are not relevant to the WIPP design or inventory have been eliminated. Examples include FEPs related to high-level waste, copper canisters, and bentonite backfill.

- FEPs relating to engineering design changes have been eliminated because they are not relevant to a compliance application based on the DOE's design for the WIPP. Examples of such FEPs are *Design Modifications: Canister* and *Design Modification: Geometry*.

- FEPs relating to constructional, operational, and decommissioning errors have been eliminated. The DOE has administrative and quality control procedures to ensure that the facility will be constructed, operated, and decommissioned properly.

- Detailed FEPs relating to processes in the surface environment have been aggregated into a small number of generalized FEPs. For example, the SKI list includes the biosphere FEPs *Inhalation of Salt Particles, Smoking, Showers and Humidifiers*, *Inhalation and Biotic Material, Household Dust and Fumes, Deposition (wet and dry), Inhalation and Soils and Sediments, Inhalation and Gases and Vapors (indoor and outdoor)*, and *Suspension in Air*, which are represented by the FEP *Inhalation* in this application.

- FEPs relating to the containment of hazardous metals, volatile organic compounds (VOCs), and other chemicals that are not regulated by 40 CFR Part 191 are not included.

- A few FEPs have been renamed to be consistent with terms used to describe specific WIPP processes (for example, *Wicking*, *Brine Inflow*).

6.2.2 Criteria for Screening of FEPs and Categorization of Retained FEPs

The purpose of FEP screening is to identify those FEPs that should be accounted for in performance assessment calculations, and those FEPs that need not be considered further. The DOE's process of removing FEPs from consideration in performance assessment calculations involved the structured application of explicit screening criteria. The criteria used to screen out FEPs are explicit regulatory exclusions (SO-R), probability (SO-P), or consequence (SO-C). As discussed in Section 6.2.2.1, all three criteria are derived from regulatory requirements. FEPs not screened as SO-R, SO-P, or SO-C have been retained for inclusion in performance assessment calculations and are classified as undisturbed performance (UP) or disturbed performance (DP) FEPs. These screening criteria and FEP classifiers are discussed in this section, and FEP screening is discussed in Sections 6.2.3, 6.2.4, and 6.2.5.

6.2.2.1 Elimination of FEPs Based on Regulation (SO-R), Probability (SO-P), or Consequence (SO-C)

Regulation (SO-R). Specific FEP screening criteria are stated in 40 CFR Part 191 and 40 CFR Part 194. These screening criteria relating to the applicability of particular FEPs represent screening decisions made by the EPA. That is, in the process of developing and demonstrating the feasibility of the 40 CFR Part 191 standard and the 40 CFR Part 194 criteria, the EPA considered and made conclusions on the relevance, consequence, and/or probability of occurrence of particular FEPs and, in so doing, allowed for some FEPs to be eliminated from consideration. Section 6.2.5 describes the regulatory screening criteria that pertain to limitations on the type of human-initiated events and processes that need be analyzed.

Probability of occurrence of a FEP leading to significant release of radionuclides (SO-P). Low-probability events can be excluded on the basis of the criterion provided in 40 CFR § 194.32(d), which states that "performance assessments need not consider processes and events that have less than one chance in 10,000 of occurring over 10,000 years." In practice, for most FEPs screened out on the basis of low probability of occurrence, it has not been possible to estimate a meaningful quantitative probability. In the absence of quantitative probability estimates, a qualitative argument has been provided.

Potential consequences associated with the occurrence of the FEPs (SO-C). The DOE recognizes two uses for this criterion:

(1) FEPs can be eliminated from performance assessment calculations on the basis of insignificant consequence. Consequence can refer to effects on the repository or site or to radiological consequence. In particular, 40 CFR § 194.34(a) states that "The results of performance assessments shall be assembled into "complementary, cumulative distribution functions" (CCDFs) that represent the probability of exceeding various levels of cumulative release caused by all *significant* processes and events." (emphasis added). The DOE has omitted events and processes from performance assessment calculations where there is a reasonable expectation that the remaining probability distribution of cumulative releases would not be significantly changed by such omissions.

(2) FEPs that are potentially beneficial to subsystem performance may be eliminated from performance assessment calculations if necessary to simplify the analysis. This argument may be used when there is uncertainty as to exactly how the FEP should be incorporated into assessment calculations or when incorporation would incur unreasonable difficulties.

In some cases the effects of the occurrence of a particular event or process, although not necessarily insignificant, can be shown to lie within the range of uncertainty of another FEP already accounted for in the performance assessment calculations. In such cases the event or

process may be considered to be included in performance assessment calculations implicitly, within the range of uncertainty associated with the included FEP.

The distinctions between the SO-R, SO-P, and SO-C screening classifications are summarized in Figure 6-6. Although some FEPs could be eliminated from performance assessment calculations on the basis of more than one criterion, the most practical screening criterion was used for classification. In particular, a regulatory screening classification was used in preference to a probability or consequence screening classification, as illustrated in Figure 6-6. FEPs that have not been screened out based on any one of the three criteria are included in the performance assessment.

6.2.2.2 Undisturbed Performance (UP) FEPs

FEPs classified as UP are accounted for in calculations of undisturbed performance of the disposal system. Undisturbed performance is defined in 40 CFR § 191.12 as "the predicted behavior of a disposal system, including consideration of the uncertainties in predicted behavior, if the disposal system is not disrupted by human intrusion or the occurrence of unlikely natural events." The UP FEPs are accounted for in the performance assessment calculations to evaluate compliance with the Containment Requirements in 40 CFR § 191.13.

6.2.2.3 Disturbed Performance (DP) FEPs

FEPs classified as DP are accounted for only in assessment calculations for disturbed performance. As described in Appendix SCR (Sections SCR.3.1.3.2 and SCR.4), the DP FEPs that remain following the screening process relate to the potential disruptive effects of future drilling and mining events in the controlled area. Consideration of both DP and UP FEPs is required to evaluate compliance with 40 CFR § 191.13.

In the following sections, FEPs are discussed under the categories Natural FEPs, Waste- and Repository-Induced FEPs, and Human-Initiated Events and Processes (EPs).

This also allows an evaluation of compliance with the individual dose criterion in 40 CFR § 191.15 and the groundwater protection requirements in 40 CFR § 191.24 (see Chapter 8.0).

6.2.3 Natural FEPs

This subsection briefly discusses natural FEPs that have the potential to affect long-term performance of the WIPP disposal system. These FEPs and their screening classifications are listed in Table 6-3; the DOE's detailed screening arguments for natural FEPs are contained in Appendix SCR (Section SCR.1). This screening of natural FEPs fulfills, in conjunction with the performance assessment calculations, the criterion of the Future States Assumptions in

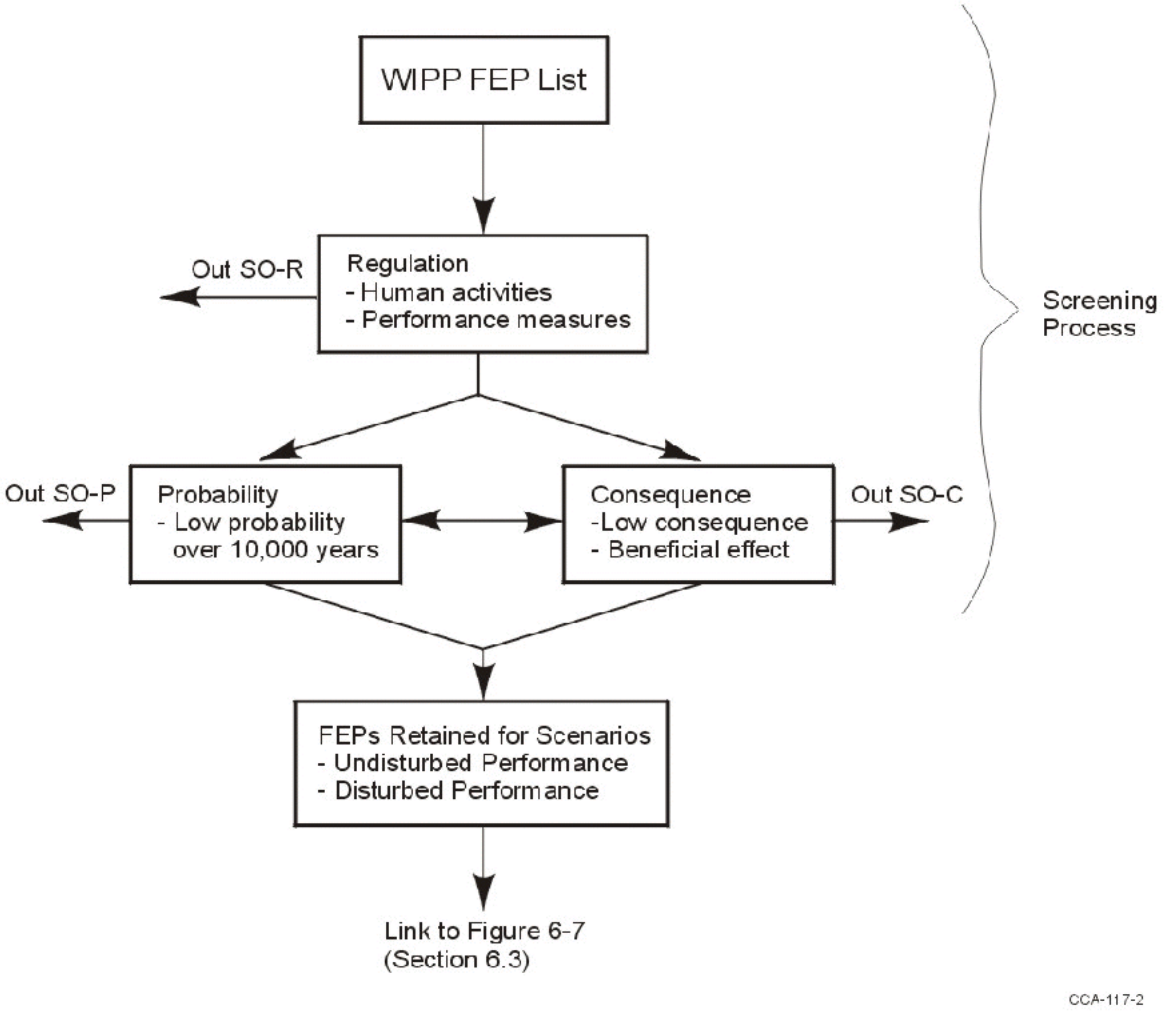

Figure 6-6. Screening Process Based on Screening Classifications

1

1 **THIS PAGE INTENTIONALLY LEFT BLANK**

Table 6-3. Natural FEPs and Their Screening Classifications

Features, Events, and Processes (FEPs)	Screening Classification	Comments	Appendix SCR Section
GEOLOGICAL FEPS			SCR.1.1
Stratigraphy			SCR.1.1.1
Stratigraphy	UP		
Brine reservoirs	DP		
Tectonics			SCR.1.1.2
Changes in regional stress	SO-C		
Regional tectonics	SO-C		
Regional uplift and subsidence	SO-C		
Structural FEPs			SCR.1.1.3
Deformation			SCR.1.1.3.1
Salt deformation	SO-P	UP near repository.	
Diapirism	SO-P		
Fracture development			SCR.1.1.3.2
Formation of fractures	SO-P	UP near repository.	
Changes in fracture properties	SO-C	UP near repository.	
Fault movement			SCR.1.1.3.3
Formation of new faults	SO-P		
Fault movement	SO-P		
Seismic activity			SCR.1.1.3.4
Seismic activity	UP		
Crustal processes			SCR.1.1.4
Igneous activity			SCR.1.1.4.1
Volcanic activity	SO-P		
Magmatic activity	SO-C		
Metamorphism			SCR.1.1.4.2
Metamorphic activity	SO-P		
Geochemical FEPs			SCR.1.1.5
Dissolution			SCR.1.1.5.1
Shallow dissolution	UP		
Lateral dissolution	SO-C		
Deep dissolution	SO-P		
Solution chimneys	SO-P		
Breccia pipes	SO-P		
Collapse breccias	SO-P		
Mineralization			SCR.1.1.5.2
Fracture infills	SO-C		
SUBSURFACE HYDROLOGICAL FEPS			SCR.1.2
Groundwater characteristics			SCR.1.2.1
Saturated groundwater flow	UP		
Unsaturated groundwater flow	UP	SO-C in Culebra.	
Fracture flow	UP		
Density effects on groundwater flow	SO-C		
Effects of preferential pathways	UP	UP in Salado and Culebra.	

Table 6-3. Natural FEPs and Their Screening Classifications (Continued)

Features, Events, and Processes (FEPs)	Screening Classification	Comments	Appendix SCR Section
Changes in groundwater flow			SCR.1.2.2
Thermal effects on groundwater flow	SO-C		
Saline intrusion	SO-P		
Freshwater intrusion	SO-P		
Hydrological response to earthquakes	SO-C		
Natural gas intrusion	SO-P		
SUBSURFACE GEOCHEMICAL FEPS			SCR.1.3
Groundwater geochemistry			SCR.1.3.1
Groundwater geochemistry	UP		
Changes in groundwater chemistry			SCR.1.3.2
Saline intrusion	SO-C		
Freshwater intrusion	SO-C		
Changes in groundwater Eh	SO-C		
Changes in groundwater pH	SO-C		
Effects of dissolution	SO-C		
GEOMORPHOLOGICAL FEPS			SCR.1.4
Physiography			SCR.1.4.1
Physiography	UP		
Meteorite impact			SCR.1.4.2
Impact of a large meteorite	SO-P		
Denudation			SCR.1.4.3
Weathering			SCR.1.4.3.1
Mechanical weathering	SO-C		
Chemical weathering	SO-C		
Erosion			SCR.1.4.3.2
Aeolian erosion	SO-C		
Fluvial erosion	SO-C		
Mass wasting	SO-C		
Sedimentation			SCR.1.4.3.3
Aeolian deposition	SO-C		
Fluvial deposition	SO-C		
Lacustrine deposition	SO-C		
Mass wasting	SO-C		
Soil development			SCR.1.4.4
Soil development	SO-C		
SURFACE HYDROLOGICAL FEPS			SCR.1.5
Fluvial			SCR.1.5.1
Stream and river flow	SO-C		
Lacustrine			SCR.1.5.2
Surface water bodies	SO-C		
Groundwater recharge and discharge			SCR.1.5.3
Groundwater discharge	UP		

Table 6-3. Natural FEPs and Their Screening Classifications (Continued)

Features, Events, and Processes (FEPs)	Screening Classification	Comments	Appendix SCR Section
Groundwater recharge	UP		
Infiltration	UP	UP for climate change effects.	
Changes in surface hydrology			SCR.1.5.4
Changes in groundwater recharge and discharge	UP		
Lake formation	SO-C		
River flooding	SO-C		
CLIMATIC FEPS			SCR.1.6
Climate			SCR.1.6.1
Precipitation (for example, rainfall)	UP		
Temperature	UP		
Climate change			SCR.1.6.2
Meteorological			SCR.1.6.2.1
Climate change	UP		
Glaciation			SCR.1.6.2.2
Glaciation	SO-P		
Permafrost	SO-P		
MARINE FEPS			SCR.1.7
Seas			SCR.1.7.1
Seas and oceans	SO-C		
Estuaries	SO-C		
Marine sedimentology			SCR.1.7.2
Coastal erosion	SO-C		
Marine sediment transport and deposition	SO-C		
Sea level changes			
Sea level changes	SO-C		SCR.1.7.3
ECOLOGICAL FEPS			SCR.1.8
Flora & fauna			SCR.1.8.1
Plants	SO-C		
Animals	SO-C		
Microbes	SO-C	UP for colloidal effects and gas generation	

Table 6-3. Natural FEPs and Their Screening Classifications (Continued)

Features, Events, and Processes (FEPs)	Screening Classification	Comments	Appendix SCR Section
Changes in flora & fauna			SCR.1.8.2
Natural ecological development	SO-C		

Legend:

UP	FEPs accounted for in the assessment calculations for undisturbed performance for 40 CFR § 191.13 (as well as 40 CFR § 191.15 and Subpart C of 40 CFR Part 191).
DP	FEPs accounted for (in addition to all UP FEPs) in the assessment calculations for disturbed performance for 40 CFR § 191.13.
SO-R	FEPs eliminated from performance assessment calculations on the basis of regulations provided in 40 CFR Part 191 and criteria provided in 40 CFR Part 194.
SO-C	FEPs eliminated from performance assessment (and compliance assessment) calculations on the basis of consequence.
SO-P	FEPs eliminated from performance assessment (and compliance assessment) calculations on the basis of low probability of occurrence.

40 CFR § 194.25(b) that the DOE shall "document in any compliance application, to the extent practicable, effects of potential future hydrogeologic, geologic and climatic conditions on the disposal system over the regulatory time frame."

Consistent with 40 CFR § 194.32(d), the DOE has screened out several natural FEPs from performance assessment calculations on the basis of a low probability of occurrence at or near the WIPP site. In particular, natural events for which there is no evidence indicating that they have occurred within the Delaware Basin have been screened on this basis. In this analysis, the probabilities of occurrence of these events are assumed to be zero. Quantitative, nonzero probabilities for such events, based on numbers of occurrences, cannot be ascribed without considering regions much larger than the Delaware Basin, thus neglecting established geological understanding of the events and processes that occur within particular geographical provinces. No disruptive natural FEPs are likely to occur during the regulatory time frame that could result in the creation of new pathways or significant alteration of existing pathways.

In considering the overall geological setting of the Delaware Basin, the DOE has eliminated many FEPs from performance assessment calculations on the basis of low consequence. Events and processes that have had little effect on the characteristics of the region in the past are expected to be of low consequence for the regulatory time period.

6.2.4 Waste- and Repository-Induced FEPs

The waste- and repository-induced FEPs are those that relate specifically to the waste material, waste containers, shaft seals, MgO backfill, panel closures, repository structures, and investigation boreholes. All FEPs related to radionuclide chemistry and radionuclide migration are included in this category. FEPs related to radionuclide transport resulting from future borehole intersections of the WIPP excavation are defined as waste- and repository-

induced FEPs. Waste- and repository-induced FEPs and their screening classification are listed in Table 6-4. The DOE's detailed screening discussions for these FEPs are contained in Appendix SCR (Section SCR.2).

The DOE has screened out many FEPs in this category on the basis of low consequence to the performance of the disposal system. For example, the DOE has shown that the heat generated by radioactive decay of the emplaced RH- and CH-TRU waste will not result in temperature increases sufficient to induce significant thermal convection, thermal stresses and strains, or thermally induced chemical perturbations within the disposal system (see Appendix SCR, Sections SCR.2.2.2 and SCR.2.5.7). Also, hydration of the emplaced concrete seals and chemical conditioner will be exothermic, but the DOE has shown that the heat generated will not have a significant effect on the performance of the disposal system (see Appendix SCR, Section SCR.2.5.7).

Other waste- and repository-induced FEPs have been eliminated from performance assessment calculations on the basis of beneficial effect to the performance of the disposal system, if necessary to simplify the analysis.

Waste- and repository-induced FEPs eliminated on the basis of low probability of occurrence over 10,000 years are generally those for which no mechanisms have been identified that could result in their occurrence within the disposal system. Such FEPs include explosions resulting from nuclear criticality, and the development of large-scale reduction-oxidation fronts.

6.2.5 Human-Initiated Events and Processes

Assessments of compliance with the Containment Requirements in 40 CFR § 191.13 require consideration of "all significant processes and events" including human-initiated EPs. These EPs and their screening classifications are listed in Table 6-5. The DOE's detailed screening arguments for human-initiated EPs are presented in Appendix SCR (Section SCR.3).

The scope of performance assessments is clarified with respect to human-initiated events and processes in 40 CFR § 194.32. At 40 CFR § 194.32(a) the EPA states that

> Performance assessments shall consider natural processes and events, mining, deep drilling, and shallow drilling that may affect the disposal system during the regulatory time frame.

Thus, performance assessments must include consideration of human-initiated EPs relating to mining and drilling activities that might take place during the regulatory time frame. In particular, performance assessments must consider the potential effects of such activities that might take place within the controlled area at a time when institutional controls cannot be assumed to completely eliminate the possibility of human intrusion.

Table 6-4. Waste- and Repository-Induced FEPs and Their Screening Classifications

Features, Events, and Processes (FEPs)	Screening Classification	Comments	Appendix SCR Section
WASTE AND REPOSITORY CHARACTERISTICS			SCR.2.1
Repository characteristics			SCR.2.1.1
Disposal geometry	UP		
Waste characteristics			SCR.2.1.2
Waste inventory	UP		
Heterogeneity of waste forms	DP		
Container characteristics			SCR.2.1.3
Container form	SO-C		
Container material inventory	UP		
Seal characteristics			SCR.2.1.4
Seal geometry	UP		
Seal physical properties	UP		
Seal chemical composition	SO-C	Beneficial SO-C	
Backfill characteristics			SCR.2.1.5
Backfill physical properties	SO-C		
Backfill chemical composition	UP		
Postclosure monitoring			SCR.2.1.6
Postclosure monitoring	SO-C		
RADIOLOGICAL FEPS			SCR.2.2
Radioactive decay			SCR.2.2.1
Radionuclide decay and ingrowth	UP		
Heat from radioactive decay			SCR.2.2.2
Heat from radioactive decay	SO-C		
Nuclear criticality			SCR.2.2.3
Nuclear criticality: heat	SO-P		
Radiological effects on material properties			SCR.2.2.4
Radiological effects on waste	SO-C		
Radiological effects on containers	SO-C		
Radiological effects on seals	SO-C		
GEOLOGICAL AND MECHANICAL FEPS			SCR.2.3
Excavation-induced fracturing			SCR.2.3.1
Disturbed rock zone	UP		
Excavation-induced changes in stress	UP		
Rock creep			SCR.2.3.2
Salt creep	UP		
Changes in the stress field	UP		
Roof falls			SCR.2.3.3
Roof falls	UP		
Subsidence			SCR.2.3.4
Subsidence	SO-C		
Large scale rock fracturing	SO-P		

Table 6-4. Waste- and Repository-Induced FEPs and Their Screening Classifications (Continued)

Features, Events, and Processes (FEPs)	Screening Classification	Comments	Appendix SCR Section
Effects of fluid pressure changes			SCR.2.3.5
Disruption due to gas effects	UP		
Pressurization	UP		
Effects of explosions			SCR.2.3.6
Gas explosions	UP		
Nuclear explosions	SO-P		
Thermal effects			SCR.2.3.7
Thermal effects on material properties	SO-C		
Thermally-induced stress changes	SO-C		
Differing thermal expansion of repository components	SO-C		
Mechanical effects on material properties			SCR.2.3.8
Consolidation of waste	UP		
Movement of containers	SO-C		
Container integrity	SO-C	Beneficial SO-C	
Mechanical effects of backfill	SO-C		
Consolidation of seals	UP		
Mechanical degradation of seals	UP		
Investigation boreholes	SO-C		
Underground boreholes	UP		
SUBSURFACE HYDROLOGICAL AND FLUID DYNAMICAL FEPS			SCR.2.4
Repository-induced flow			SCR.2.4.1
Brine inflow	UP		
Wicking	UP		
Effects of gas generation			SCR.2.4.2
Fluid flow due to gas production	UP		
Thermal effects			SCR.2.4.3
Convection	SO-C		
GEOCHEMICAL AND CHEMICAL FEPS			SCR.2.5
Gas generation			SCR.2.5.1
Microbial gas generation			SCR.2.5.1.1
Degradation of organic material	UP		
Effects of temperature on microbial gas generation	UP		
Effects of pressure on microbial gas generation	SO-C		
Effects of radiation on microbial gas generation	SO-C		
Effects of biofilms on microbial gas generation	UP		

Table 6-4. Waste- and Repository-Induced FEPs and Their Screening Classifications (Continued)

Features, Events, and Processes (FEPs)	Screening Classification	Comments	Appendix SCR Section
Corrosion			SCR.2.5.1.2
Gases from metal corrosion	UP		
Galvanic coupling	SO-P		
Chemical effects of corrosion	UP		
Radiolytic gas generation			SCR.2.5.1.3
Radiolysis of brine	SO-C		
Radiolysis of cellulose	SO-C		
Helium gas production	SO-C		
Radioactive gases	SO-C		
Chemical speciation			SCR.2.5.2
Speciation	UP	UP in disposal rooms and Culebra. SO-C elsewhere, and beneficial SO-C in cementitious seals.	
Kinetics of speciation	SO-C		
Precipitation and dissolution			SCR.2.5.3
Dissolution of waste	UP		
Precipitation	SO-C	Beneficial SO-C	
Kinetics of precipitation and dissolution	SO-C	Kinetics of waste dissolution is a beneficial SO-C	
Sorption			SCR.2.5.4
Actinide sorption	UP	UP in the Culebra and Dewey Lake. Beneficial SO-C elsewhere	
Kinetics of sorption	UP		
Changes in sorptive surfaces	UP		
Reduction-oxidation chemistry			SCR.2.5.5
Effect of metal corrosion	UP		
Reduction-oxidation fronts	SO-P		
Reduction-oxidation kinetics	UP		
Localized reducing zones	SO-C		
Organic complexation			SCR.2.5.6
Organic complexation	SO-C		
Organic ligands	SO-C		
Humic and fulvic acids	UP		
Kinetics of organic complexation	SO-C		
Exothermic reactions			SCR.2.5.7
Exothermic reactions	SO-C		
Concrete hydration	SO-C		
Chemical effects on material properties			SCR.2.5.8
Chemical degradation of seals	UP		
Chemical degradation of backfill	SO-C		

Table 6-4. Waste- and Repository-Induced FEPs and Their Screening Classifications (Continued)

Features, Events, and Processes (FEPs)	Screening Classification	Comments	Appendix SCR Section
Microbial growth on concrete	UP		
CONTAMINANT TRANSPORT MODE FEPS			SCR.2.6
Solute transport			SCR.2.6.1
Solute transport	UP		
Colloid transport			SCR.2.6.2
Colloid transport	UP		
Colloid formation and stability	UP		
Colloid filtration	UP		
Colloid sorption	UP		
Particulate transport			SCR.2.6.3
Suspensions of particles	DP	SO-C for undisturbed conditions	
Rinse	SO-C		
Cuttings	DP	Repository intrusion only	
Cavings	DP	Repository intrusion only	
Spallings	DP	Repository intrusion only	
Microbial transport			SCR.2.6.4
Microbial transport	UP		
Biofilms	SO-C	Beneficial SO-C	
Gas transport			SCR.2.6.5
Transport of radioactive gases	SO-C		
CONTAMINANT TRANSPORT PROCESSES			SCR.2.7
Advection			SCR.2.7.1
Advection	UP		
Diffusion			SCR.2.7.2
Diffusion	UP		
Matrix diffusion	UP		
Thermochemical transport phenomena			SCR.2.7.3
Soret effect	SO-C		
Electrochemical transport phenomena			SCR.2.7.4
Electrochemical effects	SO-C		
Galvanic coupling	SO-P		
Electrophoresis	SO-C		
Physicochemical transport phenomena			SCR.2.7.5
Chemical gradients	SO-C		
Osmotic processes	SO-C	Beneficial SO-C	
Alpha recoil	SO-C		
Enhanced diffusion	SO-C		

Table 6-4. Waste- and Repository-Induced FEPs and Their Screening Classifications (Continued)

Features, Events, and Processes (FEPs)	Screening Classification	Comments	Appendix SCR Section
ECOLOGICAL FEPS			SCR.2.8
Plant, animal, and soil uptake			SCR.2.8.1
Plant uptake	SO-R	SO-C for 40 CFR § 191.15	
Animal uptake	SO-R		
Accumulation in soils	SO-C	Beneficial SO-C	
Human uptake			SCR.2.8.2
Ingestion	SO-R	SO-C for 40 CFR § 191.15	
Inhalation	SO-R	SO-C for 40 CFR § 191.15	
Irradiation	SO-R	SO-C for 40 CFR § 191.15	
Dermal sorption	SO-R	SO-C for 40 CFR § 191.15	
Injection	SO-R	SO-C for 40 CFR § 191.15	

Legend:

UP FEPs accounted for in the assessment calculations for undisturbed performance for 40 CFR § 191.13 (as well as 40 CFR § 191.15 and Subpart C of 40 CFR Part 191).

DP FEPs accounted for (in addition to all UP FEPs) in the assessment calculations for disturbed performance for 40 CFR § 191.13.

SO-R FEPs eliminated from performance assessment calculations on the basis of regulations provided in 40 CFR Part 191 and criteria provided in 40 CFR Part 194.

SO-C FEPs eliminated from performance assessment (and compliance assessment) calculations on the basis of consequence.

SO-P FEPs eliminated from performance assessment (and compliance assessment) calculations on the basis of low probability of occurrence.

Further criteria concerning the scope of performance assessments are provided at 40 CFR § 194.32(c):

> Performance assessments shall include an analysis of the effects on the disposal system of any activities that occur in the vicinity of the disposal system prior to disposal and are expected to occur in the vicinity of the disposal system soon after disposal. Such activities shall include, but shall not be limited to, existing boreholes and the development of any existing leases that can be reasonably expected to be developed in the near future, including boreholes and leases that may be used for fluid injection activities.

Table 6-5. Human-Initiated EPs and Their Screening Classifications

Events and Processes (EPs)	Screening Classification Historical/ Ongoing/ Near Future	Future	Comments	Appendix SCR Section
GEOLOGICAL EPs				SCR.3.2
Drilling			DP for boreholes that penetrate the waste and boreholes that penetrate Castile brine underlying the waste disposal region. SO-C for other future drilling.	SCR.3.2.1
Oil and gas exploration	SO-C	DP		
Potash exploration	SO-C	DP		
Water resources exploration	SO-C	SO-C		
Oil and gas exploitation	SO-C	DP		
Groundwater exploitation	SO-C	SO-C		
Archeological investigations	SO-R	SO-R		
Geothermal	SO-R	SO-R		
Other resources	SO-C	DP		
Enhanced oil and gas recovery	SO-C	DP		
Liquid waste disposal	SO-R	SO-R		
Hydrocarbon storage	SO-R	SO-R		
Deliberate drilling intrusion	SO-R	SO-R		
Excavation activities				SCR.3.2.2
Potash mining	UP	DP	UP for mining outside the controlled area. DP for mining inside the controlled area.	
Other resources	SO-C	SO-R		
Tunneling	SO-R	SO-R		
Construction of underground facilities (for example storage, disposal, accommodation)	SO-R	SO-R		
Archeological excavations	SO-C	SO-R		
Deliberate mining intrusion	SO-R	SO-R		
Subsurface explosions				SCR.3.2.3
Resource recovery				SCR.3.2.3.1
Explosions for resource recovery	SO-C	SO-R		
Underground nuclear device testing				SCR.3.2.3.2
Underground nuclear device testing	SO-C	SO-R		

Table 6-5. Human-Initiated EPs and Their Screening Classifications (Continued)

Events and Processes (EPs)	Screening Classification Historical/ Ongoing/ Near Future	Future	Comments	Appendix SCR Section
SUBSURFACE HYDROLOGICAL AND GEOCHEMICAL EPs				SCR.3.3
Borehole fluid flow				SCR.3.3.1
Drilling-induced flow				SCR.3.3.1.1
Drilling fluid flow	SO-C	DP	DP for boreholes that penetrate the waste. SO-C for other future drilling.	
Drilling fluid loss	SO-C	DP	DP for boreholes that penetrate the waste, SO-C for other future drilling	
Blowouts	SO-C	DP	DP for boreholes that penetrate the waste and boreholes that penetrate Castile brine underlying the waste disposal region. SO-C for other future drilling.	
Drilling-induced geochemical changes	UP	DP	SO-C for units other than the Culebra.	
Fluid extraction				SCR.3.3.1.2
Oil and gas extraction	SO-C	SO-R		
Groundwater extraction	SO-C	SO-R		
Fluid injection				SCR.3.3.1.3
Liquid waste disposal	SO-C	SO-R		
Enhanced oil and gas production	SO-C	SO-R		
Hydrocarbon storage	SO-C	SO-R		
Fluid-injection induced geochemical changes	UP	SO-R	SO-C for units other than the Culebra	
Flow through abandoned boreholes			Classification distinguishes the time when drilling occurs.	SCR.3.3.1.4
Natural borehole fluid flow	SO-C	DP	DP for boreholes that penetrate Castile brine underlying the waste disposal region. SO-C for other future boreholes.	
Waste-induced borehole flow	SO-R	DP	DP for boreholes that penetrate the waste. SO-C for other future boreholes.	

Table 6-5. Human-Initiated EPs and Their Screening Classifications (Continued)

Events and Processes (EPs)	Screening Classification Historical/ Ongoing/ Near Future	Future	Comments	Appendix SCR Section
Flow through undetected boreholes	SO-P	NA		
Borehole-induced solution and subsidence	SO-C	SO-C		
Borehole-induced mineralization	SO-C	SO-C		
Borehole-induced geochemical changes	UP	DP	SO-C for units other than the Culebra	
Excavation-induced flow			Classification distinguishes the time when excavation occurs.	SCR.3.3.2
Changes in groundwater flow due to mining	UP	DP	UP for mining outside the controlled area. DP for mining inside the controlled area.	
Changes in geochemistry due to mining	SO-C	SO-R		
Explosion-induced flow				SCR.3.3.3
Changes in groundwater flow due to explosions	SO-C	SO-R		
GEOMORPHOLOGICAL EPs				SCR.3.4
Land use and disturbances				SCR.3.4.1
Land use changes	SO-R	SO-R		
Surface disruptions	SO-C	SO-R		
SURFACE HYDROLOGICAL EPs				SCR.3.5
Water control and use				SCR.3.5.1
Damming of streams or rivers	SO-C	SO-R		
Reservoirs	SO-C	SO-R		
Irrigation	SO-C	SO-R		
Lake usage	SO-R	SO-R		
Altered soil or surface water chemistry by human activities	SO-C	SO-R		
CLIMATIC EPs				SCR.3.6
Anthropogenic climate change				SCR.3.6.1
Greenhouse gas effects	SO-R	SO-R		
Acid rain	SO-R	SO-R		
Damage to the ozone layer	SO-R	SO-R		

Table 6-5. Human-Initiated EPs and Their Screening Classifications (Continued)

Events and Processes (EPs)	Screening Classification Historical/ Ongoing/ Near Future	Future	Comments	Appendix SCR Section
MARINE EPs				SCR.3.7
Marine activities				SCR.3.7.1
Coastal water use	SO-R	SO-R		
Sea water use	SO-R	SO-R		
Estuarine water use	SO-R	SO-R		
ECOLOGICAL EPs				SCR.3.8
Agricultural activities				SCR.3.8.1
Arable farming	SO-C	SO-R		
Ranching	SO-C	SO-R		
Fish farming	SO-R	SO-R		
Social and technological developments				SCR.3.8.2
Demographic change and urban development	SO-R	SO-R		
Loss of records	NA	DP		

Legend:

UP	FEPs accounted for in the assessment calculations for undisturbed performance for 40 CFR § 191.13 (as well as 40 CFR § 191.15 and Subpart C of 40 CFR Part 191).
DP	FEPs accounted for (in addition to all UP FEPs) in the assessment calculations for disturbed performance for 40 CFR § 191.13.
SO-R	FEPs eliminated from performance assessment calculations on the basis of regulations provided in 40 CFR Part 191 and criteria provided in 40 CFR Part 194.
SO-C	FEPs eliminated from performance assessment (and compliance assessment) calculations on the basis of consequence.
SO-P	FEPs eliminated from performance assessment (and compliance assessment) calculations on the basis of low probability of occurrence.
NA	FEPs not applicable to the particular category.

Performance assessments must include consideration of all human-initiated EPs relating to activities that have taken place or are reasonably expected to take place outside the controlled area in the near future.

In order to implement the criteria in 40 CFR § 194.32, relating to the scope of performance assessments, the DOE has divided human activities into three categories. Distinctions are made between (1) human activities that are currently taking place and those that took place prior to the time of the compliance application, (2) human activities that might be initiated in the near future after submission of the compliance application, and (3) human activities that might be initiated after repository closure. The first two categories of EPs are considered

under undisturbed performance, and EPs in the third category lead to disturbed performance conditions.

(1) Historical and current human activities include resource extraction activities that have historically taken place and are currently taking place outside the controlled area. These activities are of potential significance insofar as they could affect the geological, hydrological, or geochemical characteristics of the disposal system or groundwater flow pathways outside the disposal system. Current human activities taking place within the controlled area are essentially those associated with development of the WIPP repository. Historical activities include existing boreholes.

(2) Near-future human activities include resource extraction activities that may be expected to occur outside the controlled area based on existing plans and leases. Thus, the near future includes the expected lives of existing mines and oil and gas fields, and the expected lives of new mines and oil and gas fields that the DOE expects will be developed based on existing plans and leases. These activities are of potential significance insofar as they could affect the geological, hydrological, or geochemical characteristics of the disposal system or groundwater flow pathways outside the disposal system. The only human activities that are expected to occur within the controlled area in the near future are those associated with development of the WIPP repository. The DOE assumes that any activity that is expected to be initiated in the near future, based on existing plans and leases, will be initiated prior to repository closure. Activities initiated prior to repository closure are assumed to continue until their completion.

(3) Future human activities include activities that might be initiated within or outside the controlled area after repository closure. This includes drilling and mining for resources within the disposal system at a time when institutional controls cannot be assumed to completely eliminate the possibility of such activities. Future human activities could influence the transport of contaminants within and outside the disposal system by directly removing waste from the disposal system or altering the geological, hydrological, or geochemical characteristics of the disposal system.

In order to satisfy the criteria in 40 CFR § 194.32, performance assessments must consider the potential effects of historical, current, near-future, and future human activities on the performance of the disposal system. The criterion in 40 CFR § 194.25(a) concerned with predictions of the future states of society requires that performance assessments and compliance assessments "shall assume that the characteristics of the future remain what they are at the time the compliance application is prepared." This criterion has been applied to eliminate the following human-initiated EPs from performance assessment calculations:

- drilling associated with geothermal energy production, liquid waste disposal, hydrocarbon storage, and archeological investigations (Appendix SCR, Sections SCR.3.2.1.1 and SCR.3.2.1.2),

- excavation activities associated with tunneling and construction of underground facilities (for example, storage, disposal, and accommodation) (Appendix SCR, Sections SCR.3.2.2.1 and SCR.3.2.2.2),

- changes in land use (Appendix SCR, Section SCR.3.4.1.2),

- anthropogenic climate change (Appendix SCR, Section SCR.3.6.1),

- changes in agricultural practices (Appendix SCR, Section SCR.3.8.1.2),

- demographic change, urban developments, and technological developments (Appendix SCR, Section SCR.3.8.2).

As discussed in Chapter 8.0, compliance assessments (to determine compliance with 40 CFR § 191.15 and Subpart C of 40 CFR Part 191) need consider the undisturbed performance of the disposal system.

6.2.5.1 Historical, Current, and Near-Future Human Activities

The observational data obtained as part of WIPP site characterization reflect any effects of historical and current human activities in the vicinity of the WIPP, such as groundwater extraction and oil and gas production. As discussed in Appendix SCR (Section SCR.3), historic and current human activities are modeled or found to be of low consequence to long-term performance.

Historical, current, and near-future human activities could affect WIPP site characteristics subsequent to the submission of this application, and could influence the performance of the disposal system. The hydrogeological impacts of historical, current and near-future potash mining outside the controlled area are accounted for in calculations of the undisturbed performance of the disposal system. Near-future potash mining is assumed to continue for the expected economic life of each mine. The potential consequences to the performance of the disposal system of other human-initiated EPs expected to occur in the Delaware Basin in the near future are discussed in Appendix SCR (Section SCR.3), which describes how these EPs are eliminated on the basis of low consequence.

6.2.5.2 Future Human Activities

Performance assessments (but not compliance assessments, as discussed in Chapter 8.0) must consider the effects of future human activities on the performance of the disposal system. The EPA has provided criteria relating to future human activities in 40 CFR § 194.32(a), which limits the scope of consideration of future human actions in performance assessments to mining and drilling.

Criteria concerning future mining: The EPA provides additional criteria concerning the type of future mining that should be considered by the DOE in 40 CFR § 194.32(b):

> Assessments of mining effects may be limited to changes in the hydraulic conductivity of the hydrogeologic units of the disposal system from excavation mining for natural resources. Mining shall be assumed to occur with a one in 100 probability in each century of the regulatory time frame. Performance assessments shall assume that mineral deposits of those resources, similar in quality and type to those resources currently extracted from the Delaware Basin, will be completely removed from the controlled area during the century in which such mining is randomly calculated to occur. Complete removal of such mineral resources shall be assumed to occur only once during the regulatory time frame.

Thus, consideration of future mining may be limited to mining within the controlled area at the locations of resources that are similar in quality and type to those currently extracted from the Delaware Basin. Potash is the only resource that has been identified within the controlled area in quality similar to that currently mined from underground deposits elsewhere in the Delaware Basin. Within the controlled area, the McNutt of the Salado provides the only potash of appropriate quality. The hydrogeological impacts of future potash mining within the controlled area are accounted for in calculations of the disturbed performance of the disposal system. Consistent with 40 CFR § 194.32(b), all economically recoverable resources in the vicinity of the disposal system (outside the controlled area) are assumed to be extracted in the near future.

Criteria concerning future drilling: With respect to consideration of future drilling, in the preamble to 40 CFR Part 194, the EPA "reasoned that while the resources drilled for today may not be the same as those drilled for in the future, the present rates at which these boreholes are drilled can nonetheless provide an estimate of the future rate at which boreholes will be drilled." Criteria concerning the consideration of future deep and shallow drilling[2] in performance assessments are provided in 40 CFR § 194.33. These criteria require that, to calculate future drilling rates, the DOE should examine the historical rate of drilling for resources in the Delaware Basin. Historical drilling for purposes other than resource exploration and recovery (such as WIPP site investigation) need not be considered in determining future drilling rates.

In particular, in calculating the frequency of future deep drilling, 40 CFR § 194.33(b)(3)(i) states that the DOE should

> Identify deep drilling that has occurred for each resource in the Delaware Basin over the past 100 years prior to the time at which a compliance application is prepared.

Oil and gas are the only known resources below 2,150 feet (655 meters) that have been exploited over the past 100 years in the Delaware Basin. However, some potash and sulfur exploration boreholes have been drilled in the Delaware Basin to depths in excess of 2,150 feet (655 meters) below the surface relative to where the drilling occurred. Thus, consistent with 40 CFR § 194.33(b)(3)(i), the DOE has used the historical record of deep

[2] The EPA has defined two types of drilling in 40 CFR § 194.2: deep drilling is defined as "drilling events in the Delaware Basin that reach or exceed a depth of 2,150 feet below the surface relative to where such drilling occurred"; shallow drilling is defined as "drilling events in the Delaware Basin that do not reach a depth of 2,150 feet below the surface relative to where such drilling occurred."

drilling associated with oil, gas, potash and sulfur exploration, and oil and gas exploitation in the Delaware Basin in calculations to determine the rate of deep drilling within the controlled area and throughout the basin in the future, as discussed in Appendix DEL, Section DEL.7.4 (see also Table DEL-6). Deep drilling may occur within the controlled area after the end of the period of active institutional control (100 years after disposal).

In calculating the frequency of future shallow drilling, 40 CFR § 194.33(b)(4)(i) states that the DOE should

> Identify shallow drilling that has occurred for each resource in the Delaware Basin over the past 100 years prior to the time at which a compliance application is prepared.

An additional criterion with respect to the calculation of future shallow drilling rates is provided in 40 CFR § 194.33(b)(4)(iii):

> In considering the historical rate of all shallow drilling, the Department may, if justified, consider only the historical rate of shallow drilling for resources of similar type and quality to those in the controlled area.

As an example of the use of the criterion in 40 CFR § 194.33(b)(4)(iii) the EPA states in the preamble to 40 CFR Part 194 that "if only non-potable water can be found within the controlled area, then the rate of drilling for water may be set equal to the historical rate of drilling for non-potable water in the Delaware Basin over the past 100 years." Thus, the DOE may limit the rate of future shallow drilling based on a determination of the potential resources in the controlled area. Shallow drilling associated with water, potash, sulfur, oil, and gas extraction has taken place in the Delaware Basin over the past 100 years. However, of these resources, only water and potash are present at shallow depths (less than 2,150 feet [655 meters] below the surface) within the controlled area. Thus, consistent with 40 CFR § 194.33(b)(4), the DOE has used the historical record of shallow drilling associated with water and potash extraction in the Delaware Basin in calculations to determine the rate of shallow drilling within the controlled area, as discussed in Appendix DEL (Sections DEL.7.2 and DEL.7.4).

The EPA also provides a criterion in 40 CFR § 194.33(d) concerning the use of future boreholes subsequent to drilling:

> With respect to future drilling events, performance assessments need not analyze the effects of techniques used for resource recovery subsequent to the drilling of the borehole.

Thus, performance assessments need not consider the effects of techniques used for resource extraction and recovery, that would occur subsequent to the drilling of a borehole in the future.

The EPA provides an additional criterion that limits the severity of human intrusion scenarios that must be considered in performance assessments. In 40 CFR § 194.33(b)(1) the EPA states that

> Inadvertent and intermittent intrusion by drilling for resources (other than those resources provided by the waste in the disposal system or engineered barriers designed to isolate such waste) is the most severe human intrusion scenario.

Thus, human intrusion scenarios involving deliberate intrusion need not be considered in performance assessments.

Screening of future human-initiated EPs: Future human-initiated EPs accounted for in performance assessment calculations for the WIPP are those associated with mining and deep drilling within the controlled area at a time when institutional controls cannot be assumed to eliminate completely the possibility of such activities. All other future human-initiated EPs, if not eliminated from performance assessment calculations based on regulation, have been eliminated based on low consequence or low probability. For example, the effects of future shallow drilling within the controlled area have been eliminated from performance assessment calculations on the basis of low consequence to the performance of the disposal system. These screening decisions are listed in Table 6-5 and are discussed in Appendix SCR (Section SCR.3).

6.3 Scenario Development and Selection

This section addresses the formation of scenarios from FEPs that have been retained for performance assessment calculations, and introduces the specification of scenarios for consequence analysis. Specification of probabilities associated with scenarios is discussed in Section 6.4.12.

Logic diagrams are used to illustrate the formation of scenarios for consequence analysis from combinations of FEPs that remain after FEP screening (Cranwell et al. 1990) (Figure 6-7). Each scenario shown in Figure 6-7 is defined by a combination of occurrence and nonoccurrence of all potentially disruptive EPs. Disruptive EPs are defined as those EPs that result in the creation of new pathways, or significant alteration of existing pathways, for fluid flow and, potentially, radionuclide transport within the disposal system. Each of these scenarios also contains a set of features and nondisruptive EPs that remain after FEP screening. As shown in Figure 6-7, undisturbed performance and disturbed performance scenarios are considered in consequence modeling for the WIPP performance assessment. The undisturbed performance scenario, as discussed in Chapter 8.0, is used for compliance assessments. Important aspects of undisturbed and disturbed performance are summarized in this section.

6.3.1 Undisturbed Performance

Undisturbed performance is defined in 40 CFR § 191.12 to mean "the predicted behavior of a disposal system, including consideration of the uncertainties in predicted behavior, if the disposal system is not disrupted by human intrusion or the occurrence of unlikely natural events." Consideration of only undisturbed performance is required for compliance assessments with respect to the Individual and Groundwater Protection Requirements (40 CFR § 191.15 and 40 CFR § 191.24) (see Chapter 8.0). Undisturbed performance is also

considered, together with disturbed performance, for performance assessments with respect to the Containment Requirements (40 CFR § 191.13).

No potentially disruptive natural EPs are likely to occur during the regulatory time frame (Section 6.2.3 and Appendix SCR, Section SCR.1). Therefore, all naturally occurring EPs retained for scenario construction are nondisruptive and are considered as part of undisturbed performance. The only natural features and waste- and repository-induced FEPs retained after screening that are not included in the undisturbed performance scenario but are included in disturbed performance are those directly associated with the potential effects of future deep drilling within the controlled area. These drilling-related FEPs are discussed in Section 6.3.2. Potash mining outside the controlled area does not constitute a disruption of the disposal system by human intrusion and is included in the undisturbed performance scenario. In total, 67 undisturbed performance FEPs have been identified (Section 6.2.3). These FEPs have been assigned a screening designator UP in tables in Section 6.2.3 and Appendix SCR and are listed separately in Table 6-6. Table 6-6 also contains references to text in Section 6.4 that describes the conceptual models that account for the undisturbed performance FEPs.

Among the most significant FEPs that will affect the undisturbed performance within the disposal system are excavation-induced fracturing, gas generation, salt creep, and MgO backfill in the disposal rooms:

- The excavation of the repository and the consequent changes in the stress field in the rock surrounding the excavated opening will result in the creation of a DRZ immediately adjacent to excavated openings. The DRZ will exhibit mechanical and hydrological properties different than those of the intact rock.

- Organic material in the waste may degrade because of microbial activity, and brine will corrode metals in the waste and waste containers, with concomitant generation of gases. Gas generation may result in pressures sufficient to both maintain or develop fractures and change the fluid flow pattern around the waste disposal region.

- At the repository depth, salt creep will tend to heal fractures and reduce the permeability of the DRZ and the crushed salt component of the long-term shaft seals to near that of the host rock salt.

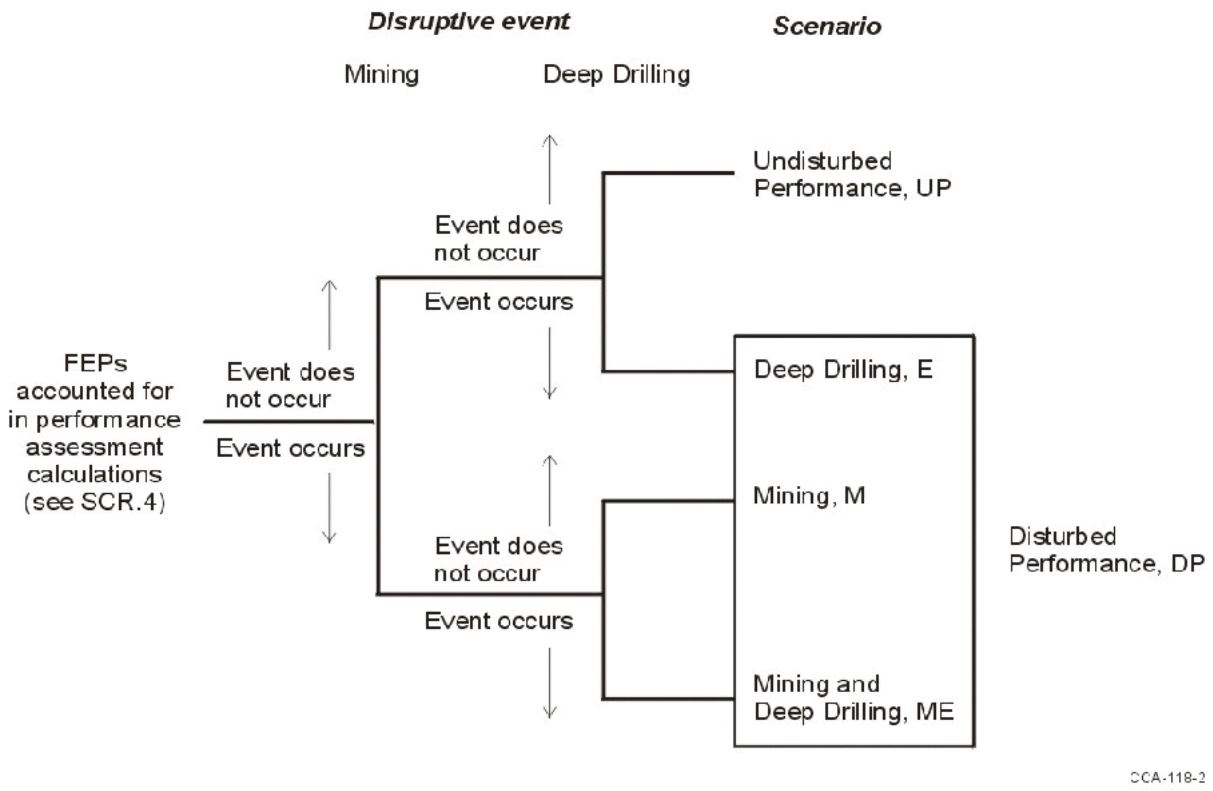

Figure 6-7. Logic Diagram for Scenario Analysis

1

1 **THIS PAGE INTENTIONALLY LEFT BLANK**

Table 6-6. Undisturbed Performance (UP) FEPs

Undisturbed Performance Features, Events, and Processes (FEPs)	Chapter Section
NATURAL FEPs	
Geological	
Stratigraphy	
Stratigraphy	6.4.2
Structural effects	
Seismic activity	
Seismic activity	6.4.5.3
Geochemical	
Dissolution	
Shallow dissolution	6.4.6.2
Subsurface hydrological	
Groundwater characteristics	
Saturated groundwater flow	6.4.5 6.4.6
Unsaturated groundwater flow	6.4.6
Fracture flow	6.4.6.2
Effects of preferential pathways	6.4.6.2
Subsurface geochemical	
Groundwater geochemistry	
Groundwater geochemistry	6.4.3.4 6.4.6.2
Geomorphological	
Physiography	
Physiography	6.4.2
Surface hydrological	
Groundwater recharge and discharge	
Groundwater discharge	6.4.10.2
Groundwater recharge	6.4.10.2
Infiltration	6.4.10.2
Changes in surface hydrology	
Changes in groundwater recharge and discharge	6.4.9
Climatic	
Climate	
Precipitation (for example, rainfall)	6.4.9
Temperature	6.4.9
Climate change	
Meteorological	
Climate change	6.4.9
WASTE- AND REPOSITORY-INDUCED FEPs	
Waste and repository characteristics	
Repository characteristics	
Disposal geometry	6.4.2.1
Waste characteristics	
Waste inventory	6.4.3.3

Table 6-6. Undisturbed Performance (UP) FEPs (Continued)

Undisturbed Performance Features, Events, and Processes (FEPs)	Chapter Section
Container characteristics	
Container material inventory	6.4.3.3
Seal characteristics	
Seal geometry	6.4.3
Seal physical properties	6.4.4
Backfill characteristics	
Backfill chemical composition	6.4.3.4
Radiological	
Radioactive decay	
Radionuclide decay and ingrowth	6.4.5.4.2 6.4.12.4
Geological and Mechanical	
Excavation-induced fracturing	
DRZ	6.4.5.3
Excavation-induced changes in stress	6.4.3.1
Rock creep	
Salt creep	6.4.3.1
Changes in the stress field	6.4.3.1
Roof falls	
Roof falls	6.4.5.3
Effects of fluid pressure changes	
Disruption due to gas effects	6.4.5.2
Pressurization	6.4.5.2
Effects of explosions	
Gas explosions	6.4.5.3
Mechanical effects on material properties	
Consolidation of waste	6.4.3.1
Consolidation of seals	6.4.4
Mechanical degradation of seals	6.4.4
Underground boreholes	6.4.5.3
Subsurface hydrological and fluid dynamics	
Repository-induced flow	
Brine inflow	6.4.3.2
Wicking	6.4.3.2
Effects of gas generation	
Fluid flow due to gas production	6.4.3.2
Geochemical and chemical	
Gas generation	
Microbial gas generation	
Degradation of organic material	6.4.3.3
Effects of temperature on microbial gas generation	6.4.3.3
Effects of biofilms on microbial gas generation	6.4.3.3
Corrosion	
Gases from metal corrosion	6.4.3.3
Chemical effects of corrosion	6.4.3.3

Table 6-6. Undisturbed Performance (UP) FEPs (Continued)

Undisturbed Performance Features, Events, and Processes (FEPs)	Chapter Section
Chemical speciation	
Speciation	6.4.3.4 6.4.3.5
Precipitation and dissolution	
Dissolution of waste	6.4.3.5
Sorption	
Actinide sorption	6.4.3.6 6.4.6.2.1
Kinetics of sorption	6.4.6.2.1
Changes in sorptive surfaces	6.4.6.2.1
Reduction-oxidation chemistry	
Effect of metal corrosion	6.4.3.5
Reduction-oxidation kinetics	6.4.3.5
Organic complexation	
Humic and fulvic acids	6.4.3.6 6.4.6.2.2
Chemical effects on material properties	
Chemical degradation of seals	6.4.4
Microbial growth on concrete	6.4.4
Contaminant transport mode	
Solute transport	
Solute transport	6.4.5.4 6.4.6.2.1
Colloid transport	
Colloid transport	6.4.6.2.2
Colloid formation and stability	6.4.3.6
Colloid filtration	6.4.6.2.2
Colloid sorption	6.4.6.2.2
Microbial transport	
Microbial transport	6.4.6.2.2
Contaminant transport processes	
Advection	
Advection	6.4.5.4 6.4.6.2
Diffusion	
Diffusion	6.4.5.4 6.4.6.2
Matrix diffusion	6.4.6.2
HUMAN-INITIATED EPs	
Geological	
Excavation activities	
Potash mining outside controlled area	6.4.6.2.3 6.4.12.8 6.4.13.8

Table 6-6. Undisturbed Performance (UP) FEPs (Continued)

Undisturbed Performance Features, Events, and Processes (FEPs)	Chapter Section
Subsurface hydrological and geochemical	
Borehole fluid flow	
Drilling-induced flow	
Drilling induced geochemical changes	6.4.6.2
Fluid injection	
Fluid injection-induced geochemical changes	6.4.6.2
Flow through abandoned boreholes	
Borehole-induced geochemical changes	6.4.6.2
Excavation-induced flow	
Changes in groundwater flow due to mining	6.4.6.2.3 6.4.12.8 6.4.13.8

- The MgO backfill emplaced in the disposal rooms will react with carbon dioxide and maintain mildly alkaline conditions. Corrosion of metals in the waste and waste containers will maintain reducing conditions. These effects will control radionuclide solubility.

Radionuclides can become mobile as a result of waste dissolution and colloid generation following brine flow into the disposal rooms. Colloids may be generated from the waste (humics, mineral fragments, and actinide intrinsic colloids) or from other sources (humics, mineral fragments, and microbes).

Conceptually, there are several pathways for radionuclide transport within the undisturbed disposal system that may result in releases to the accessible environment (Figure 6-8). Contaminated brine may migrate away from the waste-disposal panels if pressure within the panels is elevated by the generation of gas from corrosion or microbial degradation. Radionuclide transport may occur laterally, through the anhydrite interbeds toward the subsurface boundary of the accessible environment in the Salado, or through access drifts or anhydrite interbeds (primarily MB139) to the base of the shafts. In the latter case, if the pressure gradient between the panels and overlying strata is sufficient, then contaminated brine may migrate up the shafts. As a result, radionuclides may be transported directly to the ground surface, or they may be transported laterally away from the shafts, through permeable strata such as the Culebra, toward the subsurface boundary of the accessible environment. These conceptual pathways are shown in Figure 6-8.

The modeling system described in Section 6.4 includes potential radionuclide transport along other pathways, such as migration through Salado halite. However, the natural properties of the undisturbed system make radionuclide transport to the accessible environment via these other pathways unlikely.

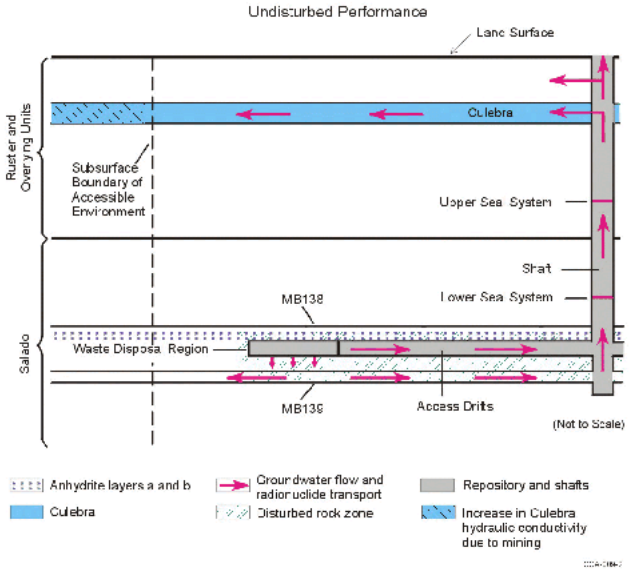

Figure 6-8. Conceptual Release Pathways for the Undisturbed Performance Scenario

1

1 **THIS PAGE INTENTIONALLY LEFT BLANK**

6.3.2 Disturbed Performance

Assessments for compliance with 40 CFR § 191.13 need to consider the potential effects of future disruptive natural and human-initiated EPs on the performance of the disposal system. As discussed in Section 6.2.3, no potentially disruptive natural EPs are considered to be sufficiently likely to require inclusion in analyses of either undisturbed or disturbed performance. The only future human-initiated EPs retained after FEP screening are those associated with mining and deep drilling (but not the subsequent use of a borehole) within the controlled area at a time when institutional controls cannot be assumed to eliminate the possibility of such activities (Sections 6.2.5.2 and 6.4.12.1). In total, 21 disturbed performance FEPs associated with future mining and deep drilling have been identified. These FEPs have been assigned a screening designator DP in tables in Section 6.2 and Appendix SCR and are listed separately in Table 6-7. Table 6-7 also contains references to text in Section 6.4 that describes the conceptual models which account for the disturbed performance FEPs.

For evaluation of the consequences of disturbed performance the DOE has defined the mining scenario, M, the deep drilling scenario, E, and a mining and drilling scenario, ME. These scenarios are described in the following sections.

6.3.2.1 The Disturbed Performance Mining Scenario (M)

The disturbed performance mining scenario, M, involves future mining within the controlled area.

Consistent with the criteria stated by the EPA in 40 CFR § 194.32 (b), for performance assessment calculations, the effects of potential future mining within the controlled area are limited to changes in hydraulic conductivity of the Culebra that result from subsidence (as described in Section 6.4.6.2.3).

Radionuclide transport may be affected in the M scenario if a head gradient between the waste-disposal panels and the Culebra causes brine contaminated with radionuclides to move from the waste-disposal panels to the base of the shafts and up the shafts to the Culebra. The changes in the Culebra transmissivity field may affect the rate and direction of radionuclide transport within the Culebra. Features of the M scenario are illustrated in Figure 6-9. The three disturbed performance FEPs labeled M in Table 6-7 relate to the occurrence and effects of future mining. The modeling system used for the M scenario is similar to that developed for the undisturbed performance scenario, but with a modified Culebra transmissivity field within the controlled area to account for the effects of mining.

Table 6-7. Disturbed Performance (DP) FEPs

Disturbed Performance Features, Events, and Processes (FEPs)	Scenario	Chapter Section
ALL UNDISTURBED PERFORMANCE (UP) FEPS		
NATURAL FEPs		
Geological		
Stratigraphy		
Brine reservoirs	E1	6.4.8 6.4.12.6
WASTE- AND REPOSITORY-INDUCED FEPs		
Waste and repository characteristics		
Waste characteristics		
Heterogeneity of waste forms	E1, E2	6.4.12.4
Contaminant transport mode		
Particulate transport		
Suspensions of particles	E1, E2	6.4.7.1
Cuttings	E1, E2	6.4.7.1
Cavings	E1, E2	6.4.7.1
Spallings	E1, E2	6.4.7.1 6.4.13.7
HUMAN-INITIATED EPs		
Geological		
Drilling		
Oil and gas exploration	E1, E2	6.4.7 6.4.12.2
Potash exploration	E1, E2	6.4.7 6.4.12.2
Oil and gas exploitation	E1, E2	6.4.7 6.4.12.2
Other resources	E1, E2	6.4.7 6.4.12.2
Enhanced oil and gas recovery	E1, E2	6.4.7 6.4.12.2
Excavation activities		
Potash mining	M	6.4.6.2.3 6.4.12.8 6.4.13.8
Subsurface hydrological and geochemical		
Borehole fluid flow		
Drilling-induced flow		
Drilling fluid flow	E1, E2	6.4.7.1
Drilling fluid loss	E2	6.4.7.1.1
Blowouts	E1, E2	6.4.7.1.1
Drilling-induced geochemical changes	E1, E2	6.4.6.2
Flow through abandoned boreholes		

Table 6-7. Disturbed Performance (DP) FEPs (Continued)

Disturbed Performance Features, Events, and Processes (FEPs)	Scenario	Chapter Section
Natural borehole fluid flow	E1, E2	6.4.7.2 6.4.12.7 6.4.13
Waste-induced borehole flow	E1, E2	6.4.7.2 6.4.12.7 6.4.13
Borehole-induced geochemical changes	E1, E2	6.4.6.2
Excavation-induced flow		
Changes to groundwater flow due to mining	M	6.4.6.2.3 6.4.12.8 6.4.13.8
Ecological		
Social and technological developments		
Loss of records	M, E1, E2	6.4.7 6.4.12.1

Legend:

M Mining within the controlled area.
E1 Deep drilling that intersects the waste disposal region and a brine reservoir in the Castile.
E2 Deep drilling that intersects a waste disposal panel.

6.3.2.2 The Disturbed Performance Deep Drilling Scenario (E)

The disturbed performance deep drilling scenario, E, involves at least one deep drilling event that intersects the waste disposal region. The EPA provides criteria concerning analysis of the consequences of future drilling events in performance assessments in 40 CFR § 194.33(c):

> Performance assessments shall document that in analyzing the consequences of drilling events, the Department assumed that:
> (1) Future drilling practices and technology will remain consistent with practices in the Delaware Basin at the time a compliance application is prepared. Such future drilling practices shall include, but shall not be limited to: the types and amounts of drilling fluids; borehole depths, diameters, and seals; and the fraction of such boreholes that are sealed by humans; and
> (2) Natural processes will degrade or otherwise affect the capability of boreholes to transmit fluids over the regulatory time frame.

Consistent with these criteria, there are several pathways for radionuclides to reach the accessible environment in the E scenario. During the period before any deep drilling intersects the waste, potential release pathways are identical to those in the undisturbed performance scenario.

If a borehole intersects the waste in the disposal rooms, releases to the accessible environment may occur as material entrained in the circulating drilling fluid is brought to the surface, as discussed further in Section 6.4.7.1. Particulate waste brought to the surface may include cuttings, cavings, and spallings. Cuttings are the materials cut by the drill bit as it passes through waste. Cavings are the materials eroded by the drilling fluid in the annulus around the

drill bit. Spallings are the materials that may be forced into the circulating drilling fluid if there is sufficient pressure in the waste disposal panels. During drilling, contaminated brine may flow up the borehole and reach the surface, depending on fluid pressure within the waste disposal panels.

When abandoned, the borehole is assumed to be plugged in a manner consistent with current practice in the Delaware Basin (see Section 6.4.7.2; Appendix DEL, Sections DEL.5 and DEL.6; and Appendix MASS, Section MASS.16.3 and MASS Attachment 16-1). An abandoned intrusion borehole with degraded casing and/or plugs may provide a pathway for fluid flow and contaminant transport from the intersected waste panel to the ground surface if the fluid pressure within the panel is sufficiently greater than hydrostatic. Additionally, if brine flows through the borehole to overlying units, such as the Culebra, it may carry dissolved and colloidal actinides that can be transported laterally to the accessible environment by natural groundwater flow in the overlying units.

Alternatively, the units intersected by an intrusion borehole may provide sources for brine flow to a waste panel during or after drilling. For example, in the northern Delaware Basin, the Castile, which underlies the Salado, contains isolated volumes of brine at fluid pressures greater than hydrostatic (as discussed in Section 2.2.1.2.2). The WIPP-12 penetration of one of these reservoirs provided data on one brine reservoir within the controlled area. The location and properties of brine reservoirs cannot be reliably predicted; thus, the possibility of a deep borehole penetrating both a waste panel and a brine reservoir is accounted for in consequence analysis of the WIPP, as discussed in Section 6.4.8. Such a borehole could provide a connection for brine flow from the Castile to the waste panel, thus increasing fluid pressure and brine volume in the waste panel.

Also, a borehole that is drilled through a disposal room pillar, but does not intersect waste, could penetrate the brine reservoir underlying the waste disposal region. Such an event would, to some extent, depressurize the brine reservoir, and thus would affect the consequences of any subsequent intersections of the reservoir. The possibility for boreholes that do not penetrate the waste to depressurize a brine reservoir underlying the waste disposal region is accounted for in the consequence analysis of the WIPP.

The DOE has distinguished two types of deep drilling events by whether or not the borehole intersects a Castile brine reservoir. A borehole that intersects a waste disposal panel and penetrates a Castile brine reservoir has been designated an E1 event. The 18 disturbed performance FEPs labeled E1 in Table 6-7 relate to the occurrence and effects of an E1 drilling event. A borehole that intersects a waste panel but does not penetrate a Castile brine reservoir has been designated an E2 event. The 18 disturbed performance FEPs labeled E2 in Table 6-7 relate to the occurrence and effects of an E2 drilling event.

1

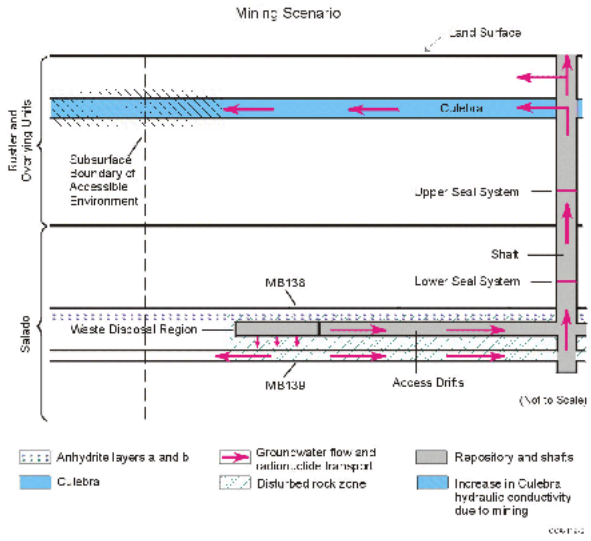

Figure 6-9. Conceptual Release Pathways for the Disturbed Performance Mining Scenario

1 **THIS PAGE INTENTIONALLY LEFT BLANK**

In order to evaluate the consequences of future deep drilling, the DOE has divided the E scenario into three drilling subscenarios, E1, E2 and E1E2, distinguished by the number of E1 and E2 drilling events that are probabilistically assumed to occur in the regulatory time frame. These subscenarios are described in order of increasing complexity in the following sections.

6.3.2.2.1 The E2 Scenario

The E2 scenario is the simplest scenario for inadvertent human intrusion into a waste disposal panel. In this scenario, a panel is penetrated by a drill bit; cuttings, cavings, spallings, and brine flow releases may occur; and brine flow may occur in the borehole after it is plugged and abandoned. Sources for brine that may contribute to long-term flow up the abandoned borehole are the Salado or, under certain conditions, the units above the Salado. An E2 scenario may involve more than one E2 drilling event. Features of the E2 scenario are illustrated in Figure 6-10. A modeling system has been developed to evaluate the consequences of an E2 scenario during which single or multiple E2 events occur.

6.3.2.2.2 The E1 Scenario

Any scenario with one inadvertent penetration of a waste panel that also penetrates a Castile brine reservoir is called E1. Features of this scenario are illustrated in Figure 6-11.

Sources of brine in the E1 scenario are the brine reservoir, the Salado and, under certain conditions, the units above the Salado. However, the brine reservoir is conceptually the dominant source of brine in this scenario. The model configuration developed for the E1 scenario is used to evaluate the consequences of futures that have only one E1 event. A future during which more than one E1 event occurs is described as an E1E2 scenario.

6.3.2.2.3 The E1E2 Scenario

The E1E2 scenario is defined as all futures that have multiple penetrations of a waste panel of which at least one intrusion is an E1 type. One case of this scenario, with a single E1 event and a single E2 event penetrating the same panel, is illustrated in Figure 6-12. However, the E1E2 scenario can include many possible combinations of intrusion times, locations, and types of event (E1 or E2). The sources of brine in this scenario are those listed for the E1 scenario, and multiple E1-type sources may be present. The E1E2 scenario potentially has a flow path not present in the E1 or E2 scenarios: flow from an E1 borehole through the waste to another borehole. This flow path has the potential to (1) bring large quantities of brine in direct contact with waste and (2) provide a less restrictive path for this brine to flow to the units above the Salado (via multiple boreholes) compared to either the E1 or E2 individual scenarios. It is both the presence of brine reservoirs and the potential for flow through the waste to other boreholes that make this scenario different in terms of potential consequences from combinations of E2 boreholes. The extent to which flow occurs between boreholes, as estimated by modeling, determines whether combinations of E1 and E2 boreholes at specific locations in the repository should be treated as E1E2 scenarios or as independent E1 and E2 scenarios in the consequence analysis. Because of the number of possible combinations of

drilling events, the modeling configuration for the E1E2 scenario differs in significant ways from the model configuration used for evaluating E1 and E2 scenarios. This configuration is described in Section 6.4.13.5.

6.3.2.3 The Disturbed Performance Mining and Deep Drilling Scenario (ME)

Mining in the WIPP site (the M scenario) and deep drilling (the E scenario) may both occur in the future. The DOE calls a future in which both of these events occur the ME scenario. The occurrence of both mining and deep drilling do not create processes in addition to those already described separately for the M and E scenarios. For example, the occurrence of mining does not influence any of the interactions between deep boreholes and the repository or brine reservoirs. As well, the occurrence of drilling does not impact the effects of mining on Culebra hydrogeology. The difference between the M and E scenarios considered separately and the ME scenario is that the combination of borehole transport to the Culebra (E) and a transmissivity field impacted by mining (M) may result in more rapid transport of actinides to the accessible environment. For example, because the M scenario does not include drilling the only pathway for actinides to reach the Culebra is up the sealed shafts. For clarity in describing computational results, the ME scenario has been subdivided according to the types of deep drilling subscenarios into the ME1 scenario (M and E1), the ME2 scenario (M and E2), and the ME1E2 scenario (M and E1E2).

The system used for modeling flow and transport in the Culebra for the ME scenario is similar to that used for the E scenario. However, in the ME scenario the Culebra transmissivity field is modified to account for the effects of mining within the controlled area.

6.3.3 Scenarios Retained for Consequence Analysis

These scenarios described in Sections 6.3.1 and 6.3.2 have been retained for consequence analysis to determine compliance with the Containment Requirements in 40 CFR § 191.13. The modeling systems used to evaluate the consequences of these undisturbed and disturbed performance scenarios are discussed in Section 6.4. For consequence analysis, the scenarios and subscenarios described in this section are further subdivided into scenarios, S_i. The S_i scenarios are distinguished by, for example, the time of occurrence of disruptive events. The S_i scenarios are generated, and their probabilities determined, by probabilistic sampling of selected processes and events (see Sections 6.1.5.2 and 6.4.12).

6.4 Calculation of Scenario Consequences

Scenario consequence, cS_i, is the third element of the ordered triples shown in Equation 2 in Section 6.1.1. Estimation of cS_i requires quantitative modeling; performance assessment uses a linked system of individual computer codes. This section discusses the conceptual and computational models and some parameter values used to estimate the consequence of the

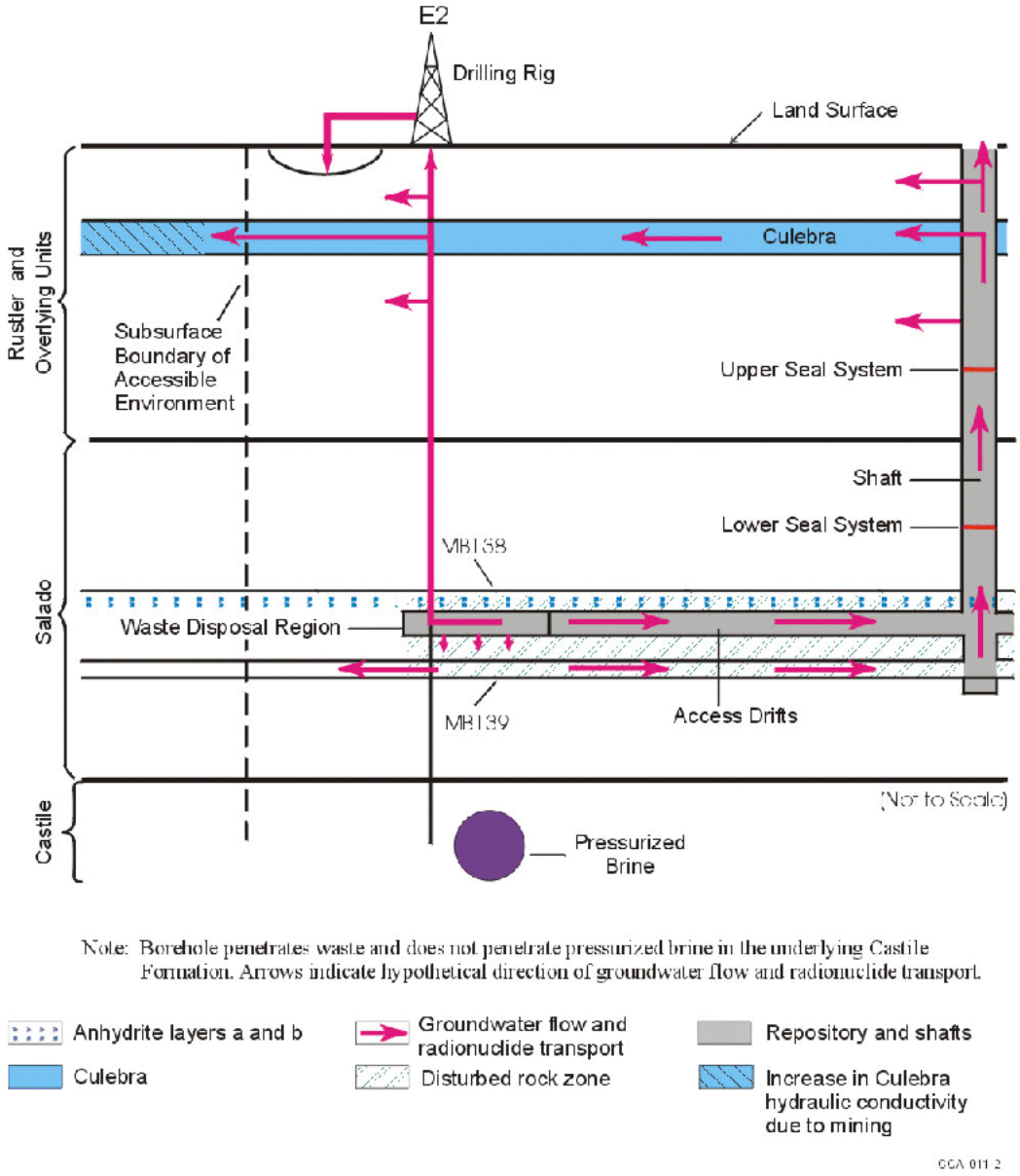

Figure 6-10. Conceptual Release Pathways for the Disturbed Performance Deep Drilling E2 Scenario

1 **THIS PAGE INTENTIONALLY LEFT BLANK**

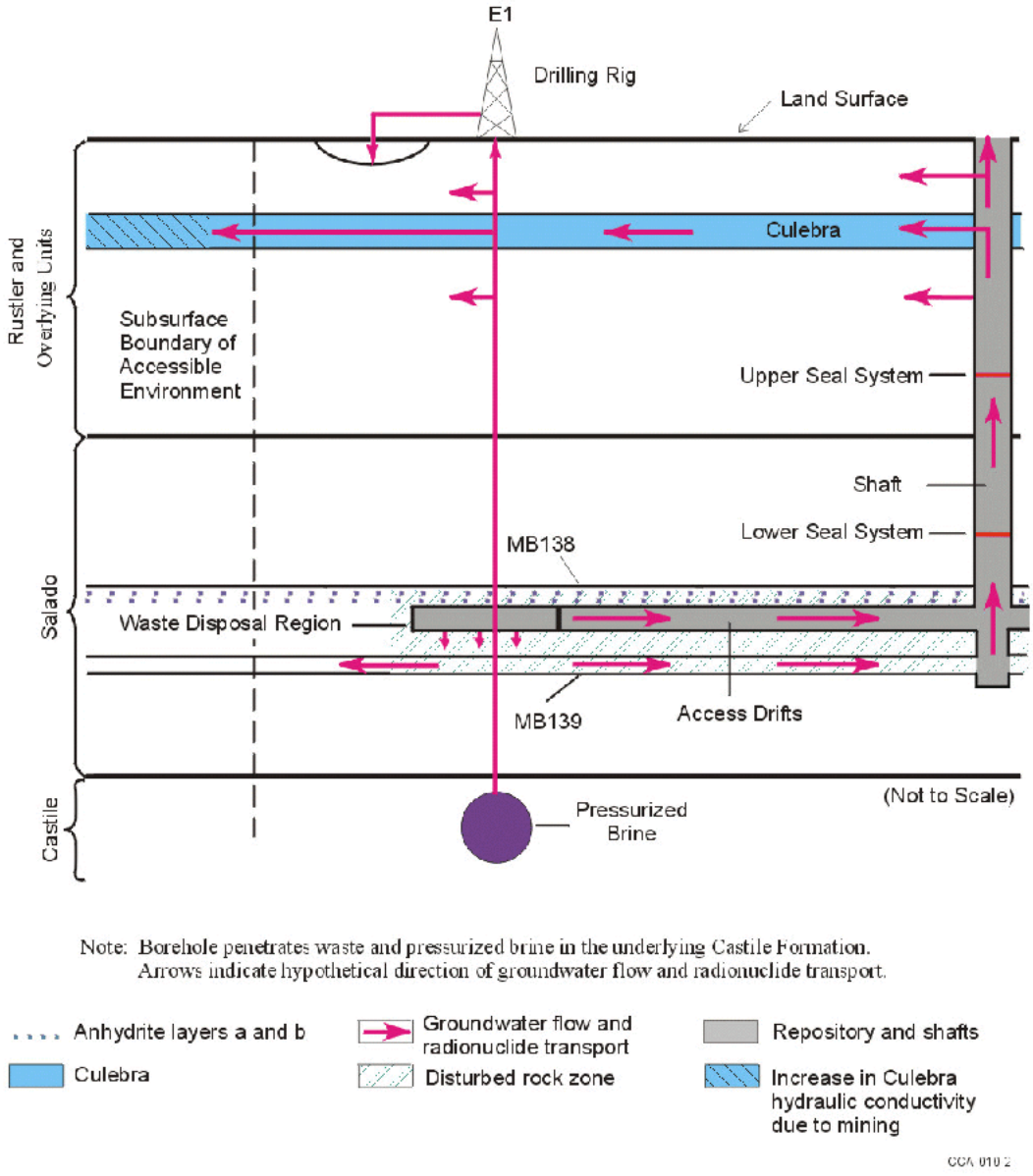

Figure 6-11. Conceptual Release Pathways for the Disturbed Performance Deep Drilling Scenario E1

1

1 **THIS PAGE INTENTIONALLY LEFT BLANK**

1

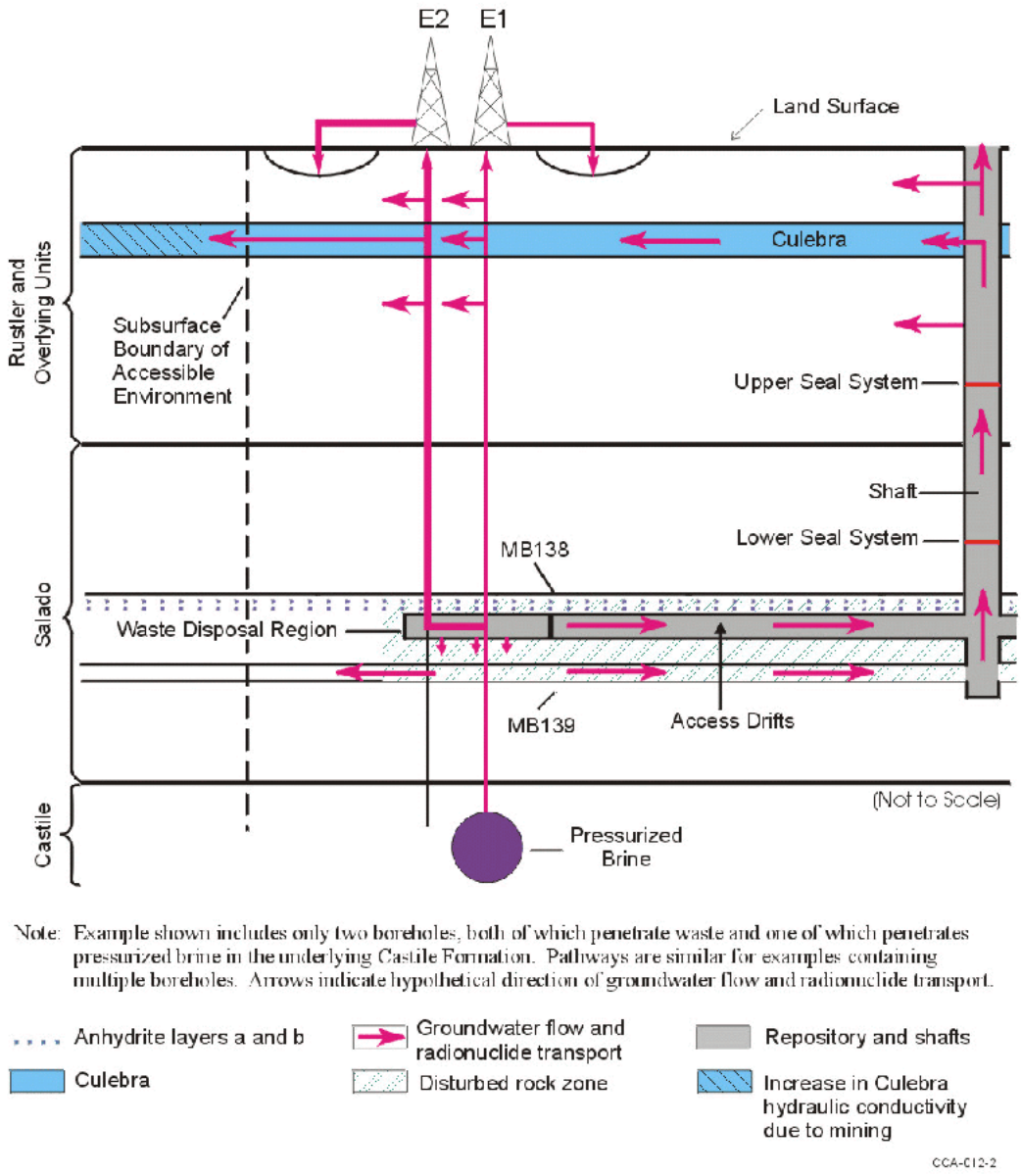

Figure 6-12. Conceptual Release Pathways for the Disturbed Performance Deep Drilling Scenario E1E2

1 **THIS PAGE INTENTIONALLY LEFT BLANK**

scenarios described in Section 6.3. Additional discussion of conceptual models and modeling assumptions is provided in Appendix MASS. Additional descriptions of sampled parameter values are included in Appendix PAR (Parameters 1 to 57).

6.4.1 Types of Models

A single modeling system was used to represent the disposal system and calculate the CCDFs presented in Section 6.5. The modeling system, however, can be conveniently described in terms of various submodels with each describing a part of the overall system. This section is organized to provide, for each submodel defined, an integrated, summary description of the conceptual model, mathematical model, numerical model, computational model, experimental data, and model parameters used. These terms are described below.

The models used in the WIPP performance assessment, as in other complex analyses, exist at four different levels:

(1) **Conceptual models** are a set of qualitative assumptions used to describe a system or subsystem for a given purpose. At a minimum, these assumptions concern the geometry and dimensionality of the system, initial and boundary conditions, time dependence, and the nature of the relevant physical and chemical processes. The assumptions should be consistent with one another and with existing information within the context of the given purpose.

(2) **Mathematical models** are developed to represent the processes at the site. The conceptual models provide the context within which these mathematical models must operate and define the processes they must characterize. The mathematical models are predictive in the sense that, once provided with the known or assumed properties of the system and possible perturbations to the system, they predict the response of the system. The processes represented by these mathematical models include fluid flow, mechanical deformation, radionuclide transport in groundwater, and removal of waste through intruding boreholes.

(3) **Numerical models** are developed to provide approximations of mathematical model solutions because most mathematical models do not have closed-form solutions.

(4) The complexity of the system requires the use of computer codes to solve the numerical models. The implementation of the numerical model in the computer code with specific initial and boundary conditions and parameter values is generally referred to as the **computational model**.

Data are descriptors of the physical system being considered, normally obtained by experiment or observation. Parameters are values necessary in mathematical, numerical, or computational models. The distinction between data and parameters can be subtle. Parameters are distinct from data, however, for three reasons. First, data may be evaluated, statistically or otherwise, to generate parameters for a model to account for uncertainty in

data. Second, some parameters have no relation to the physical system, such as the parameters in a numerical model specified to determine when an iterative solution scheme has converged. Third, many model parameters are applied at a different scale than one that can be directly observed or measured in the physical system. The distinction between data and parameter values is described further in Appendix PAR, where the derivations of distributions for specific parameters are given. The interpretation and the scaling of experimental and field data are discussed in Appendix PAR for individual and sampled parameters, as appropriate.

6.4.2 Model Geometries

Although the specific geometries used in performance assessment models are developed after the conceptual and mathematical models are defined, they are introduced here because they provide a useful framework for presenting the full discussion of the modeling system. Performance assessment represents the three-dimensional geometry of the disposal system (repository, shafts, and controlled area) using two primary two-dimensional simplifications. In the first two-dimensional geometry, processes that act on the entire disposal system occur within the repository and are simulated in the BRAGFLO (BRine And Gas FLOw) computer code using a geometry that approximates a north-south vertical cross section through the disposal system and some surrounding rock. This geometry is used to simulate processes in the disposal system, such as two-phase flow and movement of actinides, as well as processes acting only within the repository, such as creep closure of disposal rooms and gas generation. In the second two-dimensional geometry, groundwater flow and actinide transport in the Culebra, which provides a potential pathway for lateral transport of actinides to the accessible environment, are simulated in the SECOFL2D and SECOTP2D computer codes using a two-dimensional horizontal geometry that treats the Culebra as a single layer. These two geometries are discussed in the following sections. Additional geometries used to simulate system behavior during drilling intrusions are discussed in Sections 6.4.7 and 6.4.13. Performance assessment codes and the flow of numerical information through the performance assessment are described in Section 6.4.11 and referenced appendices.

6.4.2.1 Disposal System Geometry

A single disposal system geometry is used in the BRAGFLO computational model (see Appendix BRAGFLO) with four different maps of material properties: one for undisturbed conditions; one for the E1 intrusion event, in which a borehole penetrates the panel and a Castile brine reservoir; one for the E2 intrusion event, in which a borehole penetrates the repository but not a Castile brine reservoir; and one for the E1E2 intrusion event, in which at least one E1 borehole and one other borehole penetrate a disposal panel (see Section 6.4.13.5). The geometry and material maps used in BRAGFLO are similar; each is a model for fluid flow calculations that represents the three-dimensional physical system in a two-dimensional plane that cuts vertically through the repository and surrounding strata. Side views of the vertical cross section and two of the material maps are presented in Figures 6-13 and 6-14. In these figures, the boundaries of grid blocks discretized in the model (see

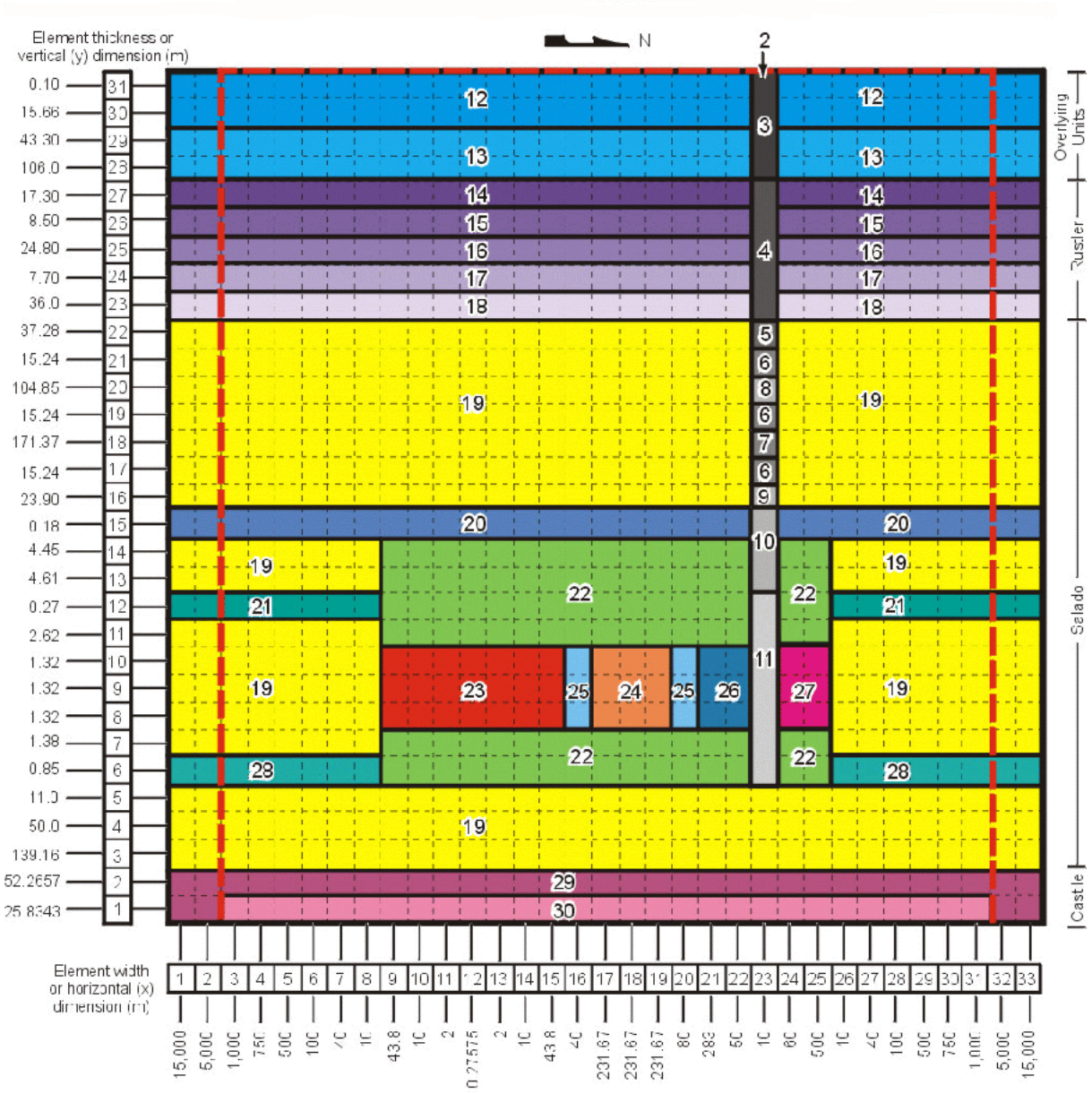

Figure 6-13. A Side View of the BRAGFLO Elements and Material Regions Used for Simulation of Undisturbed Performance

1 **THIS PAGE INTENTIONALLY LEFT BLANK**

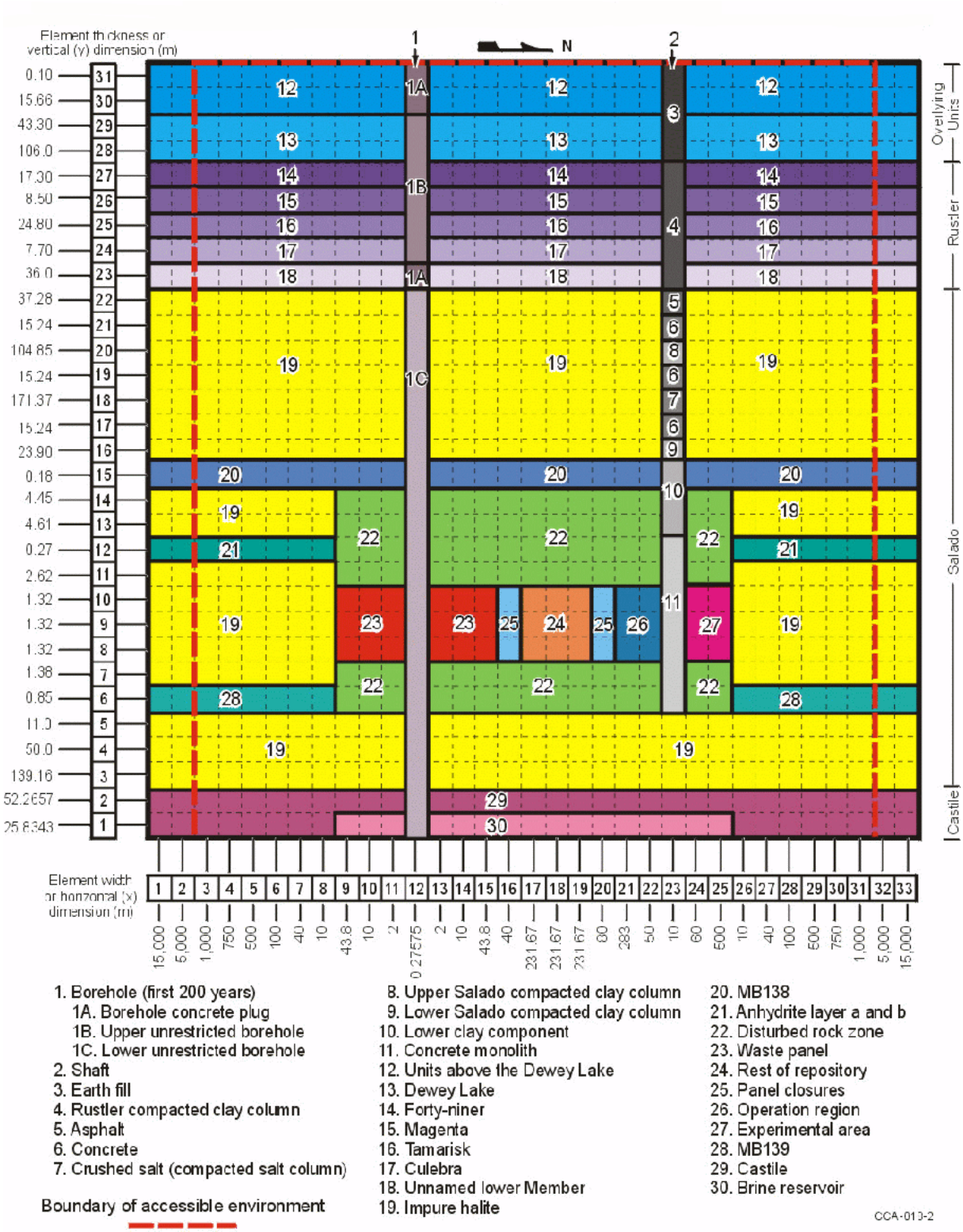

Figure 6-14. A Side View of the BRAGFLO Elements and Material Regions Used to Simulate the E1 Event (For E2 Event, the Borehole Extends Only Between the Surface and the Base of the Repository)

1 **THIS PAGE INTENTIONALLY LEFT BLANK**

Appendix BRAGFLO, Section 4.5, for details of the finite-difference method) are shown with dashed lines; each grid block is associated with material properties representing an important feature of the disposal system. These associations between grid blocks and material properties are shown by color and number in the figures. The two figures differ in that the material property map used for E1 intrusion events (Figure 6-14) includes a material region representing the borehole (Region 1) that is not present in the undisturbed case. The borehole region vertically transects other material regions and connects the single panel (Region 23) with the Castile brine reservoir (Region 30), marker beds, overlying units, and the surface. The E2 intrusion event material regions are similar to those of E1, except that the modeled borehole region does not extend below the repository and therefore does not contact a brine reservoir. Additionally, the extent of the Castile brine reservoir is different from undisturbed to disturbed performance. This difference has no impact on results because no natural FEPs are retained that can create a pathway from the Castile to the repository.

Figures 6-13 and 6-14 show the relationship among material regions in the model and how connections are made within the finite-difference scheme. However, by illustrating equidimensional grid blocks, the volumetric relationship between grid blocks is greatly distorted. To show the volumetric relationship among nodal blocks and between the repository and host formations, a scaled side view of the vertical cross section used in BRAGFLO is shown in Figure 6-15. An undistorted 1:1 vertical:horizontal scale side view is in the upper left corner of Figure 6-15; at this scale, important model features are not resolvable. Therefore, two other views are provided in which the vertical scale has been exaggerated 50:1 to show model features. Notice that the modeling system extends more than 15 miles (25 kilometers) to the north and 14 miles (22.5 kilometers) to the south from the borehole, which intersects the approximate center of the waste disposal region and includes the uppermost 2,990 feet (911 meters) of rock at the WIPP site. Colors in Figure 6-15 are consistent with colors for material regions in Figures 6-13 and 6-14.

Effects of flow in the third (out-of-plane) dimension are approximated with a two-dimensional element configuration that simulates convergent or divergent flow to the north and south, centered on the repository, in intact rocks laterally away from the repository. A top-down (plan) view of the model is shown in Figure 6-16 and illustrates the discretization adopted to simulate convergent or divergent flow. Colors in Figure 6-16 are consistent with colors for material regions in Figures 6-13 through 6-15 at the repository depth (node rows 8, 9, and 10). In this text, the term width corresponds to the x (lateral) dimension of nodes, thickness refers to the y (vertical) dimension, and depth refers to the z (out-of-plane) dimension. The effects of the grid assumptions on fluid flow processes in the Salado are discussed in Appendix MASS (Section MASS.4 and MASS Attachment 4-1).

Based on observations in the existing excavations, the DOE approximates the regionally variable dip in the Salado by incorporating a 1-degree dip to the south in the BRAGFLO computational mesh. This dip is not indicated in Figures 6-13, 6-14, and 6-15.

The BRAGFLO definition of hydrostratigraphic units follows formation and member divisions. Inside the Salado, however, further subdivision of hydrostratigraphy has been made

based on the observed differences in permeability between anhydrite-rich interbeds and halite-rich intervals. This further subdivision has been made only at elevations near the repository horizon because only in this region are such distinctions important. The models and assumptions used to represent the various regions of material properties shown in Figures 6-13 and 6-14 are discussed beginning in Section 6.4.3 and in Appendices MASS and PAR. The thickness of hydrostatigraphic units used in BRAGFLO are tabulated in Appendix PAR (Table PAR-57).

6.4.2.2 Culebra Geometry

Although the BRAGFLO model contains a discretization of the Culebra and calculates flow there, the DOE uses a more detailed representation of this unit to estimate potential radionuclide releases to the accessible environment resulting from lateral subsurface transport. The conceptual model for flow and transport in this geometry is discussed in Section 6.4.6.2. The boundary and initial conditions applied to this geometry are discussed in Section 6.4.10.2. SECOFL2D and SECOTP2D are the computer codes used to simulate groundwater flow and radionuclide transport in the Culebra. The manner in which this geometry is linked to the BRAGFLO geometry described in the preceding section is discussed in Sections 6.4.6.2, 6.4.11, and Appendix CODELINK (Section CODELINK.6). The grids used for modeling the Culebra are discussed in Section 6.4.6.2.

6.4.3 The Repository

The repository, as shown in Figure 3-2 (see Chapter 3.0), is represented by Regions 23 to 27 in Figures 6-13 and 6-14. These regions include a waste disposal panel (Region 23), panel closures (Region 25), the panels and access drifts in the rest of the waste disposal region (Region 24), the operations region (Region 26), and the experimental region at the north end of the repository (Region 27). The shaft (Region 2, which is further subdivided into Regions 3 through 11) intersects the repository between the operations region and the experimental region. The shaft is discussed in detail in Section 6.4.4. For human-intrusion events, the borehole (Region 1) intersects the waste disposal region in the panel. In two-dimensional fluid flow codes, a grid block's length, volume, and cross-sectional area of faces connected to other grid blocks are important model features. For each region of the repository depicted, the BRAGFLO model geometry preserves the true excavated volume. Lateral dimensions have been determined to preserve volume and retain important cross-sectional areas and distances between defined regions, as discussed below. These simplifications are conservative with respect to fluid contact with waste, which is a critical factor in determining the quantity of actinides mobilized in the aqueous phase. The simplifications are conservative because (1) all pillars have been removed from the modeled panel, resulting in homogeneous waste regions through which fluid can flow directly; and (2) the panels in the rest of the repository have neither pillars nor closures, resulting in a large homogeneous region that is assigned an average

1

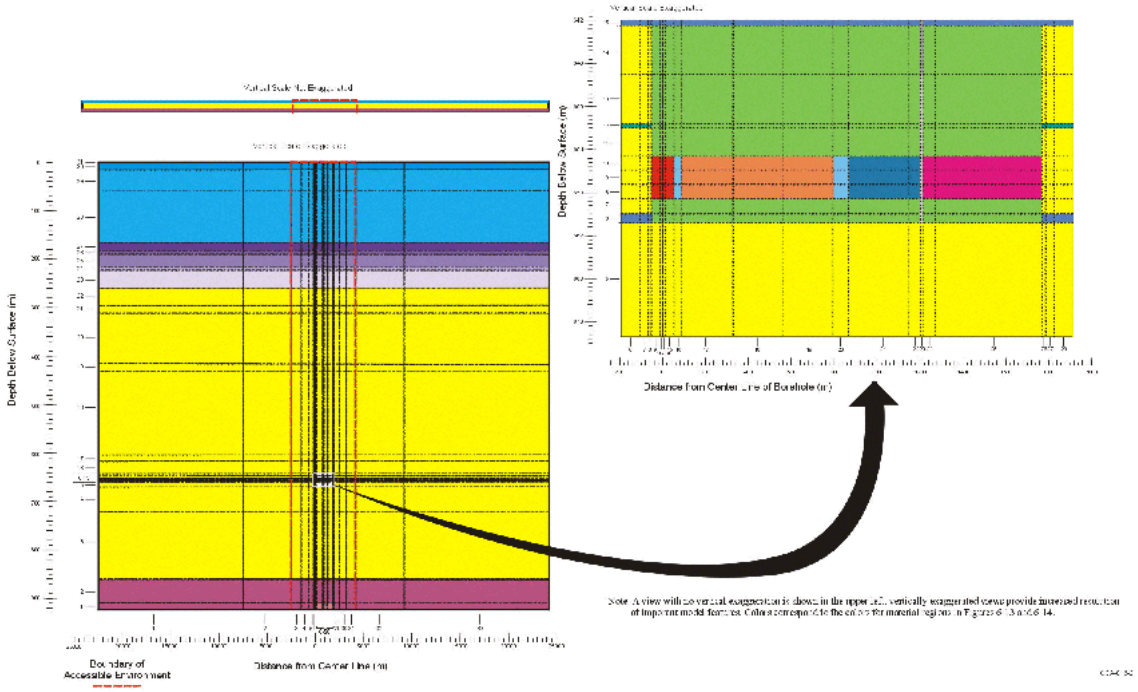

Figure 6-15. A Side View of the BRAGFLO Geometry Drawn to Scale Used for this Performance Assessment

1 **THIS PAGE INTENTIONALLY LEFT BLANK**

1

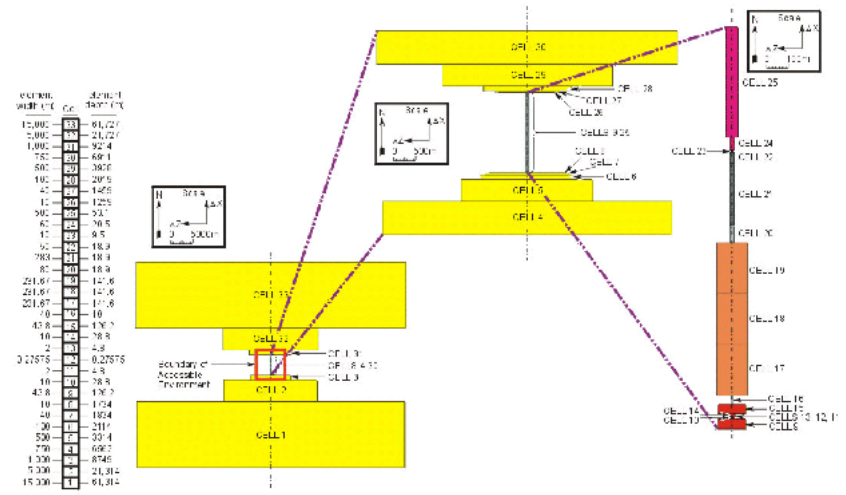

Note: This view illustrates the variation in element depth present in the model for simulation of radially convergent flow.

Figure 6-16. A Top-Down View of a Row of Elements in BRAGFLO Used for Undisturbed Performance

1 **THIS PAGE INTENTIONALLY LEFT BLANK**

permeability within the range of experimentally determined permeabilities (see Section 6.4.3.2 and Appendix MASS, Section MASS.5).

The single panel that is represented individually (Region 23) is discretized to simulate radial flow to and from the borehole that intersects it. The true distance from the south end of the waste disposal region to the waste handling shaft is preserved in the model as the distance from the south end of the modeled panel to the modeled single shaft. In BRAGFLO, the single panel region is the southernmost portion of the repository. It occupies this position because separate modeling activities indicate that slightly larger releases may result from a panel in this position than from alternative placements (see Vaughn et al. 1995).

The panel closure between the panel and the rest of the repository has a cross-sectional area equal to the cross-sectional area of the drifts between panels. The length and total volume of modeled panel closures is consistent with their design. The panel closure between the rest of the repository and the operations region has a cross-sectional area equal to the cross-sectional area of the drifts between the north end of the waste disposal region and the operations region. Because there are two closures between the waste disposal region and the shafts in the operations region, the modeled panel closures between the rest of the repository and the operations region have a length and volume consistent with two panel closures.

A number of submodels have been defined within the repository region and are described in this section. The submodels that have been defined for repository processes are Creep Closure (6.4.3.1), Repository Fluid Flow (6.4.3.2), Gas Generation (6.4.3.3), Chemical Conditions in the Repository (6.4.3.4), Dissolved Actinide Source Term (6.4.3.5), and Source Term for Colloidal Actinides (6.4.3.6).

6.4.3.1 Creep Closure

Salt creep occurs naturally in the Salado halite in response to deviatoric stress. Inward creep of rock and the repository response is a process generally referred to as creep closure. Creep closure of excavated regions begins immediately because of excavation-induced deviatoric stress. If the rooms were empty, closure would proceed to the point where the void volume created by the excavation would be eliminated as the surrounding formation returns to a uniform stress state. In the waste disposal region, waste consolidation will continue until loading in the surrounding rock is uniform, at which point salt creep ceases. The amount of waste consolidation that occurs and the time it takes to consolidate are governed by properties of the waste (waste strength, modulus, etc.), properties of the surrounding rock, the dimensions and location of the room, and the quantities of fluids present in the room.

Fluids that could affect closure are brine that may enter the repository from the Salado or an intrusion borehole, air present in the repository when it is sealed, and gas produced by reactions occurring during waste degradation. Closure and consolidation can be slowed by fluid pressure in the repository. This can be quantified according to the principle of effective stress:

$$\sigma_T = \sigma_e + p \,, \tag{11}$$

where σ_T is the stress caused by the weight of the overburden (an essentially constant value), p is the pressure of the repository pore fluid, and σ_e is the stress that is applied to the waste matrix. In this formulation, the waste is considered a skeleton structure containing pore fluids. As the pore pressure increases, an increasing amount of overburden stress is supported by pore fluid pressure, P, and less overburden stress is supported by the strength of the waste matrix. Waste consolidation will cease when the sum of the stresses felt by the waste matrix and fluid pressure reaches lithostatic pressure. If gas and brine quantities in the repository stabilize, creep closure will act to establish a constant pressure and pore volume.

In summary, creep closure of waste disposal areas will cause their volume to decrease as the Salado deforms to consolidate and encapsulate the waste, changing waste porosity and permeability. Resistance to creep closure will be caused by waste strength and fluid pressure.

Three major material-response models are required for closure analyses. The first model describes how the halite creeps as a function of time and stress. The second model describes the state of consolidation of the waste as a function of applied stress. A third constitutive model is used to model inelastic behavior of anhydrite marker beds (see Appendix PORSURF, PORSURF Attachment 1).

Halite deformation is predicted using a multimechanism deformation steady-state creep model with work hardening and recovery transient response. For the conditions of the WIPP, creep mechanisms are governed by the temperature and shear stress at a given location in the surroundings at any time. Although WIPP conditions are expected to be nearly isothermal at the ambient natural underground temperature, several of the mechanisms can be active at the same time because of the large range of stress states that occur around underground rooms and shafts. The focus of the mechanistic part of the model is definition of steady-state creep strain, with transient creep strain described through a multiplier on the steady-state rate, thus accommodating both transient changes in stress loading and unloading.

The volumetric plasticity model is the mathematical model for room closure and waste consolidation. The experimental data used in this model are summarized and interpreted in Butcher et al. (1991, 65 – 76) and Luker et al. (1991).

The volumetric plasticity model, multimechanism deformation model, and the inelastic constitutive model for anhydrite were numerically implemented in the SANTOS computer code to calculate the closure of disposal rooms for performance assessment (Appendix PORSURF, PORSURF Attachment 1). SANTOS is described in Appendix PORSURF (Section PORSURF.3).

As a boundary condition, SANTOS requires estimates of the fluid pressure and hence the quantity of gas present in a disposal room. These estimates are obtained using the average stoichiometry model of gas generation (Section 6.4.3.3) with different rates of gas generation that reflect different assumptions about the quantity of brine that might be available in a waste

disposal room. The different rates of gas generation used in SANTOS bound the possible conditions for gas content in the repository. With the volumetric plasticity model and the fluid pressure boundary condition, SANTOS calculates the pore volume of the disposal room through time.

In performance assessment, the time-dependent effects on volume of creep closure calculated by SANTOS are linked to the fluid-flow code BRAGFLO by a porosity surface, which is a look-up table relating porosity (void volume) to (1) time after sealing and (2) gas pressure. At the beginning of a time step, BRAGFLO evaluates the pressure of a cell in the waste disposal regions; the pressure is sensitive to brine and gas flow and the previous pore volume of the cell. The code then consults the porosity surface to find the void volume of the cell appropriate for a given time and pressure. The void volume in the cell is iteratively adjusted during a time step for consistency with gas generation, fluid movement, and repository pressure. Additional details about the porosity surface method are included in Appendix BRAGFLO (Section 4.11) and Appendix PORSURF (Sections PORSURF.1, PORSURF.2, and PORSURF Attachments 1 through 6). The porosity surface method of incorporating the dynamic effect of creep closure in performance assessment has been compared to more complex techniques that are computationally impractical in a performance assessment (Freeze et al. 1995). In these comparisons, the porosity surface method was found to be a reasonable representation of behavior observed in more complex models.

The operations area and experimental area (Regions 26 and 27 in Figures 6-13 and 6-14, respectively) are modeled as unfilled after closure in this performance assessment. These regions are expected to close in less than 200 years and do not require a porosity surface, in contrast to the region containing waste (Vaughn et al. 1995).

6.4.3.2 Repository Fluid Flow

Fluid flow modeling within the repository is concerned with (1) fluid flow and distribution in the waste, (2) fluid flow to and from the Salado and shafts, and (3) fluid flow between the repository and intrusion boreholes. These are important in assessing gas generation rates (Section 6.4.3.3), repository pressure, and the mobility of radionuclides in the disposal system. Additional discussion of this topic is provided in Appendix MASS (Section MASS.7).

Disposal region fluid flow is affected by the geometrical association of pillars, rooms, drifts, panel closures, possible borehole locations, the time-dependent properties of waste areas resulting from creep closure, flow interactions with other parts of the disposal system, and reactions that generate gas. As described in Section 6.4.3.1, creep closure changes disposal region porosity. Depending on material properties and conditions, brine may flow into the disposal region by moving down shafts and through the DRZ or operations region, or during disturbed conditions, through a borehole. Brine contained in the Salado may flow to the waste disposal region because of pressure gradients created by the excavation. Brine flow into the repository may be reduced as repository pressure increases, and brine may be expelled from the repository if pressure in the repository exceeds brine pressure in the immediately surrounding rock or borehole. Gas may be generated as waste decomposes, causing a

pressure increase. Gas may flow away from the waste into lower pressure areas, which may include disturbed areas surrounding the repository, the interbeds, the shafts, or an intrusion borehole. Gas flow into intact, halite-rich rock is not expected because of the expected high threshold pressure of halite (see Section 6.4.5.1).

Fluid flow in the disposal system is conceptualized using principles of multiphase flow, except for Culebra flow and transport modeling. In multiphase flow, a residual brine saturation (S_{br}), is defined, which is the minimum saturation at which the brine phase has a nonzero relative permeability; below this saturation brine is immobile. In accordance with two-phase flow theory, the residual gas saturation (S_{gr}) in the disposal system corresponds to the gas saturation necessary to create an incipient gas-phase relative permeability; below this saturation waste-generated gas is immobile. The multiphase flow techniques adopted by the DOE are described in Appendix BRAGFLO (Section 4.8).

The intrinsic permeability of waste at a given time can influence repository system performance by affecting the flow rate of gas or brine through the waste. Tests reported by Luker et al. (1991, 693 – 702) on simulated waste have shown material permeabilities from about 10^{-12} to 10^{-16} square meters on waste compacted under a lithostatic load. Performance assessment assigns a permeability of the waste as a constant at 1.7×10^{-13} square meters (Table 6-8). This permeability value is representative of the average value of compacted waste. Use of a constant value rather than a variable has been found acceptable (Vaughn et al. 1995).

Because two-phase relationships have not been measured for waste, performance assessment determines a range of possible two-phase conditions for the repository by applying the LHS technique to parameters within the Brooks-Corey two-phase equations. These and other parameters in the disposal room and repository flow model are shown in Tables 6-8 and 6-9. Details about the two-phase equations and parameters used in performance assessment are included in Appendix BRAGFLO (Sections 4.8 and 4.9) and Appendix PAR (Parameters 6 and 7).

Material properties in the waste are assumed to be homogeneous and are distributed in the BRAGFLO model in cells whose volumes are much larger than an individual waste container. Two processes that may occur on scales smaller than the cell volumes in BRAGFLO are wicking (the retention of brine in a capillary fringe) and puddling (the capture of brine in isolated pockets of waste caused by waste heterogeneity). Wicking is accounted for in the gas generation model (Section 6.4.3.3). Vaughn et al. (1995) found that puddling can be neglected.

Table 6-8. Repository[a] and Panel Closures Parameter Values

Parameter (units)	Maximum	Minimum	Median or Constant
Permeability, k (square meters) - Waste Region	-	-	1.70×10^{-13}
Permeability, k (square meters) - Operations and Experimental Regions	-	-	10^{-11}
Permeability (square meters) - Panel Closures	-	-	10^{-15}
Initial Effective Porosity (percent) - Waste Region	-	-	84.8
Effective Porosity (percent) - Operations and Experimental Regions	-	-	18.0
Effective Porosity (percent) - Panel Closures	-	-	7.5
Threshold Pressure, P_t (pascals) - Repository[a]	-	-	0
Threshold Pressure, P_t (pascals) - Panel Closures[b]	-	-	8.67×10^{4}
Residual Brine Saturation, S_{br} (unitless) - Repository	0.552	0	0.276
Residual Brine Saturation, S_{br} (unitless) - Operations and Experimental Regions	-	-	0
Residual Brine Saturation, S_{br} (unitless) - Panel Closures	-	-	0.20
Residual Gas Saturation, S_{gr} (unitless) - Repository	0.15	0	0.075
Residual Gas Saturation, S_{gr} (unitless) - Operations and Experimental Regions	-	-	0
Residual Gas Saturation, S_{gr} (unitless) - Panel Closures	-	-	0.20
Pore Distribution Parameter, λ (unitless) - Repository	-	-	2.89
Pore Distribution Parameter, λ (unitless) - Operations and Experimental Regions	-	-	0.7
Pore Distribution Parameter, λ (unitless) - Panel Closures	-	-	0.94
Maximum Capillary Pressure (pascals) - Repository and Panel Closures	-	-	10^{8}
Pore Compressibility (1/pascals) - Repository[c]	-	-	0
Pore Compressibility (1/pascals) - Panel Closures	-	-	2.64×10^{-9}

[a] Unless specifically listed, Repository refers to operations, experimental, and waste regions.
[b] Threshold pressure (P_t) determined from the relationship: $P_t = PCT\_A \cdot k^{PCT\_EXP}$ where PCT_A and PCT_EXP are constants and k is the permeability.
[c] Accounted for in porosity surface.

Table 6-9. BRAGFLO Fluid Properties

Parameter (units)	Value
Reference Temperature (kelvin)[a]	300.15
Liquid Density (kilograms per cubic meter)[a,b] at	
• Atmospheric Pressure	1,220.0
• 8 megapascals	1,223.0
• 15 megapascals	1,225.7
Liquid Viscosity (pascals * seconds)[b]	2.1×10^{-3}
Liquid Compressibility (1/pascals)[b]	3.1×10^{-10}
Gas Density (kilograms per cubic meter)[a,b] at:	
• Atmospheric Pressure	0.0818
• 8 megapascals	6.17
• 15 megapascals	11.1
Gas Viscosity (pascals * seconds)[b]	8.93×10^{-6}

[a] These values applied to fluids in all material regions in BRAGFLO.
[b] See Appendix BRAGFLO (Section 4.4) for equations of state.

The experimental and operations regions (Regions 26 and 27 in Figures 6-13 and 6-14) are represented in performance assessment with a porosity of 18.0 percent and a permeability of 10^{-11} square meters as a conservative upper bound. For postoperational performance, the panel closures (Region 25 in Figures 6-13 and 6-14) are represented with a porosity of 7.5 percent and a permeability of 10^{-15} square meters, as discussed in Appendix MASS (MASS Attachment 7-1).

6.4.3.3 Gas Generation

Gas will be produced in the repository because of a variety of chemical reactions, primarily those occurring between brine, metals, microbes, cellulosics and similar materials, plastics, and rubber materials, and via liberation of dissolved gases to the gas phase. The dominant processes are anoxic corrosion of metals in the waste containers and the waste and microbial degradation of cellulosics, plastics, and rubbers in the waste. Anoxic corrosion reactions will occur between brine and steel, aluminum, and aluminum alloys, producing H_2. Microbial degradation of cellulosics may produce a variety of gases; however, for the waste inventory and expected conditions, CO_2 and CH_4 (methane) are expected to be the dominant gases for the process. Radiolysis has been demonstrated by laboratory experiment and model calculations to be insignificant (see Appendix MASS, Section MASS.8; Appendix SCR, Section SCR.2.5.1.3).

Gas generation will affect repository pressure, which is important in other submodels of the disposal system, such as those calculating creep closure (Section 6.4.3.1), interbed fracturing (Section 6.4.5.2), two-phase flow (Section 6.4.3.2), and the radionuclide release associated

with spallings during an inadvertent drilling intrusion (Section 6.4.7). Thus, gas generation must be estimated in performance assessment.

Performance assessment uses the average stoichiometry model to estimate gas generation occurring in the waste disposal region. This model was developed for WIPP performance assessment based on gas generation experiments performed for the WIPP (see Appendix MASS, Section MASS.8 and MASS Attachment 8-2). The average stoichiometry model accounts for the formation of gas by anoxic corrosion of steels and microbial degradation of cellulosics, including plastics and rubbers. For the purpose of calculating repository pressure and gas flow, the density and viscosity of the generated gas are assumed to be those of H_2. In the average stoichiometry model, gas is assumed to be generated at a rate dependent on the availability of brine in the computational cell. Gas can be generated by anoxic corrosion in all realizations, and is assumed to be generated by microbial degradation in half of the realizations. The average stoichiometry model is based on experimental data on the rates of corrosion and microbial degradation under inundated and humid conditions. These data were used to develop ranges of possible gas-generation rates, as shown in Table 6-10. In BRAGFLO, a gas-generation rate is determined from the rates listed in Table 6-10 by a linear interpolation method that combines humid and inundated rates based on the effective liquid saturation (Appendix BRAGFLO, Section 4.13). The effective liquid saturation in a computational cell in BRAGFLO for the purpose of gas generation is the computed liquid saturation in that cell, plus an adjustment to account for uncertainty in the capillary rise (wicking) characteristics of the waste. Refer to Appendices PAR (Parameter 8) and BRAGFLO (Sections 4.13 and 7.2.9) for details on the treatment of wicking in the gas generation model.

Anoxic corrosion is represented by a generic equation given in Appendix BRAGFLO (Section 4.13). This equation accounts for corrosion only of the steel content in the repository by the reaction expected to dominate. Because the total quantity of aluminum and aluminum alloys is a small compared to the quantity of iron base metals, corrosion of aluminum is omitted for simplicity. The steel content of the repository is depleted separately in each computational cell (that is, a cell-by-cell basis), and gas generation can continue in cells, depending on parameter values, until all steel in a cell is consumed. Brine in cells is consumed as gas generation proceeds. If a cell has a brine saturation equal to zero, it cannot produce gas by anoxic corrosion.

It is assumed that there is no passivation of anoxic corrosion of steel by CO_2 and H_2S produced by microbial degradation because microbial gas generation is too slow and also because CO_2 will be removed from the gaseous phase by reaction with MgO backfill. Details of the equations and parameter values are given in Appendix BRAGFLO (Section 4.13), Appendix PAR (Parameter 1), and Appendix MASS (Section MASS.8).

Microbial degradation occurs in only half of the realizations because of uncertainties in viability of the microbial colonies (Appendix MASS, Section MASS.8 and MASS Attachment 8-2). Like anoxic corrosion, microbial degradation is represented by a generic

Table 6-10. Average-Stoichiometry Gas Generation Model Parameter Values

Parameter (units)	Maximum	Minimum	Median or Constant
Inundated Corrosion Rate for Steel without CO_2 Present (meters per second)	1.59×10^{-14}	0	7.94×10^{-15}
Humid Corrosion Rate for Steel	-	-	0
Probability of Microbial Degradation of Plastics and Rubbers in the Waste in the Event of Significant Microbial Gas Generation (see figure PAR-1) where 0 represents corrosion and no significant microbial gas generation. 1 represents cellulosic degradation only, and 2 represents cellulosic, plastic, and rubber degradation	2	0	2
Rate for Microbial Degradation Under Humid Conditions (mole per kilogram∗ second)	1.27×10^{-9}	0	6.34×10^{-10}
Rate for Microbial Degradation under Brine-Inundated Conditions (mole per kilogram∗ second)	9.51×10^{-9}	3.17×10^{-10}	4.92×10^{-9}
Factor β for Microbial Reaction Rates (unitless)	1.0	0	0.5
Anoxic Corrosion Stoichiometric Factor X (unitless)	-	-	1.0
Average Density of Cellulosics in CH Waste (kilograms per cubic meter)	-	-	54.0
Average Density of Cellulosics in RH Waste (kilograms per cubic meter)	-	-	17.0
Average Density of Iron-Based Materials in CH Waste (kilograms per cubic meter)	-	-	170.0
Average Density of Iron-Based Materials in RH Waste (kilograms per cubic meter)	-	-	100.0
Average Density of Plastics in CH Waste (kilograms per cubic meter)	-	-	34.0
Average Density of Plastics in RH Waste (kilograms per cubic meter)	-	-	15.0
Average Density of Rubber in CH Waste (kilograms per cubic meter)	-	-	10.0
Average Density of Rubber in RH Waste (kilograms per cubic meter)	-	-	3.3
Bulk Density of Iron Containers, CH Waste (kilograms per cubic meter)	-	-	139.0
Bulk Density of Iron Containers, RH Waste (kilograms per cubic meter)	-	-	2.59×10^{3}

Table 6-10. Average-Stoichiometry Gas Generation Model Parameter Values (Continued)

Parameter (units)	Maximum	Minimum	Median or Constant
Bulk Density of Plastic Liners, CH Waste (kilograms per cubic meter)	-	-	26.0
Bulk Density of Plastic Liners, RH Waste (kilograms per cubic meter)	-	-	3.1
BIR Total Volume of CH Waste (cubic meters)	-	-	1.69×10^5
BIR Total Volume of RH Waste (cubic meters)	-	-	7.08×10^3
Wicking Saturation (unitless)	1.0	0	0.5

equation, given along with other details in Appendix BRAGFLO (Section 4.13). The cellulose inventory is depleted on a cell-by-cell basis. Depending on parameter values, gas generation by microbial degradation can continue until all cellulosics in the cell are degraded. Reaction with MgO added to the repository consumes CO_2 (see Section 6.4.3.4 and Appendix SOTERM, Section SOTERM.2.2.2). Thus, the net quantity of gas developed by microbial degradation is correlated with constituents of the waste disposal region. Details are provided in Appendix BRAGFLO (Section 4.13). It is assumed that the microbial degradation process neither produces nor consumes water, but its rate is dependent on the amount of liquid present in a computational cell.

Microbial degradation may consume plastic and rubber materials in the repository. The DOE assumes that in half of those simulations in which microbial degradation of cellulosics occurs, microbial degradation also acts on plastic and rubber materials in the waste disposal region. As with cellulosics, these materials are depleted on a cell-by-cell basis. Parameter values for the average stoichiometry model are summarized in Table 6-10 and detailed in Appendix PAR (Parameters 1 through 5).

6.4.3.4 Chemical Conditions in the Repository

The chemical conditions in the repository determine actinide solubility, a property demonstrated in past analyses as important to disposal system performance. In scenarios that have the potential to result in releases to the accessible environment, the DOE has determined that chemical conditions in the repository can be modeled as constant in performance assessment. This use of constant conditions is based on an assumption of equilibrium for most processes between the brine in the repository (determined by the scenario being considered), waste, MgO backfill, and abundant minerals. Some exceptions to the equilibrium assumption are present in some performance assessment models and are discussed where appropriate. In addition to the following discussion, information supporting this position is presented in Appendix SOTERM.

Brine and waste within the WIPP repository are modeled as a uniform mixture of dissolved and solid-state species. Thermodynamic equilibrium is assumed for dissolved actinide

concentrations, but oxidation-reduction reactions between the actinides and other waste components are not assumed to proceed to equilibrium. Although materials in the waste will actually dissolve at different rates, the presumption of homogeneity and solubility equilibrium, along with assumed disequilibrium reduction-oxidation conditions, yields the largest reasonable concentration of aqueous actinides in the repository. No chemical microenvironments that influence the overall chemical environment are expected to persist, nor is supersaturation expected during the 10,000-year regulatory period. The average temperature of the WIPP is expected to increase by less than 6°C as a result of radioactive decay and exothermic reactions, such as MgO hydration and carbonization, and the effect of this small increase is assumed negligible (see Appendix WCA, Section WCA.5.3, and Appendix SCR, Sections SCR.2.2.2 and SCR.2.5.7).

Brine composition in the repository can vary depending on the sequence of future human events. Calculating mixing of brine from different sources is not amenable to performance assessment. The DOE has made the reasonable simplification that in the undisturbed performance and E2 scenarios, which do not include penetration of a Castile brine reservoir, all brine in the repository will have the composition of Salado brine (see Appendix SOTERM, Section SOTERM.2.2.1). In these scenarios, there is no process that could introduce Castile brine into the repository. For the E1 and E1E2 scenarios, which include penetration of a brine reservoir in the Castile, brine in the repository is assumed to have the composition of Castile brine at all times. Even though some Salado brine may enter the repository in these scenarios, it is reasonable to assume that Castile brine is the dominant portion of brine because the quantity of brine that can flow from a reservoir through a borehole and into the repository is substantial compared to the quantity of brine entering from the Salado.

The chemical environment in the repository after closure is expected to be reducing (that is, lowered oxidation states are expected to be favored). Any gaseous or dissolved oxygen present in the repository will be consumed quickly either by aerobic microbes or by oxic corrosion after repository closure. Moreover, the repository will contain large amounts of iron, and anoxic corrosion has been shown to produce considerable quantities of hydrogen gas and Fe^{2+} under expected repository conditions (see Appendix MASS, MASS Attachment 8-3). Despite the overall reducing conditions, however, a condition of reduction-oxidation disequilibrium is assumed in that reduction-oxidation reactions between dissolved actinides in possible oxidation states are assumed to not occur.

Based on experimental data reported in Appendix SOTERM (Sections SOTERM.2.2.2, SOTERM.3.4, and SOTERM.3.6), the DOE has determined that alkaline conditions in the repository favor lower actinide solubility. As discussed in Section 3.3.3 and Appendix BACK, MgO will be emplaced in the repository with the waste, in order to ensure alkaline conditions in the repository. MgO emplaced with the waste will react with the CO_2 that forms, creating magnesium carbonate minerals such as $MgCO_3$. The fugacity of CO_2 will be low and controlled by equilibrium considerations, rather than controlled by its rate of production by microbial degradation, because the DOE will emplace enough MgO with sufficient surface area to ensure CO_2 uptake will exceed the CO_2 production rate. Thus, by adding MgO to the repository, the DOE not only maintains alkaline conditions but also minimizes a property of

the repository, its CO_2 fugacity, that would be expected to vary with time and potentially complicate the estimation of actinide solubilities in performance assessment.

MgO reacts with brine to form $Mg(OH)_2$. $Mg(OH)_2$ will react with CO_2 produced by the microbial degradation of cellulosics by reactions such as

$$Mg(OH)_2 + CO_2 = MgCO_3 + H_2O \; . \qquad (12)$$

There is a small amount of other alkaline components in the waste, such as $Ca(OH)_2$, contained in the cementitious waste. Their effect will be minimal because they will be consumed by reactions with $MgCl_2$ in the Salado brine and microbially generated CO_2. Details of those buffering reactions are described in Appendix SOTERM (Section SOTERM.2.2.2).

Because the processes that might cause time-dependent changes in important chemical conditions in the repository have been eliminated by the addition of MgO and by the assumptions made regarding brine composition, performance assessment uses constant chemical conditions. The chemical conditions in the repository, including the pmH (the $-\log_{10}$ of the molality of the hydrogen ion), are assumed to be controlled by equilibrium between minerals (that is, MgO, Salado halite, and anhydrite present in interbeds), brine present, and waste. In Salado brine, the pmH in this system will be about 9.4. In Castile brine, the pmH in this system will be about 9.9. In both systems, the carbon dioxide fugacity will be low and will be determined by the equilibrium system (see Appendix SOTERM, Section SOTERM.2.2.2, for a detailed discussion).

The waste contains chemical compounds, known as organic ligands, that can enhance the concentration of actinide ions by forming soluble complexes of these ions. The ligands of concern in the repository are acetate, citrate, oxalate, and ethylenediaminetetraacetate (EDTA) because they are soluble in brine and are known to be present in the waste (see WCA Section 8.11). However, these organic ligands also bond strongly to other metal species known to be in the repository system. The DOE assumes that because of this competition effect, the organic ligands will have no significant impact on the repository performance (see Appendix SOTERM, Section SOTERM.5, and Appendix SCR, Section SCR.2.5.6, for discussion).

6.4.3.5 Dissolved Actinide Source Term

Analysis reported in Appendix WCA (Section WCA.3) has demonstrated that the mobility in brine of the following actinides may be significant in the performance assessment of the WIPP: Th, U, Np, Pu, Cm, and Am. Although commonly referred to as actinides in the waste inventory, these substances are almost always present in the waste as solid actinide oxides or solid actinide salts, and if they dissolve in the WIPP brines, they will dissolve as complex ions. Additional discussion of actinide solubility modeling and the oxidation state distribution of the actinides is presented in Appendix SOTERM (Sections SOTERM.3 and SOTERM.4, respectively).

Actinides may be mobilized either by dissolution in brine as aqueous species, by bioaccumulation or sorption onto colloidal particles, or by condensation into colloidal forms as actinide-intrinsic colloids that could be carried by brine (see Section 6.4.3.6 for a discussion of colloidal actinides). The dissolved actinide source term model calculates the dissolved concentration of each actinide in solution by applying the modeled solubility for the particular oxidation state, as determined by the oxidation state distribution for that actinide, at the repository conditions presented in Section 6.4.3.4. Several oxidation states are not stable in the chemically reducing conditions described in Section 6.4.3.4. The unstable oxidation states are Np(VI), Pu(V), Pu(VI), and Am(V), as described in Appendix SOTERM (Section SOTERM.4).

Thorium will exist only in the IV oxidation state (see Appendix SOTERM, Section SOTERM.4.1). Am and Cm will exist in only the III oxidation state (see Appendix SOTERM, Sections SOTERM.4.4 and SOTERM.4.5). For the remaining actinides, Pu, U, and Np, it is uncertain whether repository conditions will favor the lower or higher of the remaining oxidation states (see Appendix SOTERM, Sections SOTERM.4.2, SOTERM.4.3, and SOTERM.4.6). The DOE has captured the range of possible behavior by assuming that in half the realizations, conditions within the repository are extremely reducing and the solubility of all three of these actinides will be adequately represented by the solubility of their lower oxidation states. In the other half of the realizations, the solubilities of these actinides are well represented by the solubilities of the higher of the possible oxidation states. The factors controlling the aqueous actinide concentration in a possible oxidation state are equilibrium with anhydrite, halite, MgO, and brine.

The solubility of the actinides as a function of equilibrium between anhydrite, halite, MgO, and brine is calculated outside of the performance assessment using FMT, a computer code for calculating actinide concentration limits based on thermodynamic parameters. The parameters for FMT are derived both from experimental investigations specifically designed to provide parameter values for this model and from the published literature. FMT and its application are described in Appendix SOTERM (Section SOTERM.3.5). Table 6-11 presents a summary of solubility parameter values for each actinide oxidation state consistent with the assumptions regarding chemical conditions stated in this section and Section 6.4.3.4. These values are documented in Table 6-11 and in Appendix PAR (Parameters 36 through 45 and Table PAR-39). Details of the generation of Table 6-11 are given in Appendix SOTERM (Section SOTERM.3).

Actinide concentration may not be equal to the values sampled in LHS. This condition could arise when there are not sufficient actinides in the solid phase in a particular cell, when combined with the dissolved actinides that may have been transported into that cell from an

Table 6-11. Summary of Dissolved Actinide Solubilities (moles per liter) in Castile and Salado Brines[a]

Actinides	Brine	Maximum	Minimum	Median[b] or Constant
Am(III), Pu(III), Cm(III)	Salado	1.46×10^{-5}	5.82×10^{-9}	4.73×10^{-7}
Pu(IV), Th(IV), U(IV)	Salado	1.11×10^{-4}	4.40×10^{-8}	3.58×10^{-6}
Np(IV)	Salado	-	-	4.40×10^{-6}
Np(V)	Salado	-	-	2.30×10^{-6}
U(VI)	Salado	2.19×10^{-4}	8.70×10^{-8}	7.07×10^{-6}
Am(III), Pu(III), Cm(III)	Castile	1.64×10^{-6}	6.52×10^{-10}	5.30×10^{-8}
Pu(IV)	Castile	1.51×10^{-7}	6.00×10^{-11}	4.88×10^{-9}
Th(IV)	Castile	-	-	6.00×10^{-9}
U(IV)	Castile	-	-	6.00×10^{-9}
Np(IV)	Castile	-	-	6.00×10^{-9}
Np(V)	Castile	-	-	2.20×10^{-6}
U(VI)	Castile	2.21×10^{-4}	8.80×10^{-8}	7.15×10^{-6}

[a] Inorganic chemistry controlled by the $Mg(OH)_2$ - $MgCO_3$ pair.
[b] Appendix SOTERM (Sections SOTERM.3.6 and SOTERM.7.2) discusses the relationship of this distribution to the modeled solubility.

adjacent cell, to achieve the concentration value as determined by LHS sampling. This situation is referred to as inventory limited.

The actinide inventory is depleted on a cell-by-cell basis by the computer code NUTS (NUclide Transport Systems) for the undisturbed, E1, and E2 scenarios. The treatment of the E1E2 scenario is described in Section 6.4.13.5. In a computational cell, the processes affecting actinide dissolved concentration are dissolution of solid actinide compounds, advection of dissolved actinides by brine flow from neighboring cells and interaction with colloidal particles (see Section 6.4.3.6). NUTS dissolves each actinide until the maximum concentration determined by the actinide source term algorithms is obtained or an inventory limit is reached. In the repository, the transfer of actinides between solid phase and solution is tracked to preserve mass balance of the actinide inventory. Outside the repository, the model does not precipitate actinides into the solid phase, thereby giving a conservative measure of mobile actinide quantities (see Appendix SCR, Section SCR.2.5.3.2).

6.4.3.6 Source Term for Colloidal Actinides

Colloidal actinides are discussed in greater detail in Appendix SOTERM (Section SOTERM.6). Colloidal particles form in the repository by a variety of processes, including waste degradation, microbial activity, rock decomposition, and chemical condensation. These particles may also be carried into the repository by liquids moving from the Salado or through boreholes. Because of the presence of soils, nutrients, and cellulosic substrates for microbial

action in WIPP waste (see Appendix BIR), humic substances and microbes will be present in disposal room brines, or may form in situ. Actinide-intrinsic colloids may form in the disposal rooms from condensation of dissolved actinides. Mineral fragments, as well as humic substances and microbes, may provide surfaces on which dissolved actinides may sorb.

Four types of colloidal particles are believed to cover the range of possible behavior of all colloid types (see Appendix SOTERM, Section SOTERM.6.1.2). The four particle types considered in performance assessment are microbes, humic and fulvic acids (humic substances), actinide-intrinsic (intrinsic), and mineral fragments. The concentration of actinides carried by each colloidal particle type depends on many of the same chemical conditions that govern the concentration of dissolved actinides.

Actinide concentrations associated with humic substances and microbes are linked to dissolved actinide concentrations through proportionality constants based on experimental results. For humic substances, actinide complexation constants from WIPP-specific experiments or from published literature are coupled with experimentally determined site-binding densities and solubilities of different types of humic substances in WIPP brines. For microbes, actinide uptake was experimentally determined through experiments with WIPP-relevant bacteria cultures. Actinide concentrations associated with mineral fragment-type colloidal particles are estimated based on results from experiments designed to determine mobile concentrations in brines, coupled with site-binding densities of mineral substrates. For the Pu(IV)-polymer, actinide concentrations are determined through solubility experiments conducted from over- and undersaturation over a range of pmH values. Intrinsic colloids of other actinides were determined to be of negligible importance and are eliminated from performance assessment calculations. For more discussion on this topic refer to Appendix SOTERM (Section SOTERM.6.3.2.2).

Actinides associated with microbes and humics are related to the concentration of dissolved actinides in the repository through proportionality constants determined from interpretation of WIPP-relevant experiments and the literature (Appendix SOTERM, Sections SOTERM.6.3.3 and SOTERM.6.3.4). The proportionality-constant relationship is not based rigorously on thermodynamic equilibrium but is simply an empirical relationship. The concentration of actinides associated with the Pu(IV)-polymer is a constant value determined from experimental results at the pmH conditions dictated by the presence of MgO backfill. Likewise, the concentration of actinides associated with mineral colloids is also a constant value, not linked to the concentration of dissolved actinides. Actinides associated with humics and microbes represent most of the colloidal actinide source term. Consequently, the colloidal actinide source term is closely related to the dissolved actinide source term. As discussed in Section 6.4.6.2, however, the source terms are considered separately for transport in the Culebra.

For performance assessment, the concentration of each actinide element on each colloidal particle type during a realization is a fixed value. The concentration parameters are summarized in Table 6-12. Actual values of actinide concentration on colloidal particles are constrained by inventory limits.

Table 6-12. Colloid Concentration Factors

	Concentration on Mineral Fragments[a]	Concentration as Intrinsic Colloid[a]	Proportion Sorbed on Microbes[b]	Maximum Sorbed on Microbes[c]	Proportion Sorbed on Humics[b]		Maximum Sorbed on Humics[a]
					Salado	Castile	
Th(IV)	2.6×10^{-8}	0.0	3.1	0.0019	6.3	6.3	1.1×10^{-5}
U(IV)	2.6×10^{-8}	0.0	0.0021	0.0021	6.3	6.3	1.1×10^{-5}
U(VI)	2.6×10^{-8}	0.0	0.0021	0.0023	0.12	0.51	1.1×10^{-5}
Np(IV)	2.6×10^{-8}	0.0	12.0	0.0027	6.3	6.3	1.1×10^{-5}
Np(V)	2.6×10^{-8}	0.0	12.0	0.0027	9.1×10^{-4}	7.4×10^{-3}	1.1×10^{-5}
Pu(III)	2.6×10^{-8}	0.0	0.3	6.8×10^{-5}	0.19	1.37[d]	1.1×10^{-5}
Pu(IV)	2.6×10^{-8}	1.0×10^{-9}	0.3	6.8×10^{-5}	6.3	6.3	1.1×10^{-5}
Am(III)	2.6×10^{-8}	0.0	3.6	NA	0.19	1.37[d]	1.1×10^{-5}

[a] In units of moles colloidal actinide per liter
[b] In units of moles colloidal actinide per mole dissolved actinide
[c] In units of moles total mobile actinide per liter
[d] A cumulative distribution from 0.065 to 1.60 with a mean value of 1.1 was used.
NOTE: The colloidal source term is added to the dissolved source term to arrive at a total source term. Mineral fragments were provided with distributions, but the maximum was used as described in Appendix SOTERM (Section SOTERM.7.1.3). Humic proportionality constants for III, IV, and V were provided with distributions, but only the Castile Am(III) and Pu(III) were sampled.

The concentrations of colloidal actinides indicated in this section are assumed to be concentrations of actinides mobilized on colloidal particles. The indicated concentrations will be entrained in moving brine. For conservatism, it is assumed that no actinides sorb onto colloidal particles that are not mobile in the repository. Thus all actinides in the repository will be present in the solid phase, dissolved in the aqueous phase, or as colloidal actinides suspended in the aqueous phase.

When actinide inventory in a model cell is sufficient, the concentration of colloidal actinides will be at the values indicated in Table 6-12. The total concentration of an actinide in solution and suspension is limited by the amount of solid available to dissolve from the inventory. This condition is called inventory-limited when it occurs.

Colloid concentrations are calculated by the source term procedure described in Appendix SOTERM (Sections SOTERM.7.1.4 and SOTERM.7.2). Processes affecting the transport of colloids in the Culebra are addressed in Section 6.4.6.2.2.

6.4.4 Shafts and Shaft Seals

The four shafts connecting the repository to the surface are represented in performance assessment with a single shaft, represented by Regions 2 through 11 on Figures 6-13 and 6-14. This single shaft has a cross section and volume equal to the total cross section and volume of the four real shafts it represents and is separated from the waste disposal regions in the model by the true north-south distance from the waste to the nearest shaft (the Waste Shaft). Upon closure of the repository, the shafts will be sealed as described in Section 3.3.1. The seal system is represented in performance assessment by discretizing 11 model regions in the shaft. These regions are as follows: an earthen fill region above the Rustler; a compacted clay column in the Rustler; an asphalt region at the top of the Salado; three concrete sections within the Salado; an upper Salado compacted clay column; a thick section of compacted crushed salt; a lower Salado compacted clay column separated into upper and lower segments; and a concrete monolith at the repository horizon (see Appendix SEAL, Section 4 and Appendix A). The concrete components in the Salado represent the concrete asphalt waterstops in the seal system design. Seal material parameter values used in the performance assessment are provided in Table 6-13.

Conceptually, the shafts are assumed to be surrounded by a DRZ in the Salado. Within the bedded halite, the DRZ begins to form immediately after excavation and develops progressively as a function of unloading as the formation creeps toward the excavated area. From a sealing perspective, the most important characteristic of the DRZ is the higher permeability that results from dilatant deformation and the increased pore volume.

The properties of the DRZ are known to vary with the type of adjacent material, time, and depth. When the shaft seals are emplaced, back pressures will progressively develop over time as the surrounding salt creeps inward. The back pressure applied by the seal material will progressively reduce the magnitude of the stress differential, which is the source for the DRZ microfracturing mechanism. The back pressure also results in a higher mean stress, which induces healing of the DRZ. The shaft DRZ permeability will, over time, approach that of the intact halite. Also, since the creep rate of the salt surrounding the shafts depends on depth, the back pressures supplied by the seal materials will result in DRZ healing at rates that increase with depth. The relative stiffness of the seal material is a factor, as well.

In the performance assessment model, the radial extent of the DRZ around the shaft seal materials is an input parameter obtained by numerical model calculations and is corroborated by field data (see Appendix SEAL, Section 8 and SEAL Appendix C). The permeability of the DRZ around the shaft versus distance is assumed to follow a log linear relationship. Permeability of the DRZ at the shaft wall is based on experimental data collected in the air intake shaft (Dale and Hurtado 1996) and Room M (Van Pelt 1995). More information on how the DRZ is incorporated into the shaft parameters is contained in Appendix PAR (Parameter 12).

Table 6-13. Shaft Materials Parameter Values

Parameter (units)	Maximum	Minimum	Median or Constant
ALL SHAFT MATERIALS			
Residual Brine Saturation, S_{br} (unitless)	0.6	0	0.2
Residual Gas Saturation, S_{gr} (unitless)	0.4	0	0.2
Pore Distribution, λ (unitless)	8.10	0.11	0.94
Maximum Capillary Pressure (pascals)[a]	-	-	10^8
Threshold Pressure, P_t (pascals)	-	-	0
CLAY SHAFT MATERIALS			
Permeability (square meters) - Rustler Compacted Clay[b]	5×10^{-18}	1.0×10^{-21}	5×10^{-19}
Permeability (square meters) - Upper Salado Compacted Clay[b]	5×10^{-18}	1.0×10^{-21}	5×10^{-19}
Permeability (square meters) - Lower Salado Compacted Clay[b]	5×10^{-18}	1.0×10^{-21}	5×10^{-19}
Permeability (square meters) - Bottom Clay[b]	5×10^{-18}	1.0×10^{-21}	5×10^{-19}
Thickness (meters) - Rustler Compacted Clay	-	-	94.3
Thickness (meters) - Upper Salado Compacted Clay	-	-	104.85
Thickness (meters) - Lower Salado Compacted Clay	-	-	23.9
Thickness (meters) - Bottom Clay	-	-	9.24
Effective Porosity (percent) - All Clays	-	-	24.0
Pore-Volume Compressibility (1/pascals) - Rustler Compacted Clay	-	-	1.96×10^{-9}
Pore-Volume Compressibility (1/pascals) - Upper Salado Compacted Clay	-	-	1.81×10^{-9}
Pore-Volume Compressibility (1/pascals) - Lower Salado Compacted Clay and Bottom Clay	-	-	1.59×10^{-9}
SALT SHAFT MATERIAL			
Permeability (square meters) - Salt[b]	2×10^{-18}	1×10^{-23}	5.4×10^{-21}
Thickness (meters) - Salt	-	-	171.37
Effective Porosity (percent) - Salt	-	-	5.0
Pore-Volume Compressibility (1/pascals) - Salt	-	-	1.60×10^{-9}
CONCRETE SHAFT MATERIALS			
Permeability (square meters) - Concrete (T < 400 years)	1×10^{-17}	1×10^{-23}	1.78×10^{-19}
Permeability (square meters) - Concrete (T > 400 years) and Concrete Monolith	-	-	1×10^{-14}
Thickness (meters) - Concrete	-	-	45.72
Thickness (meters) - Concrete Monolith	-	-	9.08
Effective Porosity (percent)	-	-	5.00
Threshold Pressure P_t (pascals) - All Concrete[a]	-	-	0
Pore-Volume Compressibility (1/pascals) - All Concrete	-	-	2.64×10^{-9}

Table 6-13. Shaft Materials Parameter Values (Continued)

Parameter (units)	Maximum	Minimum	Median or Constant
ASPHALT SHAFT MATERIAL			
Permeability (square meters) - (T = 0 - 10,000 years)	10^{-18}	10^{-21}	10^{-20}
Thickness (meters)	-	-	37.28
Effective Porosity (percent)	-	-	1.00
Pore-Volume Compressibility (1/pascals)	-	-	2.97×10^{-8}
EARTHEN FILL MATERIAL ABOVE RUSTLER			
Permeability (square meters) (T = 0 - 10,000 years)	-	-	1×10^{-14}
Thickness (meters)	-	-	165.06
Effective Porosity (percent)	-	-	32.0
Pore-Volume Compressibility (1/pascals)	-	-	3.1×10^{-8}

[a] Capillary pressure for all shaft materials is set to 0.
[b] These values represent the permeabilities of the seal material without the surrounding DRZ incorporated. See Appendix IRES, Section IRES.2, for time-dependent values.

The DRZ surrounding the shaft is not represented explicitly in the BRAGFLO mesh (Figures 6-13 to 6-15). Rather, the mesh has been simplified to represent only the cross-sectional area of the four WIPP shafts, and the permeability values for the various seal components at different times have been adjusted to account for the presence of the shaft DRZ. This adjustment, which yields effective permeabilities, can be done because in Darcy flow the flux through a porous medium is a linear function of the product of the permeability of the medium and the cross-sectional area across which flow occurs. Thus, the flux that would occur through a shaft and its surrounding DRZ can be modeled equivalently using the shaft cross-sectional area with a higher seal component permeability. Equations for the derivation of the effective permeabilities are given in Appendix PAR (Parameter 12) and Appendix IRES (Section IRES.2). The permeabilities of shaft components are calculated in the SCMS (see Section 6.4.11) from LHS parameter values according to these equations. Appendix IRES (Section IRES.2) shows calculated shaft component effective permeabilities.

6.4.5 The Salado

The Salado is the principal natural barrier to fluid flow between the waste disposal panels and the accessible environment. Fluid flow in natural conditions in the Salado is discussed in Section 2.2.1.3. Excavation of the repository has altered natural pressure gradients in the Salado, creating the potential for fluid flow into the excavation. Fluid flow, gas generation, and volume changes from creep closure cause changes in pressure gradients through time. Salt creep, as well as possible fracturing from high repository pressure, alters the permeability and other flow properties of the rock near the repository. Depending on pressure gradients

developed and altered material properties, gas and brine flow may be enhanced in affected portions of the Salado.

For performance assessment, the DOE conceptualizes the Salado as a porous medium composed of several rock types arranged in layers, through which flow occurs according to Darcy's law. Two rock types, impure halite and anhydrite, are used to represent the intact Salado. Once sampled, model parameters for all layers are uniform and constant, with two exceptions, porosity and permeability. Conceptually, this assumption of constant properties is based on observations of compositional and structural regularity in layers exposed by the repository and on the inference that there is little variation in large-scale averages of rock or flow properties across the disposal system. For several meters above and below the repository, a DRZ has increased permeability compared to intact rock and offers little resistance to flow between anhydrite interbeds and the repository. In all rock units, porosity can vary from initial values due to compressibility, depending on pressure changes in a computational grid block. As discussed in Section 6.4.5.2, a model has been implemented in interbeds to simulate the effects of fracturing caused by high repository pressure as pore pressure approaches or exceeds lithostatic.

Specific information about the three submodels used to represent impure halite, Salado interbeds, and the DRZ is presented in the following sections.

6.4.5.1 Impure Halite

The DOE uses a single porous medium with spatially constant rock and hydrologic properties (Region 19 in Figures 6-13 and 6-14) in performance assessment to represent intact, halite-rich layers in the Salado and minor interbeds contained within those layers that are not explicitly represented. A comparison has been made between the simplified stratigraphy used in the performance assessment model and a model with a more detailed stratigraphy in the vicinity of the repository; this comparison supports use of the stratigraphic representation used for performance assessment. This model comparison is described in Christian-Frear and Webb (1996).

Gas may not be able to flow through intact, halite-rich strata of the Salado under realistic conditions for the repository. Gas flow in liquid-saturated rock depends on the gas pressure required to overcome capillary resistance to initial gas penetration and development of interconnected gas pathways that allow gas flow (threshold pressure). While the permeability of halite is known to be low, its threshold pressure has never been measured. An empirical relationship between threshold pressure and permeability in non-WIPP rocks (Davies 1991, 17 – 19) suggests that threshold pressure will be sufficiently high that gas will not be able to flow through the halite-rich strata of the Salado under any conditions foreseeable for the WIPP (see Appendix MASS, Section MASS.13.1). Values used by the DOE for halite threshold pressure are consistent for generic material of low permeability and prevent the flow of gas into the impure halite regions (Table 6-14). This is a conservative assumption because gas flow in halite would decrease the pressure in the repository and the driving force available for flow elsewhere. Table 6-14 shows various parameter values used in modeling the Salado

impure halite. Additional information on parameter values is contained in Appendix PAR (Parameters 17 through 19 and Table PAR-32).

Table 6-14. Salado Impure Halite Parameter Values

Parameter (units)[a]	Maximum	Minimum	Median or Constant
Permeability (square meters)	10^{-21}	10^{-24}	3.16×10^{-23}
Effective Porosity (percent)	3.0	0.10	1.0
Threshold Pressure, P_t (pascals)[b]	1.13×10^{8}	1.03×10^{7}	3.41×10^{7}
Residual Brine Saturation, S_{br} (unitless)	-	-	0.3
Residual Gas Saturation, S_{gr} (unitless)	-	-	0.2
Pore Distribution Parameter, λ (unitless)	-	-	0.7
Maximum Capillary Pressure (pascals)	-	-	10^{8}
Rock Compressibility (1/pascals)[c]	1.92×10^{-10}	2.94×10^{-12}	9.75×10^{-11}

[a] See Table 6-9 for fluid properties.
[b] Threshold pressure (P_t) determined from the relationship: $P_t = PCT\_A \cdot k^{PCT\_EXP}$ where PCT_A and PCT_EXP are constants and k is the permeability.
[c] Pore compressibility = Rock compressibility/effective porosity.

6.4.5.2 Salado Interbeds

Three distinct anhydrite interbeds are modeled in BRAGFLO, representing MB138 (Region 20 in Figures 6-13 and 6-14), anhydrite layers a and b (Region 21), and MB139 (Region 28). The three intact interbeds have the same set of model parameters, and the parameters are initially spatially constant. Porosity and permeability can vary spatially during a simulation depending on the extent of interbed fracturing. The interbeds differ only in position and thickness.

The three interbeds explicitly represented in the BRAGFLO model are included because they exist in the disturbed region around the repository within which fluid is expected to be able to flow with relative ease compared to the surrounding formation. MB139 and anhydrite layers a and b are present within the DRZ that forms around excavations. MB138 is included along with a thick DRZ because of uncertainty in the extent and properties of the DRZ and the associated long-term isolation of MB138 from the repository.

In BRAGFLO, brine flows between the Salado and the repository in response to fluid potential gradients that may form over time. Because of the low permeability of the impure halite and relatively small surface area involved, direct brine flow between the impure halite and the repository is relatively small. The interbeds included in the BRAGFLO model of the Salado (Regions 20, 21, and 28), however, can serve as conduits for brine flow between the impure halite and the repository. Conceptually, brine flows laterally along higher permeability interbeds towards or away from the repository and vertically between the interbeds and the

lower permeability halite. Because the interbeds have a very large contact area with adjacent halite-rich rock, even a very small flux from the halite into the interbeds (for brine inflow) or to the halite from the interbeds (for brine outflow) can accumulate into a significant quantity of brine. In this manner, halite serves as a source or sink for brine in the repository. It is expected that, because of density differences between gas and brine and their stratification within the repository, brine outflow will be dominantly in MB139, and gas outflow will occur in anhydrite a and b or MB138. However, the model does not preclude other flow patterns.

Interbeds contain natural fractures that may be partially healed. If high pressure is developed in an interbed, its preexisting fractures may dilate or new fractures may form, altering its porosity and permeability. Pressure-dependent changes in permeability are supported by experiments conducted in the WIPP underground and in the laboratory (Beauheim et al. 1993). Accordingly, the DOE has implemented in BRAGFLO a porous-media model of interbed dilation and fracturing that causes the porosity and permeability of a computational cell in an interbed to increase as its pore pressure rises above a threshold value. Model details are presented in Appendix BRAGFLO (Section 4.10) and Appendix MASS (Section MASS.13.3). To the extent that it occurs, dilation or fracturing of interbeds is expected to increase the transmissivity of interbed intervals. The threshold pressure of dilated or fractured interbeds is expected to be low because apertures of the fractures increase; thus, fluid is expected to be able to flow outward readily if adequate pressure is available to dilate the interbeds.

The model used to simulate the effects of interbed dilation or fracturing is explained in detail in Appendix BRAGFLO (Section 4.10). In summary, it assigns a fracture initiation pressure above the initial pressure at which local fracturing takes place, and changes in permeability and porosity occur above this pressure. Below this fracture initiation pressure, an interbed has the permeability and compressibility assigned by LHS and representative of intact rock. Below the fracture initiation pressure, the initial sampled porosity is modified slightly with pressure caused by compressibility. Above the fracture initiation pressure, the local compressibility of the interbed is assumed to increase linearly with pressure. This greatly increases the rate at which porosity increases with increasing pore pressure. Additionally, permeability increases by a power function of the ratio of altered porosity to initial porosity. For numerical reasons (that is, to prevent unbounded changes in parameter values that would create numerical instabilities in codes), a pressure is specified above which porosity and permeability change no further.

Parameters associated with the interbeds are shown in Table 6-15. Table 6-16 lists parameters used in the model of interbed dilation and fracture. Additional information about interbed parameters is included in Appendix PAR (Table PAR-36 and Parameters 20 through 25).

Table 6-15. Parameter Values for Salado Anhydrite Interbeds a and b, and MB138 and MB139

Parameter (units)[a]	Maximum	Minimum	Median or Constant
Permeability (square meters)	7.94×10^{-18}	10^{-21}	1.29×10^{-19}
Effective Porosity (percent)	-	-	1.1
Threshold Pressure, P_t (pascals)[b]	5.28×10^{6}	2.32×10^{5}	9.74×10^{5}
Residual Brine Saturation, S_{br} (unitless)	0.174	0.007846	0.084
Residual Gas Saturation, S_{gr} (unitless)	0.197	0.014	0.077
Pore Distribution Parameter, λ (unitless)	0.842	0.491	0.644
Maximum Capillary Pressure (pascals)	-	-	10^{8}
Rock Compressibility (1/pascals)[c]	2.75×10^{-10}	1.09×10^{-11}	8.26×10^{-11}
Brine Far-Field Pore Pressure at elevation of MB139 and shaft intersection (pascals)	13.9×10^{6}	11.0×10^{6}	12.5×10^{6}

[a] See Table 6-9 for fluid properties.
[b] Threshold pressure (P_t) determined from the relationship: $P_t = PCT\_A \cdot k^{PCT\_EXP}$ where PCT_A and PCT_EXP are constants and k is the permeability.
[c] Pore compressibility = Rock compressibility/effective porosity.

Table 6-16. Fracture Parameter Values for Salado Anhydrite Interbeds a and b, and MB138 and MB139

Parameter (units)	Constant
Fracture Initiation Pressure at MB139, base of shaft (pascals)	12.7×10^{6}
Increment to give Full Fracture Porosity (percent), MB139 and MB138[a]	3.9
Increment to give Full Fracture Porosity (percent), Anhydrite a and b[a]	23.9
Full Fracture Permeability (square meters)	10^{-9}
Increment above Fracture Initiation Pressure to Obtain Full Fracture Pressure (pascals)[a]	3.8×10^{6}

[a] A fitting parameter to yield desired dilation over a variation in pressure.

6.4.5.3 DRZ

In the DRZ (Region 22 in Figures 6-13 and 6-14) near the repository, permeability and porosity are expected to generally increase in both halite and interbeds. These increases are due to a variety of processes. Creep closure and stress-field alterations as the result of the excavation are the dominant causes, similar to the processes discussed for the formation of the DRZ around the shaft (see Section 6.4.4). The increases in permeability and porosity in interbeds are not expected to be completely reversible with creep closure of the disposal rooms. The increase in DRZ permeability increases the ability of fluid to flow from interbeds to the waste disposal region. The increase in DRZ porosity provides a volume in which some

fluid could be retained so that it does not contact waste, or slows actinide movement. Performance assessment approximates the effects of the DRZ conservatively with respect to brine flow to the repository (see Appendix MASS, Section MASS.13.4). In the model, the permeability of this region is increased relative to intact Salado rock for the duration of a realization. The porosity of the modeled DRZ is increased by a fixed value of 0.0029 (0.29 percent) above the sampled intact Salado impure halite. The modeled DRZ extends above and below the repository from the base of MB138 to MB139. The performance assessment treatment of the DRZ creates a permanent high-permeability region that does not significantly impede flow between the repository and affected interbeds. Table 6-17 shows parameter values used in the performance assessment representation of the DRZ.

Table 6-17. DRZ Parameter Values

Parameter (units)[a]	Maximum	Minimum	Median or Constant
Permeability (square meters)	-	-	10^{-15}
Effective Porosity (percent)[b]	-	-	1.29
Threshold Pressure, P_t (pascals)	-	-	0
Residual Brine Saturation, S_{br} (unitless)	-	-	0
Residual Gas Saturation, S_{gr} (unitless)	-	-	0
Pore Distribution Parameter, λ (unitless)	-	-	0.7
Maximum Capillary Pressure (pascals)	-	-	10^8
Rock Compressibility (1/pascals)[c]	-	-	7.41×10^{-10}

[a] See Table 6-9 for fluid properties.
[b] The DRZ effective porosity value for each realization is equivalent to the sampled value for the Salado halite plus 0.0029 (0.0029 is the difference between the medians for the DRZ and the halite).
[c] Pore compressibility = rock compressibility/effective porosity.

6.4.5.4 Actinide Transport in the Salado

Actinide transport in the Salado is considered by the DOE to be a possible mechanism for release to the accessible environment. As in other areas of the disposal system, actinides in the Salado may be transported as dissolved species or as colloidal particles. Actinide transport is affected by a variety of processes that may occur along the flow path.

The DOE uses the NUTS code (see Appendix NUTS) to model the migration of radionuclides in the repository and surrounding formations. NUTS models radionuclide transport within all regions for which BRAGFLO computes brine and gas flow, and uses as input for each realization the corresponding BRAGFLO velocity field, pressures, porosities, saturations, and other model parameters including, for example, the geometrical grid, residual saturation, material map, and compressibility.

NUTS is used in two ways in the performance assessment. First, the code is used in a computationally fast tracer mode to identify those BRAGFLO realizations for which it is not necessary to do full transport calculations because contaminated brine never reaches the top of the salt or the accessible environment within the Salado. Such realizations have no potential to contribute to the total integrated release of radionuclides from the disposal system. If the tracer calculation indicates a possibility of consequential release, a computationally slow calculation of the full transport of each radionuclide is performed.

6.4.5.4.1 NUTS Tracer Calculations

All BRAGFLO realizations are evaluated using NUTS in a tracer mode to identify those realizations for which there is no possibility of radionuclides reaching the accessible environment. The tracer simulations consider an infinitely soluble, nondecaying, nondispersive, and nonsorbing species as a tracer element. The tracer is given a unit concentration in all waste disposal areas of 1 kilogram per cubic meter. If this tracer does not reach the selected boundaries (the top of the Salado and the land withdrawal boundary within the Salado) in a cumulative mass greater than or equal to 10^{-7} kilograms within 10,000 years, then it is assumed that there is no consequential release to these boundaries. If a cumulative mass greater than or equal to 10^{-7} kilograms does reach the selected boundaries within 10,000 years, a complete transport analysis is conducted. The value of 10^{-7} kilograms is selected because, regardless of the isotopic composition of the release, it corresponds to a normalized release less than 10^{-6} EPA units, which is the smallest release displayed in CCDF construction. The largest normalized release corresponding to 10^{-7} kilograms would occur if the release were entirely ^{241}Am and would be 9.98×10^{-7} EPA units.

6.4.5.4.2 NUTS Transport Calculations

For those BRAGFLO realizations with greater than 10^{-7} kilograms reaching the boundaries in the tracer calculations, NUTS models the transport of five different species of radionuclides (^{241}Am, ^{239}Pu, ^{238}Pu, ^{234}U, and ^{230}Th). These radionuclides represent a lumping of a larger number of radionuclides, as discussed in Appendix WCA (Sections WCA.3 and WCA.8.3). For decay purposes, radionuclides have been lumped together based on similarities to simplify the calculations, as discussed in Appendix WCA. For transport purposes, solubilities are lumped to represent both dissolved and colloidal forms. These lumpings simplify and expedite calculations.

NUTS models radionuclide transport by advection (see Appendix MASS, Section MASS.13.5). NUTS disregards sorptive and other retarding effects throughout the entire flow region. Physically, some degree of retardation must occur at some locations within the repository and the geologic media, and the disregard of retardation processes is therefore conservative. NUTS also disregards reaction-rate aspects of dissolution and colloid formation processes, and mobilization is assumed to occur instantaneously. Neither molecular nor mechanical dispersion is modeled in NUTS. These processes are assumed to be insignificant in comparison to advection, as discussed further in Appendix MASS (Section MASS.13.5).

Colloidal actinides are subject to retardation by chemical interaction between colloids and solid surfaces and by clogging of small pore throats (that is, sieving). It is expected that there will be some interaction of colloids with solid surfaces in the anhydrite interbeds. As well, because of the low permeability of intact interbeds, it is expected that pore apertures are small and some sieving will occur. However, colloidal particles, if not retarded, are transported slightly more rapidly than the average velocity of the bulk liquid flow. Because the effects on transport of slightly increased average pore velocity and retarding interactions with solid surfaces and sieving are offsetting, the DOE assumes residual effects of these opposing processes will be either small or beneficial and does not incorporate them in modeling of the transport of actinides in the Salado interbeds.

If brine that has been in the repository moves into interbeds, it is likely that mineral precipitation reactions will occur. Precipitated minerals may contain actinides as trace constituents. The beneficial effects of the possible mineral co-precipitation process are neglected in performance assessment. Furthermore, colloidal-sized precipitates will behave like mineral-fragment colloids, which are destabilized by brines, quickly agglomerate and settle by gravity. The beneficial consequence of colloid precipitation is disregarded in performance assessment also.

Additional processes that may impact transport in Salado interbeds are related to fractures, channeling, and viscous fingering. Interbeds contain natural fractures. Because of the low permeability of unfractured anhydrite, it is expected that most fluid flow occurring in interbeds will occur in fractures. Even though some properties of naturally fractured interbeds are characterized by in-situ tests (see Section 2.2.1.3), other uncertainty exists in the characteristics of the fracture network that may be created if gas pressure in the repository becomes high. The performance assessment modeling system accounts for the possible effects on porosity and permeability of fracturing through the implementation of a fracturing model (see Section 6.4.5.2). It is considered that the processes and effects associated with fracture dilation or fracture propagation that are not already captured by the performance assessment fracture model will be negligible (see Appendix MASS, Section MASS.13.3 and MASS Attachment 13.2). Of those processes not already incorporated, channeling is considered to have the greatest potential effect.

Channeling is the movement of fluid through the larger aperture portions of a fracture network (that is, areas of local high permeability). It could locally enhance actinide transport. However, it is assumed that the effects of channeled flow in existing or altered fractures will be negligible on the scale of the disposal system. The DOE believes this assumption to be reasonable because processes that act to limit the effectiveness of channels or disperse actinides in them are likely to occur. First, if gas is present in the fracture network, it will be present as the nonwetting phase and will occupy the portions of the fracture network with relatively large apertures, where the highest permeabilities will exist locally. The presence of gas thus removes the most rapid transport pathways from the contaminated brine and decreases the impact of channeling. Second, brine penetrating the Salado from the repository is likely to be completely miscible with in-situ brine. Because of miscibility, diffusion or other

local mixing processes will probably broaden fingers (reduce concentration gradients) until the propagating fingers are indistinguishable from the advancing front.

It is expected that gas will penetrate the liquid-saturated interbeds as a fingered front rather than as a uniform front. Fingers form because of the difference in viscosity between the invading fluid (gas) and the resident fluid (liquid brine), and because of channeling effects. This process does not affect actinide transport, however, because actinides of interest are transported only in the liquid phase, and the liquid phase will not displace gas in the relatively high-permeability regions because of capillary effects.

6.4.6 Units Above the Salado

The geology and hydrology of units above the Salado are discussed in Sections 2.1.3 and 2.2.1.4, respectively. In this section, the assumptions, simplifications, and models used in performance assessment modeling of these units are described. Because it is unlikely that these units will be impacted by undisturbed performance, modeling of these units is performed mainly because regulations require consideration of the effects of inadvertent human intrusions. See Appendix MASS (Section MASS.14) for additional discussion on the units above the Salado.

The principal purpose of BRAGFLO calculations for units above the Salado is to determine the quantity of brine entering each unit from an intrusion borehole or the shaft. It is unrealistic to assume that all flow up an intrusion borehole enters the Culebra. Accordingly, BRAGFLO parameters are specified such that brine flow from the intrusion borehole is possible not only into the Culebra but also into the Magenta, Dewey Lake, and overlying units (as well as to the ground surface), depending on whether liquid rises above the Culebra in the intrusion borehole. Some of the assumptions regarding the properties of the units above the Salado are made specifically because they allow model simplification and are conservative with respect to actinide transport in the Culebra (that is, tend to cause overestimates of release).

Consistent with accepted stratigraphic conventions for the area, discussed in Section 2.1.3, the units above the Salado are subdivided into seven layers in performance assessment; these are, in order of lower-to-higher, the unnamed lower member, the Culebra, the Tamarisk, the Magenta, the Forty-niner, the Dewey Lake, and the units above the Dewey Lake. The conceptual model for each of these layers is described sequentially in the following sections.

A fundamental assumption in the conceptual model used in performance assessment for modeling actinide transport to the accessible environment in units above the Salado is that lateral actinide transport through rock formations is possible within the next 10,000 years only in the Culebra. This assumption is appropriate for several reasons relating to the properties of the other rock units and the groundwater basin conceptual model, which are discussed in following sections.

Section 2.2.1.4 describes the hydrology of the units above the Salado in terms of the groundwater basin conceptual model. Insight into the processes occurring in the groundwater basin obtained by modeling and other lines of evidence indicates that significant simplification of the hydrologic models in the units above the Salado is possible to obtain reasonable estimates of actinide transport (see Corbet and Knupp 1996; Appendix MASS, Section MASS.14.2). Therefore, the DOE calculates actinide transport in the units above the Salado with a two-dimensional conceptual and mathematical model. The models used for actinide transport in the units above the Salado are a simplified implementation of the groundwater basin conceptual model. The mathematical model is implemented in the computer codes SECOFL2D and SECOTP2D.

6.4.6.1 Unnamed Lower Member

The unnamed lower member of the Rustler (Region 18 in Figures 6-13 and 6-14) rests above the Salado. Its transmissivity has been measured (see Section 2.2.1.4.1.1) and was found to be low, which is consistent with expectations based on its anhydrite, gypsum, halite, clay, and siltstone composition (see Section 2.1.3.5.1). In performance assessment, this member is treated as impermeable, which prevents liquid flow and actinides from entering this unit. The DOE assumes that because of the low permeability of the unnamed lower member, any brine entering it adjacent to an intrusion borehole would be contained well within the site boundary for more than 10,000 years. Therefore, this treatment is conservative, regarding estimated releases into the Culebra, because allowing flow from a borehole or shaft into the unnamed lower member would, if anything, decrease flow into the Culebra. This would have a tendency to reduce the release of actinides from the Culebra to the accessible environment. In performance assessment, the thickness of the unnamed lower member is 118 feet (36 meters), and its permeability is zero.

6.4.6.2 The Culebra

The Culebra is represented in BRAGFLO as Region 17 in Figures 6-13 and 6-14. The model geometries for Culebra flow calculations and transport calculations are discussed in this section. Boundary and initial conditions for this geometry are discussed in Section 6.4.10.2. Supplementing the discussion in this section are additional details about the Culebra modeling provided in Section 6.4.13 and Appendices SECOFL2D, SECOTP2D, MASS (Section MASS.15), and TFIELD (Sections TFIELD.2.2 and TFIELD.4).

Conceptually, radionuclides might be introduced into the Culebra through brine flow up the sealed shafts. However, the chief source of actinides in the Culebra is modeled as long-term releases from a borehole that intersects the repository. If radionuclides are introduced into the Culebra, they may be transported from the point of introduction by groundwater flowing naturally through the Culebra.

The Culebra is conceptualized as a horizontal, confined aquifer. For fluid flow, it is conceptualized as a heterogeneous porous medium which is represented by variations in transmissivity. A heterogeneous velocity field is used for transport calculations, but all other rock properties are conceptualized as constant (homogeneous) across the model area. The Culebra is conceptualized as having two types of porosity; a portion of the porosity is associated with high-permeability features where transport occurs by advection, and the rest of the porosity is associated with low-permeability features where flow does not occur and retardation occurs by physical processes (diffusion) and chemical processes (sorption). This type of conceptual model is commonly referred to as double-porosity. In this conceptual model, transport and retardation of colloidal particles is also considered. In this section, the principal topic will be fluid flow in the Culebra. The transport and retardation of dissolved actinides will be discussed principally in Section 6.4.6.2.1. The transport and retardation of colloidal particles will be discussed principally in Section 6.4.6.2.2.

In the Culebra conceptual model used in performance assessment, the spatial distribution of transmissivity in the Culebra is important. Other potentially important processes acting on Culebra flow and transport are climate change (Section 6.4.9 and Appendix MASS, Section MASS.17) and the effects of subsidence caused by potash mining in the McNutt (Section 6.4.6.2.3 and Appendix MASS, Section MASS.15.4).

The SECOFL2D code uses two-dimensional horizontal grids to simulate groundwater flow. A regional grid approximately 14 miles by 19 miles (22 kilometers by 30 kilometers) with spatially varying transmissivity (Figure 6-17) is used to determine the flow fields in the WIPP region resulting from hydraulic head distributions that are controlled by distant topographic and hydrologic features (that is, boundary conditions). Because this grid is used to define the boundary conditions for the flow and transport calculations, it is discussed in detail in Section 6.4.10.2, together with the specification of initial and boundary conditions. For transport in the region of interest within the disposal system, a local grid 4 miles by 4 miles (7 kilometers by 7 kilometers) with finer discretization is used in both SECOFL2D and SECOTP2D (Figure 6-18). Boundary heads and fluxes for the local grid are obtained by interpolation from the regional flow field. The grid for the local domain contains 75 columns and 65 rows, resulting in 4,875 grid blocks.

Boundaries of the local domain were chosen to capture important flow paths and facilitate the computation of integrated release to the accessible environment. Because past analyses have indicated that transport in the Culebra will occur within a region that lies from southeast of the repository to west of the repository, the local domain extends slightly beyond the southern and western boundaries of the controlled area. Because it is not needed, a strip in the northern portion of the controlled area has been omitted from the local domain to ease the computational burden.

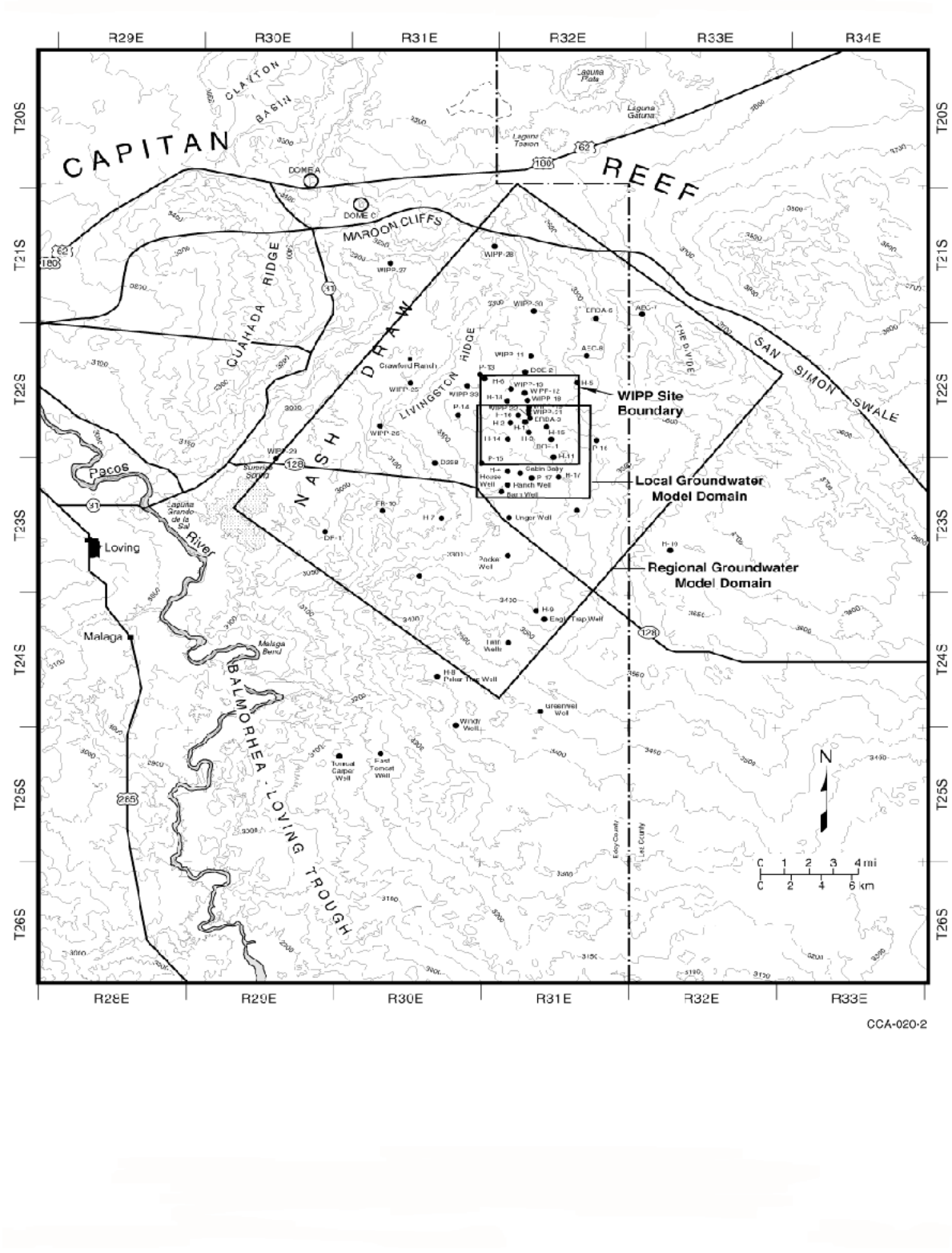

Figure 6-17. The Regional and Local Domains Used in the Horizontal Groundwater Model of the Culebra

1 **THIS PAGE INTENTIONALLY LEFT BLANK**

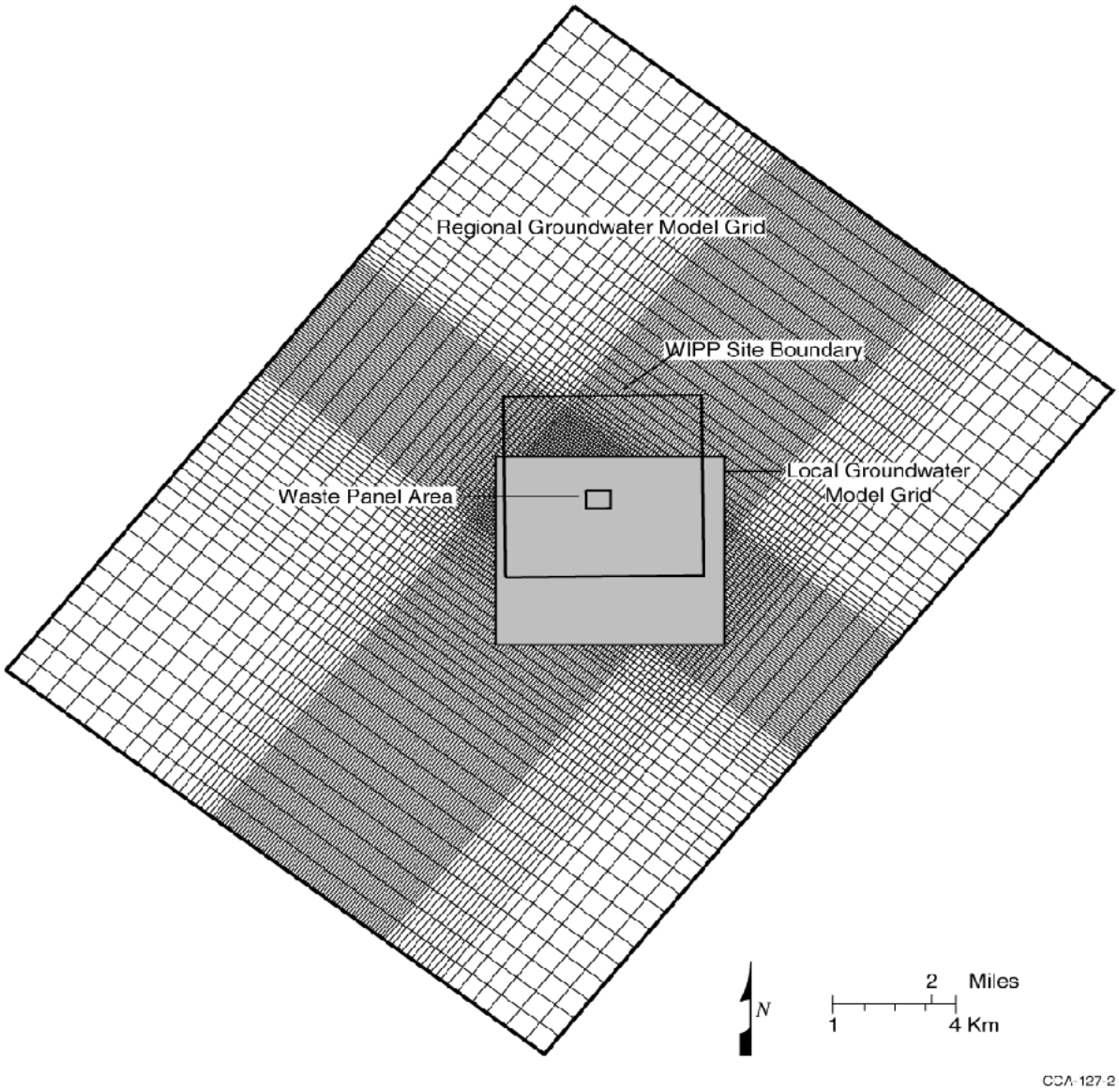

Figure 6-18. The Discretization Used in Modeling Groundwater Flow in the Culebra

THIS PAGE INTENTIONALLY LEFT BLANK

Flow directions and transmissivities in the Culebra vary significantly from location to location to a considerable distance from the site boundary. Consequently, the effects of flow in the region around the WIPP site are considered important in the conceptual model. The boundaries to the flow model are discussed in Section 6.4.10.2; the grid itself is shown in Figure 6-18.

The conceptual model for the Culebra assumes that fluid fluxes and directions in the future will be the same as they are projected to be at repository closure, unless future mining within the site occurs, in which case changes to fluid flow are calculated. A steady-state flow field is used to represent this assumption. Conditions assumed at site closure are the subsidence effects of mining in the near future outside the site boundary, climate change, and a reasonable estimate of the hydraulic conditions that existed prior to disturbances to the Culebra caused by site characterization activities (see Appendix MASS, Sections MASS.15.4 and MASS.14.2, and Appendix TFIELD, Section TFIELD.2.2).

The factors controlling fluid flow in the Culebra are conceptualized to be the hydraulic gradient, transmissivity distribution, and porosity. The hydraulic gradient and transmissivities used in performance assessment are coupled because they are calibrated to observed conditions by a process described in Appendix TFIELD (Section TFIELD.3). Flow fields are calculated with the code SECOFL2D using an assumption of homogeneous porosity in the Culebra. This single value is the total porosity for the Culebra, including both advective and diffusive porosity, as discussed below. Use of a single porosity for the flow calculation does not introduce inconsistency with transport calculations because (1) steady-state flow fields are used so flux through the system is not dependent on porosity, and (2) the velocity of liquid for transport is calculated based on a double-porosity model implemented in the code SECOTP2D. Thus, the important factors for flow calculations are the hydraulic gradient and transmissivity variation.

Because BRAGFLO models a vertical section of the disposal system, the spatial distribution of transmissivity cannot be represented in the BRAGFLO grid. The source term of actinides in the Culebra is calculated in part from BRAGFLO flow fields, so parameters for the Culebra are required in BRAGFLO. Specifically, a single value of Culebra permeability representative for the Culebra in the area immediately over the waste-emplacement panels is input to partition fluid flow among the stratigraphic units along the human-intrusion borehole.

BRAGFLO calculates gas flow and brine flow that may occur up a borehole (see Section 6.4.7). The SECO codes model flow of the liquid phase only. The possible effects of gas on Culebra flow are not modeled in the SECO codes. This simplification is reasonable because after gas pressure is relieved by flow to the surface during drilling, little gas will remain in the repository. This gas will move up the borehole at low rates and tend to move directly to the top of the liquid-saturated section of the borehole, bypassing the Culebra. Any gas that does enter the Culebra will tend to displace brine from fractures and reduce the potential for actinide transport. Based on previous modeling (Lappin et al. 1989, Appendix E.1.5.1), the effect of the mass of brine being injected into the Culebra on the natural flow in the Culebra is negligible. Parameter values used in BRAGFLO to describe the Culebra are shown in

Table 6-18. Parameter values used in SECOFL2D are shown in Table 6-19. See Appendix PAR (Table PAR-30) and relevant Culebra parameter sheets, for additional information.

Table 6-18. Culebra Parameter Values for the BRAGFLO Model

Parameter (units)[a]	Value
Permeability (square meters)	2.1×10^{-14}
Effective Porosity (percent)	15.1
Rock Compressibility (1/pascals)[b]	10^{-10}
Threshold Pressure, P_t (pascals)[c]	1.5×10^{4}
Residual Brine Saturation, S_{br} (unitless)	0.084
Residual Gas Saturation, S_{gr} (unitless)	0.077
Pore Distribution Parameter, λ (unitless)	0.644
Maximum Capillary Pressure (pascals)	10^{8}
Thickness (meters)	7.70
Initial Pressure (pascals)	8.22×10^{5}

[a] See Table 6-9 for fluid properties in BRAGFLO.
[b] Pore compressibility = rock compressibility/effective porosity.
[c] Threshold pressure (p_t) determined from relationship: $P_t = PCT\_A \cdot k^{PCT\_EXP}$, where PCT_A and PCT_EXP are constants and k is the permeability.

Table 6-19. SECO Fluid Properties

Parameter (units)	Value
Liquid Density (kilograms per cubic meter)	1,000
Liquid Compressibility (1/pascals)	4.4×10^{-10}

Three different thicknesses of the Culebra have been assumed in performance assessment modeling. BRAGFLO uses a thickness of 25.3 feet (7.7 meters), representative of the Culebra over the waste disposal panels. For calibrating transmissivity fields (see Appendix TFIELD, Section 4.4.1) and calculating flow in the Culebra with SECOFL2D, a thickness of 25.4 feet (7.75 meters) is assumed, consistent with an average thickness over the area modeled. For transport calculations using the code SECOTP2D, a thickness of 13 feet (4 meters) is assumed, consistent with observations of the thickness of the Culebra active in transport, which are discussed in Section 6.4.6.2.1. Use of different thicknesses does not introduce inconsistencies in the modeling, however, because the transmissivities used in these codes are consistent, and it is this parameter that governs the total flux of fluid through the Culebra. Furthermore, the fluid flux used in the SECOTP2D model is the same as that calculated by SECOFL2D, ensuring consistency.

The spatial variation in transmissivity observed in the Culebra is incorporated by assigning different transmissivity values to every computational cell in the model. Because there is uncertainty in the estimated value of Culebra transmissivity in areas where measurements have not been made, a large set of transmissivity fields is developed. Each transmissivity field is a statistical representation of the natural variation in transmissivity that honors measured data according to certain criteria. For a set of transmissivity fields generated with identical constraints, each field is equally likely to represent actual conditions. Monte Carlo simulations using a large number of equally-likely transmissivity fields is a statistically sound method of characterizing the uncertainty associated with transmissivity in the Culebra. For details of the generation and use of transmissivity fields, refer to Appendix TFIELD (Section TFIELD.4.1).

Regional flow directions and fluxes are calculated with the regional domain, as described earlier and shown in Figures 6-17 and 6-18. For increased resolution of transport processes in the region where transport is important, a finer grid is used. Consistency between the flow calculated in the regional domain and flow in the local domain is important, and is assured by interpolation of the boundary conditions and transmissivity field properties of the regional domain onto the local domain. This process of calculating two flow fields with domains of different extent and different resolution is implemented for practical reasons only. It is a method of incorporating regional effects in finely discretized local flow fields that has relatively low computational burden, compared to other possible methods. Additional discussion of this process is provided in Section 6.4.10.2.

In summary, flow in the Culebra is calculated with the code SECOFL2D, using a conceptual model of a horizontal confined aquifer, regional flow effects, uniform porous media, steady state, and transmissivity variation. In addition, the effects of subsidence caused by potash mining in the McNutt are incorporated during the flow calculation, as discussed in Section 6.4.6.2.3.

6.4.6.2.1 Transport of Dissolved Actinides in the Culebra

Actinides may be introduced into the Culebra by brine flowing up a borehole or by brine flowing up the shaft. Three principal processes have been demonstrated to occur naturally that affect the transport and retardation of dissolved actinides. Dissolved actinides will be carried by advection in the natural flow of Culebra groundwater. Dissolved actinides will diffuse into the matrix. Dissolved actinides will sorb to varying extents onto the different minerals lining pore walls or fractures. It is possible that dissolved actinides may participate as trace constituents in reactions between water and rock and be bound up in newly formed minerals, but this phenomenon is not included in the conceptual model. These processes are complicated to characterize because of known stratigraphic variation in the Culebra and expected heterogeneity in solution chemistry along the possible flow paths from the injection point to the accessible environment.

The basic stratigraphy of the Culebra is continuous across the WIPP site (Appendix FAC, Section FAC.4.1.2), and it contains layers with significantly different properties (Holt and

Powers 1984, 1986, 1990, and Appendix FAC, Section FAC.5.2). Hydraulically, there appear to be two distinct layers in the Culebra. Mercer and Orr (1979) report the result of a tracer and temperature survey that suggests there is not significant flow in the upper 14 feet (4.3 meters) of the Culebra. Culebra hydraulic testing at well H-14 indicates generally low permeabilities but a slightly higher permeability in the upper portion (Beauheim 1987). In descriptions from the air intake shaft, Holt and Powers (1990) noted that most of the fluid produced came out of the lower portion of the Culebra. Hydraulic tests at the H-19 hydropad indicate that the permeability of the upper portion of the Culebra is significantly lower than the permeability of the lower portion. Consistent with hydraulic indicators, tracer tests conducted at H-19 confirmed that the upper portion of the Culebra makes no significant contribution to the transport of dissolved species, although it may act to retard solute transport by diffusion into it. The Culebra at the WIPP site is conceptualized as having very low permeability in the upper approximately 9.8 feet (3 meters), and variable permeability in the lower portion, which can be lower than the upper portion in regions where the Culebra as a whole is relatively impermeable. Thus, the bulk of the data indicates that the majority of the flow and transport takes place in the lower portions of the Culebra. Accordingly, for flow and transport calculations, an effective thickness of the Culebra of 13.1 feet (4 meters) is assumed.

There is considerable variability in the structure and size of porous features in the Culebra, including fractures (of a variety of dimensions and interconnectedness), vugs, interparticle and intercrystalline porosity. The principal flow occurs within those features with the high permeability, and slower flow and diffusion are primary processes in the lower permeability features. Tracer test interpretations indicate that at some locations flow occurs predominantly through fractures (advective porosity is low) and at other locations slower transport indicates that flow is occurring in other permeable features such as vugs connected by microfractures, and possibly interparticle porosity (higher advective porosity). Tracer test interpretations also indicate that matrix diffusion is an important process in high-permeability regions of the Culebra. In other words at least two scales of porosity are needed to reasonably represent the transport processes in the Culebra (that is, a double-porosity model). At some locations of low permeability, fractures may be absent or filled with gypsum. An alternative conceptual model for transport at these locations is uniform single porosity with a high porosity. To simplify calculations, the uniform single porosity model was not implemented; the double porosity model implemented results in faster transport.

In SECOTP2D, advective porosity represents the porous features in which flow occurs. Advective porosity values are low, which is representative of flow in fractures. Diffusive porosity represents those porous features in which no flow is assumed to occur and diffusion and sorption occur. Diffusive porosities are large relative to advective porosity, representative of the vugs, interparticle, and intercrystalline porosity of the bulk rock.

The processes that occur in the advective porosity portion of the Culebra are advection (flow), dispersion (spreading caused by heterogeneity), diffusion within the advective porosity, and diffusion into the diffusive porosity. Important factors in this conceptual model are the velocities of fluid in the advective porosity, free-water diffusion coefficients, and

dispersion coefficients. The most important factor is the fluid velocity. Free-water tracer diffusion coefficients are specified for actinides. Dispersive spreading at the scale of disposal-system modeling is dominated by the effects of heterogeneities explicitly incorporated in the transmissivity fields input to SECOFL2D. This eliminates the need to account for larger-scale features by specifying a dispersion coefficient for SECO modeling larger than those observed at the hydropad-test scale.

Fluid velocity in SECOTP2D is coupled to the results of the fluid flow modeling conducted with SECOFL2D on the local domain (see the preceding section). Fluid flow directions and volumetric fluxes in SECOTP2D are calculated in SECOFL2D. The flow velocities in the transport calculation are determined using the fluxes from the fluid flow calculation, the Culebra thickness specified for the transport calculation, and the advective porosity specified for the transport calculation. Because a different transmissivity field is used and the values of several important parameters are sampled, each realization uses a different velocity field. Retardation is conceptualized to be a function of physical effects of diffusion into diffusive porosity, and sorption. Diffusion is parameterized by the diffusive porosity (which can essentially be thought of as a reservoir for diffusion) tortuosity, matrix block length and free-water diffusion coefficient. Tortuosity represents the tortuous structure of the porosity within the matrix; it acts to slow the diffusion process. The matrix block length is a conceptual construct representing the ratio of the surface area between advective and diffusive porosity to the volume of diffusive porosity features; physical retardation increases as the matrix block length decreases. Physical retardation also increases if tortuosity or the free-water diffusion coefficient of diffusive porosity are larger. See Appendix MASS (Section MASS.15.2 and MASS Attachment 15-6) and Appendix SECOTP2D (Section 2, Governing Equations) for more details.

Chemical retardation of dissolved actinides is conceptualized to occur by sorption onto dolomite grains exposed in diffusive porosity because of the large amount of dolomite present in the Culebra. Chemical retardation increases if diffusive porosity is smaller because there is a larger volume of rock for sorption. Although clay minerals are present and would sorb actinides in the Culebra, their effects are not included in the conceptual model or parameter values specified. Effective properties for the rock matrix, which is assumed to be homogeneous, and solution chemistry are assumed and are incorporated directly in specification of the parameters for the retardation model (see Appendix MASS, Section MASS.15.2, and Appendix PAR, Parameters 49 through 57).

The DOE uses a linear isotherm model to represent the retardation that occurs as dissolved actinides are sorbed onto dolomite. This model uses a single parameter K_d to express a linear relationship between sorbed concentration and liquid concentration. The K_ds used in performance assessment have been determined from experimental data and are conservatively chosen such that the model predictions of sorption are less than or equal to actual sorption expected along the possible flow paths in the Culebra should a release occur (Appendix MASS, Section MASS.15.2 and MASS Attachment 15-1). Other important parameters in the linear isotherm model are the diffusive porosity and the grain density of the Culebra because these determine the mass of dolomite available on which sorption can occur. Consistent with

the assumption of homogeneous rock properties in the conceptual model, K_ds and grain densities are selected and then applied to the entire transport domain and are held constant for an entire realization. See Appendices SECOTP2D (Section 7, User Interactions, Input and Output Files) and PAR (Parameters 49 through 57) for details of parameter definitions and values.

Selection of the parameter values required by the SECOTP2D model for physical retardation and chemical retardation is performed in LHS according to the CDFs described in Appendix PAR. Important parameter values are summarized in Tables 6-20 and 6-21.

In summary, the conceptual model for dissolved actinide transport includes the following: transport in advective porosity, physical retardation (diffusion) into diffusive porosity, chemical retardation (sorption) in diffusive porosity, homogeneous rock properties, and a linear isotherm to describe the sorption process. Some of the more important parameters are advective porosity, diffusive porosity, tortuosity, matrix block length, molecular diffusion coefficients, K_d, and the grain density of dolomite in the Culebra.

6.4.6.2.2 Transport of Colloidal Actinides in the Culebra

Colloidal particles are subject to many of the same processes that affect dissolved actinides, but because of their size several additional processes affect them. There are three process differences. Colloidal particles in general are preferentially carried in the center of pore throats by faster-moving fluid, which could cause slightly increased rates of transport compared to dissolved species. Colloidal particles can be filtered from flowing groundwater when they encounter small-aperture features in the pore network. Finally, colloidal particles may undergo different sorption processes than dissolved species.

The primary distinction in the transport behavior of the different colloidal particles is whether particles diffuse into the matrix from fractures. This is controlled by the difference between the size of colloidal particles and the mean pore-throat diameters in the diffusive porosity of the Culebra. Colloidal particles that are smaller than the pore throats can diffuse into the diffusive porosity. Actinide intrinsic colloids and humic materials are small enough for this to occur. The conceptual model for these particles includes the processes of advection, diffusion, and dispersion in the advective porosity, diffusion into diffusive porosity, and sorption of actinides in diffusive porosity. This model is analogous to the model specified for dissolved actinides, although the parameter values are different. The conceptual model assumes that other retardation processes (for example, filtration) will not occur for actinide-intrinsic colloids and humic materials.

In contrast, colloidal particles that are larger than pore throats will be excluded from the matrix and will remain in advective porosity. Microbes and mineral fragments are

Table 6-20. Matrix Distribution Coefficients (K_ds) and Molecular Diffusion Coefficients for Dissolved Actinides in the Culebra

Actinide	K_d (cubic meters per kilogram) Maximum	Minimum	Median	Molecular Diffusion Coefficients (square meters per second)[a] Constant
U(IV)	20.0	0.90	10.0	1.53×10^{-10}
U(VI)	0.030	3.0×10^{-5}	0.015	4.26×10^{-10}
Th(IV)	20.0	0.90	10.0	1.53×10^{-10}
Pu(III)	0.50	0.02	0.26	3.00×10^{-10}
Pu(IV)	20.0	0.90	10.0	1.53×10^{-10}
Am(III)	0.50	0.02	0.26	3.00×10^{-10}

[a] See Appendix MASS, MASS Attachment 15-3

Table 6-21. Culebra Actinides Flow and Transport Parameters Required for SECO Codes

Parameter (units)	Maximum	Minimum	Median or Constant
Advective Porosity (percent)	1.0	0.01	0.10
Diffusive Porosity (percent)	25.0	10.0	16.0
Half Matrix Block Length (meters)	0.50	0.05	0.275
Longitudinal Dispersivity, α_L (meters)	-	-	0
Transverse Dispersivity, α_T (meters)	-	-	0
Grain Density (cubic kilograms per cubic meter)	-	-	2.82
Effective Thickness (meters)	-	-	4.0
Fracture Tortuosity (unitless)	-	-	1.0
Diffusive Tortuosity (unitless)	-	-	0.11

conceptualized as being larger than the mean pore-throat diameter in Culebra diffusive porosity. The conceptual model for these particles includes the processes of advection in advective porosity and filtration by small-aperture features that occur within the advective porosity. See Appendix MASS (Section MASS.15.3 and MASS Attachment 15-9) for additional discussion.

Experiments have demonstrated that mineral fragments and microbes are attenuated so effectively by the advective porosity in the Culebra that it was deemed unnecessary to include those colloids in performance assessment calculations. Under the neutral to slightly basic geochemical conditions expected in the Culebra, humic substances were found to not influence the sorption behavior of dissolved actinides. Therefore, actinides associated with

humic substances were treated as dissolved species in the performance assessment calculations. The only actinide-intrinsic colloid found to exist in significant concentrations was the Pu(IV)-polymer. At the WIPP, the total amount of Pu(IV)-polymer introduced to the Culebra was found to be insignificant with respect to the EPA normalized release limit and so was not included in transport calculations. See Appendix SOTERM (Section SOTERM.6) and Appendix MASS (Section MASS.15.3.1) for details. See Appendix MASS (Section MASS.15.3.3) for alternative modeling approaches considered.

Indigenous microbes, humics, and mineral fragment colloids in the Culebra may react with actinides introduced to the Culebra in dissolved form to create new colloidal actinides. Newly formed actinide-bearing microbial and mineral colloids, however, will be attenuated similarly to colloidal actinides introduced from the repository. Therefore, disregarding the impact of newly formed microbial and mineral fragment colloidal actinides is conservative. Experimental results indicate that humics do not interact with dissolved actinides under Culebra geochemical conditions. Consequently, the quantity of newly formed humic actinides will be insignificant.

6.4.6.2.3 Subsidence Due to Potash Mining

Subsidence effects caused by potash mining are included in this performance assessment because of specific criteria in the EPA's 40 CFR Part 194. For incorporating the effects of subsidence caused by mining, the DOE uses the conceptual model provided by the EPA in 40 CFR Part 194 and supporting documents.

The EPA's conceptual model for mining is introduced in 40 CFR § 194.32 (b) and (c) and clarified in the Preamble and Background Information. 40 CFR § 194.32 (b) and (c) state

> (b) Assessments of mining effects may be limited to changes in the hydraulic conductivity of the hydrogeologic units of the disposal system from excavation mining for natural resources. Mining shall be assumed to occur with a one in 100 probability in each century of the regulatory time frame. Performance assessments shall assume that the mineral deposits of those resources, similar in quality and type to those resources currently extracted from the Delaware Basin, will be completely removed from the controlled area during the century in which such mining is randomly calculated to occur. Complete removal of such minerals resources shall be assumed to occur only once during the regulatory time frame.
>
> (c) Performance assessments shall include an analysis of the effects on the disposal system of any activities that occur in the vicinity of the disposal system prior to disposal and are reasonably expected to occur in the vicinity of the disposal system soon after disposal. Such activities shall include, but shall not be limited to, existing boreholes and the development of any existing leases that can be reasonably expected to be developed in the near future, including boreholes and leases that may be used for fluid injection activities.

40 CFR § 194.32 (b) and (c) state what gets mined, when it gets mined, and the effects of mining on the disposal system—a conceptual model. Within the disposal system, mineral resources similar in quality and type to those currently being mined outside the disposal system may be mined at an uncertain time in the future. Outside the disposal system, mineral

resources reasonably expected to be mined in the near future should be assumed to be mined. These effects are included in analyses of both disturbed and undisturbed performance. Inside the disposal system, whether and when a mining event occurs after the active institutional control period is determined by a probabilistic model. Outside the disposal system, what is reasonably expected to be mined is assumed to be mined by the end of WIPP disposal operations. With respect to consequence analysis, mining affects only the hydraulic conductivity of the units of the disposal system.

The DOE has identified areas that are assumed to be mined in a manner consistent with the conceptual model and other guidance presented by the EPA in 40 CFR Part 194. The only natural resource being mined currently near WIPP is potash in the McNutt, and it is the only mineral considered for future mining. Appendix MASS (Sections MASS.15.4 and MASS Attachment 15-4) provides a description of the method used to determine the extent of mining in the McNutt both inside and outside the disposal system. This description also presents additional relevant discussion by the EPA on the extent of mining. The extent of mining outside the disposal system used in this performance assessment is shown in Figure 6-19. It is based on the map of existing leases presented in Chapter 2.0 (Figure 2-37), setbacks from existing boreholes, and the presence of ore in the lease (see Appendix MASS, Section MASS.15.4 and MASS Attachment 15-5). Inside the disposal system, a region that could be mined in the future is specified based exclusively on the quality and type of ore present. This region was presented in Figure 2-38 (see Chapter 2.0) and is reproduced here for convenience as Figure 6-20.

The EPA clarifies its conceptual model on the effects of mining on hydraulic conductivity of the units of the disposal system in the Preamble to 40 CFR Part 194 (EPA 1996a, 61 FR 5229). The EPA states

> Some natural resources in the vicinity of WIPP can be extracted by mining. These natural resources lie within the geologic formations found at shallower depths than the tunnels and shafts of the repository and do not lie vertically above the repository. Were mining of these resources to occur, this could alter the hydrologic properties of overlying formations—including the most transmissive layer in the disposal system, the Culebra dolomite—so as to either increase or decrease groundwater travel times to the accessible environment. For the purposes of modeling these hydrologic properties, this change can be well represented by making corresponding changes in the values for the hydraulic conductivity. The Agency has conducted a review of the data and scientific literature discussing the effects mining can induce in the hydrologic properties of a formation. Based on its review of available information, the Agency expects that mining can, in some instances, increase the hydraulic conductivity of overlying formations by as much as a factor of 1,000, although smaller and even negligible changes can also be expected to occur. Thus, the final rule requires DOE to consider the effects of mining in performance assessments. In order to consider the effects of mining in performance assessments, the DOE may use the location-specific values of hydraulic conductivity, established for the different spatial locations within the Culebra dolomite, and treat them as sampled parameters varying between unchanged and increased 1,000-fold relative to the value that would exist in the absence of mining.

This section adds four important clarifying concepts. First, the EPA has concluded that there are no minerals vertically above the repository similar in quality and type to those currently

being extracted elsewhere in the Delaware Basin. Second, the EPA does not draw conclusions about whether mining will increase or decrease groundwater travel times to the accessible environment. Third, it may be assumed that the important effects of change in hydraulic conductivity occur only in the Culebra. Fourth, the spatially variant hydraulic conductivities established in the Culebra by the DOE may be multiplied, where they are impacted by mining, by a factor from 1 to 1,000. The DOE has applied the EPA's guidance regarding hydraulic conductivity to the transmissivity at locations in the Culebra.

In using the EPA's conceptual model for mining, the DOE makes assumptions with respect to two topics in order to formulate the mathematical model. The angle of draw is a parameter necessary to translate the area mined in the McNutt to the area affected in the Culebra. In its Background Information Document for 40 CFR Part 194, the EPA discusses the possible range in the value of angle of draw (EPA 1996b, 9-36). The DOE has examined the Background Information for 40 CFR Part 194 (see EPA 1996b, 9-47) and concluded that an angle of draw of 45° is the value most consistent with the EPA's discussions and calculations. Second, the Agency does not specify a distribution to the multiplicative factor. As discussed in Appendix PAR (Parameter 34), the DOE has assigned a uniform distribution to this variable. As discussed in the introduction to Appendix PAR, a uniform distribution is appropriate when only lower and upper bounds of the range are known.

Applying the angle of draw to the mined areas presented in Figures 6-19 and 6-20 makes the area impacted in the Culebra larger than the area actually mined in the McNutt. The area in the Culebra impacted by mining is shown in Figure 6-21, for outside the controlled area, and in Figure 6-22, for inside and outside the controlled area. These figures are plotted on the regional domain of the SECOFL2D model, which is used to calculate the effects of subsidence caused by mining on flow directions and rates in performance assessment.

The effects of mining outside the disposal system are included in the undisturbed performance scenario, and, therefore, the effects of this mining are included in all scenarios. In other words, all calculations of transport in the Culebra include the effects of mining outside the controlled area. This is the undisturbed mining case because mining within the controlled area has not occurred.

These effects are incorporated by multiplying location-specific values in the transmissivity field in the area labeled "Impacted by Mining" in Figure 6-21 by a factor (mining multiplier) between 1 and 1,000 that is randomly sampled in LHS. The same factor is applied to all affected nodal blocks. In every vector of the LHS, the steady-state flow fields used in the 10,000-year transport simulation incorporate this change to the transmissivity field. These simulations, followed by a transport simulation as discussed in preceding sections, develop reference conditions for the transport of actinides in the Culebra in the undisturbed mining case.

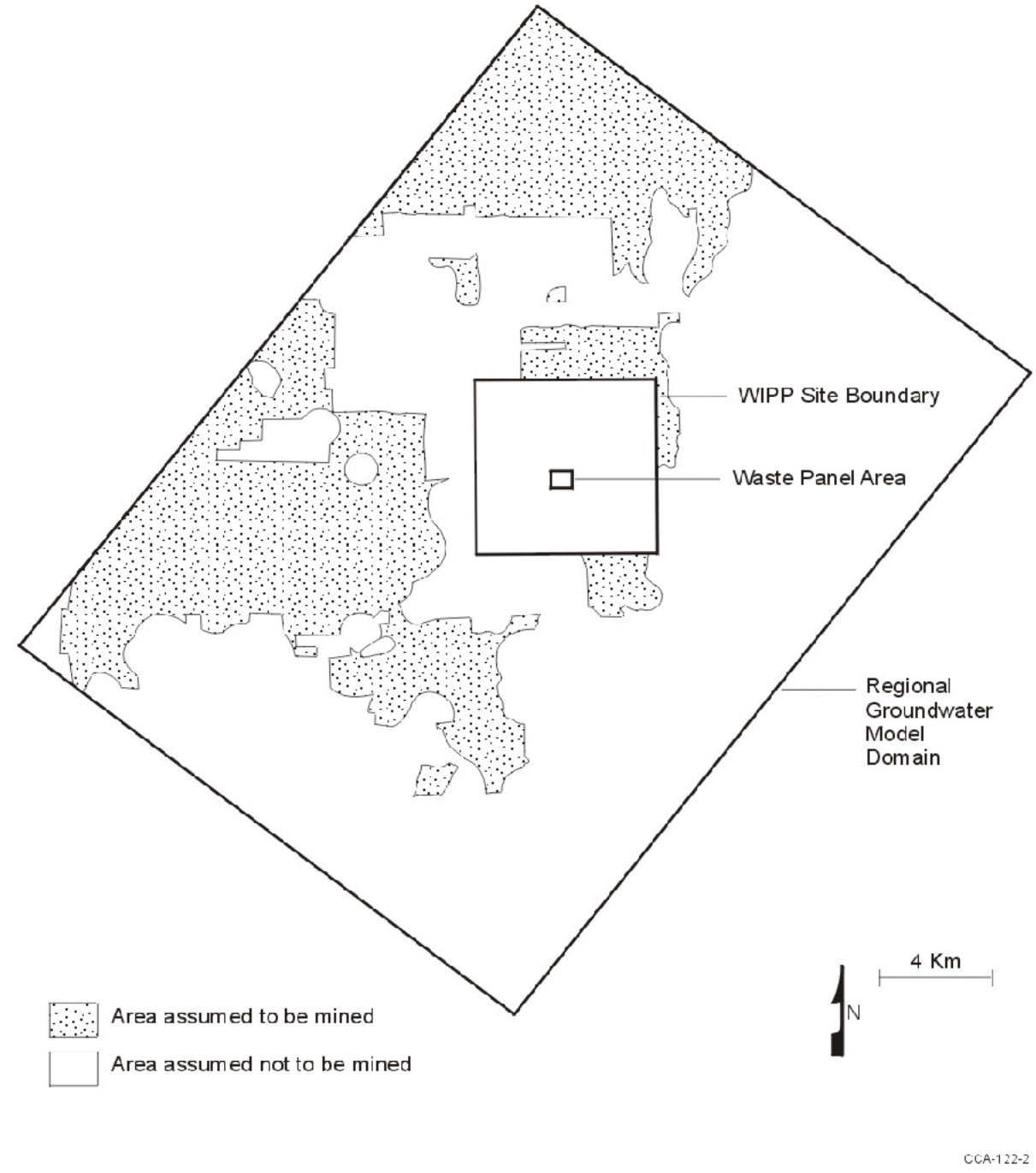

Figure 6-19. Extent of Mining in the McNutt in Undisturbed Performance within SECOFL2D Regional Model Domain

1

1 **THIS PAGE INTENTIONALLY LEFT BLANK**

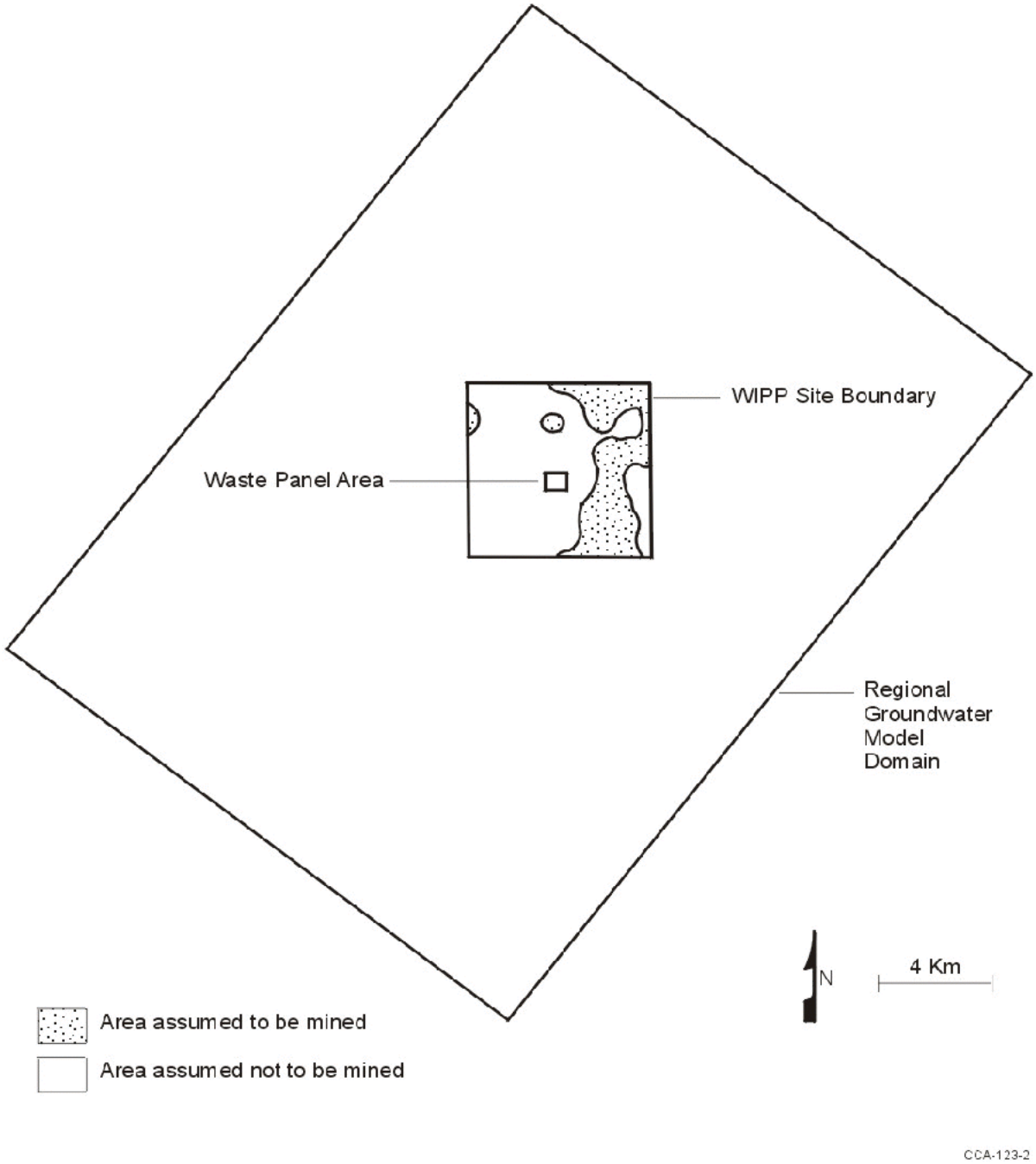

Figure 6-20. Extent of Future Mining in the McNutt within the Controlled Area Considered in Disturbed Performance

1 **THIS PAGE INTENTIONALLY LEFT BLANK**

Figure 6-21. Extent of Impacted Area in the Culebra from Mining in the McNutt Outside the Controlled Area for Undisturbed Performance

1 **THIS PAGE INTENTIONALLY LEFT BLANK**

Figure 6-22. Extent of Impacted Area in the Culebra for Disturbed Performance if Mining In the McNutt Occurs in the Future Within the Controlled Area

1 **THIS PAGE INTENTIONALLY LEFT BLANK**

If mining occurs within the controlled area, an area of the Culebra inside and outside the disposal system is affected. This is the disturbed mining case. To evaluate the impact of disturbed mining, a second simulation of Culebra flow directions and rates is executed on the regional and local domains. In this second simulation, the affected location-specific values in the transmissivity field within the controlled area are multiplied by the same mining multiplier used for the undisturbed mining case outside the controlled area. These simulations, followed by a transport simulation as discussed in preceding sections, develop reference conditions (see Section 6.4.11) for the transport of actinides following mining inside the controlled area.

The implementation of the EPA's probability model for future mining is presented in Section 6.4.12.8. A discussion of how the reference simulations for the undisturbed and disturbed mining cases are used in CCDF construction is presented in Section 6.4.13.

6.4.6.3 The Tamarisk

The Tamarisk (Region 16 in Figures 6-13 and 6-14) rests between the more transmissive Culebra and Magenta. An in-situ hydraulic test determined that the transmissivity of the Tamarisk is lower than the transmissivity of the unnamed lower member (see Section 2.2.1.4.1.3). This low transmissivity is consistent with expectations because of its anhydrite, gypsum, and clay composition (see Section 2.1.3.5.3). In performance assessment, this member is treated as impermeable. This may cause an increase in flow through the adjacent Culebra and Magenta. This treatment is considered conservative in that allowing flow from the intrusion borehole or shaft into the Tamarisk would, if anything, decrease flow into the Culebra, which would tend to reduce the consequence of radionuclide release to the Rustler. In performance assessment, the thickness of the Tamarisk is assumed to be 81.4 feet (24.8 meters) and its permeability is effectively zero (Appendix PAR, Table PAR-29).

6.4.6.4 The Magenta

The Magenta is described in Sections 2.1.3.5.4 and 2.2.1.4.1.4 and is shown as Region 15 in Figures 6-13 and 6-14. Transport of actinides through the Magenta to the accessible environment is not modeled. The assumption that no releases will occur from the Magenta is based on the hydraulic test results from wells on the WIPP site (Beauheim 1987, 110 – 118) that indicate that the Magenta is a porous medium with no hydraulically significant fractures (in contrast to the Culebra) and that its conductivity is lower than that of the Culebra. Early numerical simulations of flow and transport in the Magenta suggested much slower transport than in the Culebra (Barr et al. 1983, 26 – 27). Therefore, no radionuclides entering the Magenta will reach the accessible environment boundary within the 10,000-year time frame. Accordingly, the BRAGFLO model geometry reasonably approximates the effects of Magenta flow. The Magenta permeability is chosen conservatively as the lowest of measured values near the center of the WIPP site, in order to yield a lower reasonable amount of brine (and radionuclide) storage within the Magenta, while continuing to yield an upper bounding flow into the Culebra. The volumes of brine and radionuclides calculated to be stored in the Magenta are tracked and documented, however. Magenta parameter values are summarized in Table 6-22 and are described in more detail in Appendix PAR (Table PAR-28).

Table 6-22. Model Parameter Values for the Magenta

Parameter (units)	Value
Permeability (square meters)	6.31×10^{-16}
Effective Porosity (percent)	13.8
Rock Compressibility (1/pascals)[a]	2.64×10^{-10}
Threshold Pressure, P_t (pascals)[b]	5.06×10^{5}
Residual Brine Saturation, S_{br} (unitless)	0.084
Residual Gas Saturation, S_{gr} (unitless)	0.077
Pore Distribution Parameter, λ (unitless)	0.644
Maximum Capillary Pressure	10^{8}
Thickness (meters)	8.5
Initial Pressure (pascals)	9.17×10^{5}

[a] Pore compressibility = rock compressibility/effective porosity.
[b] Threshold Pressure (P_t) determined from the relationship: $PCT\_A \cdot k^{PCT\_EXP}$, where PCT_A and PCT_EXP are constants and k is the permeability.

6.4.6.5 The Forty-niner

In evaluations of radionuclide transport, flow in the Forty-niner is considered insignificant because of its low transmissivity (see Section 2.2.1.4.1.5). As with the Tamarisk and unnamed lower members, the Forty-niner is assigned a permeability of effectively zero in performance assessment (Appendix PAR, Table PAR-27). This treatment is considered conservative in that allowing flow from the intrusion borehole or shaft into the Forty-niner would, if anything, decrease flow into the Culebra, which would tend to reduce the consequence of radionuclide release to the Rustler. Its modeled thickness is 56.8 feet (17.3 meters). It is shown as Region 14 in Figures 6-13 and 6-14.

6.4.6.6 Dewey Lake

Release of actinides to the accessible environment from transport in the Dewey Lake is assumed not to occur even if contaminated brine reaches the unit because the sorptive capacity of this unit appears large. This assumption is based on an analysis (Wallace et al. 1995) that demonstrated that the potential sorption capacity of the Dewey Lake is sufficient to prevent releases for 10,000 years. This analysis consisted of (1) a literature review of sorptive capacity of redbeds and (2) an estimate of the minimum sorption required to prevent release of actinides that enter the Dewey Lake to the accessible environment in 10,000 years. Comparison of the sorption values for the Dewey Lake analogues established by literature review with the minimum sorption required to prevent release indicates that the likely sorptive capacity of the Dewey Lake is orders of magnitude greater than would likely be required to prevent release. Therefore, the DOE assumes that chemical retardation occurring in the Dewey Lake will prevent release within 10,000 years of any actinides that might enter it. Geological and hydrological information on the Dewey Lake is presented in Sections 2.1.3.6

and 2.2.1.4.2, respectively. Dewey Lake parameter values are summarized in Table 6-23 (see also Appendix PAR, Table PAR-26). The Dewey Lake is shown as Region 13 in Figures 6-13 and 6-14.

Table 6-23. Dewey Lake Parameters for the BRAGFLO Model

Parameter (units)	Value
Permeability (square meters)	5.01×10^{-17}
Effective Porosity (percent)	14.3
Rock Compressibility (1/pascals)[a]	10^{-8}
Threshold Pressure, P_t (pascals)[b]	0
Residual Brine Saturation, S_{br} (unitless)	0.084
Residual Gas Saturation, S_{gr} (unitless)	0.077
Pore Distribution Parameter, λ (unitless)	0.644
Maximum Capillary Pressure (pascals)	10^8
Thickness (meters)	149.3
Initial Pressure (below water table at 980 meters, 43.3 meters below top of formation) (pascals)	hydrostatic
Initial Pressure, 20 percent liquid saturation above water table (atmospheres)	1

[a] Pore compressibility = rock compressibility/effective porosity.

[b] Threshold Pressure (P_t) determined from the relationship: $PCT\_A \cdot k^{PCT\_EXP}$, where PCT_A and PCT_EXP are constants and k is the permeability.

6.4.6.7 Supra-Dewey Lake Units

The units overlying the Dewey Lake are discussed in Sections 2.1.3.7 through 2.1.3.10 and are shown as Region 12 in Figures 6-13 and 6-14. Because these units are thin and predominantly unsaturated at the WIPP site, brine that might enter from the borehole (assuming brine can reach this elevation) is assumed to flow downward to the Dewey Lake, where any actinides will be sorbed. These units are included in BRAGFLO, however, and the possibility of actinide transport into them from a borehole is considered in the performance assessment. Actinide transport within the Supra-Dewey Lake units is not modeled, and it is assumed that there can be no actinide release to the accessible environment through these units. For performance assessment, the units overlying the Dewey Lake are represented as a single hydrostratigraphic unit whose parameters are shown in Table 6-24.

Table 6-24. Supra-Dewey Lake Unit Parameters for the BRAGFLO Model

Parameter (units)	Value
Permeability (square meters)	10^{-10}
Effective Porosity (percent)	17.5
Rock Compressibility (1/pascals)[a]	5.71×10^{-8}
Threshold Pressure, P_t (pascals)[b]	0
Residual Brine Saturation, S_{br} (unitless)	0.084
Residual Gas Saturation, S_{gr} (unitless)	0.077
Pore Distribution Parameter, λ (unitless)	0.644
Maximum Capillary Pressure (pascals)	10^8
Thickness (meters)	15.76
Initial Pressure, 8.36 percent liquid saturation (atmospheres)	1

[a] Pore compressibility = rock compressibility/effective porosity.
[b] Threshold Pressure (P_t) determined from the relationship: $PCT\_A \cdot k^{PCT\_EXP}$, where PCT_A and PCT_EXP are constants and k is the permeability.

6.4.7 The Intrusion Borehole

In accordance with the requirements of 40 CFR § 194.33(b)(1), the DOE models consequences of inadvertent and intermittent intrusion into the repository during drilling for natural resources as the most severe human intrusion scenario that may affect long-term performance of the disposal system. This section discusses the conceptual models used for drilling (particulate release during drilling, direct brine release during drilling, and long-term brine flow) and provides references to appropriate discussions of numerical modeling codes.

This section does not address the likelihood that inadvertent human intrusion will occur. As discussed in Chapter 7.3.4, the DOE believes passive institutional controls will be effective in reducing the likelihood of intrusion (see Appendix EPIC); however, regulatory guidance requires consideration of a nonzero probability of intrusion (40 CFR § 194.43[c]). The DOE's treatment of the probability of inadvertent human intrusion is discussed in Section 6.4.12.

Human intrusion scenarios require simulating penetration of an intrusion borehole into the waste disposal region. There are two effects associated with drilling: releases from the drilling itself and possible releases because of the long-term effects on fluid flow in the disposal system after the borehole casing and plugs have degraded. Both types of releases are estimated for two different types of intrusions: those that intersect pressurized brine in the Castile (E1 events, see Section 6.3.2.2.2), and those that do not (E2 events, see Section 6.3.2.2.1).

6.4.7.1 Releases During Drilling

Consistent with the criterion of 40 CFR § 194.33(c)(1), releases that may occur during and immediately following the drilling event are modeled under the assumption that future drilling practices will be the same as those of the present (see Appendix DEL, Sections DEL.5 and DEL.6, for a complete description of present drilling practices). Figure 6-23 shows a schematic representation of a standard rotary drilling operation inadvertently penetrating the repository. A drill bit is attached to the bottom of a string of steel pipe, the lowest segments of which are reinforced collars. The drill bit, collars, and pipe are collectively referred to as the drill string. As the drill string rotates, liquid, referred to as drilling mud, is pumped down the interior of the pipe and out through the bit. The drilling fluid cools and lubricates the bit and then returns to the surface outside the pipe in the annulus between the pipe and the borehole wall. During its return flow, the mud carries the cuttings to the surface where they settle out in a mud pit. The mud is typically a water-based brine that is weighted with additives to maintain a hydrostatic pressure in the borehole equal to or greater than the normally anticipated fluid pressures in the formations being drilled. Salt-saturated brines are generally used in evaporites to prevent dissolution of the formation. Steel casing is installed in boreholes before entering the salt section to protect the near-surface units from contamination with fluids from deeper units and, after drilling through the salt section, to prevent hole closure on the drill string and subsequent in-hole hardware.

If a rotary drill bit penetrates the waste, radionuclides may be brought to the surface by four means. First, some quantity of cuttings, which contain material intersected by the drill bit, will be brought to the surface. Second, cavings, which contain material eroded from the borehole wall by the circulating drill fluid, may also be brought to the surface by the circulating drilling mud. Third, releases of radionuclides may occur if the repository contains fluids at pressures higher than the pressure exerted by the drilling fluid. Spalling of waste material into the borehole may occur if high-pressure gas flows into the borehole. Brine as well as gas may enter the borehole from the repository if the driller is unable to control the pressure within the well or if the driller chooses not to control the pressure. The brine may flow to the surface, and if it has been in contact with waste, it may contain dissolved or suspended radionuclides.

Releases of particulate waste material (that is, cuttings, cavings, and spallings) are modeled using the CUTTINGS_S code as described in Section 6.4.11 and Appendix CUTTINGS. Appendix MASS (Section MASS.16.1) discusses the conceptual basis for the model. As discussed in Section 6.4.12.4, cuttings and cavings are calculated separately for CH-TRU and RH-TRU waste, with distinct waste streams considered. Spallings are calculated as homogeneous waste obtained by averaging over all CH-TRU waste. For all releases during drilling, appropriate corrections are made for radioactive decay. Releases of dissolved or suspended radionuclides contained in brine are modeled using the BRAGFLO and PANEL codes as described in the next section. Casing is assumed to be intact through the Rustler and overlying units during drilling, and there is assumed to be no communication between the borehole and those units. For all direct releases, actinides that enter the borehole are conservatively assumed to reach the surface.

6.4.7.1.1 Direct Brine Release During Drilling

Direct brine release refers to the possibility that brine containing actinides may flow from the waste panels up a borehole to the surface during drilling (Appendix MASS, Section MASS.16.2). It is conceptualized that direct brine release to the surface will not occur every time a borehole penetrates the waste panels but rather that it can occur only when two conditions are met. The first condition is the presence of mobile brine in the waste panels. Because of brine consumption by corrosion and low initial saturation, it is possible for liquid saturations below the residual saturation to exist in the repository, in which case direct brine release cannot occur. The second condition is the pressure in the waste panels must be greater than the pressure at the base of the column of drilling mud. Drillers in the Delaware Basin use a salt-saturated mud with a specific gravity of about 1.23 while drilling through the Salado. This corresponds to a pressure of approximately 8 megapascals at the repository horizon (see Appendix MASS, Section MASS.16.2, and MASS Attachment 16-2). If fluid in the waste panels is below this pressure, no direct brine release during drilling can occur because liquid flow in the repository will be away from the borehole.

In the conceptual model, resolution of the details of flow near the borehole is considered important, as the changing physical conditions over the short duration of this flow can significantly impact estimates of the total volume released. It is not assumed that a direct brine release would be noticed by the driller (EPA 1996a, 61 FR 5230). Also important to the conceptual model is how long direct brine release occurs. There are several ways in which the direct brine release could be stopped. A driller might detect higher flow rate to the mud pit and take action to mitigate consequences. Alternatively, direct brine release will stop when the driller cases the hole after reaching the base of the salt section. As discussed in Appendix MASS (MASS Attachment 16-2) and Appendix DEL (Section 7.5), the DOE assumes that for low volumes of fluid flow, the borehole will be controlled and cased within 72 hours after the penetration of the repository. In all cases, all fluid flow to the surface during drilling is assumed to cease within 11 days after penetration of the repository.

In the conceptual model for direct brine release, several other assumptions are made that relate to other conceptual models. The processes of direct solids release from cuttings, cavings, spall, and direct brine release are treated separately, although the direct brine release model does account for the effects of solids removal (spall) on fluid flow near the well bore. Direct brine release will affect the pressure and saturation in the repository. However, it is assumed that these effects are negligible over the long-term because of their transient and local nature, and they are not accounted for in long-term (10,000-year) BRAGFLO disposal system calculations. This assumption simplifies modeling because it allows detailed consideration of direct brine release over a short time period, without having to couple the results of these calculations back into the disposal system simulations.

1

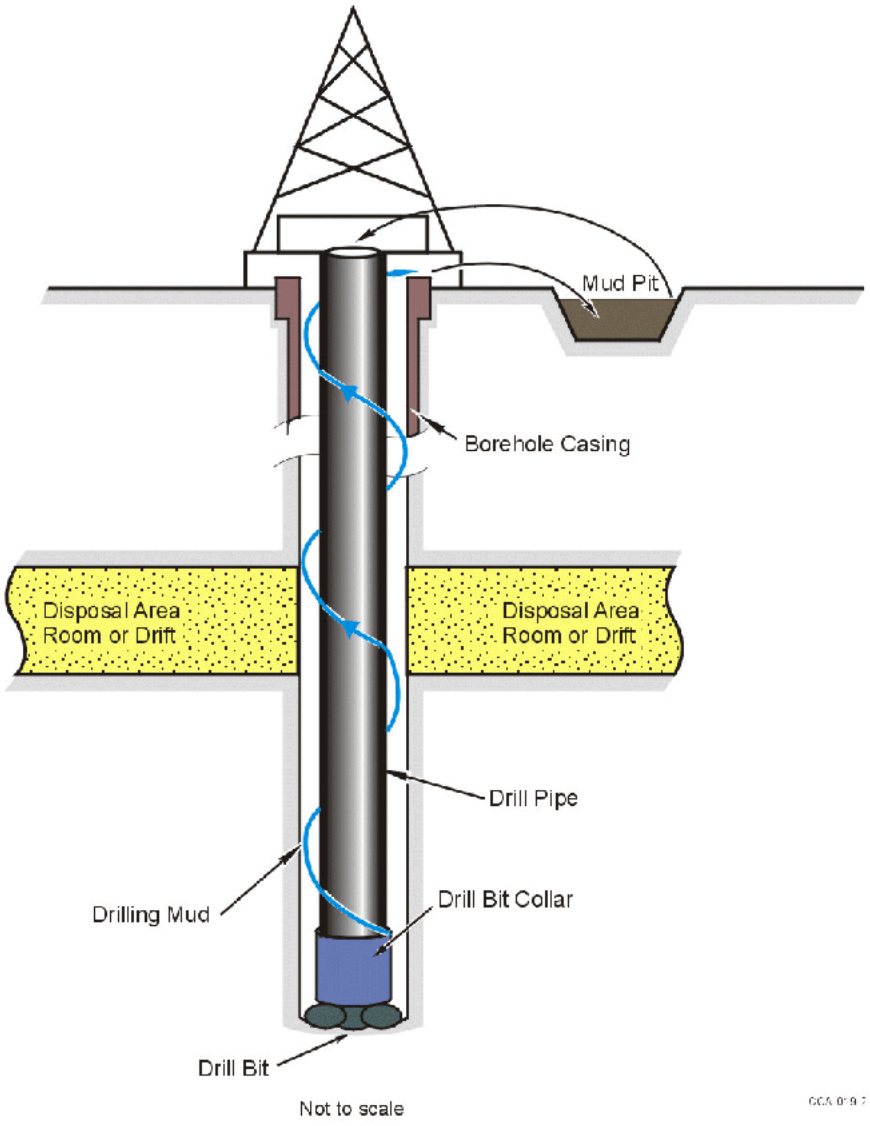

Figure 6-23. Schematic Representation of a Rotary Drilling Operation Penetrating the Repository

1 **THIS PAGE INTENTIONALLY LEFT BLANK**

The area over which fluid flow can occur during direct brine release is assumed to be the rooms and drifts of waste panels, the DRZ, room pillars, and panel closures. Because local-scale, short-duration flow is important, the geometry of the waste panels is considered important and is represented in the model. It is assumed that the flow interactions with the Salado other than the DRZ are not important during direct brine release. For this model, pillars are arbitrarily assumed to have the properties of the DRZ rather than intact halite, although in reality their properties are probably like a DRZ at their edge and like intact halite in their core. Since the DRZ permeability is greater than the permeability of intact halite, this assumption is conservative. A two-dimensional geometry is used parallel to the repository horizon, with a 1° dip from north to south. The geometry of the grid used is shown in Figure 6-24.

The BRAGFLO code is used to calculate direct brine release, and the mathematical and computational model is called the BRAGFLO direct brine release (BRAGFLO_DBR) model (Appendix MASS, Section MASS.16.2 and MASS Attachment 16-2). The initial and boundary conditions for this model are derived from the corresponding BRAGFLO disposal system simulation through several codes, including CUTTINGS_S. Some of the parameters derived from the BRAGFLO disposal system model are permeabilities, porosities, two-phase flow properties, and the height of the waste region. Initial saturations and pressures in the BRAGFLO direct brine release model are mapped from the BRAGFLO disposal system model. Other parameters used in the BRAGFLO direct brine release models are consistent with those used in the BRAGFLO disposal system model (Appendix MASS, Section MASS.16.2 and MASS Attachment 16-2, 3 – 5).

It is possible that a direct brine release could occur from a panel that is connected by a previously-drilled, abandoned borehole to a brine reservoir in the Castile. If this were to happen, flow directly between the two boreholes, analogous to the E1E2 scenario for long-term performance, may affect the estimate of the total brine released. The direct brine release for this possibility is calculated by BRAGFLO_DBR by placing a constant-pressure, flowing injection well as a boundary condition in the model. The locations used for these boreholes are shown in Figure 6-24. It is assumed that a direct brine release from a panel that has a previously-drilled, abandoned borehole of the E2 type is not affected by the presence of the other borehole. Thus, reference direct brine release conditions are calculated for previously unintruded and E2-intruded panels, and for previously-intruded E1 panels. Details about the properties assigned to the flowing-well boundary condition are discussed in Appendix MASS (Section MASS.16.2 and MASS Attachment 16-2, Appendix A). Details about how the consequences of direct brine releases from other possible combinations of boreholes are accounted for in the CCDF are discussed in Section 6.4.13.

A borehole could penetrate the repository anywhere. For simplification, the BRAGFLO direct brine release model assumes that calculation of direct brine release from several defined locations provides meaningful reference results for the possible variation in release because of location. The locations of boreholes from which representative results are calculated are indicated in Figure 6-24. In construction of a CCDF (see Section 6.4.13), the direct brine release associated with a borehole whose position is randomly selected is

correlated with the reference release most consistent with the geometry near the location of the random borehole.

Accurate representation of the flow into the borehole is considered important in the BRAGFLO direct brine release model. Accordingly, a number of mathematical methods that are not used to calculate long-term releases are applied to the conditions in the borehole for calculation of direct brine releases. The methods used appear in Appendix MASS (Section MASS.16.2 and MASS Attachment 16-2).

6.4.7.2 Long-Term Releases Following Drilling

Long-term releases to the ground surface or into groundwater in the Rustler or overlying units may occur after the hole has been plugged and abandoned (Appendix MASS, Section MASS.16.3). As required by regulation, the plugging and abandonment of future boreholes are assumed to be "consistent with practices in the Delaware Basin at the time a compliance application is prepared" [40 CFR § 194.33(c)(1)]. Detailed examination of current practice in the Delaware Basin indicates that all boreholes abandoned recently are plugged to meet state and federal regulatory requirements protecting groundwater and natural resources (see Appendix DEL, Sections DEL.5.5 and DEL.6; Appendix MASS, Section MASS.16.3 and MASS Attachment 16-3). These plugs will be effective in preventing flow in abandoned boreholes for some period of time after emplacement. However, some plugs may fail and radionuclides may be transported in brine flowing up the borehole.

Borehole plug configurations used today in the Delaware Basin vary based on the local stratigraphy encountered in the hole, its total depth, and the types of fluids present. All holes are plugged with some combination of solid concrete plugs isolating different fluid-bearing horizons from each other and from the ground surface. As discussed in detail in Appendix MASS (Section MASS.16.3 and MASS Attachment 16-1) and Appendix DEL (DEL Attachment 7), six different plug configurations are identified that are potentially relevant to future borehole abandonment practice at the WIPP. As discussed in Appendix MASS (Section MASS.16.3.3 and MASS Attachment 16-3, Section 2.0), these six plug configurations can be approximated for performance assessment by three conceptual plugging patterns. The three plugging configurations addressed in the performance assessment are described in the following section. Probabilities of occurrence for each of these three plugging configurations are discussed in Section 6.4.12.7. Parameters used to describe the borehole and its plugs are summarized in Table 6-25.

6.4.7.2.1 Continuous Concrete Plug through the Salado and Castile

In this configuration, a continuous concrete plug is assumed to exist throughout the Salado and Castile (Appendix MASS, Section MASS.16.3 and MASS Attachment 16-3, Figure 1). Such a plug could be installed in keeping with current regulatory requirements of the New Mexico Oil Conservation Division Order R-111-P (State of New Mexico 1988, 10), which is applicable within the potash leasing area that includes the WIPP site. The purpose of the

1

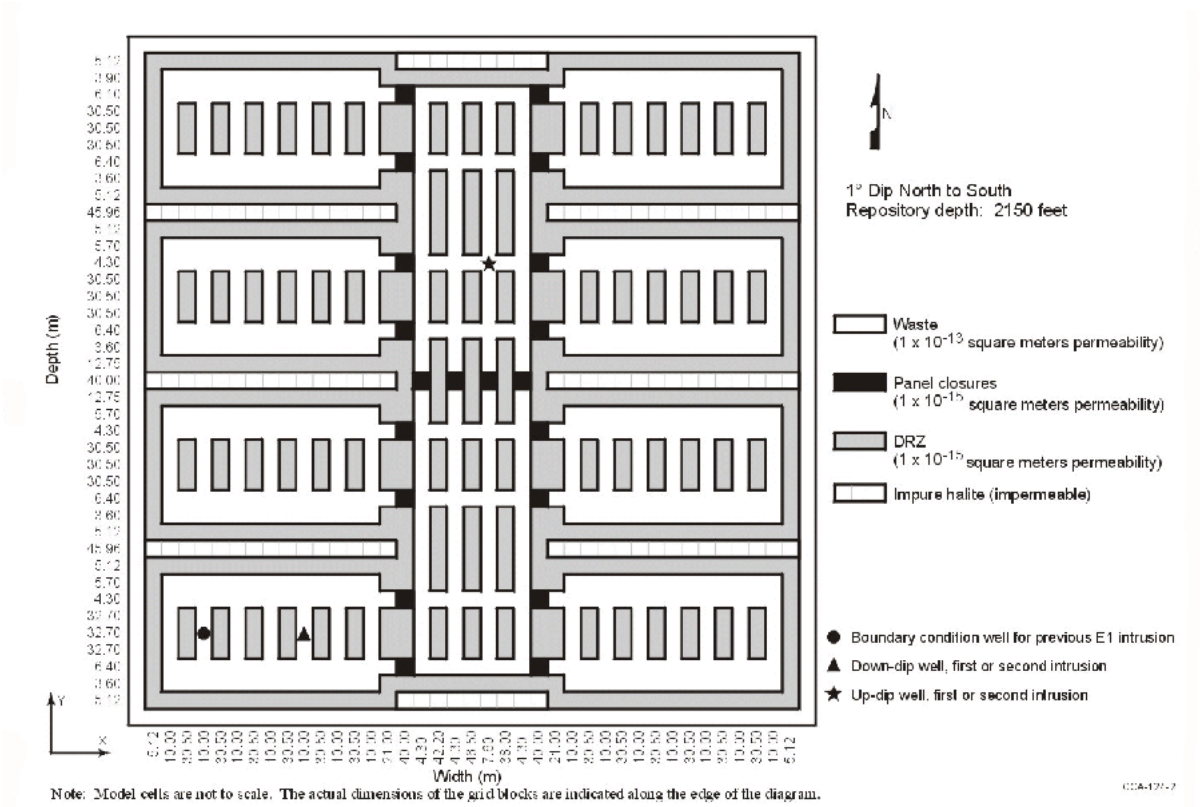

Note: Model cells are not to scale. The actual dimensions of the grid blocks are indicated along the edge of the diagram.

Figure 6-24. Repository-Scale Horizontal BRAGFLO Mesh Used for Direct Brine Release Calculations

1 **THIS PAGE INTENTIONALLY LEFT BLANK**

Table 6-25. Intrusion Borehole Properties for the BRAGFLO and CUTTINGS_S Models

Parameter (units)	Maximum	Minimum	Median or Constant[a]
Permeability of open hole (0 to 200 years) (square meters)	—	—	10^{-9}
Permeability of concrete plugs (0 to 200 years in Rustler and at surface) (square meters)[b]	—	—	5×10^{-17}
Permeability of borehole fill material (>200 years) (square meters)[b]	1×10^{-11}	1×10^{-14}	3.16×10^{-13}
Permeability of lower borehole fill material (>1,200 years) (square meters)[b]	1×10^{-12}	1×10^{-15}	3.16×10^{-14}
Effective Porosity (percent)	—	—	0.32
Pore Compressibility (1/pascals)	—	—	0
Diameter (meters)	—	—	0.311
Threshold Pressure, P_t (pascals)	—	—	0
Pore Distribution Parameter, λ (unitless)	—	—	0.94
Residual Brine Saturation, S_{br} (unitless)	—	—	0
Residual Gas Saturation, S_{gr} (unitless)	—	—	0
Effective Shear Resistance to Erosion (pascals)	0.05	10.0	5.03
Waste Particle Diameter (meters)	4×10^{-5}	0.20	2.83×10^{-3}

[a] Parameters with no maximum and minimum values are treated as constants in the performance assessment.
[b] Borehole permeabilities are for the two-plug case. Continuous three-plug case is treated as undisturbed performance.

continuous plug is to protect potash mining operations from possible hydrocarbon contamination. A continuous concrete plug is also used to approximate flow in boreholes in which numerous concrete plugs are found throughout the salt section. Examples of such plugging configurations currently used in the Delaware Basin are described in Appendix MASS (Section MASS.16.3, and MASS Attachments 16-1 and 16-3).

Because concrete within a continuous plug will be physically confined and will have very little brine flow through it, degradation will be minimal and limited to the upper and lower ends of the plug (see Appendix MASS, Section MASS.16.3.3 and MASS Attachment 16-3, Appendix C). For performance assessment, the permeability of the continuous concrete plug is 5×10^{-17} square meters. Because of the small cross-sectional area and low permeability of the potential pathway, long-term releases through a continuous concrete plug are not calculated explicitly for the performance assessment, and are assumed to be zero.

6.4.7.2.2 The Two-Plug Configuration

In the two-plug configuration, two concrete plugs are assumed to have a significant effect on long-term flow in the borehole (Appendix MASS, Section MASS.16.3 and MASS Attachment 16-3, Figure 2). The lower plug of interest is assumed to be located somewhere between the hypothetical Castile brine reservoir and underlying formations. A second plug is located within the lower portion of the Rustler, immediately above the Salado. Additional plugs that have little effect on long-term flow are also assumed to be present deeper in the hole and at the land surface.

In E1-type intrusions with two plugs, the brine reservoir and the repository are assumed to be in direct communication through an open cased hole immediately following drilling. The plugs are located in the borehole Region 1A of the BRAGFLO mesh in Figure 6-14 in Rows 30 and 31 (the surface plug) and Row 23 (the lower unnamed member). The plugs located below the brine reservoir are not modeled explicitly. Plugs are assigned initial permeabilities of 5×10^{-17} square meters, consistent with the expected properties of intact concrete (see Appendix MASS, Section MASS.16.3.2 and MASS Attachment 16-3, Appendix C.3.1.2 [C-4]). The open segments of borehole between the plugs are assigned an initial permeability of 10^{-9} square meters. Steel casing above the Salado is assumed to begin to degrade within decades after abandonment and is assumed to have failed completely after 200 years. The concrete plugs above the Salado are also assumed to fail after 200 years, as a result of chemical degradation where they are in contact with brine. The plug below the Castile brine reservoir is in a less aggressive chemical environment, and its properties remain constant in performance assessment.

After the upper plugs and casing have failed, the borehole is assumed to be filled by a silty-sand-like material containing degraded concrete, corrosion products, and material that sloughs into the hole from the walls. Thus, beginning 200 years after the time of intrusion, the entire borehole region in the BRAGFLO model, including the sections previously modeled as concrete plugs, is assigned a permeability corresponding to silty sand. This permeability is sampled from a log-uniform distribution from 10^{-11} square meters to 10^{-14} square meters.

One thousand years after the plug at the base of the Rustler has failed, or 1,200 years after the time of intrusion, permeability of the borehole region below the waste-disposal panel in the BRAGFLO model used for E1-type intrusions is decreased from its sampled value by one order of magnitude. For the remainder of the 10,000-year period, the borehole is modeled with its sampled permeability value above the repository and the adjusted value below. Conceptually, the decrease in permeability below the panel corresponds to compaction of the silty-sand-like material by partial creep closure of the lower portion of the borehole. As discussed in Appendix MASS (Section MASS.16 and MASS Attachment 16-3, Appendix D), creep closure of boreholes is not expected to be significant above the repository horizon but will be effective at greater depths because of the greater lithostatic stress. Nowhere in the borehole is creep closure assumed to close the hole completely in the regulatory time frame, but closure will be sufficient at depths below the repository to reduce the permeability of the material filling the hole.

6.4.7.2.3 The Three-Plug Configuration

In the three-plug configuration, three concrete plugs are assumed to have an effect on long-term flow in the borehole (Appendix MASS, Section MASS.16.3 and MASS Attachment 16-3, Figure 3). Two of the plugs are identical to those modeled in the two-plug configuration. The third plug is located within the Castile above the brine reservoir and below the waste-disposal panel. This plug is assumed to behave in the same manner as the lower plug in the two-plug configuration: that is, its properties remain unchanged in performance assessment. Otherwise, all portions of the borehole in the three-plug configuration are assumed to have the same material properties as the corresponding regions in the two-plug configuration, with adjustments to borehole-fill permeability occurring 1,000 years after failure of the overlying plug (Appendix MASS, Section MASS.16.3 and MASS Attachment 16-3, Section 5.3).

Because the three-plug configuration isolates the repository from the brine reservoir for the time period during which the middle plug remains effective and because the portion of the borehole above the middle plug will already be filled with silty-sand-like material before failure of the middle plug occurs, the DOE has chosen not to model this configuration explicitly in the BRAGFLO calculations. Boreholes in which the three-plug configuration is emplaced are assumed to result in long-term releases comparable to those calculated for E2 intrusions, regardless of whether they penetrate a Castile brine reservoir. Consequences of E1-type intrusions with the three-plug configuration are assumed for the purposes of CCDF construction to be identical to the consequences of E2 intrusions occurring at the same time.

6.4.8 Castile Brine Reservoir

As discussed in Section 2.2.1.2.2, high-pressure Castile brine has been encountered in several WIPP-area boreholes, including the WIPP-12 borehole within the controlled area and the U.S. Energy Research and Development Administration (ERDA)-6 borehole northeast of the site.

The E1 and E1E2 scenarios include penetration by a borehole of the repository and a brine reservoir in the Castile. The properties of the borehole are discussed in Section 6.4.7.

For performance assessment, the Castile is conceptualized as unimportant because of its expected low permeability (based on similarities to the Salado), unless a borehole penetrates both the repository and a brine reservoir in the Castile. Two regions are specified in the Castile horizon in the disposal system geometry: the Castile (Region 29 in Figure 6-13) and a reservoir (Region 30 in Figure 6-13). The Castile region is assigned an extremely low permeability, which prevents it from participating in fluid flow processes, consistent with the concept that it is unimportant.

It is not known whether a brine reservoir actually exists below the repository. Because of this fact, the conceptual model for the brine reservoirs is somewhat different from those for known major properties of the natural barrier system, such as stratigraphy. The principal difference is that a reasonable treatment of the uncertainty of the occurrence of brine reservoirs requires that assumptions be made about their spatial distribution and probability of intersection (Appendix MASS, Section MASS.18.1 and MASS Attachment 18-6). These properties are treated as stochastic uncertainty in performance assessment modeling (that is,

they are related to whether a brine reservoir exists and whether a brine reservoir intersection occurs; see Section 6.1.2). These assumptions are discussed in Section 6.4.12.

In addition to the stochastic uncertainty in the location and probability of intersecting reservoirs, there is also uncertainty in the properties of reservoirs if they are intersected (Appendix MASS, Section MASS.18 and MASS Attachments 18-2 and 18-3). This is treated as subjective uncertainty (that is, it is related to the question, If a brine reservoir is assumed to be penetrated, how does it behave?; see Section 6.1.2) and is incorporated in the BRAGFLO calculations of disposal system performance. The conceptual model for the behavior of the hypothetical brine reservoir is discussed here.

Where they exist, Castile brine reservoirs in the northern Delaware Basin are believed to be fractured systems, with high-angle fractures spaced widely enough that a borehole can penetrate through a volume of rock containing a brine reservoir without intersecting any fractures and therefore not produce brine. They occur in the upper portion of the Castile (Popielak et al. 1983, G-2). Appreciable volumes of brine have been produced from several reservoirs in the Delaware Basin, but there is little direct information on the areal extent of the reservoirs or the interconnection between them. The WIPP-12 data indicate that fractures in the network have a variety of apertures and permeabilities, and they deplete at different rates. Brine occurrences in the Castile behave as reservoirs—that is, they are bounded systems—rather than as aquifers such as groundwater in the Culebra and Magenta. The properties that need to be specified for brine reservoirs are pressure, permeability, compressibility, total brine volume, and porosity.

Brine reservoir pressure in this performance assessment is based on measured pressure in anhydrites in the Castile and Salado. The values used in this performance assessment are shown in Table 6-26. These values are determined by analysis of pressures observed in brine produced from anhydrites in the Salado and Castile, corrected for the difference in depth between the observation location and WIPP-12. The analysis is documented in Appendix MASS (Section MASS.18 and MASS Attachments 18-1 and 18-2) and Appendix PAR (Parameter 27).

The permeability of brine reservoirs is based on analysis of brine reservoirs tested by the DOE in drillholes ERDA-6 and WIPP-12 (Popielak et al. 1983, Sections H-3.4.3 and H-3.4.4). Values used in this performance assessment are shown in Table 6-26. The derivation of these values from the referenced study is documented in Appendix PAR (Parameter 28).

Table 6-26. Parameter Values Used for Brine Reservoirs in the BRAGFLO Calculations

Parameter (units)	Maximum	Minimum	Median or Constant[a]
Permeability (square meters)	1.58×10^{-10}	2.0×10^{-15}	1.58×10^{-12}
Effective Porosity (percent)	-	-	0.87
Rock Compressibility (1/pascals)[b]	10^{-8}	5.0×10^{-12}	10^{-10}
Initial Pressure (pascals)	1.70×10^{7}	1.11×10^{7}	1.27×10^{7}
Threshold Pressure, P_t (pascals)[c]	4.59×10^{-6}	2.28×10^{-4}	4.6×10^{-5}
Pore Distribution Parameter, λ	-	-	0.70
Residual Brine Saturation, S_{br} (unitless)	-	-	0.20
Residual Gas Saturation, S_{gr} (unitless)	-	-	0.20
Maximum Capillary Pressure (pascals)	-	-	10^{8}
Brine Volume (cubic meters)	160,000	32,000	80,000[d]

[a] Parameters with no maximum and minimum values are treated as constants in the performance assessment.
[b] Pore compressibility = rock compressibility/effective porosity.
[c] Threshold Pressure (P_t) determined from the relationship: $PCT\_A \cdot k^{PCT\_EXP}$, where PCT_A and PCT_EXP are constants and k is the permeability.
[d] There is equal probability of a brine volume less than 80,000 or greater than 80,000 cubic meters. However, 80,000 cubic meters is not a brine reservoir volume allowed in the model. See Appendix PAR.

The compressibility of brine reservoirs is based on analysis (Appendix MASS and MASS Attachment 18-2) of data collected from the WIPP-12 brine reservoir (Popielak et al. 1983, G-33). Values used in this performance assessment are shown in Table 6-26. The derivation of these values is documented in Appendix PAR (Parameter 29). The range for Castile brine reservoir compressibility used in BRAGFLO is broad. This range was selected in an attempt to ensure that all possible values are encompassed. Because the volume of brine that could be produced from a reservoir depends heavily upon the compressibility assumed, the brine volumes generated by the model reasonably bound those that would be produced from a Castile brine reservoir that could exist directly below the waste panels.

The brine reservoir volume is based on WIPP-12 observations and consideration of the effects of drilling 46.8 boreholes per square kilometer in the next 10,000 years in the vicinity of the site. The interconnectivity, or extent, of a fractured reservoir is uncertain. Analysis of WIPP-12 data has led to estimates of the effective radius of reservoirs from several hundred meters to several kilometers (Appendix MASS, Section MASS.18.1 and MASS Attachment 18-3), where the effective radius is the area over which the fractured network of a single reservoir extends. Reservoirs interpreted as smaller have effective radii on the order of several hundred meters—in other words, dimensions somewhat smaller than the waste panel. This interpretation is generally supported by geophysical survey data (see Section 6.4.12.6 and Appendix MASS, Section MASS.18.1 and MASS Attachment 18-5). Reservoirs interpreted as large have effective radii much larger than the waste panel dimensions, or even the site dimensions. The DOE assumes that reservoirs that may exist under the waste panels have

limited extent and interconnectivity, with brine volumes consistent with the lower values estimated from the WIPP-12 encounter. The basis for this assumption is discussed in the following paragraphs.

Consistent with regulatory criteria in 40 CFR § 194.33(b)(3) regarding the rate of drilling used in performance assessment, the DOE assumes that 46.8 deep boreholes may be drilled per square kilometer in the next 10,000 years. This drilling rate implies nearly 40-acre spacing of boreholes in the vicinity of the WIPP in 1,000 years, and nearly 5-acre spacing of boreholes at the end of 10,000 years. Even with limited probability of intersecting a brine reservoir (Section 6.4.12.6), there should be approximately one intersection per 480 acres in 1,000 years, and approximately one intersection per 48 acres in 10,000 years. Every time a reservoir of abnormally pressurized brine is penetrated, its pressure is partially depleted. Abnormally pressurized brine is defined as exhibiting pressure that exceeds the anticipated hydrostatic pressure for that depth. If reservoirs are well interconnected, they will be penetrated and partially depleted many times during 10,000 years until penetrating a reservoir no longer produces flow. If reservoirs are poorly interconnected, regions of pristine reservoirs could persist, although these would have lower producible brine volumes because of their limited extent.

There is an area in which potential brine reservoirs cannot be penetrated and depleted for some time—under the waste panels while passive institutional controls are effective. The passive institutional controls shield a region of the Castile from exploratory drilling. If brine reservoirs are well interconnected, the sheltered region could be depleted by the effects of multiple penetrations occurring in unprotected areas. If brine reservoirs are poorly interconnected, they could persevere under pristine conditions under the panels. The DOE considers that there are two reasonable conceptual models consistent with the drilling rate for the future condition of brine reservoirs in the WIPP region: (1) they are interconnected over large areas and penetrated and partially depleted many times; and (2) they are interconnected over small areas and not affected by the penetrations that occur outside but near the waste-area footprint. The DOE assumes that brine reservoirs potentially under the waste panels are poorly interconnected hydraulically (with extents similar to the lower estimates from WIPP-12), not much affected by penetrations occurring outside but near the waste-area footprint, and can persevere with pristine conditions until penetrated by a borehole drilled within the panel area. The DOE considers a pristine-condition, smaller reservoir to have potentially greater consequences than a depleted large reservoir.

The distribution of brine volumes assumed in performance assessment for determining the consequence of first penetration of a brine reservoir has five values: 32,000, 64,000, 96,000, 128,000, and 160,000 cubic meters (see Appendix MASS, Section MASS.18 and MASS Attachment 18-3). The smallest volume, 32,000 cubic meters, is the minimum volume from an analysis of WIPP-12 data (see Appendix MASS, MASS Attachment 18-3). Because this WIPP-12 reservoir volume represents an estimated effective area of about one-third of the waste panel area and because a reservoir larger than the minimum WIPP-12 volume could reasonably exist under the waste panels, the DOE also considers larger reservoir volumes in performance assessment. In BRAGFLO, the brine volume is placed in a region of rock of

constant dimensions. The porosity of the constant rock volume is set such that it contains pore volume equal to the reservoir brine volume. The porosity used for the largest reservoir is shown in Table 6-26. Porosities for smaller reservoirs are adjusted to yield the appropriate volume.

The BRAGFLO calculations develop reference system behavior for possible future events. BRAGFLO calculations of the E1 scenario are executed for every vector. In the calculations, it is assumed that a brine reservoir exists beneath the waste panels, and it is assigned properties from LHS. Because there is a probability associated with the occurrence of a brine reservoir, there may be no penetration of a brine reservoir in a randomly determined sequence of future events. In this case, the BRAGFLO reference-condition results for a brine reservoir penetration are not used. The probability assigned to penetrating a brine reservoir is discussed in Section 6.4.12.6 and Appendix MASS (Section MASS.18 and MASS Attachment 18-6).

6.4.9 Climate Change

The present climate at the WIPP and the geologic record of past climate change in southeastern New Mexico are discussed in Section 2.5 and Appendix CLI. Although meaningful quantitative predictions of future climate for the next 10,000 years are not feasible for the WIPP (or any location), effects of reasonably possible climate changes on disposal system performance must be considered. For the WIPP, uncertainty about these effects is incorporated in the performance assessment by considering the effects of various possible future climates on groundwater flow and potential radionuclide transport in groundwater. Direct effects of climate change that do not involve groundwater flow do not affect the long-term performance of the WIPP because of its depth below the land surface. Examples of such direct effects are changes in wind patterns, thermal effects related to changes in surface temperature, and near-future impacts on surface facilities. Long-term effects of climate change on the near-surface portions of the shaft seal system (see Section 6.4.4) are not incorporated in the analysis because BRAGFLO modeling conducted for this performance assessment indicates that system performance is unaffected by the behavior of the upper portion of the shaft seal system. Additional aspects of climate change screened out from the performance assessment, including glaciation at the site and possible future anthropogenic changes, are discussed in Appendix SCR (Sections SCR.1.6.2 and SCR.3.6.1).

The effects of postulated climate change on groundwater flow have been evaluated outside of the performance assessment calculations using a regional three-dimensional groundwater basin model based on the concept of basin hydrology introduced in Section 2.2.1.1. For the purposes of the regional analysis, climate-related factors that might affect groundwater flow, such as precipitation, temperature, and evapotranspiration, are treated through a single model parameter, potential recharge, which controls the rate at which water is added to the model at the water table. As described in Appendix MASS (Section MASS.17 and MASS Attachment 17-1), changes in this parameter allow simulation of regional groundwater flow under a range of different future states in which the climate may be wetter, the water table may be higher, and groundwater velocity in all units may increase. These and other simulations discussed in Appendix MASS (Section MASS.15 and MASS Attachment 15-7), show that the regional,

three-dimensional effects of climate change can be reasonably approximated in performance assessment through direct scaling of specific discharge in the two-dimensional, steady-state groundwater velocity field for the Culebra. The velocity field is calculated using SECOFL2D, as described in Section 6.4.6.2 and Appendix CODELINK (Section CODELINK.6.4). Radionuclide transport in the Culebra is then calculated by SECOTP2D using the scaled velocity fields.

Scaling of the two-dimensional velocity field is done using the Climate Index (Table 6-27), which is a dimensionless factor by which the specific discharge in each grid block of the SECOFL2D domain is multiplied. As summarized in Appendix PAR (Parameter 48), the Climate Index is a sampled parameter in the performance assessment, with a bimodal distribution ranging from 1.00 to 1.25 and from 1.50 to 2.25. A single value of the Climate Index is chosen in LHS for each sample element and held constant throughout the 10,000-year SECOFL2D simulation. Each realization of disposal system performance thus represents a different approximation of future climate. Those realizations in which the sampled value is close to its maximum of 2.25 represent the most extreme changes in groundwater flow that may result from climatic change.

Table 6-27. Climate Change Properties for the SECOFL2D Model

Parameter (units)	Maximum	Minimum	Median
Climate Index (dimensionless)	2.25	1.00	1.17

Sampled values close to the minimum of 1.00 represent climatic changes that have little effect on groundwater-flow velocities. Because all sampled values of the Climate Index are greater than 1.00, climate change as implemented in the performance assessment can only increase the rate of groundwater flow.

The distribution assigned to the Climate Index parameter is based on the results of three-dimensional basin modeling that considers future changes in the temporal pattern of potential recharge (see Appendix MASS, Section MASS.17 and MASS Attachment 17-1, Section F). Potential recharge is defined for the purposes of the regional modeling to be the maximum rate at which water can be added at the water table. Recharge itself is a model result and ranges from zero to the potential recharge. For those areas where the water table is at the ground surface and modeling indicates that water is discharging to the land surface through a seepage face, the potential recharge does not enter the model and has no effect on groundwater flow. In areas where the water table is below the land surface, potential recharge becomes actual recharge and tends to cause the elevation of the water table to rise. If potential recharge is zero, the water table in an idealized basin will tend to fall until it is a horizontal plane with an elevation equal to the lowest topographic point in the basin. Sufficiently large values of potential recharge will cause the water table to rise to the land surface everywhere. Smaller nonzero values result in solutions with water tables that are at the land surface at topographic low points (discharge areas) and at some distance below the

land surface at topographic highs (recharge areas). Changes in potential recharge cause the elevation of the water table to rise or fall. In the three-dimensional modeling of the WIPP region, potential recharge was assumed to be spatially invariant across the regional model domain and is assumed to change through time in response to changes in climate.

Both steady-state and transient three-dimensional regional analyses have been executed with values of potential recharge varied such that the elevation of the water table ranged from approximately its present position to at or near the land surface. The latter condition provides an upper bound for regional groundwater-flow velocities during future wetter climates. For all simulations examining the effects of climate change, recharge is assumed to be greater at some time in the future than it is at present. Present recharge is assumed to be the same as its minimum value during the Holocene. The dominant effects on climate change during the next 10,000 years are assumed to be natural rather than anthropogenic. This assumption is consistent with regulatory guidance provided by the EPA indicating that consideration of the effects of climate change should be limited to natural processes (EPA 1996a, 61 FR 5227).

Because of uncertainty about recharge rates during future wet periods and the timing of these periods, transient analyses use two fundamentally different patterns for the change in potential recharge. The first pattern for future potential recharge used in the analysis corresponds to a continuation of the inferred climate patterns of the Holocene (see Section 2.5.1 and Appendix CLI, Section 3), with wetter peaks occurring 500, 2,000, 4,000, 6,000, 8,000, and 10,000 years in the future. Potential recharge is assumed to increase and decrease linearly during the wet periods 500 years before and after the peaks, and the wet periods are each separated by 1,000 years of a drier climate like that of the present. Several different values were examined for the maximum potential recharge imposed at the wet peaks, with the largest value chosen to provide a steady-state solution with the water at, or close to, the land surface throughout the model domain. As discussed in Appendix MASS (Section MASS.17 and MASS Attachment 17-1, Section F), a continuation of the Holocene climatic variability is considered likely during the next 10,000 years, and this function is assigned a relatively high probability of occurrence (0.75). This recharge function and its probability of occurrence are reflected in the lower portion of the bimodal distribution assigned to the Climate Index parameter.

The second recharge pattern considered in the analysis assumes that potential recharge will increase from its present value to a specified larger value 500 years in the future and that potential recharge will then remain constant throughout the rest of the 10,000-year simulation. As with the Holocene pattern, several different values were examined, with the largest being sufficient to result in a steady-state solution with the water table at, or close to, the land surface throughout the model domain. Conceptually, this pattern corresponds to a future in which the climate either becomes continuously wetter or the frequency of wetter periods becomes sufficiently large that the hydrologic response is indistinguishable from that of a continuously wetter climate. Step-increase recharge functions were used to simulate the effects of major disruptions of the Holocene climate, analogous to those that might occur during the next 10,000 years in a transition from the present warm interglacial climate to the early stages of a future glacial climate. As discussed in Appendix MASS (Section MASS.17), such disruptions to the Holocene climate are considered unlikely, and the step function is

assigned a relatively low probability of occurrence (0.25). This recharge pattern and its probability of occurrence are represented by the upper portion of the bimodal distribution assigned to the Climate Index parameter.

As reported in Appendix MASS (Section MASS.17 and MASS Attachment 17-1, Section E), 17 transient and 54 steady-state, regional three-dimensional groundwater-flow simulations were run to examine effects of climate change. Simulations considered both potential recharge functions with varying peak recharge rates and different sets of assumptions about regional rock properties. Total specific discharge into and out of the Culebra within a model region approximately corresponding to the controlled area was calculated for each simulation. Values for the Climate Index parameter were determined by comparing the total lateral specific discharge calculated for each simulation. The largest observed increase in flow for those simulations using realistic values of rock properties was a factor of 2.1. Although some simulations produced a slight reduction in flow, Climate Index parameter values less than 1.0 are not considered in the performance assessment. Changes in flow direction in the Culebra were also noted in some three-dimensional simulations, with a shift in flow toward the west corresponding to a regional increase in the elevation of the water table. These potential changes in flow direction are not incorporated in the two-dimensional flow and transport modeling to simplify the computational process. This treatment is conservative with respect to radionuclide transport because the most rapid transport possible under any climate conditions will be through the most conductive portion of the Culebra south and east of the repository. Any shift of the flow direction away from this high conductivity zone would result in slower transport through less permeable rock. Restricting the effects of climate change to a uniform linear scaling of specific discharge in the SECOFL2D model is, therefore, a conservative assumption.

6.4.10 Initial and Boundary Conditions for Disposal System Modeling

The solution of many mathematical models used in performance assessment requires specification of a starting point, called initial conditions, and specification of how the region modeled (that is, volume) interacts with the regions not modeled, called boundary conditions. Initial values are required for all of the parameters appearing in a computer code. In practice, however, the term initial conditions refers to the values assigned to the primary variables used to describe the system, examples of which may be pressure, composition, and saturation. The term boundary conditions refers to the specification of primary variables that control the interaction of the modeled region with the regions excluded from the model. In many studies, applied boundary conditions are static in time, although computer codes that implement time-dependent boundary conditions are not uncommon. A common practice in modeling groundwater flow is to place boundaries of the modeled system somewhat distant from the region in which model results are of interest. This is done to help ensure that uncertainty in the natural boundaries of the system does not unduly influence model results in the region of interest. The DOE adopts this practice in its application of BRAGFLO and SECOFL2D to the WIPP.

The following sections describe the initial and boundary conditions specified for the major codes used in this performance assessment. Initial values of parameters not discussed in the following sections are set equal to the values assigned from the performance assessment database or LHS sampling that are discussed elsewhere in Section 6.4.

6.4.10.1 Disposal System Flow and Transport Modeling (BRAGFLO and NUTS)

In BRAGFLO, initial conditions for the simulation of the regulatory period are consistent with the following: (1) there are no gradients for flow in the far-field Salado; (2) Salado far-field pore pressures are elevated above hydrostatic from the surface but below lithostatic; and (3) near the repository, excavation and waste emplacement results in partial drainage of the DRZ and subsequent evaporation of drained brine into mine air, and then removal from the modeled system by air exchanged to the surface. The term far-field used above refers to the region that is not influenced by the drainage of the DRZ mentioned in (3). For units above the Salado, initial pressures are set to be consistent with observed pore pressures or normal hydrostatic gradients.

Estimating the effects of drainage of the DRZ that occurs during the operational period, (3) above, is not simple. For each vector sampled in LHS, the DOE estimates this by using BRAGFLO to simulate a period of time representing disposal operations. This calculation is called the start-up simulation and covers five years from $t = -5$ years to $t = 0$ years, corresponding to the amount of time a typical panel is expected to be open during disposal operations. Most of the initial parameters used during the regulatory period simulation ($t = 0$ to $t = 10{,}000$ years) are also assigned for the start-up simulations, with some exceptions that are described below.

The initial pressures in the Salado for the start-up simulation are calculated based on a sampled pressure at the elevation of MB139 at the shaft and adjusted throughout the Salado and the DRZ to account for changes in hydraulic head due to elevation change. This parameter is discussed in Appendix PAR (Parameter 26). This adjustment assumes hydrostatic equilibrium. The DRZ permeability is set at 10^{-17} square meters for the start-up simulation. Based on observed changes in the DRZ, the DRZ porosity is adjusted upwards 0.0029 (0.29 percent) from the sampled value for intact impure halite. Initial pressure for the start-up simulation in the excavated regions is set to atmospheric. The shaft exists and is modeled as unfilled with the same physical properties as the excavation.

For the start-up simulation, an initial water-table surface is specified within the Dewey Lake at an elevation of 3,215 feet (980 meters) above mean sea level. This elevation is consistent with observations discussed in Section 2.2.1.4.2.1. Above the water table, pressure is maintained at one atmosphere, 0.101 megapascals; liquid saturations in these computational cells are held constant at residual liquid saturation (Section 6.4.6.6, Table 6-23). Below the water table initial liquid saturations in all regions except the repository and shaft are 100 percent. Pressures are set consistent with a hydrostatic gradient below the water table within the Dewey Lake, as well as in the Rustler except for the Magenta and Culebra. An initial pressure for the Culebra is set at 0.822 megapascals, based on fluid level and fluid density

data collected at H-1, H-2B, H-3, H-4B, H-5B, H-6B, P-14, P-15, and P-17. An initial pressure of 0.917 megapascals is specified for the Magenta, calculated from fluid level and fluid density data from H-1, H-2A, H-3, H-4A, H-5A, and H-6A (Dotson 1996). Even though the natural properties of the units above the Salado vary considerably over the domain modeled by BRAGFLO, the BRAGFLO initial condition of constant pressure and constant properties for each layer is considered reasonable because the purpose of the BRAGFLO calculation with respect to these units is to calculate the long-term flux of brine from the borehole or shaft to each unit, or to the surface. For this purpose, the pressure and properties at the borehole or shaft are important, but details of regional hydraulic head and unit properties are not.

For the start-up simulation, permeabilities of all units above the Salado are set to zero so that flow cannot occur from these units into the shaft. This modeling assumption is adopted as a simple method of accounting for the existence of effective liners in the shafts during disposal operations.

For the start-up simulation, no-flow boundary conditions are assigned in the BRAGFLO model of the disposal system along all of the exterior boundaries of the computational mesh except at the far field boundaries of the Culebra and Magenta and the top of the model (that is, the surface of the ground). These boundaries are 20 kilometers from the edge of the land withdrawal area boundary, as discussed in Section 6.4.2.1. The ground surface is maintained at atmospheric pressure. The boundaries of the Culebra and Magenta are maintained at pressures of 0.822 megapascals and 0.917 megapascals, respectively, corresponding to the initial pressure conditions used in the Culebra and Magenta. The pressure in the Castile brine reservoir is set at its sampled value for the start-up simulation.

During the start-up simulation, fluid flow calculated by BRAGFLO from the Salado and the DRZ into the excavated region simulates the effect of drainage into the repository during the operational period. Following the completion of the start-up simulations, specification of initial conditions occurs for the regulatory period simulation. Boundary conditions for the regulatory period simulation are the same as those for the start-up simulation.

The regulatory period simulation begins with conditions specified consistent with the sealing of the repository by construction of shaft seals. Certain properties assigned for the start-up simulation are changed to make model conditions consistent with the emplacement of waste and completion of sealing. The liquid saturation in the waste-disposal region of the repository is set at 0.015, which is a conservative value (Butcher 1996), and other areas of the excavation are assigned zero liquid saturation (100 percent gas saturation), regardless of the quantity of brine that may have flowed into the excavation during the start-up simulations. This is consistent with the observed ability of circulating mine air to remove any inflowing brine by evaporation. The entire repository is assigned an initial pressure of one atmosphere. Pressures and saturations in model regions representing rock remain as they were calculated to be at the end of the start-up simulation. Permeabilities of the units above the Salado are reset to the values specified for them as discussed in Section 6.4.6. The shaft is assigned properties for shaft seal materials discussed in Section 6.4.4. The pressure in the shaft is set to

one atmosphere, and the liquid saturation of shaft materials is set to 1.0 except in asphalt, where liquid saturation is 0 percent. Waste is emplaced in the waste-disposal regions at a density of 1.63×10^{2} kilograms per cubic meters for ferrous metals and 6.52×10^{1} kilograms per cubic meters for biodegradable materials, and other waste properties are assigned as discussed in Section 6.4.3.2. Panel closure properties discussed in Section 6.4.3.2 are assigned to the panel closure regions. Permeability in the DRZ is raised to 10^{-15} square meters; this value remains constant for the regulatory period simulation. Corrosion and biodegradation reactions that produce gas are modeled to begin at the start of the regulatory period simulation, and their rates depend on the sampled parameter values for the gas generation model (see Section 6.4.3.3) and the availability of brine. Modeling of creep consolidation through the use of the porosity surface also begins at this time (see Section 6.4.3.1).

6.4.10.2 Culebra Flow and Transport Modeling (SECOFL2D, SECOTP2D)

Groundwater flow in the Culebra is computed at both a regional and local scale. Regional-scale simulations are performed over a large domain using a computational grid that is coarser than the grid used for the local scale. The regional domain covers only a portion of the natural hydrologic system. A correct flow field can be calculated for any arbitrary part of a more extensive system if the transmissivity distribution and the values of hydraulic head assigned at the boundaries are representative of observed conditions. There is therefore considerable flexibility in choosing the locations of boundaries for the regional SECOFL2D model. Several factors were considered in selecting these boundaries. One side of the rectangular domain was aligned along a natural hydrologic feature, the axis of Nash Draw. The size of the model domain was selected such that the domain does not extend a great distance beyond the region of concentrated transmissivity and hydraulic-head data but was large enough that the imposed boundary conditions would not have a large influence on the solution in the region of interest. The results of the regional-scale simulations are used to interpolate boundary conditions at the local scale. This modeling approach allows the use of high resolution computational grids in the region of interest for computing radionuclide transport and the incorporation of a flow field representing a larger area.

The regional domain is approximately 13.67 miles by 18.64 miles (22 kilometers by 30 kilometers) and is aligned with the axis of Nash Draw along a portion of the western boundary (see Figure 6-17 in Section 6.4.6.2). Nash Draw is a highly conductive region that behaves hydraulically as a groundwater divide (see Section 2.2.1.1). Therefore, that portion of the western boundary oriented along Nash Draw is represented by a no-flow boundary. The remaining regional boundary conditions are positioned to align with topographic highs or other geologic features such as the San Simon Swale on the southeast boundary. Because of uncertainty in boundary heads, the boundaries are positioned a large distance from the local problem domain (see Figure 6-18 in Section 6.4.6.2). This is done to reduce the influence of these boundary conditions on the solution in the region of interest. Because boundary head values can be easily estimated numerically during the calibration of transmissivity fields from existing well data, Dirichlet (constant head) boundary conditions are used on these boundaries (see also the discussion in Section 6.4.6.2).

Boundary conditions of the local domain are Dirichlet (constant-head) and derived by interpolating the solution of the regional domain. Because these boundary conditions are set by interpolation and because the simulations are steady state, Dirichlet and Neuman (specified flux) boundary conditions will provide essentially identical results, and specification of the type of boundary condition is not important.

An initial estimate of the undisturbed head distribution is required to analyze transient well data needed to generate the transmissivity fields (see Section 6.4.6.2 and Appendix TFIELD, Section TFIELD.2.2.4). These data were obtained from hydrographs of the WIPP boreholes measured prior to the excavation of the first shaft. The hydrographs depict hydraulic heads for up to 5 years preceding shaft excavations. The transmissivity-field calibration process develops a set of boundary heads for the regional domain that are consistent with hydrograph observations and the transmissivity field generated.

Initial conditions are not required for the Culebra flow calculations because these are steady state. Initial actinide concentrations in the transport simulations are assumed to be zero.

6.4.10.3 Initial and Boundary Conditions for Other Computational Models

In addition to BRAGFLO, SECOFL2D, and SECOTP2D, several other codes are used in performance assessment that require initial and boundary conditions. In general, these codes are strongly coupled to BRAGFLO, analogous to the manner in which SECOTP2D is coupled to SECOFL2D. These additional codes are NUTS, PANEL, the BRAGFLO direct brine release model (BRAGFLO_DBR), and CUTTINGS_S.

NUTS transports radionuclides through the BRAGFLO domain based on fluid flow characteristics as calculated by BRAGFLO and, therefore, does not need explicit definition of flow boundary conditions. As actinide transport is not of concern until the repository contains waste and is sealed, a start-up simulation is not executed with NUTS. Boundary conditions for advective transport are consistent with the boundary conditions assumed for fluid flow. Molecular transport boundary conditions for NUTS simulations consist of no diffusion or dispersion in the normal direction across far-field boundaries. Initial actinide concentrations are zero in all regions except the waste. Actinide concentrations in brine in the waste regions are assigned as discussed in Section 6.4.3.5 (Table 6-11).

PANEL is used to estimate the transport of radionuclides from the repository to the Culebra for the E1E2 scenario. PANEL assumes homogeneous mixing within a panel of the waste disposal region for determination of a source term for radionuclides. PANEL is strongly coupled to BRAGFLO, in that the flux of liquid up the borehole out of the separate panel in BRAGFLO is provided as the flux of liquid leaving the mixing volume in PANEL. Liquid leaving the mixing cell in PANEL is assumed to arrive at the Culebra, thereby maximizing the source of actinides to the Culebra.

Models for direct release to the surface are also strongly coupled to BRAGFLO. CUTTINGS_S (cuttings, cavings, and spall) and BRAGFLO_DBR acquire fluid pressure, fluid

saturation, and other necessary quantities from the appropriate BRAGFLO disposal system model simulation. It is assumed in the direct release models that radionuclides, once entrained in drilling fluid, remain in the drillhole until they reach the surface. In other words, there is no interaction between drilling fluid and the formations between the repository and the surface. Boundary conditions in the direct brine release model are no-flow except for the sources and sinks of brine through borehole nodes and at the surface.

6.4.11 Numerical Codes Used in Performance Assessment

To evaluate scenario consequences for both undisturbed and disturbed performance, the DOE uses many computer codes to simulate relevant features of the disposal system. The flow of information and primary roles of the codes used are discussed in this section; detailed discussion of the individual codes is reserved for appendices, which are referenced as appropriate. Parameter values and disposal system conditions must be passed between codes several times in an assessment.

The codes are executed under the requirements of the SCMS, which creates and maintains a complete record of the input data and results of each calculation, together with the exact codes used to create those results. For this application, performance assessment codes used in conjunction with LHS or random sampling were executed under the SCMS.

The major computer codes and the flow of information among them are illustrated in Figure 6-25. As discussed in Section 6.1.4 and indicated in Figure 6-25, some of these codes are used to calculate reference conditions for deterministic futures associated with the parameters in $\mathbf{x}_{su}$ (Equation 4b [Section 6.1.2]) and their associated uncertainty characterized by distributions D_{su} (Equation 6b [Section 6.1.2]). The results of these codes are then used in the construction of the consequences of probabilistic futures. There are three major steps in evaluating scenario consequences for deterministic futures: (1) preparation of input from submodels executed independent of LHS (for example, SANTOS, GRASP-INV), (2) LHS of the variables $\mathbf{x}_{su}$ in the performance assessment parameter database, and (3) execution of the sampling-dependent performance assessment codes (those within the deterministic futures box indicated by dashed lines in Figure 6-25).

Some performance assessment codes are used to calculate probabilistic futures, that is, future events that occur randomly in time and space, and uncertainty in associated parameters in $\mathbf{x}_{st}$ (Equation 4a [Section 6.1.2]) and their uncertainty characterized by distributions in D_{su} (Equation 6a [Section 6.1.2]). There are two major steps in evaluating scenario consequences for probabilistic futures: (1) random sampling of the parameter database, and (2) execution of the codes.

Figure 6-25 indicates only those codes that perform the bulk of the computational effort related to simulating the significant physical processes occurring within the disposal system. In addition to these codes, a variety of additional codes are used in this performance assessment. These additional codes are used for the transfer of data between codes,

preparation of input files, model output processing, and similar tasks. These codes are also executed within the SCMS.

Because these additional codes are not expressly used for simulation of physical processes, they have been omitted for clarity from discussion here and on Figure 6-25. A comprehensive description of the coupling of codes used in this performance assessment is provided in Appendix CODELINK (see Table CODELINK-1).

Figure 6-26 shows an alternative method of visualizing how the various performance assessment codes relate to each other and to the estimation of scenario consequences. This figure represents a vertical cross section of the disposal system, associating the major codes with the particular components of the system each code simulates. As shown in the figure, BRAGFLO, SANTOS, NUTS, and PANEL address the Salado. GRASP-INV, SECOFL2D, and SECOTP2D address the Culebra. CUTTINGS_S, BRAGFLO_DBR, and PANEL address the immediate consequences of inadvertent human intrusion through one or more exploratory boreholes. Combined, Figures 6-25 and 6-26 illustrate the flow of information through major performance assessment codes and the relationship between the codes and the physical system being simulated.

The parameter database is the initial element in the performance assessment process. The database includes the parameters used in performance assessment codes that pertain to the technical aspects of disposal system performance. Parameters pertaining only to the execution of the codes (for example, convergence criteria for Newton-Raphson numerical solvers) are generally not included in the database but are recorded in input files and are traceable through the SCMS. The parameters in the database fall into two categories: those that are assigned fixed values, and those that are uncertain and are therefore assigned a range of values according to a CDF.

Vectors (sets) of parameter values are created from the uncertain variables in the database by LHS of each variable for the set of simulations comprising a performance assessment of the system. In this performance assessment, 57 parameters are sampled using LHS, and 100 vectors are assembled in each replicate (see Section 6.5). The values assigned to each sampled parameter in each of the vectors in this performance assessment are included in Appendix IRES (Section IRES.1). Each of the fixed parameter values from the database and a vector of sampled parameter values are combined to form a realization (a set of input parameters). Each realization is then propagated through the performance assessment codes within the dashed lines in Figure 6-25.

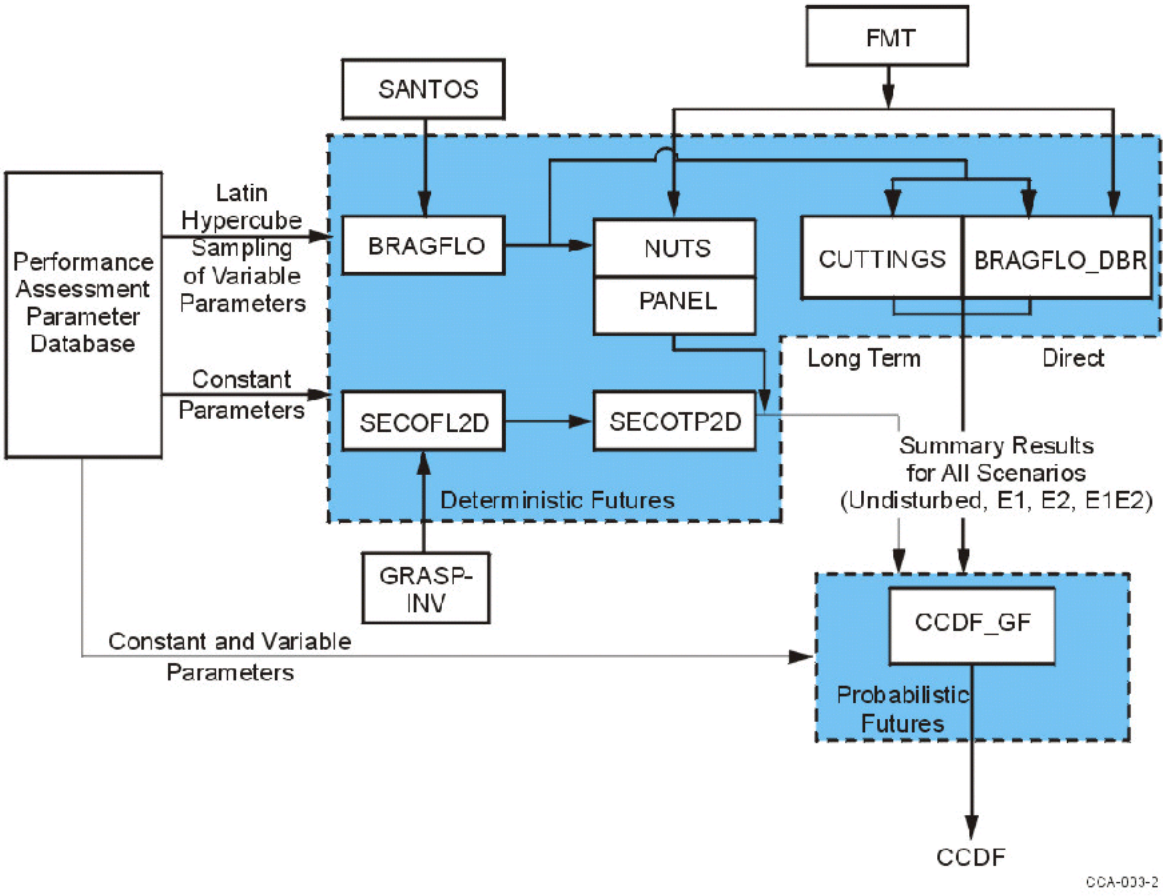

Figure 6-25. Major Codes, Code Linkages, and Flow of Numerical Information in WIPP Performance Assessment

1

1 **THIS PAGE INTENTIONALLY LEFT BLANK**

1

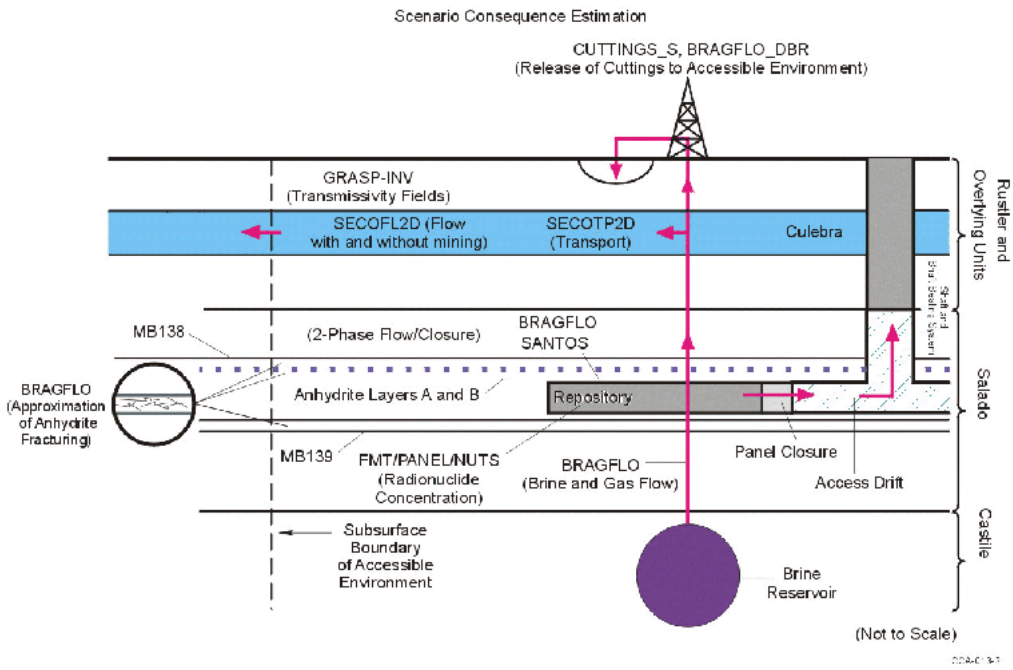

Figure 6-26. Schematic Side View of the Disposal System Associating Performance Assessment Codes with the Components of the Disposal System Each Code Simulates

1 **THIS PAGE INTENTIONALLY LEFT BLANK**

The assessment of each realization requires that the codes shown in Figure 6-25 for deterministic futures be executed under four code sequence configurations, one each for the undisturbed performance scenario, the E1 scenario, the E2 scenario, and the E1E2 scenario.

Each intrusion scenario may occur with or without mining. The techniques used for each scenario are described in Section 6.4.13.

As shown in Figure 6-25, information for some of the major codes comes from the following additional sources: the SANTOS, GRASP-INV, and FMT codes. The SANTOS code develops the porosity surface describing porosity as a function of time and pressure; this information is used in the BRAGFLO code (see Appendices BRAGFLO, Section 4.11, and PORSURF, Section PORSURF.1). GRASP-INV calculates numerous possible and equally likely Culebra transmissivity fields; these transmissivity fields are used in the SECOFL2D code (see Appendix TFIELD, Section TFIELD.4, and Appendix CODELINK, Section CODELINK.6.4). FMT is used to calculate solubility parameters that were entered into the parameter database. These parameters, as well as sampled solubility distribution parameters, were used to calculate solubilities for the performance assessment. Actinide solubility in the repository is used by the codes NUTS and PANEL.

The performance assessment codes are executed sequentially. Following LHS, BRAGFLO is the first major code executed. Notice that the code BRAGFLO is listed twice in this sequence. BRAGFLO is used in two applications for performance assessment. In the first application, BRAGFLO calculates the overall movement of gas and brine in the repository and from the Castile to the surface; this movement forms the basis for estimating radionuclide releases to the accessible environment (Appendix BRAGFLO, Sections 4.1 through 4.9). BRAGFLO also contains subsystem models for estimating gas generation in the repository, disposal room closure and consolidation, and interbed fracturing (Appendix BRAGFLO, Sections 4.10 through 4.13). BRAGFLO does not calculate the movement of radionuclides. The second application of BRAGFLO is discussed below.

NUTS calculates the overall movement and decay of radionuclides in the repository and disposal system. NUTS uses the same geometry as BRAGFLO, the brine and gas flow fields calculated by BRAGFLO, and the radionuclide source concentrations (solubilities) in the repository defined by the actinide source term models. In simulations of the E1 scenario, NUTS also tracks brine originating in the Castile brine reservoir, including the fraction of Castile brine that has flowed out from the borehole and into the waste in the repository. See Appendix NUTS (Section 4) for additional information on the use of NUTS in performance assessment. PANEL calculates actinide source term to the Culebra for the E1E2 scenario, as discussed in Section 6.4.13.5. PANEL is described in detail in Appendix PANEL.

In all scenarios, the quantity of brine flowing up the shafts or a degraded exploratory borehole to the Culebra is calculated by BRAGFLO, and the concentration of radionuclides in that brine, calculated by NUTS or PANEL, is used to determine the quantity of radionuclides released to the Culebra.

CUTTINGS_S and BRAGFLO_DBR are used to evaluate the immediate consequences of inadvertent human intrusion through exploratory drilling. Solid material and brine may be transported to the surface in the drilling fluid. After pressure in the repository is relieved through the first borehole, subsequent boreholes may release less material to the surface. CUTTINGS_S calculates the quantity of solid material transported to the accessible environment at the surface during the drilling activities. This material includes material removed directly from the borehole (cuttings), together with cavings and spallings. The code is discussed in Appendix CUTTINGS. BRAGFLO_DBR is used to calculate the quantity of brine transported up the borehole to the surface.

SECOFL2D and SECOTP2D together calculate the detailed movement of radionuclides in the Culebra that occurs if radionuclides are introduced by flow up the shafts or through a degraded exploratory borehole. SECOFL2D calculates regional Culebra flow fields using an assumption that flow occurs in a single-porosity medium. SECOFL2D uses the transmissivity fields calculated by GRASP-INV (one field in each simulation). SECOTP2D calculates radionuclide transport in a double-porosity medium, accounting for advection in fractures, matrix diffusion, retardation, and decay, as described in Section 6.4.6.2. SECOFL2D is discussed in Appendix SECOFL2D; SECOTP2D is discussed in Appendix SECOTP2D. The NUTS and PANEL codes calculate the actinide source term to the Culebra.

The computer code CCDFGF is used to (1) determine random sequences of future events that may occur over the next 10,000 years at the WIPP site; (2) estimate the radionuclide releases resulting for these random sequences of future events, using the results of the calculations described thus far in Section 6.4; and (3) construct a CCDF for each realization. The manner in which CCDFGF determines random sequences of future events is the subject of Section 6.4.12. The estimation of consequences and construction of a CCDF for these sequences of future events is the subject of Section 6.4.13.

6.4.12 Sequences of Future Events

For this application, sequences of future events that may occur are determined using a random sampling procedure described in Appendix CCDFGF (Section 3.2). A general description of the technique is presented in this section.

The incorporation of stochastic uncertainty in the performance assessment is based on repeatedly generating independent sequences of events that may occur at the WIPP over the next 10,000 years. Each 10,000-year sequence is generated by randomly sampling six parameters that characterize stochastic uncertainty about future events repeatedly. These parameters include (1) the interval of time between drilling intrusions (which yields both the number and time of intrusions), (2) the location of each drilling intrusion, (3) the activity of the waste penetrated by each drilling intrusion, (4) the plug configuration in the intrusion borehole, (5) the penetration of a Castile brine reservoir, and (6) the occurrence of mining. Probability distribution functions are assigned to each of these six parameters and are discussed in the following sections. Random sampling from these distributions is used to generate 10,000 equally likely, independent futures for the WIPP for each realization

executed and CCDF constructed. The computer code CCDFGF (Appendix CCDFGF, Section 3.2) is used to randomly sample sequences of future events, construct consequences of these sequences, and assemble CCDFs. As described in Section 6.4.13, normalized integrated radionuclide releases to the accessible environment are estimated for each history using the consequence modeling system.

The probability assigned to the occurrence of certain events in the future at the WIPP site is affected by regulatory guidance and by actions taken by the DOE to deter activities detrimental to WIPP performance. Active and passive institutional controls are discussed extensively in Chapter 7.0. A summary of their use in performance assessment begins the discussion in this section.

6.4.12.1 Active and Passive Institutional Controls in Performance Assessment

Active institutional controls and passive institutional controls will be implemented at the WIPP site to deter human activity that may be detrimental to the performance of the repository. Active institutional controls and passive institutional controls are described in detail in Chapter 7.0 and in appendices referenced in Chapter 7.0. In this section, the impact of active institutional controls and passive institutional controls to performance assessment is described.

Active institutional controls will be implemented at the WIPP after final facility closure to control access to the site and to ensure that activities detrimental to the performance of the disposal system do not occur within the controlled area. The active institutional controls will preclude human intrusion in the disposal system. A limitation for considering the effectiveness of active institutional controls in performance assessment is established in 40 CFR Part 191. That limitation is 100 years. Because of the nature of the system of active institutional controls to be implemented and regulatory restrictions, it is assumed in performance assessment that there can be no inadvertent human intrusions or mining in the controlled area for 100 years following repository closure.

Passive institutional controls have a function in deterring inadvertent human intrusion into the disposal system in performance assessment. While only minimal assumptions were made about future society for the purposes of designing the passive institutional controls to comply with the Assurance Requirements, more detailed assumptions are made in order to quantify the effectiveness of passive institutional controls for performance assessment. The preamble to 40 CFR Part 194 limits any credit for passive institutional controls in deterring human intrusion to 700 years after disposal (EPA 1996a, 61 FR 5231). This suggested time limit is important in quantifying the effectiveness of passive institutional controls for performance assessment purposes. Because active institutional controls are effective for the first 100 years, passive institutional controls are effective for the period of time from 100 to 700 years, or a duration of 600 years.

The effectiveness of passive institutional controls is implemented in performance assessment by reducing the rate of human intrusion and mining by a factor that estimates the

effectiveness of passive institutional controls. As discussed in Appendix EPIC, passive institutional controls are assumed to be 0.99 effective, meaning that the rate of deep drilling and mining for the 600-year duration of passive institutional controls is a factor of 0.01 times the respective rates for the uncontrolled period following 700 years. Because passive institutional controls are designed to protect the controlled area, this reduction factor is applied to the entire controlled area.

6.4.12.2 Number and Time of Drilling Intrusions

The number of drilling intrusions associated with each 10,000-year history is based on 40 CFR § 194.33(b)(2) and § 194.33(b)(3):

> In performance assessments, drilling shall be assumed to occur in the Delaware Basin at random intervals in time and space during the regulatory time frame. [40 CFR 194.33(b)(2)]
>
> The frequency of deep drilling shall be calculated in the following manner:
> (i) Identify deep drilling that has occurred for each resource in the Delaware Basin over the past 100 years prior to the time at which a compliance application is prepared.
> (ii) The total rate of deep drilling shall be the sum of the rates of deep drilling for each resource. [40 CFR 194.33(b)(3)]

The DOE's implementation of these criteria is described in this and the following sections.

Mathematically, events that are random in time can be described as following a Poisson process that can be written in a simple form as

(13)

where $p[E_n(\Delta t)]$ is the probability (p) that some number (n, an integer) of events (E) will occur in a time interval (Δt) given a rate constant λ with units of events per time.

Inadvertent human intrusions may occur at any time between 100 years and 10,000 years after the decommissioning of the facility. Both the number and time of intrusions are determined sequentially by sampling from a CDF derived from the Poisson model that probabilistically describes the time period that elapses between an intrusion at a fixed time and the next intrusion. The time interval to the next intrusion following an intrusion may vary from 0 years to greater than 9,900 years, with a probability determined by the rate constant λ. The rate constant is derived from the drilling rate established for the Delaware Basin and the area of the waste disposal region, 0.049 square miles (0.126 square kilometers). The drilling rate used in this analysis was 46.8 boreholes per square kilometer per 10,000 years. As discussed in Appendix DEL (Section DEL.7.4), this rate is based on a review of past and present drilling activity in the Delaware Basin. The rate constant λ is assigned different values for three time periods. While active institutional controls are effective, it is equal to zero, and while passive institutional controls are effective, it is two orders of magnitude lower than during the uncontrolled period (700 to 10,000 years).

The CDF for intrusion times while passive institutional controls are effective is called the passive institutional controls CDF. The CDF for intrusion times after passive institutional controls may no longer be considered effective is called the post-passive institutional controls CDF. Sequences of future deep drilling events are constructed as follows. The passive institutional controls CDF is sampled to determine whether an intrusion occurs while passive institutional controls are effective. If the sampled time is greater than 600 years, zero intrusions occur before 700 years. If the time is less than 600 years, the passive institutional controls CDF is sampled again to determine whether a second intrusion occurs in the interval between the time of the first intrusion and 700 years. This procedure continues until a time of intrusion greater than 700 years is determined.

Intrusions times after 700 years are determined by sampling the post-passive institutional controls CDF. If the sampled time is greater than 9300 years (700 + 9,300 = 10,000), no intrusions occur between 700 and 10,000 years. If the sampled time is less than 9,300 years, an intrusion occurs at 700 years plus the sampled time. The post-passive institutional controls CDF is sampled iteratively to determine whether intrusions occur in the time interval between the last intrusion and 10,000 years, until an intrusion is determined to occur after 10,000 years.

Evaluation of the Poisson process for a specified rate constant and time interval yields the probability of occurrence of specified numbers of intrusions. Using a different rate constant for 100 years of active institutional controls, 600 years of passive institutional controls, and 9300 years of uncontrolled activity, the most likely number of intrusions into the waste disposal region during 10,000 years is five, occurring with a probability of 0.1715. Zero intrusions occur with a probability of 0.0041. The largest number of intrusions that occur with a probability greater than 10^{-3} per 10,000 years (and which therefore can contribute to releases for comparison with the quantitative release limits) is 14, occurring with a probability of 0.0011. Probabilities for other numbers of intrusions within 10,000 years are given in Table 6-28. These probabilities are shown as a histogram in Figure 6-27.

6.4.12.3 Location of Intrusion Boreholes

Drilling events are assumed to be random in time and space, and the location of each intrusion borehole within the waste disposal region is sampled randomly. This is done in the analysis by discretizing a plan view of the area within the passive institutional control berms (see Appendix PIC, Section VIII) into 144 separate regions, and requiring each intruding borehole to penetrate one, and only one, region (Figure 6-28). The probability of intersecting each location is equal to 1/144 (about 0.00694), and slight variations in the size of regions are disregarded as unimportant.

Table 6-28. Probabilities of Different Numbers of Intrusions into the Waste Disposal Region (for 100 years of active institutional control, 600 years of passive institutional control, and 9,300 years of uncontrolled activity)

Number of Intrusions	Probability of Occurrence
0	0.0041
1	0.0227
2	0.0622
3	0.1138
4	0.1562
5	0.1715
6	0.1570
7	0.1231
8	0.0845
9	0.0516
10	0.0283
11	0.0141
12	0.0065
13	0.0027
14	0.0011
15	0.0004

Each of the 144 regions contains both excavated and unexcavated areas at the repository horizon. A borehole penetration of a region has an approximately 20 percent chance of intruding excavations and approximately 80 percent chance of passing through unexcavated Salado. The berm area and the proportion of excavated to unexcavated regions at the repository horizon are important in the Castile brine reservoir model, as discussed in 6.4.12.6.

Boreholes that penetrate excavations may penetrate CH-TRU waste, RH-TRU waste, or panel closures that contain no waste. For long-term releases and direct brine releases, all penetrations into excavations are treated as if CH-TRU waste is penetrated, and the RH-TRU waste inventory is averaged into the CH-TRU waste inventory for source-term determination. For cuttings and cavings direct releases, there is an approximately 12 percent chance that RH-TRU waste canisters are penetrated and an 88 percent chance that CH-TRU waste is penetrated, corresponding to the relative plan-view areas of each waste type. For cuttings and cavings direct releases, the small area of the panel closures is treated as CH-TRU waste and is included in the CH-TRU waste probability. Because of the low permeability of the region surrounding each RH-TRU waste canister, intrusions into RH-TRU waste are assumed to not produce spallings releases. Intrusions resulting in spallings releases are treated as CH-TRU waste for the source term determination.

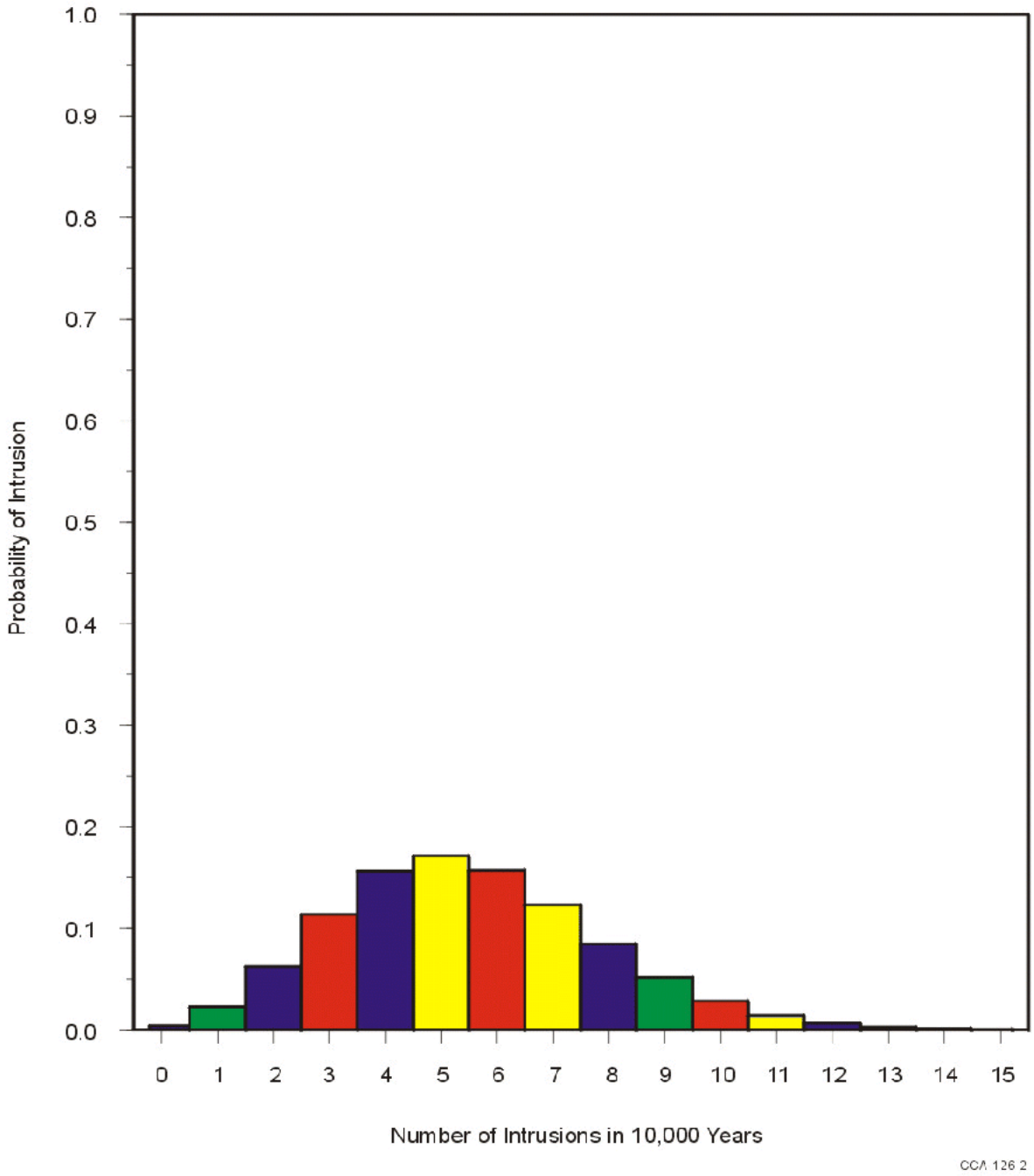

Figure 6-27. Probability of Intrusions in 10,000 Years with Active Institutional Control for 100 Years Followed by 600 Years of Passive Institutional Control

1

THIS PAGE INTENTIONALLY LEFT BLANK

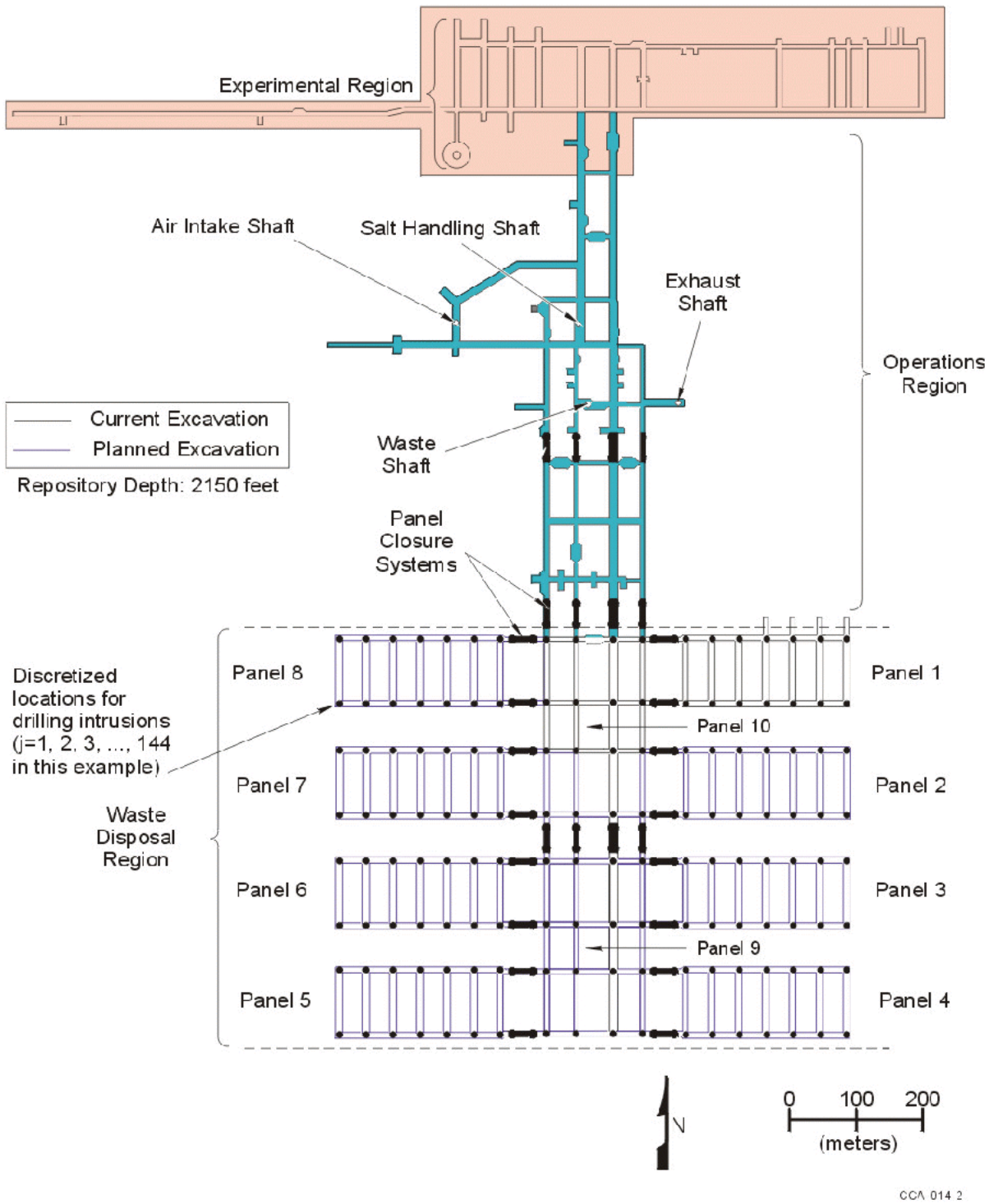

Figure 6-28. Discretized Locations for Random Intrusion by an Exploratory Borehole

1

1 **THIS PAGE INTENTIONALLY LEFT BLANK**

6.4.12.4 Activity of the Intersected Waste

Containers of waste shipped to the WIPP will contain quantities of radionuclides that will vary from container to container. Radioactivity may vary by several orders of magnitude from those waste containers with the largest quantities of radionuclides to those with the smallest.

Information about waste radioactivity has been compiled at several different levels (Figure 6-29). The waste-stream level includes information about waste activities from different processes at the generator sites that create TRU waste. At this level, a separate waste stream characteristic is maintained for RH-TRU. In total, there are approximately 970 CH- and RH-TRU waste streams, of which 569 are CH-TRU. Because the RH-TRU is approximately 1 percent (actually 1.5 percent) of the total EPA units (not activity) of CH-TRU waste, all the RH-TRU waste was grouped (binned) together into one equivalent or average (WIPP-scale) RH-TRU waste stream. It is assumed that variability in this small fraction is negligible. The waste-generator site level includes information integrated over the scale of a generator site. There are 21 generator sites identified for the WIPP. The WIPP-scale level includes integrated information about all waste destined for the WIPP, including CH- and RH-TRU. Data are present for existing waste and estimates have been made for future (to-be-generated) waste. The integration of waste data with the performance assessment is illustrated in Figure 6-30. This information is compiled for the WIPP from the Transuranic Waste Baseline Inventory Database (TWBID), an electronic version of information present in the Transuranic Waste Baseline Inventory Report (TWBIR), Rev. 3. (see Appendix BIR).

For calculation of radionuclide releases from groundwater transport (including direct brine release) and from spallings, spatial variability in the activity in the waste is assumed to have no significant impact. Concentrations of radionuclides mobilized in repository brine and quantities transported to the ground surface in spallings are assumed to be derived from a sufficiently large volume of waste that container-scale variability can be neglected. For long-term releases and direct brine releases, releases are calculated using WIPP-scale data assuming homogeneous accessibility of RH- and CH-TRU waste activities by liquid in the repository. As discussed previously, spallings releases are not calculated for RH-TRU waste; consequently, for spallings releases, activities are determined assuming homogeneous accessibility for only CH-TRU waste.

Direct releases caused by the mechanisms of cuttings and cavings access discrete and relatively small portions of the waste, and estimates of the quantity of radioactivity released to the accessible environment from these mechanisms may be sensitive to variability in activity loading. The radioactivity of cuttings and cavings releases is calculated using data from the waste-stream level in the following manner.

Containers are assumed to be placed in the WIPP from the various waste streams in a random manner. Because waste containers are to be stacked three-high for disposal, a drill bit is assumed to penetrate three containers. The direct-release consequence resulting from a drill

bit hitting the edges of containers and generating releases from more than three containers is assumed to be similar to the consequence of penetrating three containers only. Each of the three containers penetrated by the drill bit can come from different waste streams and have different activities associated with them. The waste streams penetrated are randomly sampled according to the relative quantity of waste in each waste stream. Figure 6-31 shows the discretized activities, expressed as the EPA normalized release density, of the 569 CH-TRU waste streams as a CDF, and the decay of the waste stream activities through time. Waste stream activities are maintained in performance assessment at 100, 125, 175, 350, 1,000, 3,000, 5,000, 7,500, and 10,000 years. Activities for cuttings and cavings releases at other times are interpolated from these values.

The code CUTTINGS_S calculates the volume of repository material brought to the surface by the mechanisms of cuttings and cavings. Of the volume of repository removed, approximately 40 percent is waste material, the rest is void space, backfill, and drum packing material. It is assumed that one-third of the waste material released comes from each of three containers assumed to be intersected. The activity of the release to the surface during drilling by cuttings and cavings is determined as the sum of the products of one-third the release volume times the three waste stream activities randomly sampled to be intersected. If random sampling determines that the borehole penetrates RH-TRU waste, 100 percent of the material removed is assumed to be waste and the activity of the release is equal to the volume calculated by CUTTINGS_S times the activity of RH-TRU waste.

6.4.12.5 Diameter of the Intrusion Borehole

Historical Delaware Basin drilling records were reviewed to determine the diameter of a typical intrusion borehole. In performance assessment, the borehole diameter parameter value is held constant for all future drilling and is equal to 12.25 inches (0.311 meter). Appendix DEL (DEL Attachment 1) discusses typical drill stem and drill collar diameters used to drill oil and gas wells in the Delaware Basin. Appendix DEL (Section DEL.6.1.2.2) illustrates a generalized circular cross section of a well plugged according to current practice (see Appendix DEL, DEL Attachment 7).

6.4.12.6 Probability of Intersecting a Brine Reservoir

As mentioned in Section 6.4.8, there is uncertainty about the existence of brine reservoirs and uncertainty in the probability of intersecting a brine reservoir with a deep borehole. The DOE has examined available data and concluded that there is no reasonable basis to eliminate the possibility of a brine reservoir existing under the site. Therefore, the DOE assumes that a brine reservoir may exist under the waste panels. The DOE has determined that there is a reasonable basis for determining the probability of intersecting a brine reservoir and has pursued three types of investigation relevant to this issue: geophysical methods, geological structure analysis, and geostatistical correlation.

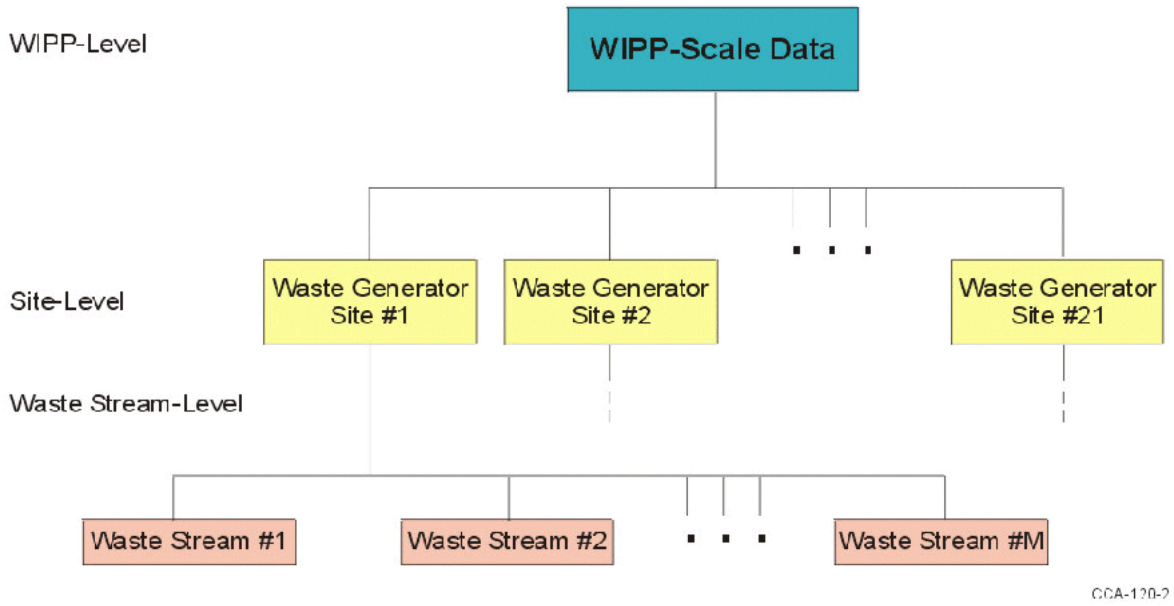

Figure 6-29. Levels of Information Available in the TWBID

1

1 **THIS PAGE INTENTIONALLY LEFT BLANK**

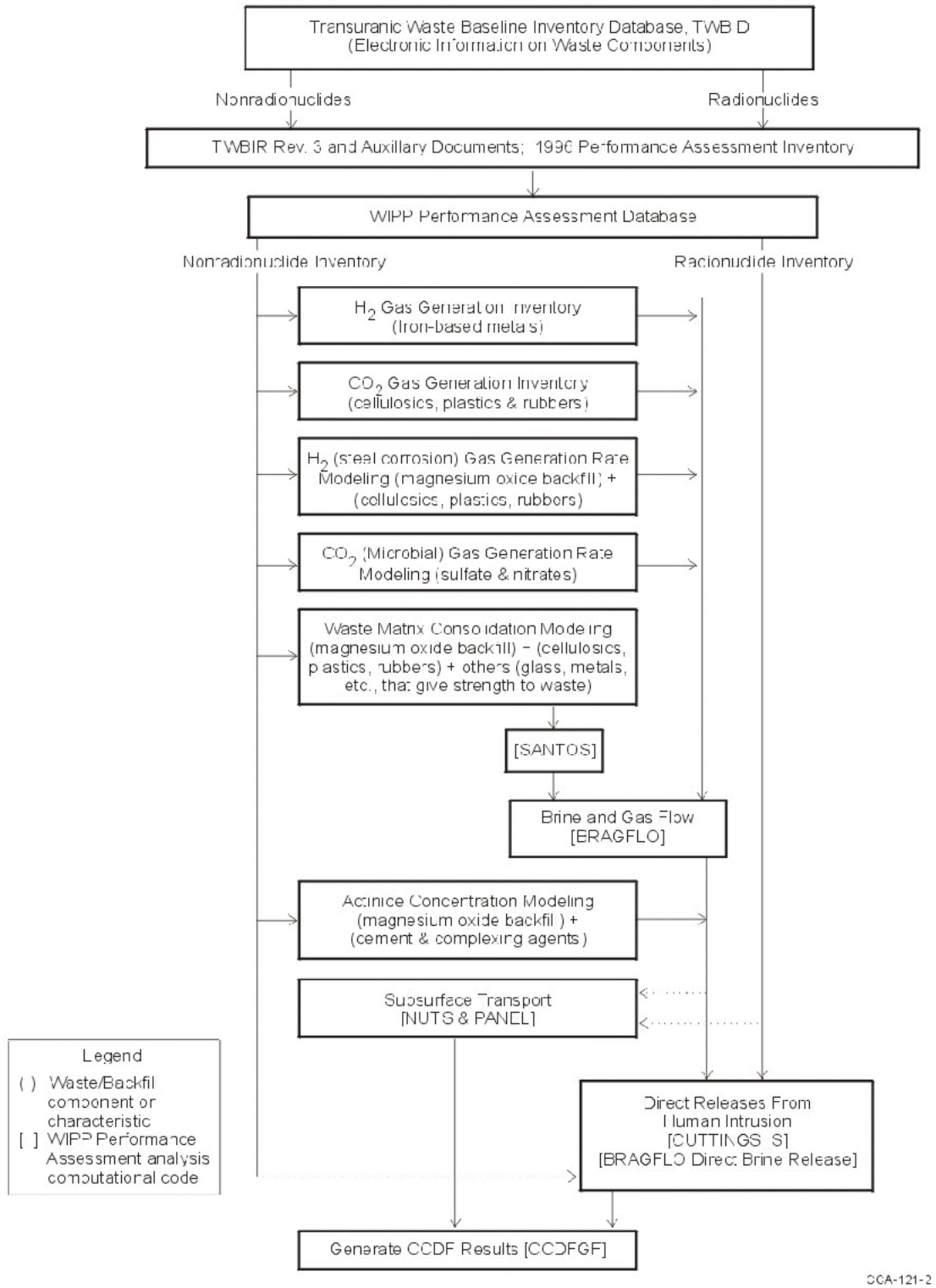

Figure 6-30. Flowchart Showing Integration of TWBID Data in Performance Assessment Calculations

1 **THIS PAGE INTENTIONALLY LEFT BLANK**

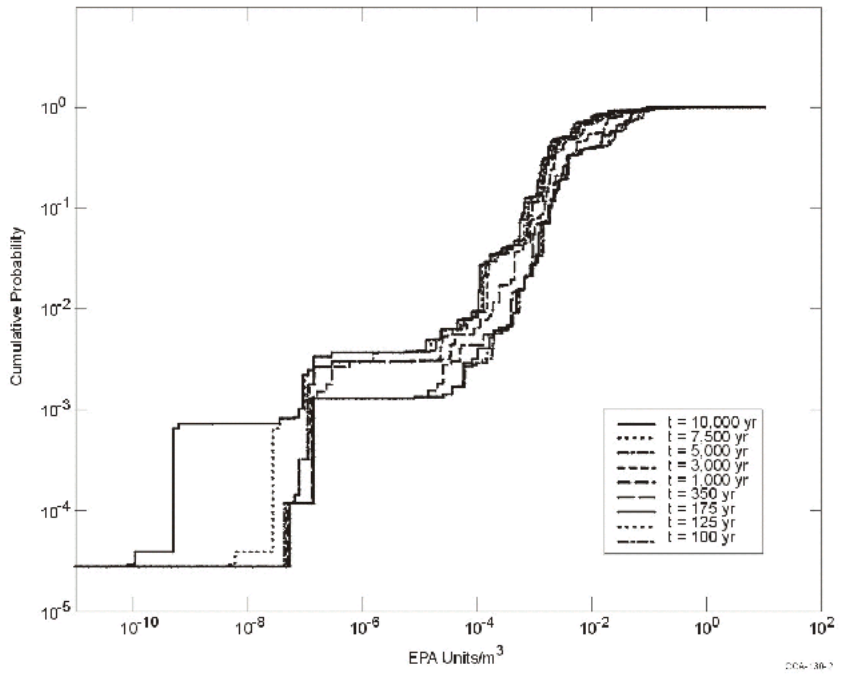

Figure 6-31. Cumulative Distribution Function for Waste Stream EPA Units/Volume

1 **Figure 6-31. Cumulative Distribution Function for Waste Stream EPA Units/Volume**

1 **THIS PAGE INTENTIONALLY LEFT BLANK**

In 1987, the DOE conducted a series of 38 time-domain electromagnetic (TDEM) soundings at the WIPP site (Earth Technology Corporation 1988; Appendix MASS, Section MASS.18.1 and MASS Attachment 18-5). Thirty-six of these soundings were executed over a 1-by-2-kilometer area, with the north-central nine soundings located directly over the waste panels. The electromagnetic data collected by the measurements indicate differences in electrical resistivity, which can be interpreted as occurring in the Castile. Regions of relatively low resistivity in the Castile are presumed to be so because of a greater abundance of interconnected brine compared to higher-resistivity regions. A sounding executed near the brine reservoir penetrated at WIPP-12 provides an independent calibration on the interpretation of the data. The study indicates the presence of electrically conductive regions below the waste panels at the WIPP. However, because of the inherent coarse resolution of the method, the data do not support the development of a unique map of the extent of conductors in the Castile. A recent interpretation of the data included in Appendix MASS (Section MASS.18.1 and MASS Attachment 18-5) suggests that between 10 percent and 55 percent of the waste panel area may be underlain by relatively conductive units, interpreted to be one or several brine reservoirs. The TDEM data do support a limited probability of intersecting brine. Because of the spatial resolution provided by TDEM data, however, the data do not support distinguishing boundaries between reservoir and nonreservoir areas. Thus, the DOE assumes that one reservoir exists below the waste panels.

The geological structure of selected units within the Castile and Salado has been mapped recently to examine more closely the relationship between identified brine intercepts and evaporite deformation. This study is described in Appendix MASS (Section MASS.18.1 and MASS Attachment 18-6). After ERDA-6 encountered brine in steeply dipping beds, studies indicated that many of the other observed brine encounters in the Delaware Basin are associated with structural deformation in the Castile. The study of structure reaffirms the concept that much of the Castile underlying the present WIPP site is generally undeformed. The DOE does not use the results of the structural study in quantifying the existence or probability of intersecting a brine reservoir.

The geostatistical study discussed in Appendix MASS (Section MASS.18 and included as MASS Attachment 18-6), was conducted using existing borehole data to estimate the probability of drilling into a fractured reservoir in areas overlain by WIPP underground workings. The database consists of boreholes in the general area of the WIPP where Castile brine has been encountered as well as a much larger number of boreholes in which brine is not reported to have been encountered. The study used geostatistical methods to estimate the probabilities that a randomly placed borehole would encounter pressurized brine in the Castile. These methods do not require assumptions about the distribution of brine reservoirs but are based on the empirical evidence available. Based on geostatistical analysis, the DOE uses a 0.08 probability that any deep borehole drilled within the waste panel penetrates the brine reservoir that is assumed to exist below the waste panels.

The DOE assumes that there is one reservoir under the quadrilateral area enclosing the waste panels with a constant probability of any deep borehole penetrating it. The location of boreholes in this area is sampled. They may lie over repository excavations, or over rock in

pillar cores or between panels. The brine reservoir under the waste panels can be depleted during the 10,000-year regulatory period by boreholes drilled anywhere within this area. Boreholes that are randomly located over rock have the same probability of intersecting the brine reservoir as boreholes located over excavations. Boreholes located over the excavations are assumed to penetrate waste, and the consequences are modeled as described throughout Section 6.4. Boreholes located over the intact rock in this area are assumed to have no consequences on the disposal system other than that they can contribute to the depletion of reservoirs, as discussed below.

Long-term depletion of pressure and the production of brine from a reservoir that may exist under the repository occurs only for the two-plug configuration boreholes. Long-term depletion does not occur during the 10,000-year regulatory period for the solid-concrete plug boreholes or three-plug configuration borehole.

BRAGFLO calculates the long-term depletion of pressure and production of brine from the reservoir for only one two-plug configuration borehole. For estimating the consequences of possible sequences of future events, the DOE assumes how the reservoir responds to additional penetrations. Subsequent penetrations are assumed to behave identically to the first until the reservoir is assumed to be completely depleted and cannot produce more brine (see Appendix MASS, Section MASS.18 and MASS Attachment 18-3). The DOE assumes the 32,000-cubic-meter reservoir is depleted after two penetrations; the 64,000-cubic-meter reservoir after four penetrations; the 96,000-cubic-meter reservoir after six penetrations; the 128,000-cubic-meter reservoir after eight penetrations; and the 160,000-cubic-meter reservoir after 10 penetrations. Because it is assumed for modeling simplicity that penetrations before depletion behave identically to the first penetration, it is possible for a reservoir to cumulatively produce more brine with multiple intrusions than it is assumed to contain for the first intrusion.

6.4.12.7 Plug Configuration in the Abandoned Intrusion Borehole

As stated in Section 6.4.7, three different plug configurations can be used to represent possible future configurations of plugged and abandoned intrusion boreholes. Based on a survey of current practice (see Appendix MASS, Section MASS.16.3 and MASS Attachment 16-1), the two-plug configuration borehole is considered most likely and is assigned a probability of 0.68. The three-plug configuration is considered less likely and is assigned a probability of 0.30. The continuous concrete plug is considered least likely and is assigned a probability of 0.02.

6.4.12.8 Probability of Mining Occurring within the Land Withdrawal Area

The EPA has specified the probability of mining in the future. In 40 CFR § 194.32 (b), the EPA states, “Mining shall be assumed to occur with a one in 100 probability in each century of the regulatory time frame.”

Also in 40 CFR § 194.32(b), the EPA limits the occurrence of mining to a maximum of once per 10,000 years. The DOE has interpreted this probability model as a Poisson model with a probability of mining of 10^{-4} per year (Appendix CCDFGF, Section 3). During the period that passive institutional controls are effective, the probability of mining is 10^{-6} per year. The occurrence of mining is sampled from a CDF of the time until mining in a manner similar to the procedure described for the time between drilling intrusions, except that multiple mining events cannot occur.

6.4.13 Construction of a Single CCDF

Construction of a single CCDF requires combining the results of numerical simulations performed for a given set of values of subjective parameters (that is, those determined by LHS) with the probabilistic futures determined by random sampling of stochastic parameters (that is, those associated with intermittent drilling) (see Appendix CCDFGF, Section 2). Because of the variety of sequences of events represented in a single CCDF and the impossibility of modeling the details of each future separately, building a CCDF necessarily involves methods for the construction of consequences for any probabilistic future from a limited number of calculations for deterministic, idealized futures. Although this methodology is conceptually straightforward, the details of the process are highly dependent on model and system-specific considerations (see Appendix CCDFGF, Section 4). Accordingly, insight gained from previous, preliminary performance assessments as well as analysis of early results for this performance assessment are used to help configure the methodology used for CCDF construction.

Depending on the scenario into which probabilistic futures are classified, different techniques are used for estimating their consequences. The deterministically determined undisturbed performance scenario consequences require no special techniques for application to probabilistic futures. For E1, E2, and E1E2 scenarios, the CCDF construction methodology is primarily based on the principle of scaling, with some simplifying assumptions made for the E2 scenario. Scaling is the estimation of consequences of probabilistic futures based on consequence estimates from deterministic futures. The use of scaling and the building of a CCDF with it is discussed in this section. Note that all of the discussions in Section 6.4.13 are for one vector of values for those parameters included in the subjective uncertainty analysis. In other words, this section addresses only stochastic variation resulting from uncertainty in the sequence of future events that may occur at the WIPP (see Section 6.1.2).

6.4.13.1 Constructing Consequences of the Undisturbed Performance Scenario

All probabilistic futures in which drilling intrusion and mining within the controlled area do not occur are included in the undisturbed performance scenario. Because there is no stochastic uncertainty for this scenario, all futures within a single LHS vector of undisturbed performance have the same releases to the accessible environment. The following major codes are used to estimate the consequences of undisturbed performance: BRAGFLO, NUTS, and, if actinides reach the Culebra, SECOFL2D and SECOTP2D. To illustrate the flow of information for the undisturbed performance scenario, these codes and the connections

between them are highlighted on the diagram of performance assessment codes in Figure 6-32. For undisturbed performance, no special techniques are required to modify the results of the deterministic calculation to fit probabilistic futures. Therefore, for a single consequence for undisturbed performance, BRAGFLO is executed once and NUTS is executed once. These calculations determine the release to the accessible environment because of transport in the Salado or up the shaft to the surface. If any actinides reach the Culebra following these calculations, SECOFL2D and SECOTP2D are executed to determine whether actinides released to the Culebra reach the lateral accessible environment. This information is sufficient to construct consequences for all probabilistic futures that have no intrusion events. This information is also used as the basis for evaluations of compliance with 40 CFR § 191.15 and 40 CFR § 191.24, described in Chapter 8.0.

6.4.13.2 Scaling Methodology for Disturbed Performance Scenarios

Although 10,000 probabilistic futures are generated for the construction of a CCDF, the major codes used in performance assessment are executed many fewer times. The results of the fewer calculations are used in part to construct the consequences of all of the probabilistic futures comprising a CCDF in a process called scaling.

The scaling methodology is simple in concept. First, several simulations are performed with a code to develop a reference behavior for a particular event or process. Each simulation has a defined event occurring at a different time. Then, a large set of futures is developed probabilistically by random sampling. The behavior of the particular event or process in each of the probabilistically sampled futures is estimated by scaling from the results of the limited number of deterministic calculations. This scaling is generally simple linear interpolation. For events or processes involving radionuclides, however, scaling becomes more complicated as it incorporates the effects of radioactive decay and ingrowth. Because scaling is generally less intensive computationally than is solving matrix equations of the type encountered in many performance assessment codes, scaling is an efficient way to develop multiple probabilistic consequence estimates from a limited number of deterministic calculations. Without scaling, fewer futures would be possible, and resolution in the CCDF would be reduced.

For an example of the application of scaling, assume that the process of interest is release of actinides to the surface during drilling. It is impossible to explicitly model the infinite possibilities present in a probabilistic conceptualization of the future. Thus, scaling is used. To develop a reference behavior for scaling, the CUTTINGS_S code is executed several times with different intrusion times. A probabilistic method is then used to develop a large number of possible, different future intrusion times. To estimate the release to the surface in probabilistic futures, scaling is used in which release at the times in the deterministic calculations closest to the probabilistic time of interest are used as reference points for scaling or interpolation.

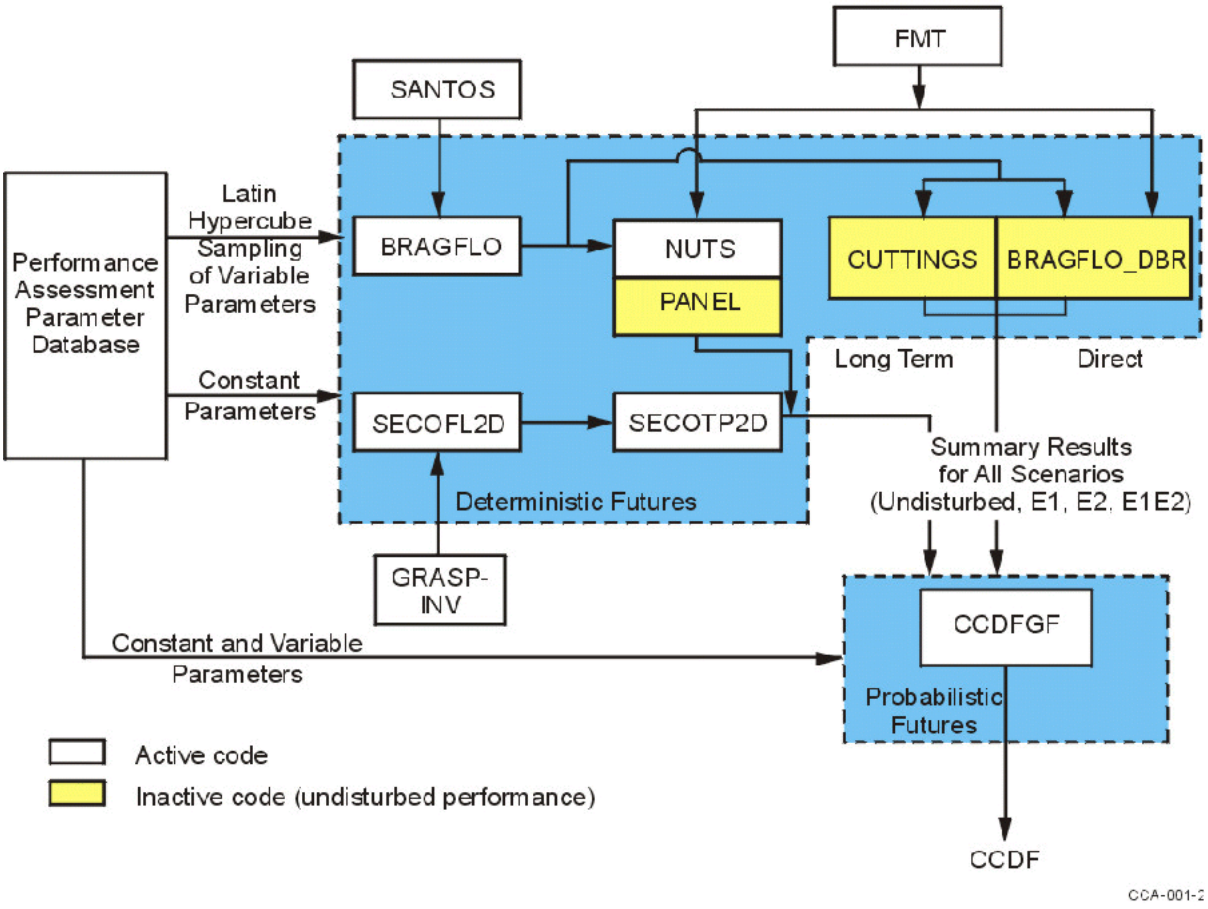

Figure 6-32. Code Configuration for the Undisturbed Performance Scenario

1

1 **THIS PAGE INTENTIONALLY LEFT BLANK**

Scaling is used for all futures with intrusion boreholes. The times when various codes are executed to develop reference behavior, and how this reference behavior is used by other codes, is the subject of the next two sections. In presenting complete descriptions of the process for each scenario, there will be some duplication of discussion.

6.4.13.3 Estimating Long-Term Releases from the E1 Scenario

The E1 scenario is defined as a single penetration of a panel by a borehole that also intersects a brine reservoir. The code configuration with which the long-term consequences of E1 scenarios are estimated is illustrated in Figure 6-33. For the E1 scenario, BRAGFLO is executed twice more for each CCDF (assuming the undisturbed performance run has already been executed), with the E1-type intrusion occurring at 350 years and 1,000 years. These three BRAGFLO calculations form the foundation for transport modeling that is used for scaling consequences to probabilistic futures.

Consistent with the BRAGFLO intrusion times, NUTS is executed with intrusions occurring at 350 and 1,000 years. These calculations form the basis for (1) estimating releases to the accessible environment via Salado interbeds or to the surface and (2) forming the actinide source term to the SECOTP2D code for Culebra transport. For computational efficiency, an intermediate scaling step is conducted prior to calculating the releases associated with probabilistic futures. In this intermediate step, NUTS reference conditions for Culebra releases by an intrusion at 100 years are calculated by using borehole flow from the 350-year intrusion, and NUTS reference conditions for intrusions at 3,000, 5,000, 7,000, and 9,000 years are calculated by using borehole flow from the 1,000-year calculation. Thus, for the scaling of consequences of E1 intrusions in probabilistic futures, reference conditions calculated by NUTS are available for 100, 350, 1,000, 3,000, 5,000, 7,000, and 9,000 years postclosure.

Consistent with the BRAGFLO intrusion times, reference behavior for actinide transport in the Culebra is calculated by SECOTP2D for the E1 intrusion occurring at 350 and 1,000 years. Because the equations governing actinide transport and retardation in SECOTP2D are linear, scaling releases to probabilistic E1 penetrations occurring at other times is easily accomplished.

6.4.13.4 Estimating Long-Term Releases from the E2 Scenario

The E2 scenario includes all futures with one or more exploratory borehole penetrations of a panel, none of which hits a brine reservoir. Estimation of long-term releases from the E2 scenario is slightly more complex than the consequences of the E1 scenario because the E2 scenario includes the possibility of multiple E2-type intrusions. The same codes used in the construction of the E1 scenario consequences are used for construction of the E2 scenario consequences. These are indicated in Figure 6-33.

As is done for the E1 scenario, BRAGFLO is executed twice more for each CCDF (assuming the undisturbed performance run has already been executed), with the E2-type intrusion

occurring at 350 years and 1,000 years. These three BRAGFLO calculations form the foundation for transport modeling that is used for scaling consequences to probabilistic futures.

NUTS is executed with intrusions occurring at 350 and 1,000 years, consistent with the BRAGFLO times of intrusion. These calculations form the basis for (1) estimating releases to the accessible environment via Salado interbeds or to the surface and (2) forming the actinide source term to the SECOTP2D code for Culebra transport. For computational efficiency, an intermediate scaling step is conducted prior to calculating the releases associated with probabilistic futures. In this intermediate step, NUTS reference conditions for Culebra release by an intrusion at 100 years is estimated by scaling borehole flow from the 350-year intrusion, and NUTS reference conditions for intrusions at 3,000, 5,000, 7,000, and 9,000 years are estimated by scaling from the 1,000-year calculation. Thus, for the scaling of consequences of E2 intrusions in probabilistic futures, reference conditions from calculations by NUTS are available for 100, 350, 1,000, 3,000, 5,000, 7,000, and 9,000 years.

Consistent with the BRAGFLO intrusion times, reference behavior for actinide transport in the Culebra is calculated by SECOTP2D for the E2 intrusion occurring at 350 and 1,000 years. Because the equations governing actinide transport and retardation in SECOTP2D are linear, scaling releases to probabilistic E2 penetrations occurring at other times is easily accomplished. For futures with two or more E2-type intrusions (and no E1-type intrusions), a simplifying assumption is made. The additional increment to the source term to the Culebra for the second and subsequent intrusions is assumed to be zero. This is considered reasonable because in the E2 scenario the flux of brine to the Culebra is limited by the rate of flow from the Salado to the waste panels rather than by borehole properties. For second and subsequent E2 scenarios, only the direct releases to the surface are therefore considered in CCDF construction.

6.4.13.5 Estimating Long-Term Releases from the E1E2 Scenario

The E1E2 scenario is defined as multiple boreholes intersecting a single waste panel, at least one of which is an E1 penetration of a brine reservoir (Section 6.3.2.2.3). The DOE uses both scaling and simplification to develop the consequences of this scenario. Similar to the E1 and E2 scenarios, BRAGFLO and related computer codes are executed with a deterministic sequence of future events to develop reference behavior for the E1E2 consequences (see Figure 6-34). Scaling is used to estimate the consequences for events occurring at different times than those used in the BRAGFLO calculations. Simplifying assumptions are used to develop the consequences of E1E2 occurrences in different waste panels or the consequences of a different sequence of future events leading to the E1E2 scenario than assumed in the deterministic BRAGFLO calculation.

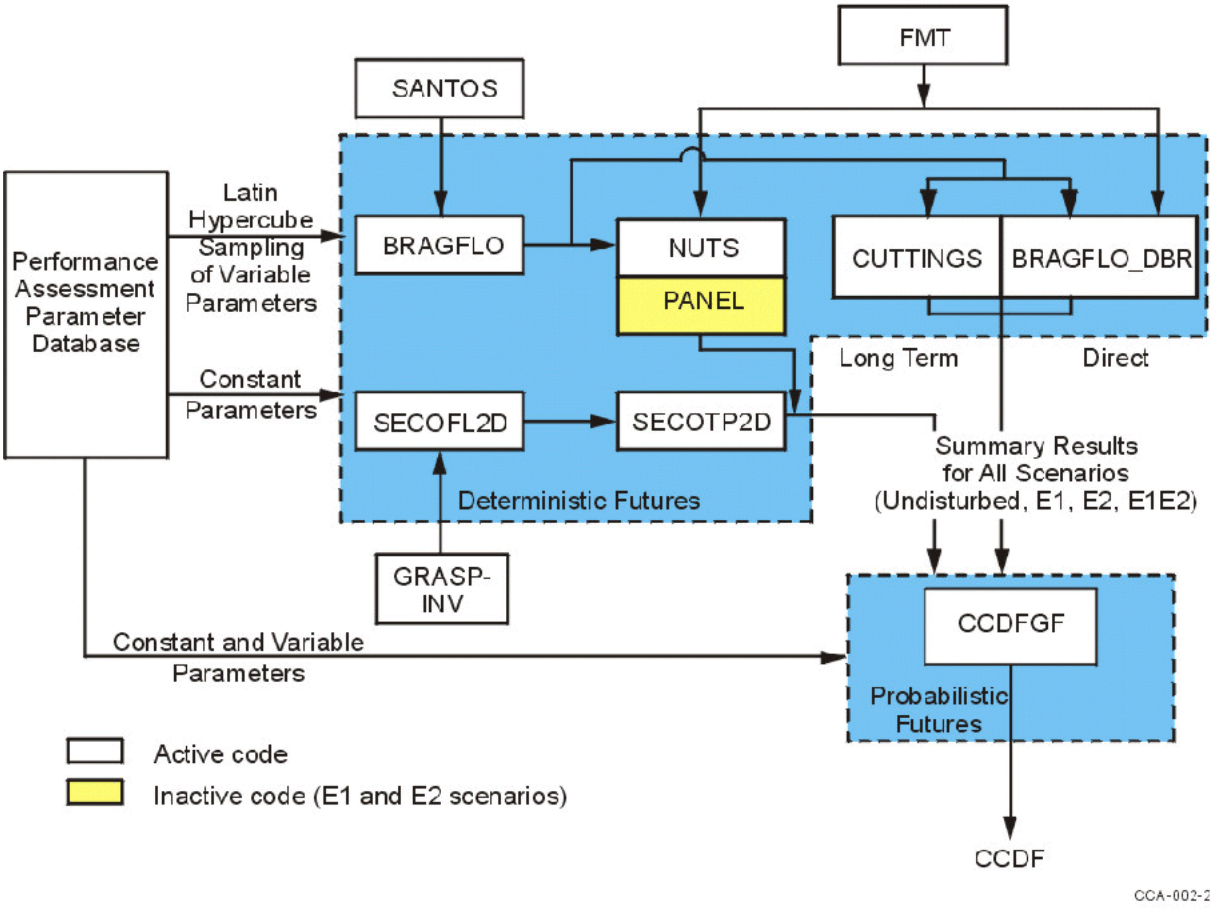

Figure 6-33. Code Configuration for Disturbed Performance Scenarios E1 and E2

1

THIS PAGE INTENTIONALLY LEFT BLANK

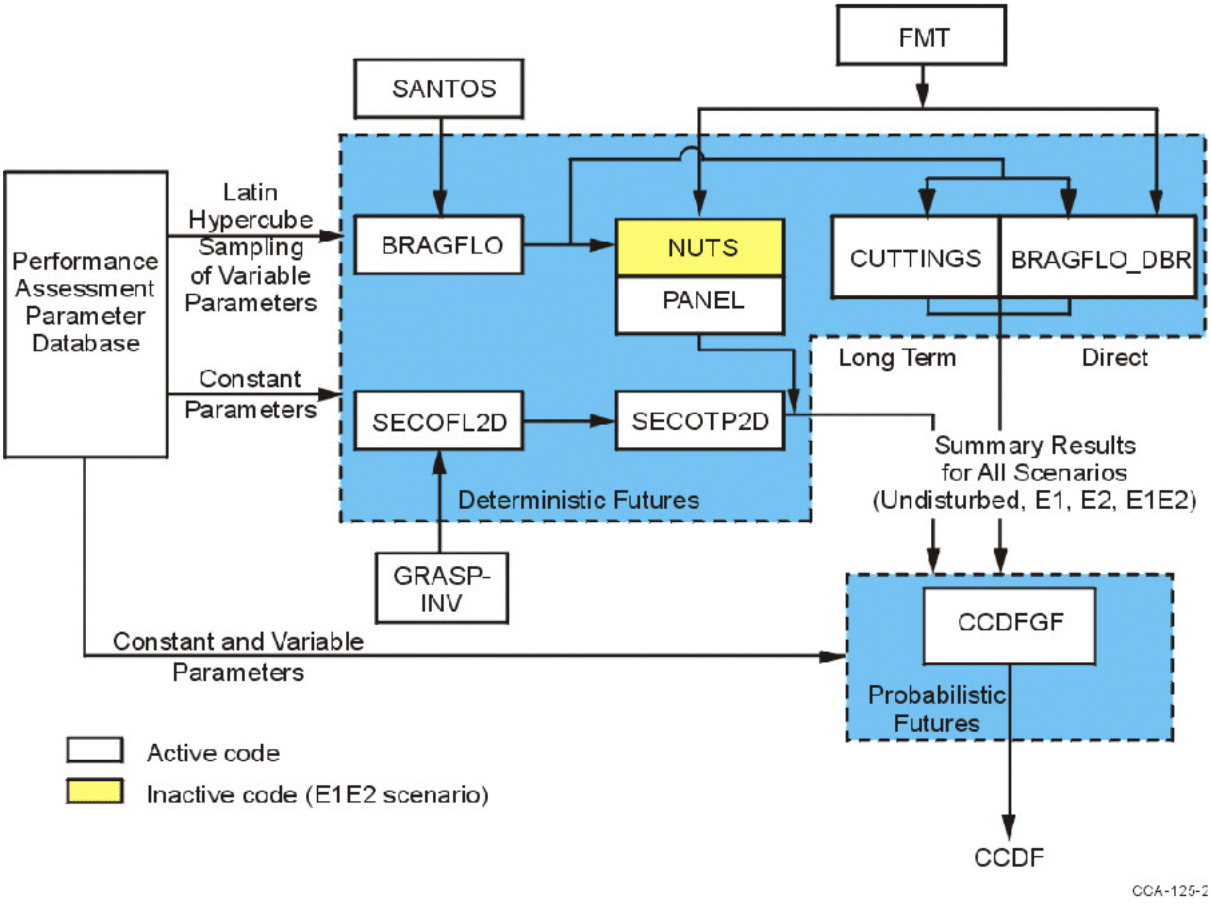

Figure 6-34. Code Configuration for Disturbed Performance Scenario E1E2

1

1 **THIS PAGE INTENTIONALLY LEFT BLANK**

Reference behavior for brine flow to the Culebra in the E1E2 scenario is predicted by the BRAGFLO disposal system model. This is the same model used to predict brine flow to the Culebra for the E1 and E2 scenarios. The geometry of the grid used is the same as that depicted in Figures 6-13 through 6-16; however, different assumptions are used about the borehole development through time. Even though the E1E2 scenario includes at least two boreholes intersecting the panel, the model used included only one borehole column. As will be described, the assumptions used about the manner in which brine mixes in the intruded panel are such that two boreholes are not needed to represent flow through the waste. The assumptions about the development of the borehole are related to the most likely (that is, most probable) sequence of events that gives rise to the E1E2 scenario.

Ninety-two percent of all deep boreholes are the E2 type (see Section 6.4.12.6). Therefore, it is most probable that the first borehole into any panel is an E2 borehole. In a BRAGFLO calculation after 1,000 years of undisturbed performance, the properties of the column of elements in BRAGFLO representing the borehole are changed. The changed properties represent the E2 borehole after the Rustler plug has degraded and silty sand fills the borehole. The period during which the plug is effective is not modeled to develop reference behavior for the E1E2 Culebra releases because relatively little happens in the disposal system during the time that the Rustler plug is effective. Reference conditions are developed with the E1 intrusion that follows the initial E2 intrusion occurring after the 200 years that it takes Rustler plugs to degrade because it is more probable that a subsequent E1 intrusion occurs after the Rustler plug has degraded. It is assumed that the E1 intrusion occurs 1,000 years after the E2 borehole becomes filled with silty sand, at a simulation time of 2,000 years. At 2,000 years, the properties of the section of the borehole below the repository horizon are changed to represent an open borehole (the E1 intrusion), allowing flow between the Castile brine reservoir and the repository. After another 200 years, the lower section is assumed to become filled with silty sand; after another 1,000 years, the permeability of the lower section is decreased one order of magnitude because of salt creep. These changes are documented in Table 6-29.

Table 6-29. Changes in BRAGFLO Borehole Properties in Developing Reference Behavior for the E1E2 Scenario

Time (years)	Borehole Portion	Properties
0-1,000	All	Undisturbed conditions
1,000-2,000	Above waste panel	Silty sand
	Below waste panel	Undisturbed conditions
2,000-2,200	Above waste panel	Silty sand
	Below waste panel	Open borehole between panel and Castile
2,200-3,200	Above waste panel	Silty sand
	Below waste panel	Silty sand
3,200-10,000	Above waste panel	Silty sand
	Below waste panel	Silty sand, permeability decreased 1 order of magnitude

Thus, above the waste panel, the E1E2 borehole evolves as an E2 borehole from 1,000 years to 10,000 years. Below the waste panel, the borehole evolves as an E1 borehole from 2,000 to 10,000 years. At 2,200 years, there will be two boreholes above the waste panels with silty-sand properties. The assumption about upper borehole permeability most consistent with the assumption made for this scenario of complete mixing in the panel (discussed below) is that the upper portion of the E1 borehole is relatively impermeable and all flow that might occur through it is diverted to the E2 borehole. Therefore, the permeability of the upper borehole remains that of the E2 borehole at 2,200 years.

The concentration of actinides in liquid moving up the borehole assumes homogeneous mixing within the panel and is calculated with the code PANEL. PANEL is a mixing-cell model that sums BRAGFLO fluxes into the waste panel from the boreholes and Salado as inputs to the cell and subtracts the flow up the borehole as a depletion from the model. Brine moving up the borehole is assumed to be at its greatest possible actinide concentration according to the dissolved and colloidal actinide source term models (Sections 6.4.3.5 and 6.4.3.6). In PANEL calculations, all actinides that enter the borehole are conservatively assumed to reach the Culebra.

Random sampling of future events can produce different timing of borehole penetrations. From the time the E2 borehole penetrates until the E1 borehole penetrates, the consequences are determined as they are in the E2 scenario. When the E1 is drilled, completing the E1E2 configuration, the consequences are assumed to be similar to the consequences modeled after the E1 penetration for the reference calculation, accounting for radionuclide decay and ingrowth.

Random sampling of future events can also produce a different sequence of borehole types. In a randomly sampled future with many E2 intrusions into a waste panel prior to the E1, the consequences are determined as they are for the E2 scenario until the E1 occurs, at which time the E1E2 consequences are used. In a randomly sampled future with the sequence E1 then E2, the consequences are assumed to be similar to an E1 event until the E2 is drilled, whereupon the consequences are assumed to be similar to the E1E2 event following the E1 drilling. In a randomly sampled future with two E1 boreholes, the consequences are assumed to be similar to an E1 borehole until the second E1 is drilled, at which time the consequences are assumed to be similar to the E1E2 behavior.

For computational simplicity, the E1E2 calculations are scaled to E1 intrusions following a prior E2 intrusion occurring at 100, 350, 3,000, 5,000, 7,000, and 9,000 years, similar to the treatment of the E1 and E2 reference conditions.

6.4.13.6 Multiple Scenario Occurrences

For long-term brine flow into the Culebra, scenario occurrences are effectively defined at the panel scale for this performance assessment. It was recognized in preliminary analysis of BRAGFLO results for this analysis that liquid flow between the separate panel and the rest of the repository is slow enough that the panel is effectively independent from the rest of the

repository. Gas flow does occur, and for this reason calculations of direct release to the surface are performed at the repository scale. For long-term brine flow to the Culebra, it is considered more reasonable, based on BRAGFLO results, to assume independent panel behavior in developing the CCDF rather than an interconnected repository.

It is very important to distinguish between model results and model assumptions on this point. For disposal system performance, the DOE is not assuming that panel closures isolate panels from one another. Rather, the DOE has assigned reasonable properties to the panel closures as input to the BRAGFLO calculations and has found that the assignment of these reasonable properties results in limited liquid flow through them. Because simplification and scaling must be used to develop CCDFs, the DOE has to assume either that the repository is well interconnected or that the panels behave fairly independently. Based on model results for this analysis, the DOE has established that it is more reasonable in constructing a CCDF to assume that brine does not flow between panels. This is a simplification of results of the detailed modeling conducted in BRAGFLO, necessary for CCDF construction. It is not an assumption used in developing conceptual models of disposal system performance. This assumption does affect how scenario consequences are developed.

There are 10 panels in the repository and the possibility of many intrusions. If panels behave independently as they are assumed to in developing consequences of long-term brine flow in the CCDF, it is possible for different configurations of boreholes (scenarios) to occur in different panels. For example, an E1E2 type situation might occur in one panel, an E2 situation in a different panel, and an E1 situation in a third panel. In this example, there are essentially three scenario types occurring. For long-term release, the repository behaves as 10 small modules (each comprising one panel), and a different borehole scenario can develop in each of those 10 modules. Long-term releases in CCDF construction are based on the premise that releases from each of these modules are independent and that the cumulative release from the repository is equal to the sum of the cumulative releases from the different modules.

6.4.13.7 Estimating Releases During Drilling for All Scenarios

The reference behavior for cuttings and cavings from the first intrusion into a pressurized repository, regardless of whether it is an E1 or E2 intrusion, is established by calculations performed in the CUTTINGS_S code. Cavings releases are also dependent on the effective shear resistance to erosion (Appendix PAR, Parameter 33). The effects of radioactive decay are captured by calculating reference behavior for cuttings and cavings by the CUTTINGS_S code at 100, 125, 175, 350, 1,000, 3,000, 5,000, 7,500, and 10,000 years.

Spall and direct brine releases during drilling are also dependent on pressure conditions in the repository, and reference releases are calculated by CUTTINGS_S for spall and by BRAGFLO_DBR at 100, 350, 1,000, 3000, 5,000, and 10,000 years for intrusions into up-dip and down-dip (that is, northern and southern) panels. Spall releases are also dependent on the waste particle diameter (Appendix PAR, Parameter 32).

Radionuclide releases from the processes in the CUTTINGS_S code and direct brine release for intrusions occurring at intermediate times are scaled from the closest calculated releases, correcting for radioactive decay (see Section 6.4.12.3 and Figure 6-28). The cuttings and cavings portion of the CUTTINGS_S releases are further adjusted to account for the distribution of CH- and RH-TRU waste streams (see Sections 6.4.12.3 and 6.4.12.4). The processes of spallings and direct brine release are assumed to involve a large enough volume of waste that it is reasonable to use homogeneous waste with average activity to estimate releases.

For multiple-intrusion scenarios, the pressure in the repository at the time of the second and subsequent intrusions may be quite different from the pressure at the time of the first intrusion. This is expected because of the assumptions of relatively permeable boreholes adopted in performance assessment. Therefore, estimates of drilling releases to the accessible environment need to be formed for penetrations of a previously intruded repository. The reference behavior for these releases for subsequent intrusions is calculated by the CUTTINGS_S code from BRAGFLO histories with E1- and E2-type intrusions at 350 and 1,000 years. Repository conditions from the calculations of the effects of a subsequent E1-type penetration are used in consequence analysis for both E1- and E2-type intrusions that follow an E1 intrusion. Conditions from the subsequent E2 calculations are used for intrusions that follow E2 intrusions only. E1 conditions are used for multiple combinations of boreholes that include at least one E1 intrusion, based on the assumption that repository conditions will be dominated by Castile brine if any borehole connects to a brine reservoir. For futures in which more than two E2-type intrusions occur (and no E1-type intrusions occur), third and subsequent spall and direct brine releases are assumed to be the same as for the second release.

For both E1 and E2 conditions following a 350-year intrusion, spall and direct brine release calculations are performed at 550, 750, 2,000, 4,000, and 10,000 years. For the 1,000-year E1 and E2 intrusions, spall and direct brine release calculations are performed at 1,200, 1,400, 3,000, 5,000, and 10,000 years. Because the subsequent intrusion may penetrate either a previously-intruded panel or an unintruded panel, these calculations are done twice, once with initial conditions drawn from the previously-intruded panel in BRAGFLO, and once with conditions drawn from the BRAGFLO subsequent intrusion of the waste-disposal region. As is done for the first intrusion into a previously undisturbed repository, radionuclide releases from spall and direct brine release for intrusions occurring at intermediate times are scaled from the closest calculated releases, correcting for radioactive decay.

After flow through the repository has occurred for some time, such as may occur in an E1E2 scenario, portions of the repository may be depleted of actinides. In the estimate of releases during drilling, however, the possibility is not accounted for that random drilling might penetrate portions of the repository that have been depleted of actinides as a consequence of processes initiated by previous drilling. This is conservative because it tends to overestimate releases during drilling.

6.4.13.8 Estimating Releases in the Culebra and the Impact of the Mining Scenario

Ten thousand-year SECOFL2D and SECOTP2D calculations are performed with Culebra transmissivity fields reflecting undisturbed performance (no future mining within the land withdrawal area) and disturbed performance (see Section 6.4.6.2.3). These calculations are performed with a unit source term of one kilogram of the actinide species of interest at 100 years. Because transport as modeled is a linear process, scaling is used to estimate the consequences of time-variable concentrations and different times of intrusion (see Appendix CCDFGF, Section 4.9). As well, mining may occur at random times in the future. The effect of mining on releases in the Culebra is determined in the following manner.

Boreholes intersecting the repository may provide a source of actinides to the Culebra with concentrations that vary through time. Until mining occurs, the transport behavior of actinides from these borehole sources is estimated by scaling the results of the undisturbed performance Culebra transport calculations. All actinides introduced into the Culebra by the time of mining are transported exclusively in the undisturbed performance flow fields. In other words, actinides in transit in the Culebra when mining occurs are assumed to be not affected by it and continue to be transported in the undisturbed flow field. Once mining occurs (it is assumed to occur instantaneously), the transport behavior of all actinides subsequently introduced into the Culebra is estimated by scaling the results of the disturbed performance flow fields.

6.4.13.9 Final Construction of a Single CCDF

After consequences for all of the sampled probabilistic futures have been estimated by the methodologies presented in the preceding sections, the information necessary to plot the CCDF associated with the probabilistic futures and the particular LHS vector is available.

The sequences of future events used in this performance assessment were generated by random sampling. Thus, each sampled future is assigned an equal weight of occurrence for the construction of a CCDF. Each sequence of future events is assigned a weight of 1/10,000 of occurrence because 10,000 futures are used for each CCDF. Before plotting, an additional step is performed in which the weights of futures with similar consequences are summed. The first step in the plotting process is to order the grouped futures according to normalized release, as discussed in Section 6.1.1, from lowest normalized release to highest. Following this ordering, the CCDF can be plotted by summing, for a given value of EPA normalized release, the probabilities of all futures whose normalized release exceeds the given value, where the probabilities are assumed to be equal to the weights. Because the releases **cS** have been ordered so that $cS_i \le cS_{i+1}$ for i=1 …, nS-1, the probability that **cS** exceeds a specific consequence value x is determined by the summation routine (duplicated from Section 6.1.1)

(14)

where i is the smallest integer such that $cS_i > x$. This completes an analysis of stochastic uncertainty for a particular vector of variable values from the LHS sampling.

6.4.14 CCDF Family

The process of CCDF construction described in Section 6.4.13 is repeated once for each vector of values of subjectively uncertain variables created by LHS. This process yields a family of CCDFs such as those presented in Section 6.5. This family of CCDFs provides a complete display of both stochastic and subjective uncertainty, as discussed in Section 6.1.2.

6.5 Performance Assessment Results

This section contains results of the performance assessment and demonstrates that the WIPP complies with the quantitative containment requirements in 40 CFR § 191.13(a). See Section 6.1 for a discussion of the containment requirements. Criteria for presenting the results of performance assessments are provided by the EPA in 40 CFR § 194.34, and are discussed in Section 6.1.3. These criteria are also summarized here for clarity.

Additional detail about the results of the performance assessment is contained in Appendix SA, which describes sensitivity analyses conducted as the final step in the Monte Carlo analysis. These sensitivity analyses indicate the relative importance of each of the sampled parameters in terms of their contribution to uncertainty in the estimate of disposal system performance. Analyses also examine the sensitivity of intermediate performance measures to the sampled parameters. Examples of such intermediate performance measures include the quantity of radionuclides released to the accessible environment by any one mechanism (for example, cuttings or direct brine releases), and other model results that describe conditions of interest such as disposal region pressure.

6.5.1 Demonstrating Convergence of the Mean CCDF

As discussed in Sections 6.4.13 and 6.4.14, individual CCDFs for the WIPP are constructed by estimating cumulative radionuclide releases to the accessible environment for 10,000 different possible futures. Each CCDF is calculated for a single LHS vector of input parameters and is conditional on the occurrence of that particular combination of parameter values. Multiple realizations of the performance assessment calculations yield a family of CCDFs in which each individual CCDF is generated from a different LHS vector. Families of CCDFs calculated for the WIPP performance assessment are based on 100 LHS vectors drawn from distributions of values for 57 imprecisely known parameters. As discussed in Section 6.1.2, mean and percentile CCDFs are constructed from families and provide summary measures of disposal system performance.

Criteria provided by the EPA in 40 CFR Part 194.34 address the statistical interpretation of CCDFs:

> The number of CCDFs generated shall be large enough such that, at cumulative releases of 1 and 10, the maximum CCDF generated exceeds the 99th percentile of the population of CCDFs with at least a 0.95 probability. Values of cumulative release shall be calculated according to Note 6 of Table 1, Appendix A of Part 191 of this chapter. (40 CFR § 194.34(d))
>
> Any compliance application shall provide information which demonstrates that there is at least a 95 percent level of statistical confidence that the mean of the population of CCDFs meets the containment requirements of § 191.13 of this chapter. (40 CFR § 194.34(f))

Information provided by the EPA in the Background Information Document for 40 CFR Part 194 clarifies the intent of these criteria.

> In 40 CFR part 194, EPA decided that the statistical portion of the determination of compliance with 40 CFR part 191 will be based on the sample mean. The LHS sample sizes should be demonstrated operationally (approximately 300 when 50 variables are considered) to improve (reduce the size of) the confidence interval for the estimated mean. The underlying principle is to show convergence of the mean. (EPA 1996b, 8-41)

The DOE has chosen to demonstrate convergence of the mean and to address the associated criteria of 40 CFR Part 194 using an operational approach of multiple replication as proposed by Iman (1982). The complete set of performance assessment calculations was repeated three times with all aspects of the analysis identical except for the random seed used to initiate the LHS procedure. Thus, performance assessment results are available for three replicates, each based on an independent set of 100 LHS vectors drawn from identical CCDFs for imprecisely known parameters and propagated through an identical modeling system. This technique of multiple replication allows evaluation of the adequacy of the sample size chosen in the Monte Carlo analysis and provides a suitable measure of confidence in the estimate of the mean CCDF used to demonstrate compliance with 40 CFR § 191.13(a).

6.5.2 Complementary Cumulative Distribution Functions for the WIPP

Families of CCDFs for each of the three replicates are shown in Figures 6-35, 6-36, and 6-37. Each figure contains 100 CCDFs. These figures address the criterion stated in 40 CFR § 194.34(e):

> Any compliance application shall display the full range of CCDFs generated.

Figures 6-35 through 6-37 show that all 300 CCDFs lie below and to the left of the limits specified in 40 CFR § 191.13(a). They also show qualitatively that the three replicates yield very similar results. Quantitative verification of the similarity of the three replicates is demonstrated in Figure 6-38, which shows the mean CCDFs calculated for each of the three replicates, together with an overall mean CCDF that is the arithmetic mean of the three individual mean CCDFs. Figure 6-38 demonstrates two key points. First, the overall mean CCDF lies entirely below and to the left of the limits specified in 40 CFR § 191.13(a). Thus, the WIPP is in compliance with the containment requirements of 40 CFR Part 191. Second, the sample size of 100 in each replicate is sufficient to generate a stable distribution of outcomes. Within the region of regulatory interest (that is, at probabilities greater than

$10^{-3}/10^{4}$ yr), the mean CCDFs from each replicate are essentially indistinguishable from the overall mean at the resolution of the figure. Figure 6-39 provides quantitative confirmation of the sufficiency of the sample size, by displaying the overall mean together with the 0.95 confidence interval of the Student's t-distribution estimated from the individual means of the three independent replicates (Iman 1982), as shown in Figure 3-38.

Figure 6-40 provides additional summary information about the distributions of CCDFs resulting from the three replicates. This figure shows CCDFs representing the mean, median, and 10th and 90th percentile CCDFs from each replicate, together with the overall mean. Note that for each type of CCDF (for example, the 10th percentile), curves from each replicate overlie closely. This provides quantitative verification of the qualitative observation that distributions from each replicate appear similar. Note also that the mean CCDFs lie to the right of the 90th percentile CCDFs at probabilities less than approximately $10^{-2}/10^{4}$ yr. This is a result of the strongly skewed distribution, with the location of the mean being dominated by the relatively small number of CCDFs associated with the largest normalized releases.

6.5.3 Release Modes Contributing to the Total Radionuclide Release

Radionuclide releases to the accessible environment can be grouped into four categories according to their mode of release:

(1) cuttings and cavings releases,

(2) spallings releases,

(3) releases resulting from the direct release of brine at the surface during drilling, and

(4) releases in the subsurface following transport in groundwater.

Each of these four modes has the potential to contribute to the total quantity of radionuclides released from the repository, and therefore each has the potential to affect the position of the mean CCDF.

Figure 6-41 provides a display of the relative contribution of each mode to the total release. Releases for each of the three replicates are similar, and results are shown for replicate 1 only for simplicity. Mean CCDFs are shown for the total normalized release (this curve is also shown in Figure 6-40 and is the mean of the family shown in Figure 6-35) and for the normalized releases resulting from cuttings and cavings, spallings, and direct brine release. The mean CCDF for subsurface releases resulting from groundwater transport is not shown because those releases were less than 10^{-6} EPA units and the CCDF cannot be shown at the scale of this figure. Releases from cuttings and cavings are shown to be the most important contributors to the location of mean CCDF, with spallings also making a small contribution. Direct brine releases are less important, and have very little effect on the location of the mean

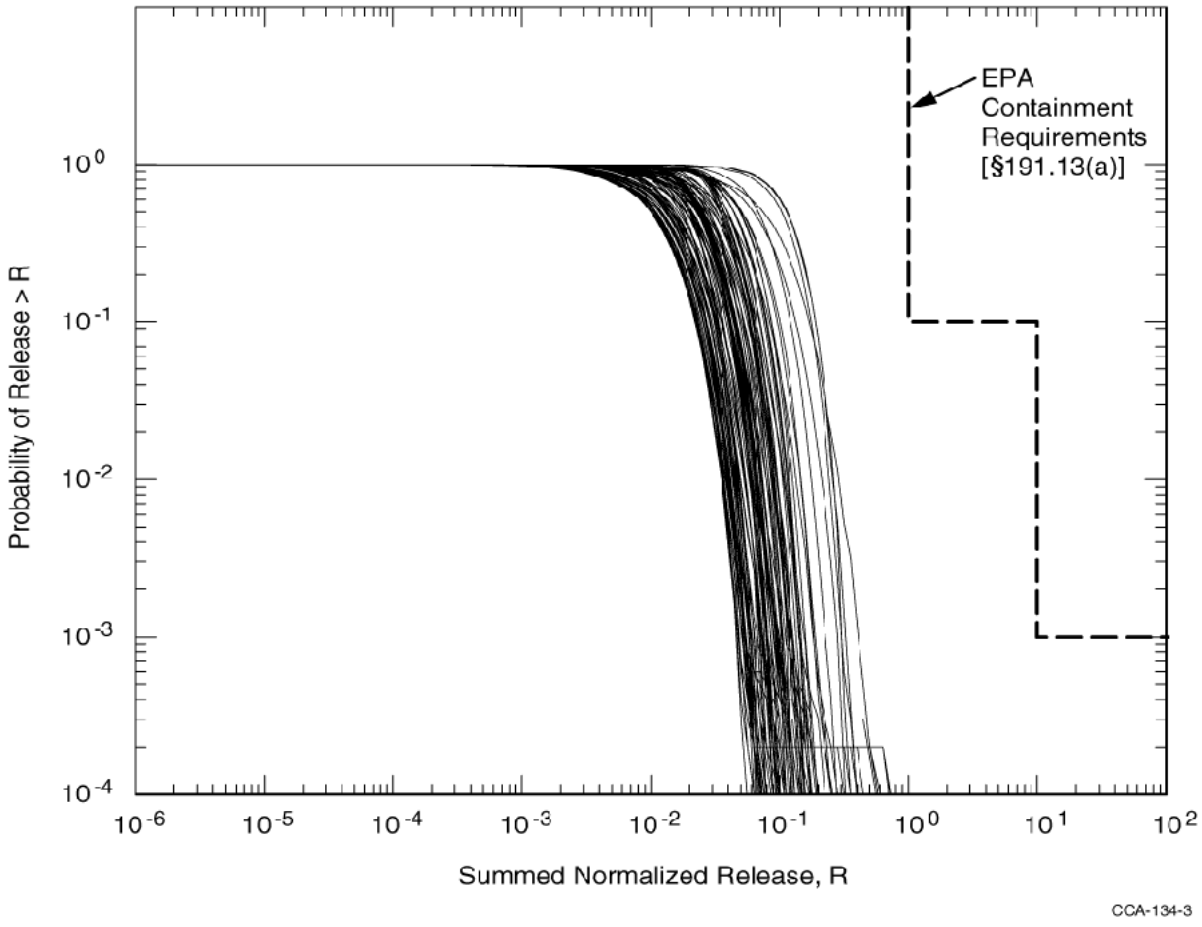

Figure 6-35. Distribution of CCDFs for Normalized Radionuclide Releases to the Accessible Environment from the WIPP, Replicate 1

1

1

1 **THIS PAGE INTENTIONALLY LEFT BLANK**

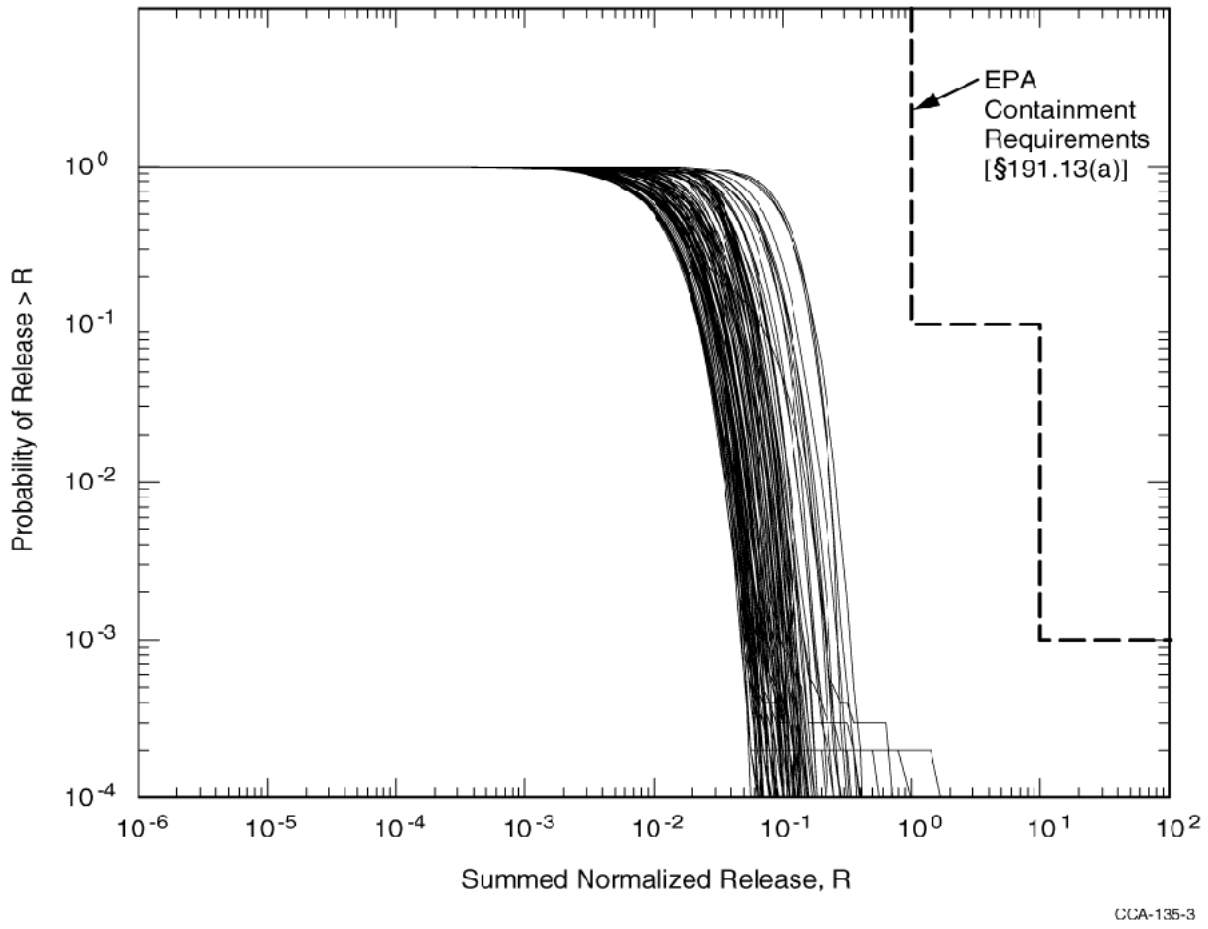

Figure 6-36. Distribution of CCDFs for Normalized Radionuclide Releases to the Accessible Environment from the WIPP, Replicate 2

1

1

1 **THIS PAGE INTENTIONALLY LEFT BLANK**

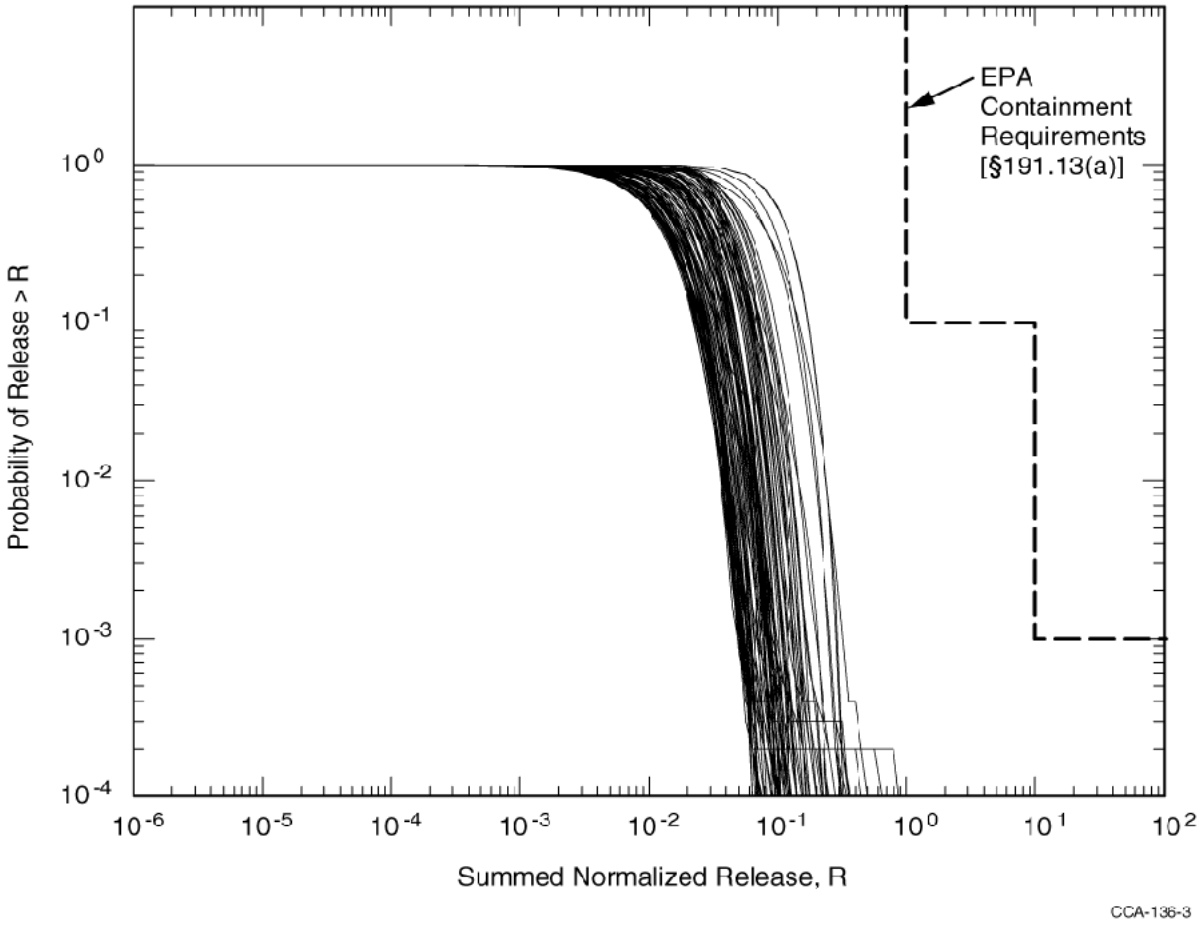

Figure 6-37. Distribution of CCDFs for Normalized Radionuclide Releases to the Accessible Environment from the WIPP, Replicate 3

1

1

1 **THIS PAGE INTENTIONALLY LEFT BLANK**

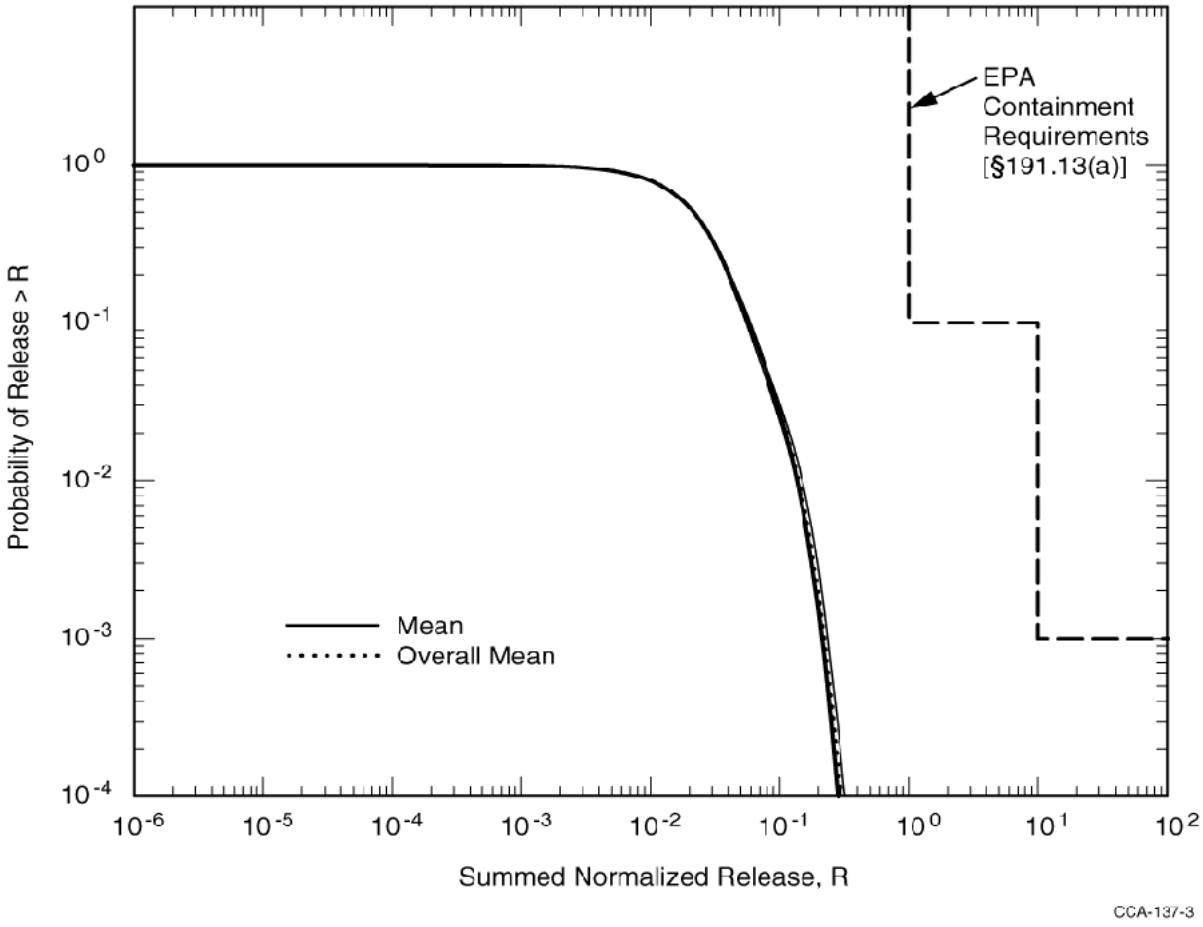

Note: Four CCDFs are shown, including three individual mean CCDFs calculated for each of the three distributions of CCDFs calculated for the three replicates and shown in Figures 6-35, 6-36, 6-37, and an overall mean CCDF that is the arithmetic mean of the three individual mean CCDFs.

Figure 6-38. Mean CCDFs for Normalized Radionuclide Releases to the Accessible Environment

1

1

1 **THIS PAGE INTENTIONALLY LEFT BLANK**

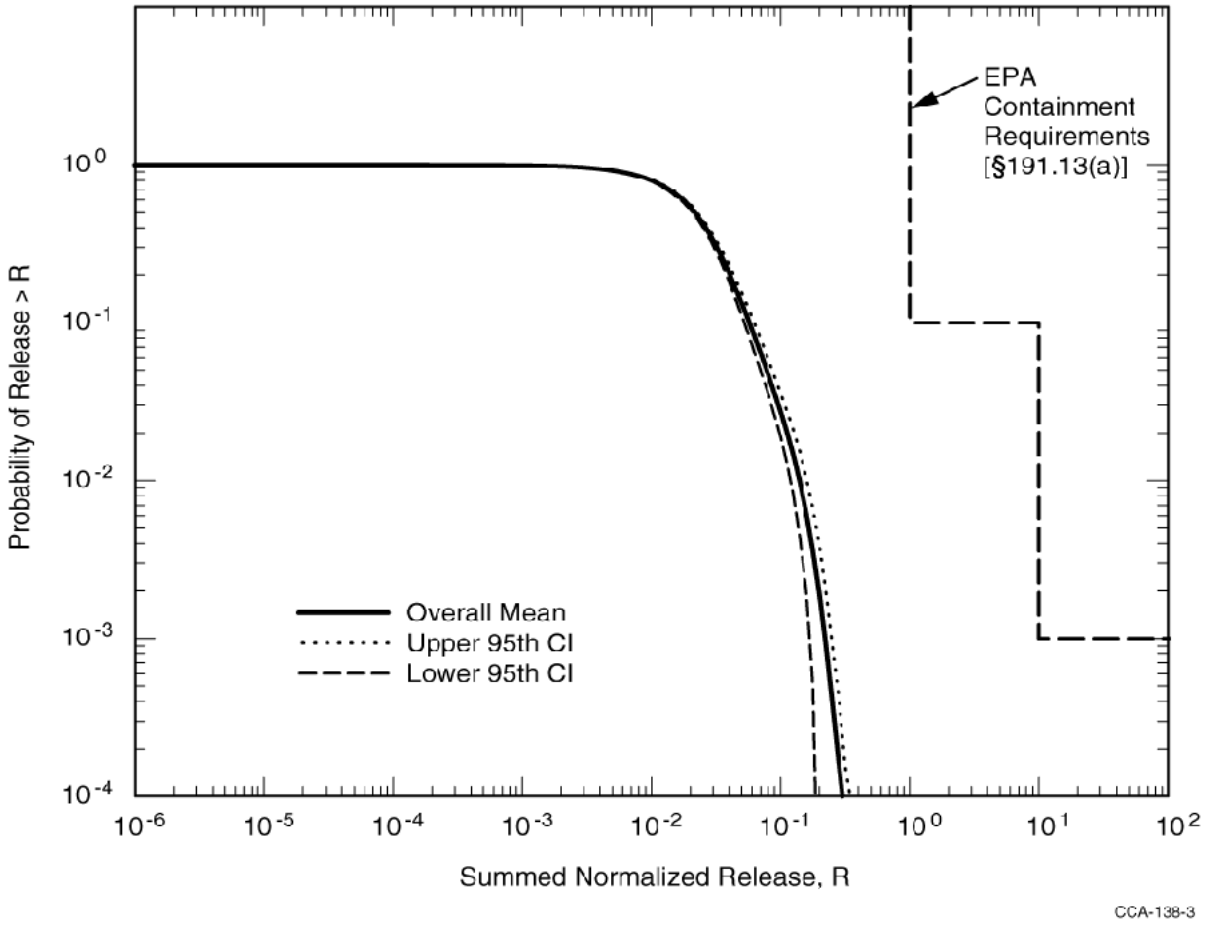

Note: The overall mean CCDF shown in Figure 6-38 is repeated together with the 0.95 confidence interval of the Student-t distribution estimated from the three individual mean CCDFs.

Figure 6-39. Confidence Levels for the Mean CCDF

1

1 **THIS PAGE INTENTIONALLY LEFT BLANK**

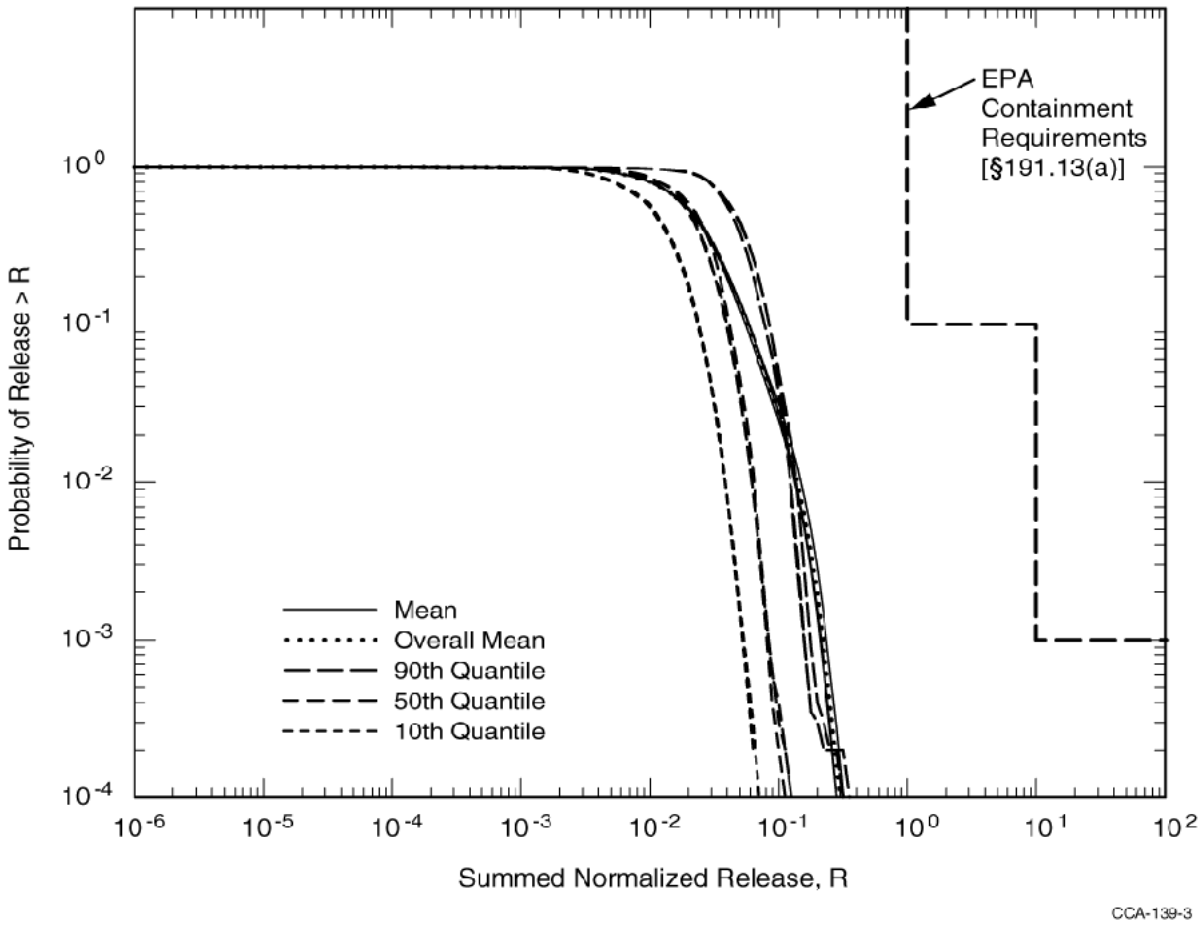

Note: Mean, median, and 10th and 90th percentile CCDFs are shown together with the overall mean. These CCDFs are based on the distributions of CCDFs shown in Figures 6-35, 6-36, and 6-37.

Figure 6-40. Summary CCDFs for Replicates 1, 2, and 3

1 **THIS PAGE INTENTIONALLY LEFT BLANK**

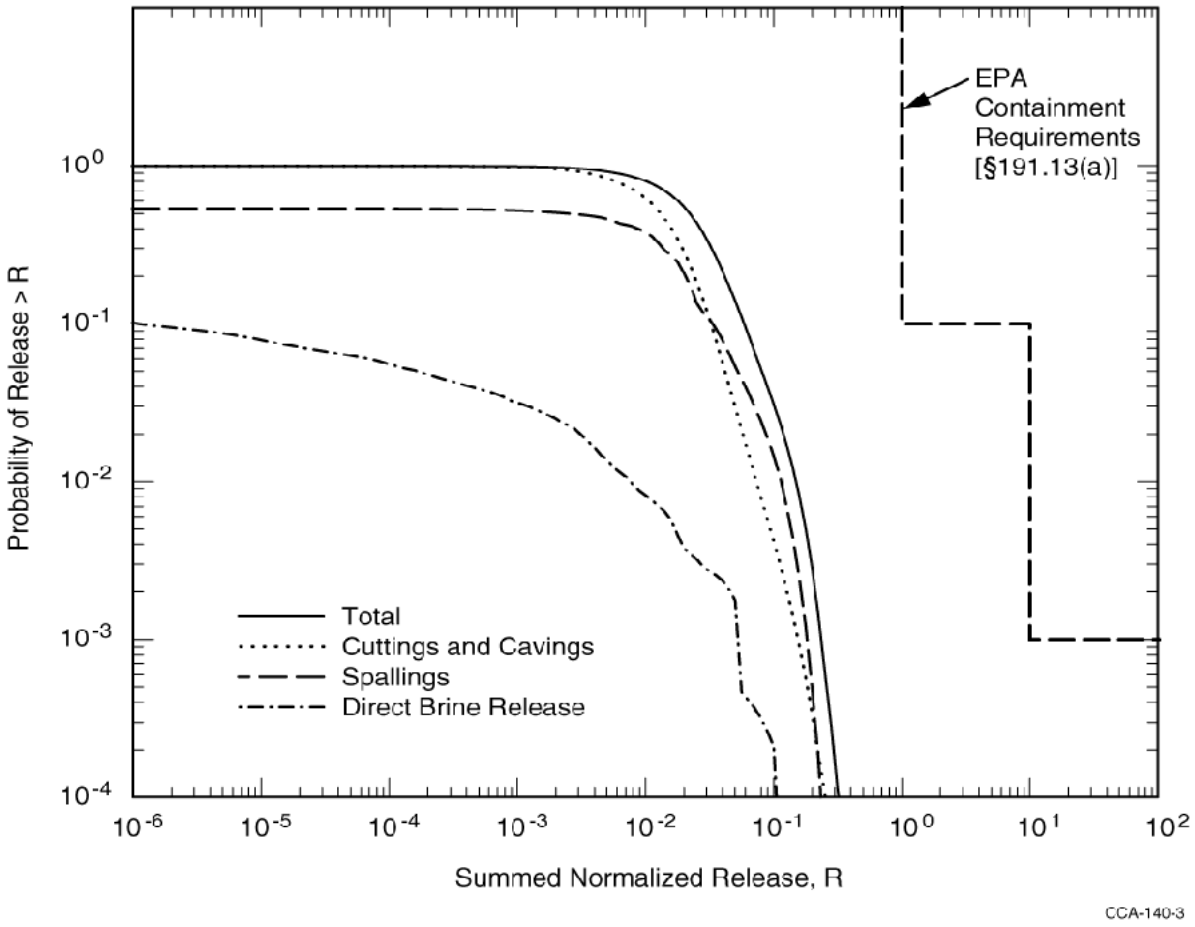

Note: Mean CCDFs are shown for the total normalized release (this curve is also shown in Figure 6-40 and is the mean of the family shown in Figure 6-35) and for the normalized releases resulting from cuttings and cavings, spallings, and direct brine release. The mean CCDF for subsurface releases resulting from groundwater transport is not shown because those releases were less then 10-6 EPA units and the CCDF cannot be shown at the scale of this figure.

Figure 6-41. Mean CCDFs for Specific Release Modes, Replicate 1

1

1 **THIS PAGE INTENTIONALLY LEFT BLANK**

CCDF. Subsurface groundwater releases are not important, and have essentially no effect on the mean CCDF. See Appendix SA for additional discussion of the relative importance of the release modes.

6.5.4 Uncertainty and the Role of Conservatism in the Compliance Demonstration

As defined in 40 CFR § 191.12, performance assessments must "estimate the cumulative releases of radionuclides, considering the associated uncertainties, caused by all significant events and processes."

Site characterization, repository design, and waste characterization activities, as described in Chapters 2.0, 3.0, and 4.0, respectively, have removed much uncertainty from the analysis. Uncertainties remain, however, about how best to characterize some aspects of the disposal system and how best to model the complex interactions between the waste and its surrounding environment. These remaining uncertainties have been incorporated in the performance assessment to the extent practicable through the use of reasonable and realistic assumptions about models and parameter values.

In general, the DOE has not attempted to bias the performance assessment toward a conservative outcome, and the mean CCDF represents a reasonable estimate of the expected and, in the case of future human activities including intrusion, prescribed, performance of the disposal system. However, where realistic approaches to incorporating uncertainty are unavailable or impractical and where the impact of the uncertainty on performance is small, the DOE has chosen to simplify the analysis by implementing reasonable and conservative assumptions. These conservative assumptions are reviewed here, not because they bias the location of the mean CCDF, but rather because an understanding of their effects contributes qualitatively to the "reasonable expectation, on the basis of the record before the implementing agency, that compliance with [§] 191.13(a) will be achieved," as required by 40 CFR § 191.13(b).

As noted in Section 6.2 and Appendix SCR, in some cases processes have been omitted from the modeling system for simplicity because the only possible effects of including them would be beneficial to system performance. Examples include the decision to model radionuclide dissolution as an equilibrium process (assuming instantaneous leaching and dissolution), and the decision not to model sorption of radionuclides in the Salado or in the seal system.

In other cases, the DOE has made conservative decisions during the design of the conceptual and computational models, as listed in Table 6-30. Some conservative assumptions listed in this table are mentioned below. For example, within the repository portion of the BRAGFLO model, fluid flow in a single panel is treated as if all rooms were a single void (that is, pillars are omitted). This treatment allows brine flow to and from an intrusion borehole to contact more waste than it would if it followed a more realistic flow path between rooms. The effect is conservative with respect to brine flow up a plugged and abandoned borehole. Similarly,

Table 6-30. Conservative Model and Parameter Assumptions Used in Performance Assessment (from Appendix MASS, Table MASS-1)

Conservative Assumption	Code	Cross-Reference
Long-term flow up plugged and abandoned boreholes is modeled as if all intrusions occur into a down-dip (southern) panel.	BRAGFLO	Section 6.4.3
Pillars and individual drifts in rooms, and panel closures in the nine lumped panels, are not modeled for long-term performance, and containers provide no barrier to fluid flow.	BRAGFLO	Section 6.4.3, Appendix MASS, Section MASS.5
Panel closures are modeled with the same permeability as the surrounding DRZ.	BRAGFLO	Sections 6.4.3.2 and 6.4.5.3 MASS Attachment 7-1
Brine in the repository will contain a uniform mixture of dissolved and solid-state species. No microenvironments that influence the overall chemical conditions will persist.	NUTS PANEL	Section 6.4.3.4 Appendix SOTERM, Section SOTERM.2.2
Radionuclide dissolution to solubility limits is instantaneous.	NUTS PANEL	Sections 6.4.3.5 and 6.4.3.4 (Appendix SOTERM, Section SOTERM.3.3, SCR.2.5.3.1)
Radionuclides are not retarded by shaft seals.	NUTS	Section 6.4.4 Section SCR.2.5.4.2
Shaft concrete components are modeled as if they degrade 400 years after emplacement.	BRAGFLO	Section 6.4.4 Appendix PAR, Table PAR-19
The permeability of the DRZ is constant and higher than intact Salado.	BRAGFLO	Section 6.4.5.3 Appendix MASS, Section MASS.13.4
The unnamed lower member, Tamarisk, and Forty-niner are assumed to be impermeable.	BRAGFLO SECOFL2D	Sections 6.4.6.1, 6.4.6.3, and 6.4.6.5 Appendix MASS, Section MASS.14
Sorption on clays present in the Culebra is not modeled.	SECOFL2D	Section 6.4.6.2.1 Appendix MASS, Section MASS.15.2
Particle waste shear based on properties of marine clays, considered a worst case.	CUTTINGS_S	Section 6.4.7.1 Appendix PAR, Parameter 33
The concentration of actinides in liquid moving up the borehole in the E1E2 scenario assumes homogeneous mixing within the panel.	CCDFGF PANEL	Section 6.4.13.5

Table 6-30. Conservative Model and Parameter Assumptions Used in Performance Assessment (from Appendix MASS, Table MASS-1) (Continued)

Conservative Assumption	Code	Cross-Reference
For all direct releases to the surface and the E1E2 source term to the Culebra, any actinides that enter the borehole are assumed to reach the surface or Culebra.	CUTTINGS_S BRAGFLO_DBR PANEL CCDFGF	Section 6.4.7.1 Section 6.4.13.5
Retardation is assumed to not occur in the Salado.	NUTS CCDFGF	Section 6.4.5.4.2
Depletion of actinides in parts of the repository that have been penetrated by boreholes is not accounted for in calculating the releases from subsequent intrusions at such locations.	CUTTINGS_S	Section 6.4.13.7
Hydraulically-significant fractures are assumed to be present everywhere in the Culebra.	SECOTP2D	Section 6.4.6.2.1

the DOE has chosen to model fluid flow through plugged and abandoned boreholes as if all intrusions occurred into a down-dip (that is, southern) panel. As modeled, downdip panels tend to have more brine in them than up-dip panels and this assumption therefore may result in overestimating the amount of brine present in intruded panels. Radionuclide dissolution to solubility limits is modeled as instantaneous. The DRZ around the panel closures is assumed not to heal and panel closures are assumed to be no more effective than the surrounding DRZ, tending to overestimate the amount of fluid flow between panels. For E1E2 scenarios, complete mixing is assumed within the intruded panel, and all brine that flows out of the panel and up the borehole is assumed to have been in contact with waste.

Within the shaft seal system, concrete components are modeled as if they degrade 400 years after emplacement, underestimating their potential to limit fluid flow over the long-term. For direct releases and E1E2 releases to the Culebra, processes of actinide transport and retardation are not modeled within the intrusion borehole and all actinides that enter the borehole are assumed to be transported to the surface or into an overlying transmissive unit. Within the Culebra (which modeling indicates will be the only transmissive unit that will receive long-term flow from the borehole), hydraulically significant fractures are assumed for modeling simplicity to be present everywhere, even though test data indicate that the portions of the Culebra above the waste disposal region behave as an unfractured, single porosity matrix.

These conservative assumptions have not significantly affected the location of the mean CCDF, which, as shown in Section 6.5.3, is dominated by cuttings and cavings releases that are, with one exception, independent of the conservative simplifications described here. As discussed in Appendix SA (Section SA.1), the parameter making the largest contribution to uncertainty in the location of the mean CCDF is the effective shear resistance of the waste,

which affects the quantity of waste eroded from the borehole wall and transported to the surface as cavings. In the absence of data describing the reasonable and realistic future properties of degraded waste and backfill, effective shear resistance of the waste is a parameter for which the DOE has selected a conservative distribution (see Appendix PAR, Parameter 33).

6.5.5 Summary of the Demonstration of Compliance with the Containment Requirements

The WIPP is in compliance with the containment requirements of 40 CFR § 191.13(a), as shown by Figures 6-35 through 6-39. Figures 6-38 and 6-39 demonstrate that the sample size of 100 chosen for this analysis is sufficient to provide the level of statistical confidence specified in 40 CFR § 194.34.

Additional confidence in the compliance determination comes from examination of Figure 6-41, which shows that the location of the mean CCDF depends almost entirely on the relatively simple processes that contribute to cuttings and cavings releases resulting from inadvertent human intrusion by drilling. Uncertainties related to the characterization of the natural system and the interaction of waste with the disposal system environment have little effect on long-term performance. The natural and engineered barrier systems, as described in Chapters 2.0 and 3.0, provide robust and effective containment of TRU waste even if the repository is penetrated by multiple borehole intrusions.

REFERENCES

Andersson, J., Ed. 1989. *The Joint SKI/SKB Scenario Development Project*. SKB Technical Report 89-35, Authors: J. Andersson, T. Carlsson, T. Eng, F. Kautsky, E. Söderman, and S. Wingefors. Swedish Nuclear Fuel and Waste Management Co., Stockholm, Sweden.

Barr, G.E., Miller, W.B., and Gonzalez, D.D. 1983. *Interim Report on the Modeling of the Regional Hydraulics of the Rustler Formation.* SAND83-0391. Sandia National Laboratories, Albuquerque, NM, pp. 26 – 27. WPO 27557.

Beauheim, R.L. 1987. *Interpretations of Single-Well Hydraulic Tests Conducted At and Near the Waste Isolation Pilot Plant (WIPP) Site, 1983 – 1987*. SAND87-0039. Sandia National Laboratories, Albuquerque, NM, pp. 110 – 118. WPO 27679.

Beauheim, R.L., Wawerisk, W.R., and Roberts, R.M. 1993. "Coupled Permeability and Hydrofracture Tests to Assess the Waste-Containment Properties of Fractured Anhydrite." *Journal of Rock Mechanics*, Vol. 30, No. 7, pp. 1159 – 1163.

Butcher, B.M. 1996. Memo to M.S. Tierney, RE: QAP 9-1 Documentation of the Initial Waste Water Content for the CCA, January 29, 1996. WPO 30925.

Butcher, B.M., Thompson, T.W., VanBuskirk, R.G., and Patti, N.C. 1991. *Mechanical Compaction of Waste Isolation Pilot Plant Simulated Waste*. SAND90-1206. Sandia National Laboratories, Albuquerque, NM. WPO 23968.

Christian-Frear, G.L., and Webb, S.W. 1996. *The Effect of Explicit Representation of the Stratigraphy on Brine and Gas Flow at the Waste Isolation Pilot Plant*. SAND94-3173. Sandia National Laboratories, Albuquerque, NM.

Corbet, T.F. and Knupp, P.M. 1996. *The Role of Regional Groundwater Flow in the Hydrogeology of the Culebra Member of the Rustler Formation at the Waste Isolation Pilot Plant (WIPP), Southeastern New Mexico.* SAND96-2133. Albuquerque, NM: Sandia National Laboratories.

Cranwell, R.M., Guzowski, R.V., Campbell, J.E., and Ortiz, N.R. 1990. *Risk Methodology for Geologic Disposal of Radioactive Waste: Scenario Selection Procedure.* NUREG/CR-1667, SAND80-1429. Sandia National Laboratories, Albuquerque, NM. WPO 26750.

Dale, T., and Hurtado, L.D. 1996. "WIPP Air-Intake Shaft Disturbed-Rock Zone Study," *4th International Conference on the Mechanical Behavior of Salt, Montreal, Quebec, June 17–18, 1996.* SAND96-1327C. Albuquerque, NM: Sandia National Laboratories.

Davies, P.B. 1991. *Evaluation of the Role of Threshold Pressure in Controlling Flow of Waste-Generated Gas into Bedded Salt at the Waste Isolation Pilot Plant.* SAND90-3246. Sandia National Laboratories, Albuquerque, NM, pp. 17 – 19. WPO 26169.

Dotson, L.J. 1996. *Non-Salado Initial Pressure*. Sandia National Laboratories, NM. WPO 30713.

Earth Technology Corporation. 1988. *Final Report for Time Domain Electromagnetic (TDEM) Surveys at the WIPP Site.* SAND87-7144. Albuquerque, NM: Sandia National Laboratories.

EPA (U.S. Environmental Protection Agency). 1985. "40 CFR Part 191: Environmental Standards for the Management and Disposal of Spent Nuclear Fuel, High-Level and Transuranic Radioactive Wastes; Final Rule." *Federal Register,* Vol. 50, No. 182, pp. 38066 – 38089, September 19, 1985. Office of Radiation and Air, Washington, D.C. WPO 39132.

EPA (U.S. Environmental Protection Agency). 1993. "40 CFR Part 191: Environmental Radiation Protection Standards for the Management and Disposal of Spent Nuclear Fuel, High-Level and Transuranic Radioactive Wastes; Final Rule." *Federal Register,* Vol. 48, No. 242, pp. 66398 – 66416, December 20, 1993. Office of Radiation and Air, Washington, D.C. WPO 39133.

EPA (U.S. Environmental Protection Agency). 1996a. "40 CFR Part 194: Criteria for the Certification and Re-Certification of the Waste Isolation Pilot Plant's Compliance with the 40 CFR Part 191 Disposal Regulations Final Rule." *Federal Register*, Vol. 61, No. 28, pp. 5224 – 5245, February 9, 1996. Office of Radiation and Indoor Air, Washington, D.C. In NWM Library as KF70.A35.C751 1996 (Reference)

EPA (U.S. Environmental Protection Agency). 1996b. *Criteria for the Certification and Re-Certification of the Waste Isolation Pilot Plant's Compliance with the 40 CFR Part 191 Disposal Regulations. Background Information Document for 40 CFR Part 194.* EPA 402-R-96-002. Environmental Protection Agency, Office of Radiation and Indoor Air, Washington, DC.

Freeze, G.A., Larson, K.W., and Davies, P.B. 1995. *A Summary of Methods for Approximating Salt Creep and Disposal Room Closure in Numerical Models of Multiphase Flow.* SAND94-0251. Sandia National Laboratories, Albuquerque, NM. WPO 29557.

Goodwin, B.W., Stephens, M.E., Davison, C.C., Johnson, L.H., and Zach, R. 1994. *Scenario Analysis for the Postclosure Assessment of the Canadian Concept for Nuclear Fuel Waste Disposal*. AECL-10969, COG-94-247. Whiteshell Laboratories, Pinawa, Manitoba, Canada.

Hodgkinson, D.P. and Sumerling, T.J. 1989. "A Review of Approaches to Scenario Analysis for Repository Safety Assessment." In *Proceedings of the IAEA/CEC/NEA (OECD)*

Symposium on Safety Assessment of Radioactive Waste Repositories (Paris, 1989). OECD/NEA, Paris, France. pp. 333 – 350.

Holt, R.M., and Powers, D.W. 1984. *Geotechnical Activities in the Waste Handling Shaft Waste Isolation Pilot Plant (WIPP) Project Southeastern New Mexico*. WTSD-TME-038. U.S. Department of Energy, Carlsbad, NM.

Holt, R.M., and Powers, D.W. 1986. *Geotechnical Activities in the Exhaust Shaft*. DOE/WIPP-86-008. U.S. Department of Energy, Carlsbad, NM.

Holt, R.M., and Powers, D.W. 1990. *Geologic Mapping of the Air Intake Shaft at the Waste Isolation Pilot Plant.* DOE/WIPP 90-051. Westinghouse Electric Corporation, Carlsbad, NM.

IAEA (International Atomic Energy Agency). 1981. *Safety Assessment for the Underground Disposal of Radioactive Wastes*. IAEA Safety Series No. 56, Vienna, Austria.

Iman, R.L., 1982. "Statistical Methods for Including Uncertainties Associated with the Geologic Isolation of Radioactive Waste Which Allow for a Comparison with Licensing Criteria," *Proceedings of the Symposium on Uncertainties Associated with the Regulation of the Geologic Disposal of High-Level Radioactive Waste*, *Gatlinsburg, Tennessee, March 9-13, 1981*, ed. D.C. Kocher. NUREG/CP-0022, CONF810372. Oak Ridge National Laboratory, Oak Ridge, Tennessee, 145-157. Available from NTIS. Order #: DE82008883.

Iman, R.L., and Conover, W.J. 1982. A Distribution-Free Approach to Inducing Rank Correlation Among Input Variables. *Communications in Statistics*: *Simulation and Computation*, Vol. B11, No. 3, pp. 311 – 334.

Kaplan, S., and Garrick, B.J. 1981. On the Quantitative Definition of Risk. *Risk Analysis*, Vol. 1, No. 1, pp. 11 – 27.

Lappin, A.R., Hunter, R.L., Garber, D.P., Davies, P.B., Beauheim, R.L., Borns, D.J., Brush, L.H., Butcher, B.M., Cauffman, T., Chu, M.S.Y., Gomez, L.S., Guzowski, R.V., Iuzzolino, H.J., Kelley, V., Lambert, S.J., Marietta, M.G., Mercer, J.W., Nowak, E.J., Pickens, J., Rechard, R.P., Reeves, M., Robinson, K.L., and Siegel, M.D., eds. 1989. *Systems Analysis, Long-Term Radionuclide Transport, and Dose Assessments, Waste Isolation Pilot Plant (WIPP), Southeastern New Mexico: March 1989.* SAND89-0462. Sandia National Laboratories, Albuquerque, NM. WPO 24125.

Luker, R.S., Thompson, T.W., and Butcher, B.M. 1991. "Compaction and Permeability of Simulated Waste." In *Rock Mechanics as a Multidisciplinary Science: Proceedings of the 32nd U.S. Symposium, University of Oklahoma, Norman, OK, July 10-12, 1991*, J.C. Roegiers, ed. SAND90-2368C, pp. 694 – 702. A.A. Balkema, Brookfield, VT. WPO 38847.

Mercer, J.W., and Orr, B.R. 1979. *Interim Data Report on Geohydrology of Proposed Waste Isolation Pilot Plant Site, Southeast New Mexico*. Water Resources Investigations 79-98. U.S. Geological Survey, Albuquerque, NM.

Miller, W.M. and Chapman, N.A., Ed. 1992. *Identification of Relevant Processes, System Concept Group Report,* UKDOE/HMIP Report TR-ZI-11, London, England.

NAGRA. 1985. *Nuclear Waste Management in Switzerland: Feasibility Studies and Safety Analyses (Project Gewahr, 1985)*. NAGRA Project Report NGB 85-09 (English Summary), Wettingen, Switzerland.

OECD Nuclear Energy Agency. 1992. *Systematic Approaches to Scenario Development.* Organisation for Economic Co-Operation and Development, Paris, France. NWM Library, NNA.920610.0027.

Popielak, R.S., Beauheim, R.L., Black, S.R., Coons, W.E., Ellingson, C.T., and Olsen, R.L. 1983. *Brine Reservoirs in the Castile Formation Waste Isolation Pilot Plant (WIPP) Project Southeastern New Mexico.* TME-3153, Vols. 1 and 2. Westinghouse Electric Corp, Carlsbad, NM.

Sandia National Laboratories. 1991. *Preliminary Comparison with 40 CFR Part 191, Subpart B for the Waste Isolation Pilot Plant, December 1991. Volume. 1: Methodology and Results.* SAND91-0893/1. Sandia National Laboratories, WIPP Performance Assessment Division, Albuquerque, NM. WPO 26404.

Sandia National Laboratories. 1992-1993. *Preliminary Performance Assessment for the Waste Isolation Pilot Plant, December 1992.* SAND92-0700, Vols. 1 – 5. Sandia National Laboratories, WIPP Performance Assessment Division, Albuquerque, NM. Vol. 1 - WPO 20762, Vol. 2 - WPO 20805, Vol. 3 - WPO 23529, Vol. 4 - WPO 20958, Vol. 5 - WPO 20929.

State of New Mexico, Oil Conservation Division, Energy, Minerals, and Natural Resources Department. 1988. "Application of the Oil Conservation Division Upon It's Own Motion to Revise Order R-111. As Amended. Pertaining to the Potash Areas of Eddy and Lea Counties, New Mexico." Case 9316, Revision to Order R-111-P, April 21, 1988. Santa Fe, NM. On file in the NWM Library as KFN2581.

Stenhouse, M.J., Chapman, N.A., and Sumerling, T.J. 1993. *SITE-94 Scenario Development FEP Audit List Preparation: Methodology and Presentation*. SKI Technical Report 93:27. Swedish Nuclear Power Inspectorate, Stockholm. Available from NTIS as DE 94621513.

Thorne, M.C. 1992. *Dry Run 3 - A Trial Assessment of Underground Disposal of Radioactive Wastes Based on Probabilistic Risk Analysis - Volume 8: Uncertainty and Bias Audit.* United Kingdom Department of Environment Report DOE/HMIP/RR/92.040, London, England.

Van Pelt, R.S. November 20, 1995. "Permeability Estimates of MGFT08 and MGFT09." SNL Technical Memorandum to M.K. Knowles. Contained in SWCF Record Package, "Small-Scale Seals Performance Test: Series A Post-Mortem," WPO 39631.

Vaughn, P., Bean, J., Garner, J., Lord, M., MacKinnon, R., McArthur, D., Schreiber, J., and Shinta, A.. 1995. FEPs Screening Analysis DR2, DR3, DR6, DR7, and S6. Record package submitted to SWCF-A:1.1.6.3:PA:QA:TSK:DR2, DR3, DR6, DR7, and S6. Sandia National Laboratories, Albuquerque, NM. WPO 38152.

Wallace, M.G., Beauheim, R., Stockman, C., Martell, M.A., Brinster, K., Wilmot, R., and Corbet, T. 1995. FEPs Screening Analysis, NS-1: Dewey Lake Data Collection and Compilation. Record package submitted to SWCF-A:1.1.6.3:PA:QA:TSK:NS1. Sandia National Laboratories, Albuquerque, NM. WPO 30650.

Wang, Y., and Brush, L.H. January 26, 1996. "Estimates of Gas Generation Parameters for the Long-Term WIPP Performance Assessment." WPO 31943.

BIBLIOGRAPHY

Adams, J.E. 1944. Upper Permian Ochoa Series of Delaware Basin, West Texas and Southeastern New Mexico. *American Association of Petroleum Geologists Bulletin,* Vol. 28, No. 11, pp. 1596 – 1625. WPO 37940.

Anderson, R.Y. 1978. *Deep Dissolution of Salt, Northern Delaware Basin, New Mexico.* Sandia National Laboratories, Albuquerque, NM. WPO 29527 - WPO 29530.

Anderson, R.Y., and Kirkland, D.W. 1980. Dissolution of Salt Deposits by Brine Density Flow. *Geology*, Vol. 8, No. 2, pp. 66 – 69.

Anderson, R.Y., Dean, Jr., W.E., Kirkland, D.W., and Snider, H.I. 1972. Permian Castile Varved Evaporite Sequence, West Texas and New Mexico. *Geological Society of America Bulletin*, Vol. 83, No. 1, pp. 59 – 85.

Argüello, J.G., Molecke, M.A., and Beraun, R. 1989. "3D Thermal Stress Analysis of WIPP T RH TRU Experiments." *Rock Mechanics as a Guide for Efficient Utilization of Natural Resources, Proceedings of the 30th U.S. Rock Mechanics Symposium, West Virginia University, Morgantown, WV, June 19-22, 1989*, A.W. Khair, Ed. SAND88-2734C, pp. 681 – 688. A.A. Balkema, Brookfield, VT. WPO 25724.

Bachman, G.O. 1973. *Surficial Features and Late Cenozoic History in Southeastern New Mexico*. Open-File Report 4339-8. U.S. Geological Survey, Reston, VA.

Bachman, G.O. 1974. *Geologic Processes and Cenozoic History Related to Salt Dissolution in Southeastern New Mexico*. Open-File Report 74-194. U.S. Geological Survey, Denver, CO.

Bachman, G.O. 1976. Cenozoic Deposits of Southeastern New Mexico and an Outline of the History of Evaporite Dissolution. *Journal of Research*, Vol. 4, No. 2, pp. 135 – 149. U.S. Geological Survey, Denver, CO.

Bachman, G.O. 1980. *Regional Geology and Cenozoic History of Pecos Region, Southeastern New Mexico.* Open-File Report 80-1099. U.S. Geological Survey, Denver, CO.

Bachman, G.O. 1981. *Geology of Nash Draw, Eddy County, New Mexico*. Open-File Report 81-31. U.S. Geological Survey, Denver, CO.

Bachman, G.O. 1984. *Regional Geology of Ochoan Evaporites, Northern Part of Delaware Basin*. Circular 184, pp. 1 – 22. New Mexico Bureau of Mines and Mineral Resources, Socorro, NM.

Bachman, G.O. 1985. *Assessment of Near-Surface Dissolution at and Near the Waste Isolation Pilot Plant (WIPP), Southeastern New Mexico.* SAND84-7178. Sandia National Laboratories, Albuquerque, NM. WPO 24609.

Bachman, G.O. 1987. *Karst in Evaporites in Southeastern New Mexico.* SAND86-7078. Sandia National Laboratories, Albuquerque, NM. WPO 24006.

Bachman, G.O., Johnson, R.B., and Swenson, F.A. 1973. *Stability of Salt in the Permian Salt Basin of Kansas, Oklahoma, Texas, and New Mexico.* Open-File Report 4339-4. U.S. Geological Survey, Denver, CO.

Baes, C.F., Jr., and Mesmer, R.E. 1976. *The Hydrolysis of Cations.* John Wiley & Sons, New York, NY.

Barker, D.S. 1977. Northern Trans-Pecos Magmatic Province: Introduction and Comparison with the Kenya Rift. *Geological Society of America Bulletin*, Vol. 88, No. 10, pp. 1421 – 1427.

Bear, J. 1988. *Dynamics of Fluids in Porous Media*. Dover Publications, Inc., New York, NY. NNA. 911127.0046.

Bear, J., and Verruijt, A. 1987. *Modeling Groundwater Flow and Pollution.* D. Reidel Publishing Company, Boston, MA. NNA. 900212.0003.

Bear, J., Tsang, C.F., and de Marsily, G. 1993. *Flow and Contaminant Transport in Fractured Rock*. Academic Press, Inc., San Diego, CA.

Beauheim, R.L. 1986. *Hydraulic-Test Interpretations for Well DOE-2 at the Waste Isolation Pilot Plant (WIPP) Site.* SAND86-1364. Sandia National Laboratories, Albuquerque, NM. WPO 27656.

Beauheim, R.L. 1987. *Interpretation of WIPP-13 Multipad Pumping Test of the Culebra Dolomite at the Waste Isolation Pilot Plant (WIPP) Site.* SAND87-2456. Sandia National Laboratories, Albuquerque, NM. WPO 28512.

Beauheim, R.L. 1987. *Analysis of Pumping Tests of the Culebra Dolomite Conducted at the H-3 Hydropad at the Waste Isolation Pilot Plant (WIPP) Site.* SAND86-2311. Sandia National Laboratories, Albuquerque, NM. WPO 28468.

Beauheim, R.L., and Holt, R.M. 1990. "Hydrogeology of the WIPP Site." In *Geological and Hydrological Studies of Evaporites in the Northern Delaware Basin for the Waste Isolation Pilot Plant (WIPP), New Mexico.* Field Trip #14 Guidebook, Geologic Society of America 1990 Annual Meeting, Dallas, TX, October 19 - November 1, 1990, pp. 131 – 179. D.W. Powers, R.M. Holt, R.L. Beauheim, and N. Rempe, leaders. SAND90-2035J. Dallas Geologic Society, Dallas, TX. WPO 29377.

Beauheim, R.L., Hassinger, B.W., and Klaiber, J.A. 1983. *Basic Data Report for Borehole Cabin Baby-1 Deepening and Hydrologic Testing, Waste Isolation Pilot Plant (WIPP) Project, Southeastern New Mexico.* WTSD-TME-020. U.S. Department of Energy, Albuquerque, NM.

Beauheim, R.L., Dale, T.F., and Pickens, J.F. 1991. *Interpretations of Single-Well Hydraulic Tests of the Rustler Formation Conducted in the Vicinity of the Waste Isolation Pilot Plant (WIPP) Site, 1988-1989.* SAND89-0869. Sandia National Laboratories, Albuquerque, NM. WPO 25862.

Beauheim, R.L., Saulnier, Jr., G.J., and Avis, J.D. 1991. *Interpretation of Brine-Permeability Tests of the Salado Formation at the Waste Isolation Pilot Plant Site: First Interim Report*. SAND90-0083. Sandia National Laboratories, Albuquerque, NM. WPO 26003.

Bechtel National. 1985. *Quarterly Geotechnical Field Data Report*. DOE/WIPP-221. U.S. Department of Energy, Carlsbad, NM.

Bell, J.T., Coleman, C.F., Costanzo, D.A., and Biggers, R.E. 1973. Plutonium Polymerization–III. The Nitrate Precipitation of Pu(IV) Polymer. *Journal of Inorganic and Nuclear Chemistry*, Vol. 35, No. 2, pp. 629 – 632.

Bell, J.T., Costanzo, D.A., and Biggers, R.E. 1973. Plutonium Polymerization–II. Kinetics of the Plutonium Polymerization. *Journal of Inorganic and Nuclear Chemistry*, Vol. 35, No. 2, pp. 623 – 628.

Bellin, A., Salandin, P., and Rinaldo, A. 1992. Simulation of Dispersion in Heterogeneous Porous Formations: Statistics, First-Order Theories, Convergence of Computations. *Water Resources Research*, Vol. 28, No. 9, pp. 2211 – 2228.

Berger, A. 1988. Milankovitch Theory and Climate. *Reviews of Geophysics*, Vol. 26, No. 4, pp. 624 – 657.

Bertram-Howery, S.G., and Hunter, R.L. Eds. 1989. *Preliminary Plan for Disposal-System Characterization and Long-Term Performance Evaluation of the Waste Isolation Pilot Plant*. SAND89-0178. Sandia National Laboratories, Albuquerque, NM. WPO 24103.

Bertram-Howery, S.G., Marietta, M.G., Rechard, R.P., Swift, P.N., Anderson, D.R., Baker, B.L., Bean, Jr., J.E., Beyeler, W., Brinster, K.F., Guzowski, R.V., Helton, J.C., McCurley, R.D., Rudeen, D.K., Schreiber, J.D., and Vaughn, P. 1990. *Preliminary Comparison with 40 CFR Part 191, Subpart B for the Waste Isolation Pilot Plant, December 1990.* SAND90-2347. Sandia National Laboratories, Albuquerque, NM. WPO 27796.

Bird, R.B., Stewart, W.E., and Lightfoot, E.N. 1960. *Transport Phenomena*. John Wiley & Sons, New York, NY. NNA. 900919.0195.

Borns, D.J. 1985. *Marker Bed 139: Study of Drillcore From A Systematic Array.* SAND85-0023. Sandia National Laboratories, Albuquerque, NM. WPO 24529.

Borns, D.J., and Shaffer, S.E. 1985. *Regional Well-Log Correlation in the New Mexico Portion of the Delaware Basin*. SAND83-1798. Sandia National Laboratories, Albuquerque, NM. WPO 24511.

Borns, D.J., and Stormont, J.C. 1988. *An Interim Report on Excavation Effect Studies at the Waste Isolation Pilot Plant: The Delineation of the Disturbed Rock Zone.* SAND87-1375. Sandia National Laboratories, Albuquerque, NM. WPO 24694.

Borns, D.J., and Stormont, J.C. 1989. "The Delineation of the Disturbed Rock Zone Surrounding Excavations in Salt." In *Rock Mechanics as a Guide for Efficient Utilization of Natural Resources, Proceedings of the 30th U.S. Symposium, Morgantown, WV, June 19-22, 1989*, A.W. Khair, ed., pp. 353 – 360. SAND88-2230C. A.A. Balkema, Brookfield, VT. WPO 29974.

Borns, D.J., Pfeifer, M.C., Andersen, H.T., and Skokan, C.K. 1990. "Electrical Methods to Delineate Fluid Flow In Situ in Bedded Salt." In *Society of Exploration Geophysicists Workshop on Permeability, Fluid Pressure and Pressure Seals in the Crust, Denver, CO, August 5-8, 1990*. SAND90-1685A. Sandia National Laboratories, Albuquerque, NM. WPO 28590.

Bredehoeft, J.D., Riley, F.S., and Roeloffs, E.A. 1987. Earthquakes and Groundwater. *Earthquakes and Volcanoes*, Vol. 19, No. 4, pp. 138 – 146.

Brush, L.H., and Anderson, D.R. 1989. "Appendix E: Estimates of Gas Production Rates, Potentials, and Periods, and Dissolved Radionuclide Concentrations for the WIPP Supplemental Environmental Impact Statement." In *Performance Assessment Methodology Demonstration: Methodology Development for Evaluating Compliance With EPA 40 CFR 191, Subpart B, for the Waste Isolation Pilot Plant*. M.G. Marietta, S.G. Bertram-Howery, D.R. Anderson, K.F. Brinster, R.V. Guzowski, H. Iuzzolino, and R.P. Rechard, eds. SAND89-2027. Sandia National Laboratories, Albuquerque, NM. pp. E-1 through E-14. In Appendix E of WPO 25952.

Buddemeier, R.W., and Hunt, J.R. 1988. Transport of Colloidal Contaminants in Groundwater: Radionuclide Migration at the Nevada Test Site. *Applied Geochemistry*, Vol. 3, No. 5, pp. 535 – 548.

Burton, P.L., Adams, J.W., and Engwall, C. 1993. "History of the Washington Ranch, Eddy County, New Mexico." In *Carlsbad Region, New Mexico and West Texas.* D.W. Love, J.W. Hawley, B.S. Kues, J.W. Adams, G.W. Austin, and J.M. Barker, eds. Forty-Fourth Annual Conference, October 6–9, 1993, pp. 65 – 67. New Mexico Geological Society, Roswell, NM.

Cauffmann, T.L., LaVenue, A.M., and McCord, J.P. 1990. *Ground-Water Flow Modeling of the Culebra Dolomite. Volume II: Data Base*. SAND89-7068/2. Sandia National Laboratories, Albuquerque, NM. WPO 10551.

Chapman, J.B. 1986. *Stable Isotopes in Southeastern New Mexico Groundwater: Implications for Dating Recharge in the WIPP Area*. EEG-35, DOE/AL/10752-35. Environmental Evaluation Group, Santa Fe, NM.

Chappell, J., and Shackleton, N.J. 1986. Oxygen Isotopes and Sea Level. *Nature*, Vol. 324, No. 6093, pp. 137 – 140.

Chaturvedi, L. 1993. "WIPP-Related Geological Issues." In *Carlsbad Region, New Mexico and West Texas*, D.W. Love, J.W. Hawley, B.S. Kues, J.W. Adams, G.S. Austin, and J.M. Barker, eds. Forty-Fourth Annual Field Conference, October 6–9, 1993, pp. 331 – 338. New Mexico Geological Society, Roswell, NM.

Choppin, G.R. 1988. Humics and Radionuclide Migration. *Radiochimica Acta*, Vols. 44/45, Pt. 1, pp. 23 – 28.

Chugg, J.C., Anderson, G.W., King, D.L., and Jones, L.H. 1952. *Soil Survey of Eddy Area, New Mexico*. U.S. Department of Agriculture, Washington, D.C.

Coats, K.H. 1989. "Implicit Compositional Simulation of Single-Porosity and Dual-Porosity Reservoirs." In *Proceedings, Tenth SPE Symposium on Reservoir Simulation, Houston, TX, February 6–8, 1989*. SPE 18427, pp. 239 – 275. Society of Petroleum Engineers, Richardson, TX.

Cooper, J.B., and Glanzman, V.M. 1971. *Geohydrology of Project Gnome Site, Eddy County, New Mexico*. United States Geological Survey Professional Paper 712-A. U.S. Geological Survey, Washington, D.C.

Corbet, T.F., and Wallace, M.G. 1993. "Post-Pleistocene Patterns of Shallow Groundwater Flow in the Delaware Basin, Southeastern New Mexico and West Texas." In *Carlsbad Region, New Mexico and West Texas*, D.W. Love, J.W. Hawley, B.S. Kues, J.W. Adams, G.S. Austin, and J.M. Barker, eds. Forty-Fourth Annual Field Conference, October 6–9, 1993, SAND93-1318J, pp. 321 – 351. New Mexico Geological Society, Roswell, NM. WPO 28643.

Cranwell, R.M., Campbell, J.E., Helton, J.C., Iman, R.L., Longsine, D.E., Ortiz, N.R., Runkle, G.E., and Shortencarier, M.J. 1987. *Risk Methodology for Geologic Disposal of Radioactive Waste: Final Report*. NUREG/CR-2452, SAND81-2573. Sandia National Laboratories, Albuquerque, NM. WPO 28296.

Davies, P.B. 1983. "Assessing the Potential for Deep-Seated Salt Dissolution and the Subsidence at the Waste Isolation Pilot Plant (WIPP)." In *State of New Mexico*

Environmental Evaluation Group Conference, WIPP Site Suitability for Radioactive Waste Disposal, Carlsbad, NM, May 12–13, 1983. (Copy on file at the Nuclear Waste Management Library, Sandia National Laboratories, Albuquerque, NM as WPO 29533.)

Davies, P.B. 1989. *Variable-Density Ground-Water Flow and Paleohydrology in the Waste Isolation Pilot Plant (WIPP) Region, Southeastern New Mexico*. Open-File Report 88-490. U.S. Geological Survey, Albuquerque, NM. WPO 38854.

Dearlove, J.P.L., Longworth, G., Ivanovich, M., Kim, J.I., Delakowitz, B., and Zeh, P. 1990. "Organic Colloid Transport of Radionuclides at Gorleben, West Germany." In *Proceedings of the Symposium on Waste Management, Tucson, AZ, February 25–March 1, 1990.* R.G. Post, ed., Vol. 2, pp. 565 – 569. University of Arizona, Tucson, AZ.

Doctor, P.G., Liebetrau, A.M., Eslinger, P.W., Reimus, P.W., Elwood, D.M., Strenge, D.L., Engel, D.W., Tanner, J.E., and Freshley, M.D. 1992. *An Example Postclosure Risk Assessment Using the Potential Yucca Mountain Site.* PNL-8081. Pacific Northwest Laboratory, Richland, WA. NNA. 930414.0031.

DOE (U.S. Department of Energy). 1980. *Final Environmental Impact Statement, Waste Isolation Pilot Plant*. DOE/EIS-0026, Vols. 1 and 2. U.S. Department of Energy, Washington, D.C. WPO 38835, WPO 38838 - WPO 38839.

DOE (U.S. Department of Energy). 1990. *Final Safety Analysis Report*. WP 02-9, Rev. 0, May 1990. Westinghouse Electric Corporation, Waste Isolation Division, Carlsbad, NM.

DOE (U.S. Department of Energy). 1990. *WIPP Test Phase Plan: Performance Assessment.* DOE/WIPP-89-011, Rev. 0. U.S. Department of Energy, Waste Isolation Pilot Plant, Carlsbad, NM.

DOE (U.S. Department of Energy). 1991. *Evaluation of the Effectiveness and Feasibility of the Waste Isolation Pilot Plant Engineered Alternatives: Final Report of the Engineered Alternatives Task Force.* DOE/WIPP 91-007, Rev. 0. Vols. 1 and 2. Waste Isolation Pilot Plant, Carlsbad, NM.

DOE (U.S. Department of Energy). 1991. *Integrated Data Base for 1991: U.S. Spent Fuel and Radioactive Waste Inventories, Projections, and Characteristics.* DOE/RW-0006, Rev. 7. Oak Ridge National Laboratory, Oak Ridge, TN. HQX. 910711.0004.

DOE (U.S. Department of Energy). 1994. *Compliance Status Report for the Waste Isolation Pilot Plant*. DOE/WIPP 94-019, Rev. 0. U.S. Department of Energy, Carlsbad Area Office, Carlsbad, NM.

DOE (U.S. Department of Energy). 1994. *Experimental Program Plan for the Waste Isolation Pilot Plant*. DOE/WIPP 94-008, Rev. 0. U.S. Department of Energy, Carlsbad Area Office, Carlsbad, NM.

DOE (U.S. Department of Energy). 1994. *Compliance Status Report for the Waste Isolation Pilot Plant*. DOE/WIPP 94-019, Rev. 0. U.S. Department of Energy, Carlsbad Area Office, Carlsbad, NM.

DOE (U.S. Department of Energy). 1995. *U.S. Department of Energy Waste Isolation Pilot Plant Transuranic Waste Baseline Inventory Report*. DOE/CAO-94-1005, Rev. 1, Vols. 1-2. WIPP Technical Assistance Contractor for U.S. Department of Energy, Carlsbad, NM.

Dowding, C.H., and Rozen, A. 1978. Damage to Rock Tunnels from Earthquake Shaking. *Journal of the Geotechnical Engineering Division, American Society of Civil Engineers*, Vol. 104, No. GT2, pp. 175 – 191.

Eager, G.P. 1983. Cores from the Lower Dewey Lake, Rustler, and Upper Salado Formation, Culberson County, Texas. *Permian Basin Cores*. R.L. Shaw and B.J. Pollan, eds. P.B.S.-S.E.P.M. Core Workshop, Vol. 2, pp. 273 – 283. Permian Basin Section, Society of Economic Paleontologists and Mineralogists, Midland, TX.

EPA (U.S. Environmental Protection Agency). 1996. *40 CFR Part 194: Criteria for the Certification and Re-Certification of the Waste Isolation Pilot Plant's Compliance with the 40 CFR Part 191 Disposal Regulations Final Rule*. *Response to Comments Document for 40 CFR Part 194*. EPA 402-R-96-001. Environmental Protection Agency, Office of Radiation and Indoor Air, Washington, D.C.

Francis, A.J., and Gillow, J.B. 1994. *Effects of Microbial Processes on Gas Generation Under Expected Waste Isolation Pilot Plant Repository Conditions*. SAND93-7036. Sandia National Laboratories, Albuquerque, NM. WPO 26555.

Freeland, M.H. 1982. *Basic Data Report for Borehole DOE-1, Waste Isolation Pilot Plant (WIPP) Project, Southeastern New Mexico*. TME 3159. U.S. Department of Energy, Waste Isolation Pilot Plant, Albuquerque, NM.

Freeze, R.A., and Cherry, J.A. 1979. *Groundwater*. Prentice-Hall, Englewood Cliffs, NJ. NNA. 870406.0444.

Galson, D.A., Hicks, T.W., Wilmot, R.D., and Swift, P.N. 1995. *Systems Prioritization Method—Iteration 2 Baseline Position Paper: Scenario Development for Long-Term Performance Assessments of the WIPP*. Sandia National Laboratories, Albuquerque, NM. WPO 28726.

Gonzales, M.M. 1989. *Compilation and Comparison of Test-Hole Location Surveys in the Vicinity of the Waste Isolation Pilot Plant Site*. SAND88-1065. Sandia National Laboratories, Albuquerque, NM. WPO 24121.

Griswold, G.B. 1977. *Site Selection and Evaluation Studies of the Waste Isolation Pilot Plant (WIPP), Los Medaños, Eddy County, NM*. SAND77-0946. Sandia National Laboratories, Albuquerque, NM. WPO 28125.

Hays, J.D., Imbrie, J., and Shackleton, N.J. 1976. Variations in the Earth's Orbit: Pacemaker of the Ice Ages. *Science*, Vol. 194, No. 4270, pp. 1121 – 1132. HQS.880517.2140.

Helton, J.C., Garner, J.W., McCurley, R.D., and Rudeen, D.K. 1991. *Sensitivity Analysis Techniques and Results for Performance Assessment at the Waste Isolation Pilot Plant.* SAND90-7103. Sandia National Laboratories, Albuquerque, NM. WPO 23803.

Helton, J.C., Garner, J.W., Rechard, R.P., Rudeen, D.K., and Swift, P.N. 1992. *Preliminary Comparison with 40 CFR Part 191, Subpart B for the Waste Isolation Pilot Plant, December 1991. Volume 4: Uncertainty and Sensitivity Analysis Results*. SAND91-0893/4. Sandia National Laboratories, Albuquerque, NM. WPO 26423.

Helton, J.C., Marietta, M.G., and Rechard, R.P. 1993. *Conceptual Structure of Performance Assessments Conducted for the Waste Isolation Pilot Plant*. SAND92-2285. Sandia National Laboratories, Albuquerque, NM. WPO 27834.

Hiemenz, P.C. 1986. *Principles of Colloid and Surface Chemistry*. 2nd ed. Marcel Dekker, Inc., New York, NY.

Hill, A.C., and Thomas, G.W. 1985. "A New Approach for Simulating Complex Fractured Reservoirs." In *Proceedings, Eighth SPE Symposium on Reservoir Simulation, Dallas, TX, February 10-13, 1985*, L.C. Young, ed. SPE 13537, pp. 429 – 440. Society of Petroleum Engineers of AIME, Richardson, TX.

Hills, J.M., and Kottlowski, F.E. 1983. *Southwest/Southwest Mid-Continent Region: Correlation of Stratigraphic Units of North America (COSUNA) Project*. Correlation Chart Series 1983. AAPG Bookstore, Tulsa, OK.

Holcomb, D.J. 1988. "Cross-Hole Measurements of Velocity and Attenuation to Detect a Disturbed Zone in Salt at the Waste Isolation Pilot Plant." In *Key Questions in Rock Mechanics: Proceedings of the 29th U.S. Symposium, University of Minnesota, Minneapolis, MN, June 13-15, 1988*, P.A. Cundall, R.L. Sterling, and A.M. Starfield, eds. SAND87-3016C, pp. 633 – 640. A.A. Balkema, Brookfield, VT. WPO 29992.

Hora, S.C. 1992. "Appendix A: Probabilities of Human Intrusion into the WIPP, Methodology for the 1992 Preliminary Comparison." In *Preliminary Performance Assessment for the Waste Isolation Pilot Plant, December 1992. Volume 3: Model Parameters.* SAND92-0700/3. Sandia National Laboratories, Albuquerque, NM. In Appendix A of WPO 23529, pp. A-69 through A-99.

Hora, S.C., von Winterfeldt, D., and Trauth, K.M. 1991. *Expert Judgment on Inadvertent Human Intrusion into the Waste Isolation Pilot Plant.* SAND90-3063. Sandia National Laboratories, Albuquerque, NM. WPO 26161.

Houghton, J.T., Jenkins, G.J., and Ephraums, J.J. 1990. *Climate Change: The IPCC Scientific Assessment*. Cambridge University Press, New York, NY.

Howard, C.L., Jensen, A.L., Jones, R.L., and Peterson, T.P. 1993. *Room Q Data Report: Test Borehole Data from April 1989 through November 1991*. SAND92-1172. Sandia National Laboratories, Albuquerque, NM. WPO 23548.

Hunter, R.L. 1985. *A Regional Water Balance for the Waste Isolation Pilot Plant (WIPP) Site and Surrounding Area*. SAND84-2233. Sandia National Laboratories, Albuquerque, NM. WPO 27628.

Hunter, R.L., Cranwell, R.M., and Chu, M.S.Y. 1986. *Assessing Compliance with the EPA High-Level Waste Standard: An Overview.* SAND86-0121, NUREG/CR-4510. Sandia National Laboratories, Albuquerque, NM. WPO 28435.

IAEA (International Atomic Energy Agency). 1989. *Evaluating the Reliability of Predictions Made Using Environmental Transfer Models*. Safety Series Report No. 100. International Atomic Energy Agency, Vienna.

Imbrie, J. 1985. A Theoretical Framework for the Pleistocene Ice Ages. *Journal of the Geological Society*, Vol. 142, Pt. 3, pp. 417 – 432.

Imbrie, J., and Imbrie, J.Z. 1980. Modeling the Climatic Response to Orbital Variations. *Science*, Vol. 207, No. 4434, pp. 943 – 953.

Imbrie, J., Hays, J.D., Martinson, D.G., McIntyre, A., Mix, A.C., Morley, J.J., Pisias, N.G., Prell, W.L., and Shackleton, J.J. 1984. "The Orbital Theory of Pleistocene Climate: Support from a Revised Chronology of the Marine $\delta^{18}O$ Record." In *Milankovitch and Climate, Understanding the Response to Astronomical Forcing, Proceedings of the NATO Advanced Research Workshop on Milankovitch and Climate, Palisades, NY, November 30-December 4, 1982,* A. Berger, J. Imbrie, J. Hays, G. Kukla, and B. Saltzman, eds., Pt. 1, pp. 269 – 305. D. Reidel, Boston, MA.

Imbrie, J., McIntyre, A., and Mix, A. 1989. Oceanic Response to Orbital Forcing in the Late Quaternary: Observational and Experimental Strategies. *Climate and Geo-sciences*, A. Berger, S. Schneider, and J.C. Duplessy, eds., pp. 121 – 164. Kluwer, Boston, MA.

Izett, G.A., and Wilcox, R.E. 1982. *Map Showing Localities and Inferred Distributions of the Huckleberry Ridge, Mesa Falls, and Lava Creek Ash Beds in the Western United States and Southern Canada*. Misc. Investigations Map I-1325, Scale 1:4,000,000. U.S. Geological Survey.

Jones, C.L. 1978. *Test Drilling for Potash Resources: Waste Isolation Pilot Plant Site, Eddy County, New Mexico*. Open-File Report 78-592, Vols. 1 and 2. U.S. Geological Survey, Denver, CO.

Jones, T.L., Kelley, V.A., Pickens, J.F., Upton, D.T., Beauheim, R.L., and Davies, P.B. 1992. *Integration of the Interpretation Results of Tracer Tests Performed in the Culebra Dolomite at the Waste Isolation Pilot Plant Site.* SAND92-1579. Sandia National Laboratories, Albuquerque, NM. WPO 23504.

Jung, Y., Ibrahim, A., and Borns, D.J. 1991. Mapping Fracture Zones in Salt; High-Resolution, Cross-Gallery Seismic Tomography. *Geophysics: The Leading Edge of Exploration*, Vol. 10, No. 4, pp. 37 – 39.

Kazemi, H., Merrill, Jr., L.S., Porterfield, K.L., and Zeman, P.R. 1976. Numerical Simulation of Water-Oil Flow in Naturally Fractured Reservoirs. *Society of Petroleum Engineers Journal*, Vol. 16, No. 6, pp. 317 – 326.

Kelley, V.A., and Saulnier, Jr., G.J. 1990. *Core Analyses for Selected Samples from the Culebra Dolomite at the Waste Isolation Pilot Plant Site*. SAND90-7011. Sandia National Laboratories, Albuquerque, NM, pp. 4-10. WPO 28629.

Kim, J.I. 1991. Actinide Colloid Generation in Groundwater. *Radiochimica Acta*, Vol. 52/53, Pt. 1, pp. 71 – 81.

Lambert, S.J. 1983. *Dissolution of Evaporites in and Around the Delaware Basin, Southeastern New Mexico and West Texas.* SAND82-0461. Sandia National Laboratories, Albuquerque, NM. WPO 27520.

Lambert, S.J. 1987. "Stable-Isotope Studies of Groundwaters in Southeastern New Mexico." In *The Rustler Formation at the WIPP Site, Report of a Workshop on the Geology and Hydrology of the Rustler Formation as it Relates to the WIPP Project*, L. Chaturvedi, ed. SAND85-1978C, EEG-34, pp. 36 – 57. Environmental Evaluation Group, Santa Fe, NM. WPO 28418.

Lenhardt, W.A. 1988. "Damage Studies at a Deep Level African Gold Mine." In *Rockbursts & Seismicity In Mines, Proceedings of the Second International Symposium, Minneapolis, MN, June 8-10, 1988,* C. Fairhurst, ed., 1990, pp. 391 – 393. A.A. Balkema, Brookfield, VT.

Lieser, K.H., Gleitsmann, B., and Steinkopff, T. 1986. Sorption of Trace Elements or Radionuclides in Natural Systems Containing Groundwater and Sediments. *Radiochimica Acta*, Vol. 40, No. 1, pp. 33 – 37.

Lieser, K.H., Gleitsmann, B., Peschke, S., and Steinkopff, T. 1986. Colloid Formation and Sorption of Radionuclides in Natural Systems. *Radiochimica Acta*, Vol. 40, No. 1, pp. 39 – 47.

Lieser, K.H., Ament, A., Hill, R., Singh, R.N., Stingl, U., and Thybusch, B. 1990. Colloids in Groundwater and Their Influence on Migration of Trace Elements and Radionuclides. *Radiochimica Acta*, Vol. 49, No. 2, pp. 83 – 100.

Litvak, B.L. 1986. "Simulation and Characterization of Naturally Fractured Reservoirs." In *Reservoir Characterization Technical Conference, Dallas, TX, April 29-May 1, 1985*, L.W. Lake and H.B. Carroll, Jr., eds., pp. 561 – 584. Academic Press, Orlando, FL.

Lowenstein, T.K. 1987. *Post Burial Alteration of the Permian Rustler Formation Evaporites, WIPP Site, New Mexico: Textural, Stratigraphic and Chemical Evidence*. EEG-36, DOE/AL/10752-36. Environmental Evaluation Group, Santa Fe, NM.

Lowenstein, T.K. 1988. Origin of Depositional Cycles in a Permian "Saline Giant": The Salado (McNutt Zone) Evaporites of New Mexico and Texas. *Geological Society of America Bulletin*, Vol. 100, No. 4, pp. 592 – 608.

Lyklema, J. 1978. Surface Chemistry of Colloids in Connection with Stability. *The Scientific Basis of Flocculation*, K.J. Ives, ed., pp. 3 – 36. Sijthoff and Noordhoff, Dordrecht.

Lyon, M.L. 1989. *Annual Water Quality Data Report for the Waste Isolation Pilot Plant*. DOE/WIPP 89-001. Westinghouse Electric Corporation, Carlsbad, NM.

Machette, M.N. 1985. "Calcic Soils of the Southwestern United States." In *Soils and Quaternary Geology of the Southwestern United States,* D.L. Weide and M.L. Faber, eds. Special Paper Vol. 203, pp. 1 – 21. Geological Society of America, Denver, CO.

Maiti, T.C., Smith, M.R., and Laul, J.C. 1989. Colloid Formation Study of U, Th, Ra, Pb, Po, Sr, Rb, and Cs in Briny (High Ionic Strength) Groundwaters: Analog Study for Waste Disposal. *Nuclear Technology*, Vol. 84, No. 1, pp. 82 – 87.

Mansure, A., and Reiter, M. 1977. *An Accurate Equilibrium Temperature Log in AEC No. 8, A Drill Test in the Vicinity of the Proposed Carlsbad Disposal Site*. Open File Report 80. New Mexico Bureau of Mines and Mineral Resources, Socorro, NM. WPO 21200.

Marietta, M.G., Bertram-Howery, S.G., Anderson, D.R., Brinster, K.F., Guzowski, R.V., Izzulino, H., and Rechard, R.P. 1989. *Performance Assessment Methodology Demonstration: Methodology Development for Evaluating Compliance with EPA 40 CFR 191, Subpart B, for the Waste Isolation Pilot Plant.* SAND89-2027. Sandia National Laboratories, Albuquerque, NM. WPO 25952.

McGrath, E.J., and Irving, D.C. 1975. *Techniques for Efficient Monte Carlo Simulation. Volume III. Variance Reduction*. ORNL-RSIC-38, Vol. 3. Oak Ridge National Laboratory, Oak Ridge, TN.

McGrath, E.J., and Irving, D.C. 1975. *Techniques for Efficient Monte Carlo Simulation. Volume II. Random Number Generation for Selected Probability Distributions.* ORNL-RSIC-38, Vol. 2. Oak Ridge National Laboratory, Oak Ridge, TN.

McGrath, E.J., Basin, S.L., Burton, R.W., Irving, D.C., and Jaquette, S.C. 1975. *Techniques for Efficient Monte Carlo Simulation*. *Volume I. Selecting Probability Distribution*s. ORNL-RSIC-38, Vol. 1. Oak Ridge National Laboratory, Oak Ridge, TN.

McKay, M.D., Beckman, R.J., and Conover, W.J. 1979. A Comparison of Three Methods for Selecting Values of Input Variables in the Analysis of Output from a Computer Code. *Technometrics*, Vol. 21, No. 2, pp. 239 – 245.

Mercer, J.W. 1983. *Geohydrology of the Proposed Waste Isolation Pilot Plant Site, Los Medaños Area, Southeastern New Mexico*. Water Resources Investigations Report 83-4016. U.S. Geological Survey, Albuquerque, NM. (This document is included as Appendix HYDRO.)

Mercer, J.W., and Snyder, R.P. 1990. *Basic Data Report for Drillholes at the H-11 Complex (Waste Isolation Pilot Plant—WIPP)*. SAND89-0200. Sandia National Laboratories, Albuquerque, NM. WPO 27705.

Mercer, J.W., Beauheim, R.L., Snyder, R.P., and Fairer, G.M. 1987. *Basic Data Report for Drilling and Hydrologic Testing of Drillhole DOE-2 at the Waste Isolation Pilot Plant (WIPP) Site*. SAND86-0611. Sandia National Laboratories, Albuquerque, NM. WPO 27646.

Mitchell, J.F.B. 1989. The "Greenhouse" Effect and Climate Change. *Reviews of Geophysics*, Vol. 27, No. 1, pp. 115 – 139.

Molecke, M.A., Argüello, J.G., and Beraún, R. 1993. *Waste Isolation Pilot Plant Simulated RH TRU Waste Experiments: Data and Interpretation Report*. SAND88-1314. Sandia National Laboratories, Albuquerque, NM. WPO 24906.

Muehlberger, W.R., Belcher, R.C., and Goetz, L.K. 1978. Quaternary Faulting on Trans-Pecos, Texas. *Geology*, Vol. 6, No. 6, pp. 337 – 340.

Myers, J., Drez, P., and James, P. 1991. "Chapter 6: The Redox State and the Occurrence and Influence of Organics in the Culebra." In *Hydrogeochemical Studies of the Rustler Formation and Related Rocks in the Waste Isolation Pilot Plant Area, Southeastern New Mexico*. M.D. Siegel, S.J. Lambert, and K.L. Robinson, eds. SAND88-0196. Sandia National Laboratories, Albuquerque, NM. In WPO 25624 (Chapter 6) pp. 6-1 throgh 6-35.

Nicholson, Jr., A., and Clebsch, Jr., A. 1961. *Geology and Ground-Water Conditions in Southern Lea County, New Mexico.* Ground-Water Report 6. New Mexico Bureau of Mines and Mineral Resources, Socorro, NM.

Nowak, E.J., Tillerson, J.R., and Torres, T.M. 1990. *Initial Reference Seal System Design: Waste Isolation Pilot Plant.* SAND90-0355. Sandia National Laboratories, Albuquerque, NM. WPO 23981.

OECD Nuclear Energy Agency. 1995. *Future Human Actions at Disposal Sites, A Report of the NEA Working Group on Assessment of Future Human Actions at Radioactive Waste Disposal Sites*. Organisation for Economic Co-Operation and Development, Paris, France.

Parry, G.W. 1988. On the Meaning of Probability in Probabilistic Safety Assessment. *Reliability Engineering and System Safety*, Vol. 23, No. 4, pp. 309 – 314.

Paté-Cornell, M.E. 1986. Probability and Uncertainty in Nuclear Safety Decisions. *Nuclear Engineering and Design*, Vol. 93, No. 2-3, pp. 319 – 327.

Pfeifer, M.C., Borns, D.J., Skokan, C.K., Andersen, H.T., and Starrett, J.M. 1989. "Geophysical Methods to Monitor the Development of the Disturbed Rock Zone Around Underground Excavations in Bedded Salt." In *Proceedings of the Symposium on the Application of Geophysics to Engineering and Environmental Problems, Golden, CO, March 13–16, 1989*. SAND89-7055A, Vol. 2, pp. 400 – 411. WPO 29630.

Powers, D.W., and Holt, R.M. 1990. "Sedimentology of the Rustler Formation near the Waste Isolation Pilot Plant (WIPP) Site." In *Geological and Hydrological Studies of Evaporites in the Northern Delaware Basin for the Waste Isolation Pilot Plant (WIPP), New Mexico.* Field Trip #14 Guidebook, Geological Society of America 1990 Annual Meeting, October 29–November 1, 1990, pp. 79 – 106. Dallas Geological Society, Dallas, TX.

Powers, D.W., and Holt, R.M. 1993. "The Upper Cenozoic Gatuna Formation of Southeastern New Mexico." In *Carlsbad Region, New Mexico and West Texas,* D.W. Love, J.W. Hawley, B.S. Kues, J.W. Adams, G.S. Austin, and J.M. Barker, eds. Forty-Fourth Annual Field Conference, October 6–9, 1993, pp. 271 – 282. New Mexico Geological Society, Socorro, NM.

Powers, D.W., Lambert, S.J., Shaffer, S-E., Hill, L.R., and Weart, W.D., eds. 1978. *Geological Characterization Report, Waste Isolation Pilot Plant (WIPP) Site, Southeastern New Mexico*. SAND78-1596, Volumes I and II. Sandia National Laboratories, Albuquerque, NM. (This document is included as Appendix GCR.) Vol. 1 - WPO 5448, Vol. 2 - WPO 26829 - WPO 26830.

Rechard, R.P. 1989. *Review and Discussion of Code Linkage and Data Flow in Nuclear Waste Compliance Assessments.* SAND87-2833. Sandia National Laboratories, Albuquerque, NM. WPO 25675.

Rechard, R.P., ed. 1992. *User's Reference Manual for CAMCON: Compliance Assessment Methodology Controller Version 3.0.* SAND90-1983. Sandia National Laboratories, Albuquerque, NM. WPO 25628.

Richey, S.F. 1987. *Water-Level Data from Wells in the Vicinity of the Waste Isolation Pilot Plant, Southeastern New Mexico*. Open-File Report 87-120. United States Geological Survey, Albuquerque, NM.

Robinson, J.Q., and Powers, D.W. 1987. "A Clastic Deposit Within the Lower Castile Formation, Western Delaware Basin, New Mexico." In *Geology of the Western Delaware Basin, West Texas and Southeastern New Mexico*, D.W. Powers and W.C. James, eds. El Paso Geological Society Guidebook 18, pp. 69 – 79. El Paso Geological Society, El Paso, TX. WPO 37942.

Robinson, T.W., and Lang, W.B. 1938. *Geology and Groundwater Conditions of the Pecos River Valley in the Vicinity of Laguna Grande de la Sal, New Mexico, with Special Reference to the Salt Content of the River Water.* Twelfth and Thirteenth Biennial Reports of the State Engineer of New Mexico for the 23rd, 24th, 25th, and 26th Fiscal Years, July 1, 1935 to July 30, 1938. State Engineer, Santa Fe, NM. WPO 37942.

Rosholt, J.N., and McKinney, C.R. 1980. *Uranium Series Disequilibrium Investigations Related to the WIPP Site, New Mexico (USA). Part II. Uranium Trend Dating of Surficial Deposits and Gypsum Spring Deposits Near WIPP Site, New Mexico*. Open-File Report 80-879. U.S. Geological Survey, Denver, CO.

Sandia National Laboratories. 1992. *Long-Term Gas and Brine Migration at the Waste Isolation Pilot Plant: Preliminary Sensitivity Analyses for Post-Closure 40 CFR 268 (RCRA), May 1992.* SAND92-1933. Sandia National Laboratories, WIPP Performance Assessment Department, Albuquerque, NM. WPO 23513.

Saulnier, Jr., G.J. 1987. *Analysis of Pumping Tests of the Culebra Dolomite Conducted at the H-11 Hydropad at the Waste Isolation Pilot Plant (WIPP) Site*. SAND87-7124. Sandia National Laboratories, Albuquerque, NM. WPO 28520.

Saulnier, Jr., G.J., Domski, P.S., Palmer, J.B., Roberts, R.M., Stensrud, W.A., and Jensen, A.L. 1991. *WIPP Salado Hydrology Program Data Report #1*. SAND90-7000. Sandia National Laboratories, Albuquerque, NM. WPO 25746.

Schiel, K.A. 1988. *The Dewey Lake Formation; End Stage Deposit of a Peripheral Foreland Basin.* [M.S. thesis.] University of Texas at El Paso, El Paso, TX.

Schlesinger, M.E., and Mitchell, J.F.B. 1987. Climate Model Simulations of the Equilibrium Climatic Response to Increased Carbon Dioxide. *Reviews of Geophysics*, Vol. 25, No. 4, pp. 760 – 798.

Sewards, T., Glenn, R., and Keil, K. 1991. *Mineralogy of the Rustler Formation in the WIPP-19 Core*. SAND87-7036. Sandia National Laboratories, Albuquerque, NM. WPO 24140.

Shinta, A.A., and Kazemi, H. 1993. "Tracer Transport in Characterization of Dual-Porosity Reservoirs." In *Reservoir Engineering Proceedings, SPE Annual Technical Conference and Exhibition, Houston, TX, October 3-6, 1993*. SPE 26636, pp. 285 – 299. Society of Petroleum Engineers, Richardson, TX.

Silva, M. 1994. *Implications of the Presence of Petroleum Resources on the Integrity of the WIPP*. EEG-55, DOE/AL/58309-55. Environmental Evaluation Group, Albuquerque, NM. WPO 9607.

Slezak, S., and Lappin, A. 1990. "Potential for and Possible Impacts of Generation of Flammable and/or Detonable Gas Mixtures during the WIPP Transportation, Test, and Operational Phases." In Memorandum to D. Mercer and C. Fredrickson, January 5, 1990. Sandia National Laboratories, Albuquerque, NM. WPO 21224.

Snyder, R.P., Gard, Jr., L.M, and Mercer, J.W. 1982. *Evaluation of Breccia Pipes in Southeastern New Mexico and Their Relation to the Waste Isolation Pilot Plant (WIPP) Site*. Open-File Report 82-968. U.S. Geological Survey, Denver, CO.

Stensrud, W.A., Bame, M.A., Lantz, K.D., Cauffman, T.L., Palmer, J.B., and Saulnier, Jr., G.J. 1988. *WIPP Hydrology Program, Waste Isolation Pilot Plant, Southeastern New Mexico, Hydrologic Data Report #6*. SAND87-7166. Sandia National Laboratories, Albuquerque, NM. WPO 29674.

Stensrud, W.A., Dale, T.F., Domski, P.S., Palmer, J.B., Roberts, R.M., Fort, M.D., Saulnier, Jr., G.J., and Jensen, A.L. 1992. *Waste Isolation Pilot Plant Salado Hydrology Program Data Report #2*. SAND92-7072. Sandia National Laboratories, Albuquerque, NM. WPO 26432.

Stone, C.M., Krieg, R.D., and Beisinger, Z.E. 1985. *SANCHO, A Finite Element Computer Program for the Quasistatic, Large Deformation, Inelastic Response of Two-Dimensional Solids.* SAND84-2618. Sandia National Laboratories, Albuquerque, NM. WPO 24658.

Stormont, J.C. 1990. Discontinuous Behavior Near Excavations in a Bedded Salt Formation. *International Journal of Mining and Geological Engineering*, SAND89-2403J, Vol. 8, No. 1, pp. 35 – 56. WPO 29472.

Stormont, J.C., Peterson, E.W., and Lagus, P.L. 1987. *Summary of and Observations About WIPP Facility Horizon Flow Measurements Through 1986.* SAND87-0176. Sandia National Laboratories, Albuquerque, NM. WPO 27053.

Stormont, J.C., Howard, C.L., and Daemen, J.J.K. 1991. *In Situ Measurements of Rock Salt Permeability Changes Due to Nearby Excavation*. SAND90-3134. Sandia National Laboratories, Albuquerque, NM. WPO 26166.

Swift, P.N. 1992. *Long-Term Climate Variability at the Waste Isolation Pilot Plant, Southeastern New Mexico, USA*. SAND91-7055. Sandia National Laboratories, Albuquerque, NM. WPO 27093.

Telander, M.R., and Westerman, R.E. 1993. *Hydrogen Generation by Metal Corrosion in Simulated Waste Isolation Pilot Plant Environments: Progress Report for the Period November 1989 through December 1992.* SAND92-7347. Sandia National Laboratories, Albuquerque, NM. pp. 6-14 to 6-27. WPO 23456.

Thorne, B.J., and Rudeen, D.K. 1980. *Regional Effects of TRU Repository Heat.* SAND80-7161. Sandia National Laboratories, Albuquerque, NM. WPO 10281.

Tierney, M.S. 1993. "PA Methodology Overview." In *Initial Performance Assessment of the Disposal of Spent Nuclear Fuel and High-Level Waste Stored at Idaho National Engineering Laboratory. Volume 1: Methodology and Results.* R.P. Rechard, ed. SAND93-2330/1. Sandia National Laboratories, Albuquerque, NM. 3-1 through 3-28. Chapter 3 of WPO 26694.

Tiller, C.L., and O'Melia, C.R. 1993. "Natural Organic Matter and Colloidal Stability: Models and Measurements." In *Colloids in the Aquatic Environment. Colloids and Surfaces A: Physicochemical and Engineering Aspects*, T.F. Tadros and J. Gregory, eds., pp. 89 – 102. Elsevier Applied Science, London.

Tipping, E. 1993. "Modelling Ion Binding by Humic Acids." In *Colloids in the Aquatic Environment. Colloids and Surfaces A: Physicochemical and Engineering Aspects*, T.F. Tadros and J. Gregory, eds., pp. 117 – 131. Elsevier Applied Science, London.

Toth, L.M., Friedman, H.A., and Osborne, M.M. 1981. Polymerization of Pu(IV) in Aqueous Nitric Acid Solutions. *Journal of Inorganic and Nuclear Chemistry*, Vol. 43, No. 11, pp. 2929 – 2934.

Van der Lee, J., de Marsily, G., and Ledoux, E. 1993. "Are Colloids Important for Transport Rate Assessment of Radionuclides? A Microscopic Modeling Approach," In *High Level Radioactive Waste Management, Proceedings of the Fourth Annual International Conference, Las Vegas, NV, April 26-30, 1993*, pp. 646 – 652. American Society of Civil Engineers, New York, NY.

Van Sambeek, L.L., Luo, D.D., Lin, M.S., Ostrowski, W., and Oyenuga, D. 1993. *Seal Design Alternatives Study*. SAND92-7340. Sandia National Laboratories, Albuquerque, NM. WPO 23445.

Vesely, W.E., and Rasmuson, D.M. 1984. Uncertainties in Nuclear Probabilistic Risk Analyses. *Risk Analysis*, Vol. 4, No. 4, pp. 313 – 322.

Vilks, P. 1994. *The Role of Colloids and Suspended Particles in Radionuclide Transport in the Canadian Concept for Nuclear Fuel Waste Disposal.* AECL-10280. Whiteshell Laboratories, Atomic Energy of Canada, Ltd., Pinawa, Manitoba. Yucca Mt. #: MOL. 19950202.0067.

Vine, J.D. 1963. Surface Geology of the Nash Draw Quadrangle, Eddy County, New Mexico. *U. S. Geological Survey Bulletin*, 1141-B. WPO 39558.

Vlassopoulos, D., Wood, S.A., and Mucci, A. 1990. Gold Speciation in Natural Waters: II. The Importance of Organic Complexing—Experiments with Some Simple Model Ligands. *Geochimica et Cosmochimica Acta,* Vol. 54, No. 6, pp. 1575 – 1586.

Wallner, M. 1981. "Critical Examination of Conditions for Ductile Fracture in Rock Salt." In *Proceedings of the Workshop on Near-Field Phenomena in Geologic Repositories for Radioactive Waste, Seattle, WA, August 31–September 3, 1981*, pp. 243 – 253. Organisation for Economic Co-Operation and Development, Paris, France.

Warrick, R., and Oerlemans, J. 1990. "Sea Level Rise." In *Climate Change: The IPCC Scientific Assessment*, J.T. Houghton, G.J. Jenkins, and J.J. Ephraums, eds., pp. 257 – 281. Intergovernmental Panel on Climate Change, Sweden.

Washington, W.M., and Meehl, G.A. 1984. Seasonal Cycle Experiment on the Climate Sensitivity Due to a Doubling of CO_2 with an Atmospheric General Circulation Model Coupled to a Simple Mixed-Layer Ocean Model. *Journal of Geophysical Research,* Vol. 89, No. D6, pp. 9475 – 9503.

Weatherby, J.R., Brown, W.T., and Butcher, B.M. 1991. "The Closure of WIPP Disposal Rooms Filled with Various Waste and Backfill Combinations." In *Rock Mechanics as a Multidisciplinary Science*, *Proceedings of the 32nd U.S. Symposium, University of Oklahoma, Norman, OK, July 10-12, 1991*, J.C. Roegiers, ed. SAND90-2399C, pp. 919 – 928. A.A. Balkema, Brookfield, VT. WPO 28617.

Westinghouse Electric Corporation. 1994. *Backfill Engineering Analysis Report, Waste Isolation Pilot Plant.* Westinghouse Electric Corporation, Waste Isolation Division, Carlsbad, NM. WPO 37909.

Wilson, C.A., and Mitchell, J.F.B. 1987. A Doubled CO_2 Climate Sensitivity Experiment with a Global Climate Model Including a Simple Ocean. *Journal of Geophysical Research*, Vol. 92, No. D11, pp. 13,315 – 13,343.

Wolery, T.J. 1992. *EQ3NR, A Computer Program for Geochemical Aqueous Speciation-Solubility Calculations: Theoretical Manual, User's Guide, and Related Documentation (Version 7.0).* UCRL-MA-110662, Pt. 3. Lawrence Livermore National Laboratory, Livermore, CA.

Wolery, T.J., and Daveler, S.A. 1992. *EQ6, A Computer Program for Reaction Path Modeling of Aqueous Geochemical Systems: Theoretical Manual, User's Guide, and Related Documentation (Version 7.0)*. UCRL-MA-110662-Pt.4. Lawrence Livermore National Laboratory, Livermore, CA.

Wood, B.J., Snow, R.E., Cosler, D.J., and Haji-Djafari, S. 1982. *Delaware Mountain Group (DMG) Hydrology—Salt Removal Potential, Waste Isolation Pilot Plant (WIPP) Project, Southeastern New Mexico*. TME 3166. U.S. Department of Energy, Albuquerque, NM.

Zoback, M.D., and Zoback, M.L. 1981. State of Stress and Intraplate Earthquakes in the United States. *Science*, Vol. 213, No. 4203, pp. 96 – 104.

1 **THIS PAGE INTENTIONALLY LEFT BLANK**

CONTENTS

FIGURES

TABLES

INDEX